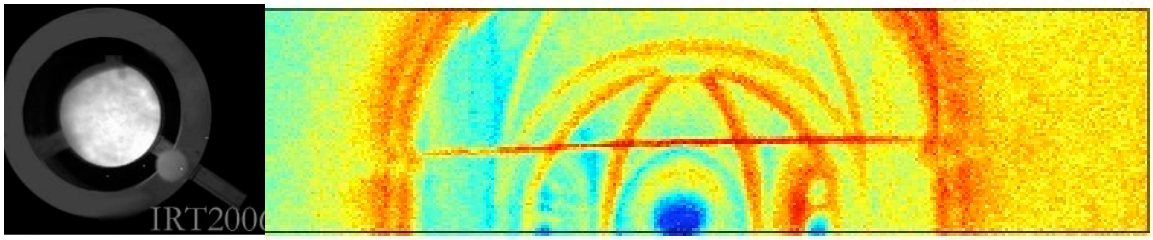

QIRT 2006

8th conference

on

Quantitative InfraRed Thermography

Book of Abstracts

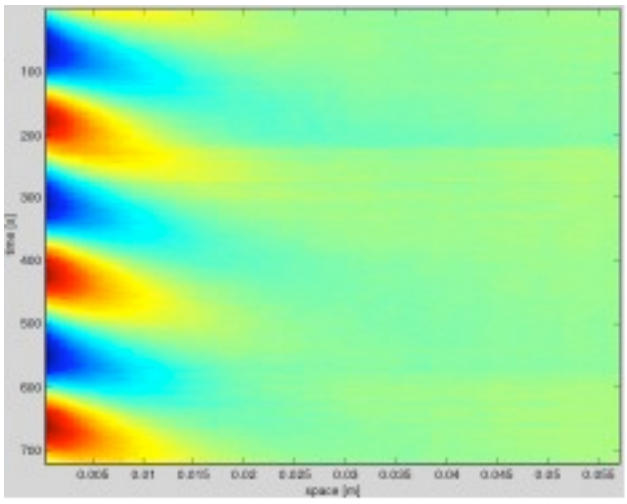

June 28-30, 2006

Organized by:
CNR ITC
Area della Ricerca
Padova – Italy

Major sponsors

Welcome

The 8th International Conference on Quantitative Infrared Thermography is taking place in Padova, Italy on June 27-30, 2006. It is a great pleasure of the organizers to welcome all the participants to the Research Area of National Research Council of Italy for this event. QIRT is an international forum, which brings together specialists from industry and academia, who share an active interest in the latest developments of science, experimental practices and instrumentation, related to infrared thermography.

Researchers have been familiar with infrared thermography for many years now. This technique took many fields by storm, sometimes to wither shortly after. While the beauty of thermographic images and the ease of getting them could explain the success of this technique, the difficulty of getting accurate measurements using "thermal cameras" has caused certain disaffection toward it. The QIRT conference addresses the quantitative use of Infrared Thermography.

The 8th International Conference, QIRT2006 will emphasise the following topics:

- State-of-the-art and evolution in the field of infrared scanners and imaging systems allowing quantitative measurements, and related data acquisition and processing.
- Integration of thermographic systems and multi spectral analysis.
- Related problems like calibration and characterization of infrared cameras (mono and multidetector systems), emissivity determination, absorption in media, spurious radiations, three dimensionality of observed objects, certification and standardization.
- Thermal effects induced e.g. by electromagnetic fields, elastic waves or mechanical stress.
- Application of infrared thermography to radiometry, thermometry, and thermal parameters identification, in all fields: industrial processes, material sciences, structures and material non destructive evaluations, medicine and biomedical science, fluid mechanics, cultural heritage, environment

Scientific Committee

Chairman of QIRT: D. Balageas, ONERA, France

QIRT Steering Committee

* D.P. Almond, University of Bath, United Kingdom
* J.-M. Buchlin, Institut von Karman, Belgium
* G. Busse, University of Stuttgart, Germany
* G. M. Carlomagno, University of Napoli, Italy
* X. Maldague, Université Laval, Canada
* S. Svaic, University of Zagreb, Croatia
* V. P. Vavilov, Tomsk Polytechnic University, Russia
* B. Wiecek, Technical University of Lodz, Poland

International Scientific Committee

* D.P. Almond, University of Bath (U. K.)
* D. Balageas, ONERA (France)
* J.-C. Batsale (France)
* C. Bissieux (France)
* J.-M. Buchlin (Belgium)
* G. Busse (Germany)
* G. Cardone (Italy)
* G. M. Carlomagno (Italy)
* E. Cramer (U.S.A.)
* E. Grinzato (Italy)
* B. Jähne (Germany)
* P. Lybaert (Belgium)
* C. Maierhofer (Germany)
* X. Maldague (Canada)
* P. Millan (France)
* A. Nowakovski (Poland)
* A. Rozlosnik (Argentina)
* F. Scarano (Italy)
* S. Svaic (Croatia)
* B. Wiecek (Poland)
* V. Vavilov (Russia)

Local Organising Committee CNR-ITC (Italy)

Chairman QIRT' 2006: Ermanno Grinzato
Board: Paolo G. Bison, Sergio Marinetti, Antonella Barizza

Courses organised before the conference:

The Courses are scheduled on Tuesday June 27, 2006.
A- Basic Thermography, 9:30-13:30
B- Application to Fluids, 15:00-18:00
C- Application to Solids, 15:00-18:00
D- Application to Works of art, 15:00-18:00.

Basic Thermography (4 hours)
X. Maldague: Université Laval, Canada
V. Vavilov: Tomsk Polytechnic University, Russia

Introduction
1. Mechanisms of heat transfer
   conduction, convection, radiation
2. Basics of InfraRed
   Radiation laws (emissivity, absorptivity, reflectivity)
   Radiometry and temperature measurement
   Noise considerations
3. Solving thermal problems by mathematical modelling
   Transient 1D analytical modelling
   Numerical modelling for 1D, 2D, 3D geometry in solids materials
4. On thermal stimulation in the active approach
   Pulse thermography
   Step heating (long pulse)
   Lockin thermography
   Vibrothermography
5. Experimental techniques
   IR Detectors
   Experimental set-up
6. Deployment, data processing and applications
   Data processing
   Applications

Applications of Thermography to fluids (3 hours)
G.-M. Carlomagno: Universtà di Napoly, Italy

1. The use of the scanner to measure convective heat fluxes
   Steady state techniques
   Unsteady state, techniques
   Measuring heat transfer in wind tunuels
2. Heat flux sensors
   Thin-film sensor
   Thin-skin sensor
   Heated-thin-foil
3. Applications to specific problems
   Natural convection
   Rotating disk
   Transition over an airfoil
   High Mach number applications
   Jet in cross flow
   U turn channels

Thermography applied to works of art (3 hours)
E. Grinzato: CNR-ITC, Italy

1. Introduction of using thermal methods for cultural heritage
   Limitations and advantages of IR thermography
   Knowledge through the IR vision
2. True and apparent temperature
   Different methods and probes integration
   Dedicated techniques
3. Historical buildings monitoring
   The moisture map
   Finishing layers (frescoes) inspection
   Hidden structures
   The microclimate evaluation
4. Application to mobiles works of art
   Painted wood
   Ceramic, pottery
   Metallic artcraft
5. Cases study
   wall painting detachment
   the moisture monitoring
6. Standards
   guidelines

Applications of Thermography to solids (3 hours)
G. Busse and, University Stuttgart, Germany

Introduction

1. Constant temperature fields
   Thermography with no heating
   Thermography with constant external heating
   Thermography with constant internal heating
   - Vibrothermography
   - Activation of internal heat sources by selective spectral heating
   - Resistive heating
2. Cooling down thermography: step function response
   Principle
   Applications
3. Pulsed thermography
   Thermal transient response of solids
   Effect of a sub-surface defeca
   Dependence of transient response on defect depth and size
   Dependence of transient response on material and defect severity
   The role of numerical modelling
   Experimental system requirements and characteristics
4. Oscillating temperature fields: permanent non-equilibrium
   Thermal waves and photothermal detection
   Lockin-thermography
   - Phase sensitive thermography
   - Multiplex photothermal imaging
5. Lockin thermography with optical excitation (OLT)
   Coatings (paint, veneered wood, ceramics on metal...)
   Laminates
6. Lockin thermography with acoustic excitation (ALT)
   Cracks
   Delamination
   Impact
   Corrosion
7. Eddy-current Lockin thermography
   Crack tips in metal
   Impact damage in CFRP

Disbond in C-SiC-Ceramics

Table of Contents

Image Processing and Data reduction

Fluid Mechanics

Thermographic Systems and Components

Process Monitoring and Industrial Applications

Radiometry and Metrology

NDT and NDE

Civil Engineering and Works of Art

Bio-Medical

Environmental Applications

Thermophysical Properties

Modeling

Thermography and microsystems-Some ways to intensify quantitative experimentation in heat transfer

by J.C. Batsale

TREFLE- ENSAM ; Esplanade des Arts et Métiers-33405 Talence cedex-France

The microfabrication technique originally devoted to electronics have reach spectacular advances in more general domains such as chemical microreactors. The spatial temperature distribution of micro-electro-mechanical systems(MEMS) is among the most important information.
At small scales, the processing of the great amount of data given by temperature IR images is then offering challenging opportunities to quickly and simultaneously estimate a great amount of parameters (thermophysical properties, source terms distribution…).
Some examples (see fig 1 nad 2) will show that a convenient way is to consider a slow in-plane 2D transfer in a conductive plate at the surface of the system and to apply linear least square estimation principles.

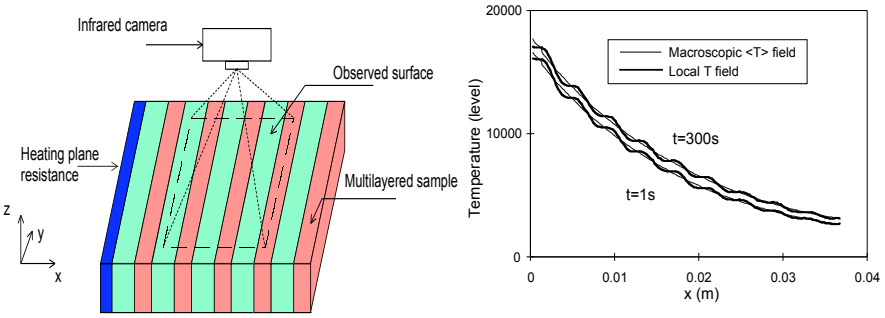

Fig 1: Estimation of local conductivities of in plane heterogeneous samples

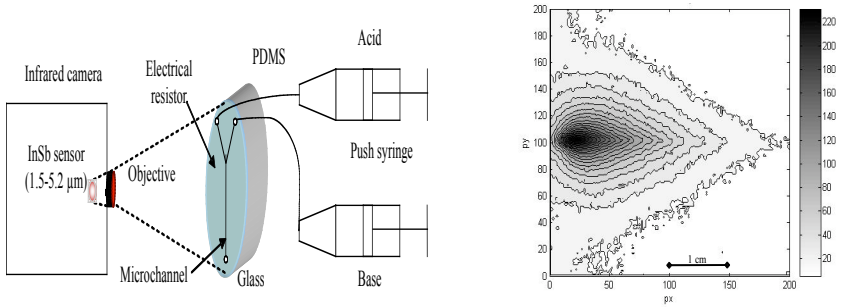

Fig. 2. *Microfluidic chip and temperature field of the front plate in the case of acid-base chemical reaction.*

Visible and Infrared Imagery for Surveillance Applications: Software and Hardware Considerations

by A. El-Maadi*, V. Grégoire*, L. St-Laurent*,**, H. Torresan*,
B. Turgeon*, D. Prévost**, P. Hébert*, D. Laurendeau*,
B. Ricard***, X. Maldague*

*ECE Dept. Université Laval, Québec, Canada
**National Optics Institute, Québec, Canada
***Research and Development for Defence Canada, Québec, Canada

Abstract

In this text we summarize recent works done in the use of visible and infrared imagery for surveillance applications. Moreover, we also present latest developments that have occurred in three partner institutions of the Québec, Canada area in this field. Our focus is on both hardware and software. Hardware here concerns channel registration and innovative optical systems while software is related to high level information extraction. Extensive literature review is provided.

AN OVERVIEW ON HYPERSONIC FLOW RESEARCH WITH INFRARED THERMOGRAPHY

by Gennaro Cardone

University of Naples"Federico II", DETEC Department, p.le Tecchio, 80127 Naples (Italy)

ABSTRACT

The most critical area of the reentry vehicle design is evaluation and the measurement, inside any ground facility, of the aerothermodynamic heating (and catalicity) of the material under test. The study of the aerothermodynamic properties in an hypersonic plasma flow represents one of the most important application fields of the optical diagnostic methodologies. The principal feature of the physical process is the non-equilibrium aspect of the plasma constituents. This peculiarity requires a specified development (theoretical and experimental) of the diagnostic techniques in order to take into account the non-equilibrium effects and the different catalicity of the constituent materials. In this paper, we present the results of the application of the thermography to two hypersonic high enthalpy plasma wind tunnel facility: SCIROCCO, located at CIRA and HEAT, located at CENTROSPAZIO PISA. The first one is devoted to test TPS materials of reentry space vehicles while the second one is devoted to aerodynamic tests of reentry space vehicles .

A first step to evaluate the applicability of IR thermography to an hypersonic arcjet facility, is the analysis and the evaluation of the radiation emitted and absorbed by the plasma flow impacting the test sample which represent the medium between the IR Thermograph system (detector and window) and the test sample surface. By using ARCSIZ by Aerotherm Co. and H2NS by CIRA codes, we carried out the estimation of all chemical species and relative concentration for the entire set of flow conditions defining the operative map of the two plasma wind tunnel facility. Then, we assume worthy of consideration any chemical species which results to be present with a significant value of concentration in terms of molar fractions. Our analysis about the behavior of such a plasma gas regarding emission and absorption of the radiation in the infrared region is performed by considering a gas mixture like the sum of the chemical species reported in Table 1 representing it the worst case. Our intention is to estimate the emission and absorption in IR spectrum in order to select a wavelength window where is possible to perform correctly the IR thermography measurements. We focus our analysis on the *short-wave* window (2-6 mm) and *long-wave* window (8-14 mm), where commercial IR systems are available. To perform the estimation of the spectral line intensity S of the chemical species reported in table 1, we used the HITRAN (acronym for high-resolution transmission molecular absorption) database. Then, from these line intensity distributions and taking into account the thermodynamical conditions (temperature and partial pressure) and the maximum plasma thickness, we compute the transmittance by using the E-TRANS code by Ontar Co. In fig 1 the spectral line intensity of considered species are reported at 1000° K for the IR *short-wave* and IR *long-wave* windows, respectively.

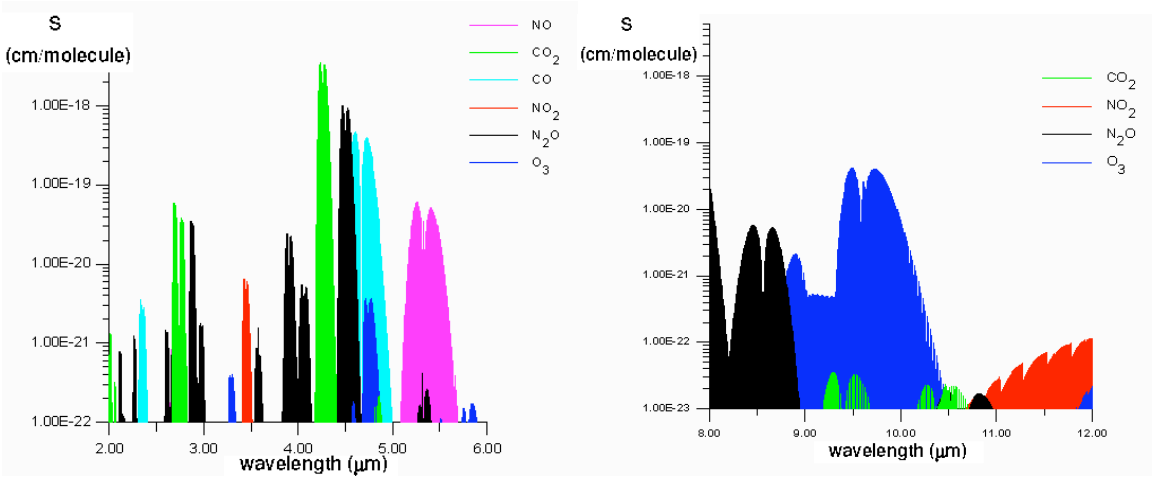

Figure 1: Spectral line intensity S in the short-wave window

In fig. 2 the transmittance in the whole infrared region 1-12 μm is shown for two different temperatures of 300° K and 1000° K, respectively.

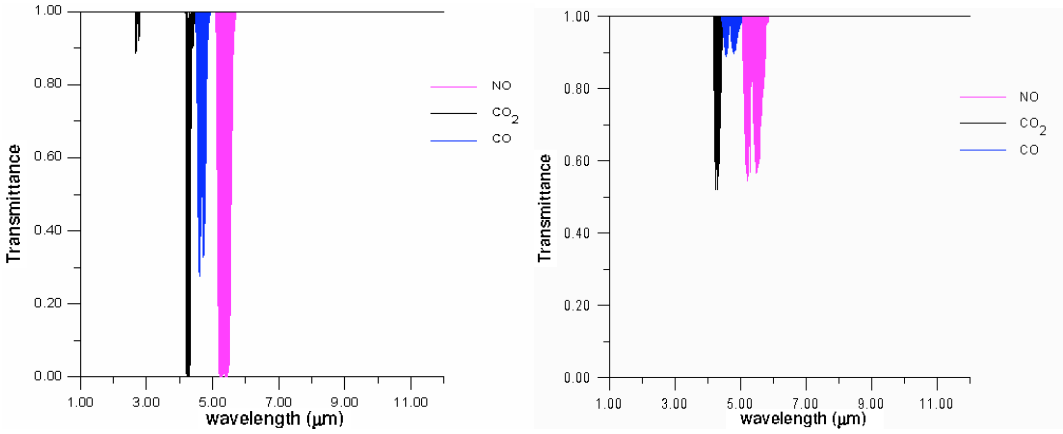

Figure 2: Transmittance at 300° K and 1000° K

Following the results of this analysis a proper detector wavelength window and optics/filter have been determined in order to minimize the noise and any undesired source of disturbance.

In a second phase, we examine the classical thin film technique and describe its inadequacy in high enthalpy hypersonic heat flux measurement and propose a new physical-mathematical model of heat flux sensor based on experimental data measured by means of IRSR and on numerical resolution of Fourier's equation in the solid model, the IR-HFS.

After the numerical validation of proposed IR-HFS we apply the same one in two test campaigns performed in the arc jet plasma wind tunnels: SCIROCCO at CIRA (NASDA HYFLEX Experiment, figs 3,4) and HEAT at CENTROSPAZIO (Shock-Wave/Boundary-Layer Interaction, figs. 5,6)

Figure 3. NASDA Hyflex test sample under test in flow condition. Total enthalpy:* 11.9 *MJ/Kg* ; *Stagnation pressure: 4.5bar

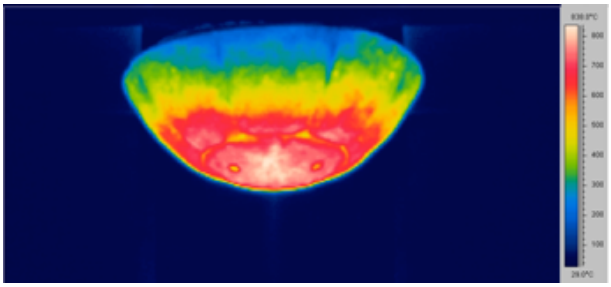

Figure 4. IR images of the NASDA Hyflex test sample in flow condition after 15s from tunnel starting Total enthalpy:* 11.9 *MJ/Kg* ; *Stagnation pressure: 4.5bar

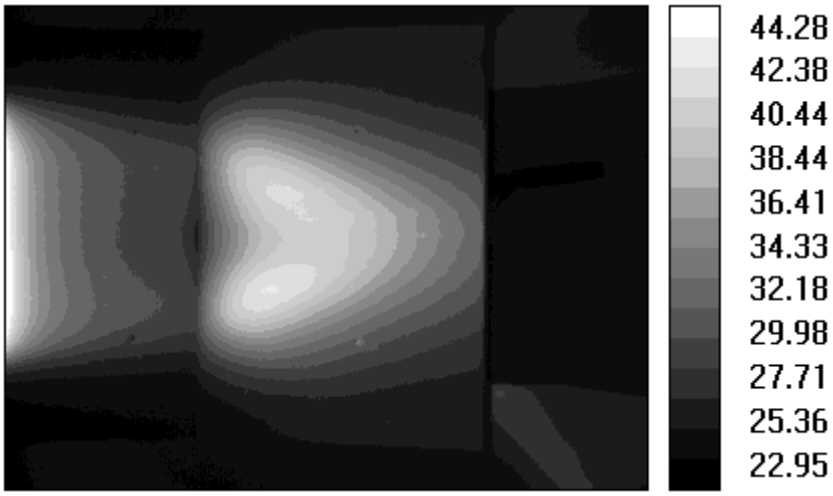

Figure 4. Temperature map(in °C) recorded on model surface after 80ms from tunnel starting. Total enthalpy:2.3 MJ/Kg; Stagnation pressure:4.6 bar

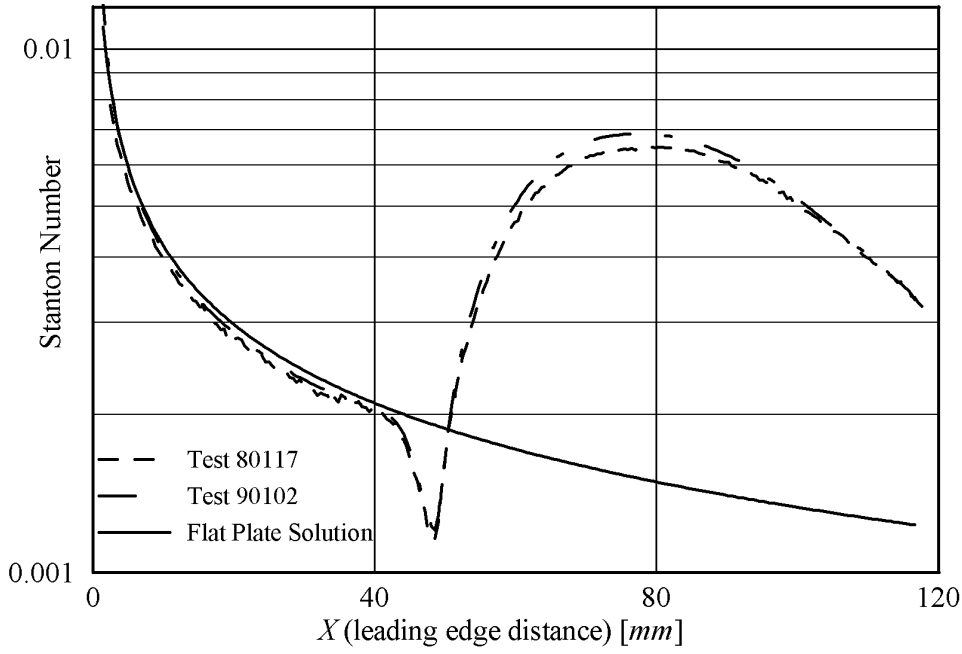

Figure 5. Stanton number profile on symmetry axis. Total enthalpy:1.8MJ/Kg; Stagnation pressure: 6bar

Thermomechanical study of TiNi shape memory alloy during low-cycling test

Elzbieta Pieczyska[1], Stefan Gadaj[1] Wojciech Nowacki[1] and Hisaaki Tobushi[2]

[1] Institute of Fundamental Technological Research, Polish Academy of Sciences, Swietokrzyska 21, 00-049 Warsaw, Poland; fax 48 22 826 9815, tel 48 22 826 1281
[2] Department of Mechanical Engineering, AICHI Institute of Technology, Toyota 470-0392, Japan; fax 81 0565 48 8555, tel 81 0565 48 8121, epiecz@aitech.ac.jp

Keywords: shape memory alloy, superelastic deformation, temperature change

(Oral presentation)

In applications to sensors, actuators, robots or solid state engines, a shape memory element (SMA) is used as a working element that performs cyclic motions. In order to evaluate the reliability of the SMA elements, cycling deformation properties of the material are of key value. In this paper low-cycling properties of TiNi SMA were studied in terms of mechanical and thermal effects. To this end, ten subsequent cycles of loading - unloading with the constant strain rate of 10^{-2} s^{-1} were repeated in room conditions (above the SMA A_f temperature) for the maximum strain value 9 %.

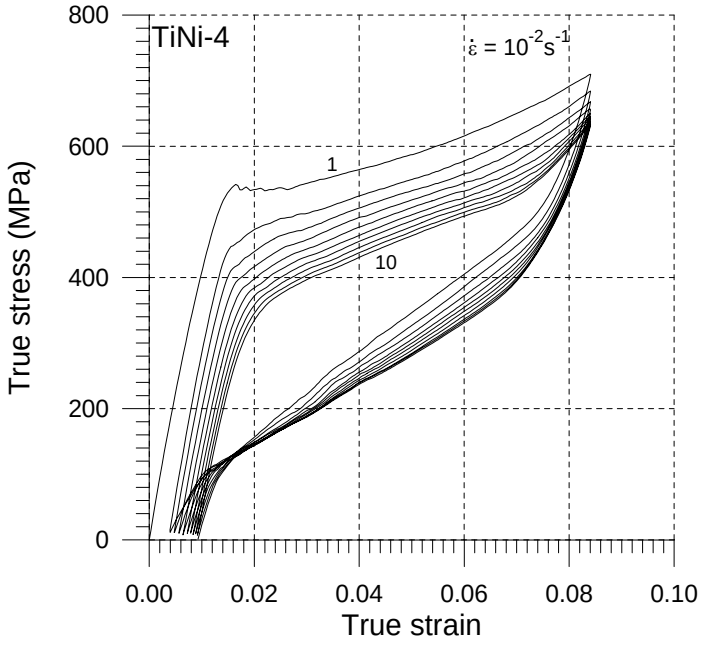

Figure 1. Stress-strain curves of TiNi SMA subjected to low-cycling test

The stress-strain curves obtained for the superelastic loading – unloading TiNi SMAs are presented in Fig. 1. One can notice that the run of the first cycle is similar to the stress-strain curve presented in [1] for the same strain rate. The yielding due to the martensite transformation occurs at a stress of 470 MPa for strain above 1.5 %. For the subsequent cycles, the martensite stress decreases with the number of the cycle,

however this amount of the decrease also decreases. The residual strain increases with the number of cycles, since both the residual martensite and microstructure defects are higher for the increasing number of cycles. The phenomena are related to temperature.

The temperature vs. true stress curves of the SMA subjected to this cycling test are presented in Fig. 2. For each cycle, an increase in temperature during the loading and the martensite transformation was observed followed by a significant temperature decrease accompanying the unloading process and the reverse transformation.

The temperature increment registered during the martensitic transformation for the first cycle was equal to 28 K, while for the subsequent cycles of loading the temperature increments were significantly lower. The temperature decreases during the reverse transformation. After the reverse transformation was completed, the temperature drops below the initial temperature. For the subsequent cycles, the drops in temperature are even higher, however the saturation effects are also observed.

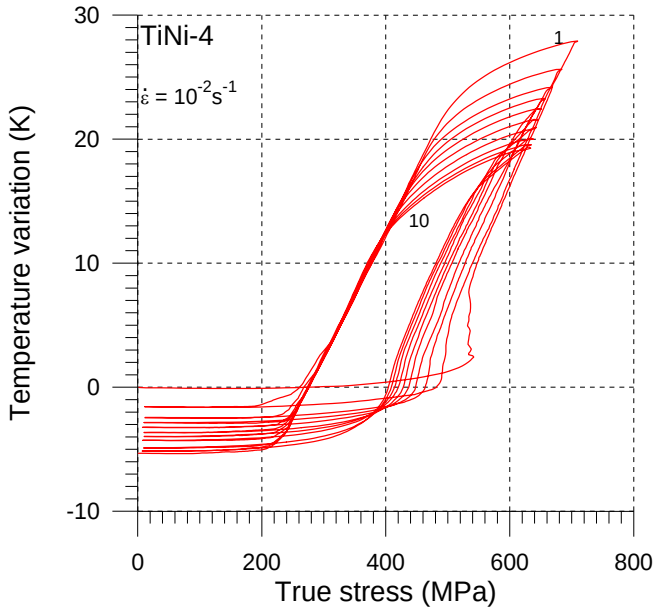

Figure 2. Stress and temperature curves of TiNi SMA subjected to subsequent cycling test with strain rate 10^{-2} s^{-1} at room temperature

Summarizing, the run of the mechanical and the temperature curves obtained during the TiNi SMA low-cling tests indicates that the temperature increments are mainly caused by the martensitic and the reverse transformations and in order to avoid too high the stress change and related to this too strong the temperature impact, the mechanical training before the material application is necessary.

References: 1) E. Pieczyska, S. Gadaj, W. Nowacki, Tobushi H., QIRT J. **1.1** (2004)
Acknowledgments: This research has been carried out under Grant No. 4 T08A 060 24, the JSPS Grants No: 13650104, Post-doc ID P04774, and Joint Research 6612.

Assessment of fatigue damage in a mild steel using Lockin-Thermography

Justus Medgenberg*, Thomas Ummenhofer*

Proposed for oral presentation

Keywords: Fatigue damage, small fatigue cracks, thermoelasticity, plasticity, finite element modelling

* Institut fuer Bauwerkserhaltung und Tragwerk, Technische Universitaet Carolo-Wilhelmina, Braunschweig, Pockelsstrasse 3, 38106 Braunschweig/Germany
Phone: +49 (0)531/3912500
Fax: +49 (0)531/3912502
Email: J.Medgenberg@tu-bs.de
T.Ummenhofer@tu-bs.de

Summary

During the last decades a large number of analytical tools and methods have been developed for the life time prediction of dynamically loaded structures. Most of these methods rely on statistical data concerning the fatigue behaviour of the specific material and/or the given construction detail. For a given loading history “the damage” of a structure is then calculated using an accumulation rule such as Palmgren-Miner. As long as no cracks can be detected in a local hot spot, the accumulated damage of a structure due to fatigue stays a quite abstract phenomenon. Nevertheless the material undergoes measurable microscopic changes as e.g. micromagnetic behaviour, sound emission, damping etc. due to the repeated loading. A couple of methods have been proposed for the quantitative determination of the actual damage state within fatigue loaded structures. The measurement of these parameters and especially the interpretation of the data with respect to the accumulated damage are sometimes difficult.

The High-Cycle Fatigue (HCF) behaviour of ductile mild steels as e.g. S355 is governed by the early microscopic onset of plastic deformation in form of persistent slip bands within several unfavourable orientated grains. The spatial extension of this early plastic deformation is highly dependent on the applied loading, stress concentration at macroscopic notches, surface treatment etc. and can be regarded as an early indicator of fatigue damage.

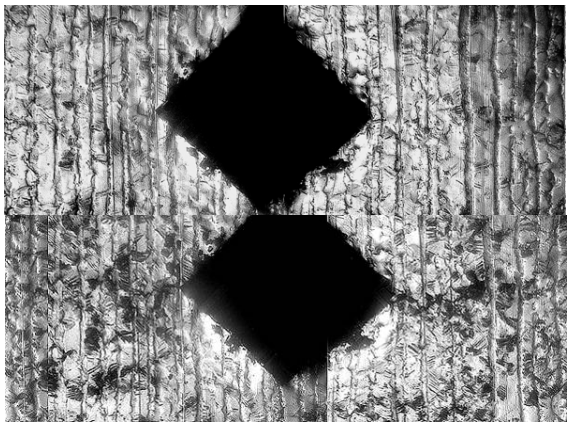

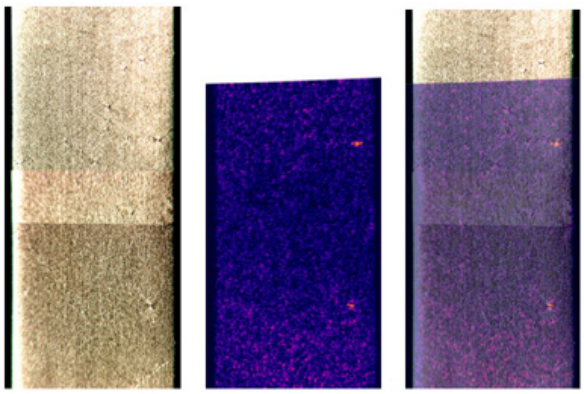

Figure 1: Persistent slip band development and fatigue crack initiation around a microhardness imprint in S355.

Figure 2: Thermographic detection of small fatigue cracks by lockin-thermography under mechanical loading.

Starting from a specific crack starter as e.g. inclusions, surface defects etc. a fatigue crack will initiate and grow until the component completely fails. Lockin-Thermography with different excitation sources offers unique opportunities for the characterisation of all states of fatigue damage: First, the local hot-spots of a complex structure under a given mechanical loading can be detected using the thermoelastic effect. Second, the onset of plastic deformation in the critical spot is coupled with a (local) temperature rise that can be distinguished from the elastic behaviour. Third, microcracks and cracks in the range of tens of microns to several millimetres length can be observed by thermographic means using ultrasound excitation or eddy current excitation. Fourth, the crack growth can be observed due to the strong plastic deformation in front of the crack tip. One of the major advantages over other methods is the close relation to the specific damage mechanisms: Fatigue damage in ductile materials is always governed by the local damping of mechanical energy, plastic deformation and therefore by a raised heat generation rate. Lockin-thermography is a very promising tool to detect these underlying processes experimentally.

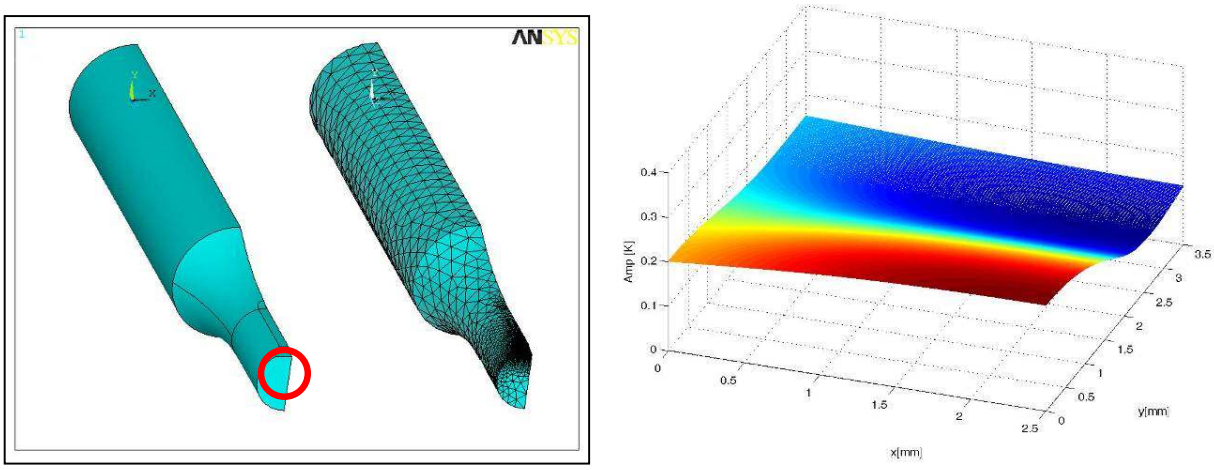

Figure 3: Thermoelastic FE-Model of a specimen (Quarter-Model of the entire specimen, using symmetry aspects). Amplitude of the temperature field in the notch region due to a mechanical sinusoidal loading of 12,3 kN at 20 Hz.

The proposed presentation shows thermographic results considering the detectablity of small fatigue cracks at artificial crack starters in the mild steel S355, comparison to microscopic pictures, plasticity effects and results of numerical simulations of the thermoelastic effect under non-adiabatic conditions. An outline for the potential of thermography within fatigue damage characterisation will also be given.

The authors of this abstract are working in the field of thermographic fatigue damage assessment of civil engineering steel structures within the framework of the SFB 477 at the Technische Universitaet Carolo-Wilhelmina Braunschweig. For the purpose of the project an experimental setup including a multipurpose servohydraulic testing machine, a long range light-microscope, a high resolution Infrared camera and a 3-axis positioning system has been build up. The setup allows for a thermographic and visual microscopic insitu-observation of fatigue damage phenomena.
Research activities include numerically and experimentally thermoelastic and thermoplastic considerations, observation of crack initiation and propagation, detectability of small fatigue with different excitation sources and framework consideration for the use of thermography within fatigue lifetime assessment.

Evaluation of storage energy of the constructional steel during plastic deformation

by A.M. Ivanov[1], E.S. Lukin[1] and B.G. Vainer[2]

[1]Institute of Physical and Technical Problems of the North, Yakutsk, Russia
[2]Institute of Semiconductor Physics, Novosibirsk, Russia

Keywords: storage energy, plastic deformation, evolved heat
Poster presentation

1. Introduction

Generally, plastic deformation of the constructional steel is associated with the generation and motion of dislocations. Change of the density and configuration of the defects always leads to energy dissipation, which causes the specimen temperature increase. Phenomenon of temperature increase in the process of plastic deformation of solids is the thermoplastic effect.

It is known from the first law of thermodynamics that the part of plastic deformation work A_P is absorbed by a material while another part is transformed into released heat Q. Thus storage energy E_S is determined as a difference between the plastic deformation work, and the heat released into surroundings [1]

$$dE_S = dA_P - dQ \quad . \tag{1}$$

Plastic deformation work is usually determined from the machine diagram. The heat Q can be evaluated with the use of calorimeter [2,3]. However, the calorimetric method is limited by its low speed of response [3].

Also, investigations of deformation in metals and steels are carried out with the use of infrared imaging cameras [4, 5]. In this case, the change in sample temperature during deformation is measured. However, the correct determination of the released heat during deformation is the problem to be studied. Here, the heat Q can be determined by simulation of the process of sample heating during deformation by applying electrical power $P(t)$ in such a way that the temperature increase with time t during the simulation is identical with that measured during tensile testing [5].

2. The materials and instruments tested

The goal of the present work is to evaluate the energy storage in the process of plastic deformation of the constructional steel. The standard sheet specimens from the steel 18G2S were subjected to static tensile test at various rates of deformation: of 9×10^{-4} s^{-1}, 2×10^{-3} s^{-1}, 4×10^{-3} s^{-1} and 9×10^{-3} s^{-1}. Temperature measurements during the specimen deformation we conducted using the infrared thermography system "TKVr-IFP/SVIT". The temperature sensitivity of that system (NETD at 30 ° C) was 0,028 ° C.

3. Evaluation of the evolved heat.

In this paper, the heat evolved in the process of plastic deformation is determined by solving the heat conduction equation with the use of thermovision measurement data.

The evolved heat Q during deformation is evaluated from the solution of one-dimensional heat conduction equation with a heat source $q(t)$. Within this problem, the specimen was simulated as an axes symmetrical finite-size bar with known boundary conditions:

$$\frac{\partial T(x,t)}{\partial t} = a\frac{\partial^2 T(x,t)}{\partial x^2} - \nu(T(x,t)-T_c) + \frac{q(t)}{c\rho} \quad , \tag{2}$$
$$T(x,0)=T_c, \qquad T(0,t)=T_c, \qquad T(l,t)=T_c \quad .$$

Here, a is the temperature conductivity and ν - the thermal diffusivity. Solutions of the heat conduct equation for the heat source is:

$$q\ (t) = \frac{\overline{T}(x,t)}{a_1 - a_2\cdot\exp[-b_1\cdot t] - a_3\cdot\exp[-b_2\cdot t]} \quad . \tag{3}$$

where a_1, a_2, a_3, b_1 and b_2 are the constants dependent on the length of bar, thermal conductivity, density, and heat capacity. The temperature distribution $\overline{T}(x,t)$ is received empirically with the use of the infrared system. Dependence of the heat source power on time is presented in Fig. 1. Then, the evolved heat q can be obtained from the integral of solutions of heat conduct equation (3):

$$q = \int_0^t q(t)\cdot dt \quad . \tag{4}$$

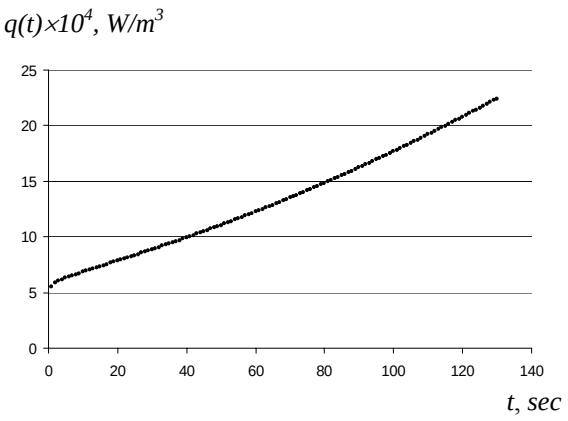

Fig. 1. Dependence of the heat source power of steel 18G2S on time.

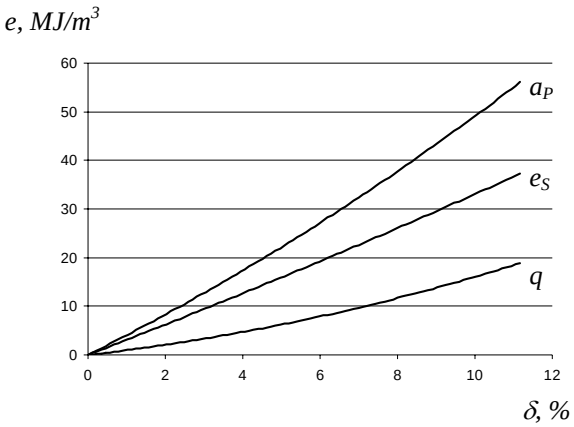

Fig. 2. Dependence of the plastic work a_P, storage energy e_S and evolved heat q in the tensile on strain of the steel 18G2S.

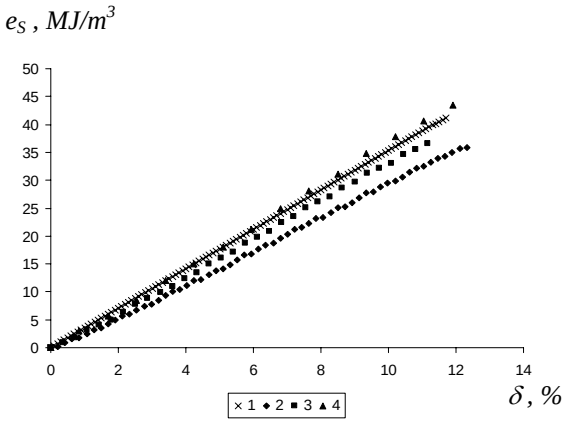

Fig. 3. Dependence of the storage energy received by the different deformation rate on strain, where 1 – by $\dot{\varepsilon} = 8{,}98\times10^{-4}$ s^{-1}; 2 – $\dot{\varepsilon} = 1{,}78\times10^{-3}$ s^{-1}; 3 – $\dot{\varepsilon} = 3{,}57\times10^{-3}$ s^{-1}; 4 – $\dot{\varepsilon} = 8{,}93\times10^{-3}$ s^{-1}.

4. Results

Dependence of the plastic work a_P, storage energy e_S and evolved heat q in the tensile tests on strain of the steel 18G2S are presented in Fig. 2. Quantity of the evolved heat amounts up to 30 percents of the plastic work, and the rest of this value is stored by material. Dependence of the storage energy at different deformation rate on strain is shown in Fig. 3. Difference between storage energies amounts to 12 percents and equals to $e_S \approx 37{,}5$ MJ/m^3.

Thus the suggested calculation-experiential technique with the use of infrared imaging cameras makes it possible to determine the energy stored by the material at static tensile test of specimens.

References

[1] Taylor G.I., Quinney H. The latent energy remaining in a metal after cold working. //Proc. Roy. Soc., 1934, vol. CXLIII.–A., p. 307-326.

[2] Maksimkin O.P., Gusev M.N. Some peculiarities of energy dissipate during plastic deformation of iron and niobium. // Pis'ma v Zhurnal Tekhnicheskoi Fiziki, 2001. – V. 27. – No.24. – p. 85-89.

[3] Astafiev I.V., Maksimkin O.P. Restoration of calorimetric thermogramms in the experiments on heat emission and energy storing during deformation. // Industrial laboratory. – 1994. – No.1. – p. 44-46.

[4] Oliferuk W. Investigation of metal deformation using thermography. // Quantitative infrared thermography 4, QIRT'98, Proceedings of Eurotherm Seminar No. 60. – Lodz, Poland, 2000. – P. 134-139.

[5] Pieczyska E.A., Gadaj S.P., Nowacki W.K. Rate of energy storage during consecutive deformation of steel. // Quantitative infrared thermography 5, QIRT'2000, Proceedings of Eurotherm Seminar No. 64. – Reims, France, 2000. – P. 260-264.

SELF-HEATING EFFECTS ON STRAIN MEASUREMENTS PERFORMED BY EMBEDDED FIBRE OPTIC SENSORS UNDER CYCLIC LOADING

Leonardo D'Acquisto[a] and Roberto Montanini[b,*]

[a] *Dipartimento di Meccanica , Università di Palermo, viale delle Scienze, 90128, Palermo, ITALY,* dacquisto@dima.unipa.it,,
[b]*DCIIM, Università di Messina, Salita Sperone, 131, 98166, Sant'Agata (ME), ITALY,* rmontanini@ingegneria.unime.it ,

Keywords: infrared thermography, fibre Bragg gratings, composite materials

State of the art

Fibre Bragg Gratings are nowadays more and more used for strain measurements in several applications for structural health monitoring. The mechanical strain variation, which is transmitted from the structure under investigation to the fiber sensor, induces a Bragg wavelength shift which represents the measured quantity. This Bragg wavelength shift depends not only on the strain level applied to the FBG sensor, but also on the temperature because of the temperature dependent change in the refraction index (thermo optic coefficient ξ). The total Bragg wavelength shift is therefore the sum of at least two terms, namely the $\Delta\lambda_{B,S}$ (strain induced wavelength shift) and $\Delta\lambda_{B,T}$ (temperature induced wavelength shift).

$$\Delta\lambda_{BS} = \lambda_B \cdot (1 - p^{eff}) \cdot \varepsilon$$
$$\Delta\lambda_{BT} = \lambda_B \cdot (1 + \xi) \cdot \Delta T$$

where λ_B is Bragg wavelength of the FBG, p^{eff} is photo-elastic coefficient of the optical fiber and ΔT is the temperature change experienced by the FBG.

Due to their very low intrusivity, FBG sensors can be embedded into composite materials, providing real-time monitoring of the structural component under working conditions. Furthermore, embedded FBG sensors can be used to predict fatigue failures of structures subjected to cyclic loads.

Commercial interrogation systems provide a static thermal compensation by the use of a reference free-strain Bragg grating which experiences only the $\Delta\lambda_{B,T}$ induced by ambient temperature at the site of the interrogation system. Structural components instrumented with embedded FBG sensors can often experience temperature levels different from the temperature level to which the *reference* FBG is exposed. It can happen if they are exposed to thermal radiation from the surrounding environment or if they undergo a self heating due to cyclic loading. This latter condition has to be carefully taken into account especially for composite materials that in certain conditions (depending on the applied load and on the cycling frequency) can experience temperature variations up to some tens of degree.

* rmontanini@ingegneria.unime.it ; phone +39(0)903977248; fax +39(0)903977464 (Corresponding author)

Aim of the work

The strain measurement error of embedded FBG sensors due to self heating will be investigated on specimens subjected to uniaxial tensile fatigue loads. Due to the dual sensitivity of Bragg grating sensors, this measurement error can be quite large, leading to unreliable evaluation of the actual stress level within the component. This aspect, which in Author's knowledge has never been deeply investigated in literature, is difficult to be managed by traditional thermal compensation techniques, because it strongly depends on the local temperature distribution within the specimen.

Proposed approach

To evaluate the strain measurement error due to self-heating of composite laminates in which a Bragg grating sensor has been embedded, experimental tests will be performed on differently shaped specimens by measuring the surface temperature distribution induced by cyclic loads with an infrared camera and by comparing it with the internal temperature distribution measured by means of either annealed distributed optical fibres thermometers or thermocouples (Fig.1). Cycling loads will be applied by an electro hydraulic testing machine. Experimental results will then be compared with a numerical model in order to predict the observed thermal flow within the specimen under specific testing conditions.

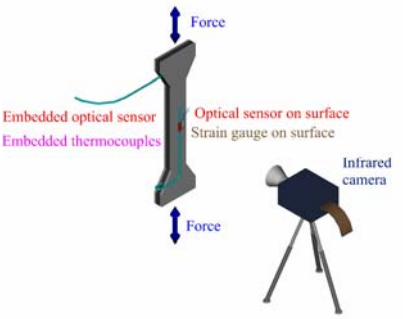

Figure 1 – Experimental setup

References

[1] Y.J. Rao, "Recent progress in applications of in-fibre Bragg grating sensor" *Opt. Laser Engineering* , Vol. 31, 1999, pp.297-324

[2] G. Fanti, "Thermo-mechanical characterization of fiber Bragg grating sensors", *Proc. of V° Congresso Nazionale di Misure Meccaniche e Termiche*, Padua, Italy 17-19/09/2002

[3] L. D'Acquisto, R. Montanini, "On the behaviour of in-fibre Bragg grating sensors for strain measurement on plane and curved surfaces" *XVII IMEKO World Congress Metrology in the 3rd Millennium June 22-27, 2003, Dubrovnik, Croatia*

[4] B. Marchetti, R. Montanini, C. Rondini, P. Maggiorana, G.L. Rossi, "Definition of FBG sensor photoelastic coefficient by laser doppler vibrometery", *Fifth International Conference on Vibration Measurements by Laser Techniques: Advances and Applications*, Proceedings of. SPIE Vol. 4827 (2002).

[5] L. D'Acquisto, R. Montanini, "Monitoraggio del processo di cura di compositi laminati mediante sensori in fibra ottica", Atti VI Congresso Nazionale di Misure Meccaniche e Termiche, Desenzano del Garda (BS), Italia, 12-14 settembre 2005.

Thermography as a routine diagnostic for mechanical testing of composites

by P. Levesque[1], P. Brunet[2], C. Cluzel[2], A. Déom[1], L. Blanchard[3] and D.L. Balageas[1]

1 ONERA, BP 72, 92320 Châtillon cedex, France - {levesque, deom, balageas}@onera.fr
2 LMT, ENS, 61 ave. Président Wilson, 94235 Cachan cedex, France - cluzel@lmt.ens-cachan.fr
3 ALCATEL ALENIA SPACE, 100 Bd du Midi, B.P. 99, 06156 Cannes La Bocca, France - laurent.blanchard@alcatelaleniaspace.com

The adequation of thermography to quantitative non-destructive evaluation (NDE) is an evidence – especially for composites -. This NDE ability is illustrated by an abundant literature starting in the 60's and still very living. In his invited lecture given at the first QIRT Conference, Vavilov presented a well documented short history of thermal NDE (Vavilov, 1992) and more recently Maldague gave to the community a very exhaustive book on the subject (Maldague, 2003).

In these conditions we can wonder why QIRT techniques are not used for improving the quality of mechanical tests. This is certainly due to the fact that until now most of the members of the solid mechanics community have neglected the thermal phenomena accompanying mechanical phenomena. Although, some research groups have recently begun to use thermography to study thermomechanical phenomena (Chrysochoos and Belmahjoub, 1992; Chrysochoos, 2000), and this is one of the most promising branches of today thermography, we do not see in the literature serious attempt to integrate this technique in the routine toolbox of experimental mechanics.

Based on some preliminary tests, the aim of this paper is to demonstrate the usefulness of infrared thermography as a routine diagnostic in mechanical tests of composite materials.

Test configuration

This experimental study concerns the characterization of the mechanical resistance and of the ruin mode (skin delamination) of sandwich composite panels used in space structures (M18/M55J carbon-epoxy skins and aluminum honeycomb core). The dimensions of the central zone of the coupons is 120x54 mm^2. There are two 17 mm-dia. drilled holes. Two types of coupons were tested. The A-type coupons in which the two skins are symmetric, quasi isotropic, and constituted of three plies (30°, -30°, 90°), and the honeycomb made of 20 μm aluminum sheet with a cell period of 4 mm and a thickness of 24,4 mm. The B-type coupons have two symmetric skins, constituted of eight plies ($0°_3$, $45°_2$, $-45°_2$, 90°), with a 22 mm-thick identical honeycomb.

The coupons are loaded in extension on a test machine capable of 50 kN. They can be heated or cooled thanks to an enclosure controlled in temperature.

The temperature field of the central zone of the coupon under test is imaged by a JADE LWIR CEDIP camera (320x240 pixels) for ambient tests and a JADE MWIR CEDIP camera for some test at -10 °C and + 70°C. Here only ambient temperature tests will be reported.

For active thermography a pulsed source (flash lamps) has been used.

Thermographic techniques used

Three strategies are possible for applying thermography during mechanical tests:

- the simplest way consists to just record the temperature-field time evolution during the test (passive thermography). The technique is essentially sensitive to the thermoelastic effect linked to compression and extension and to the dissipative phenomena. This technique is interesting for observing the progression of damage in the last phase of a mechanical test leading to rupture.

- if its possible to superimpose a modulation of the force to the static force delivered by the test machine, lock-in thermography is able to record the strain map on the coupon and the dissipative phenomena. This active technique is known since decades when applied to the elastic domain (Mountain and Webber, 1978; Brémont, 1995) and begins to be applied to the damage and fatigue observation (Krapez, 2000; Arnould et al., 2005).

- using pulsed or modulated photothermal thermography, in which a photonic source is used to stimulate the coupon. From a time or frequency analysis, damage can be detected and characterized

(occurrence depth, lateral extent, equivalent thermal resistance). Photothermal thermography is now a classical NDE technique, universally used. Here we will perform pulsed stimulation with flash lamps.

In the present study, passive and pulsed photothermal thermographies have been used. Mixing the two techniques is possible by submitting the coupon to a force-time history made of a succession of plateaus separated by ramps. During a force plateau, a pulsed stimulated experiment takes place and passive thermography is used to continuously monitor the coupon during the ramp. Each plateau, with a duration of some tens of seconds, permits to characterize the damaged state of the coupon for a given tension level, and the ramp observation allows us to detect the exact location where the rupture starts.

Results and conclusion

Examples of typical thermograms recorded during a test are given in figure 1 (left) corresponding to five locations of the coupon. These locations are seen on the right, on the IR image of the coupon recorded during the cooling following the pulse illumination. The graph shows the thermograms after the last pulse (last plateau) and during the catastrophic rupture.

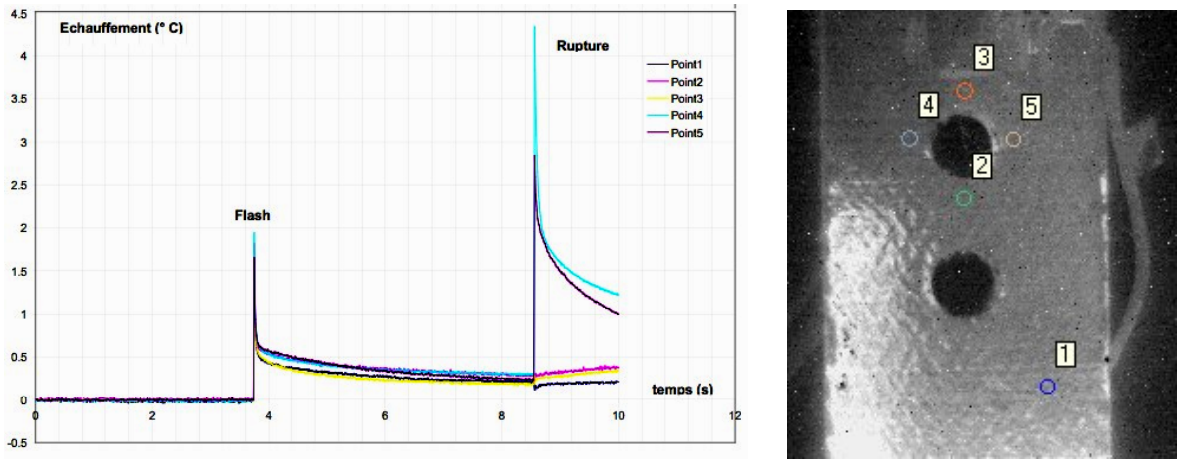

***Figure 1**. Examples of typical thermograms recorded during a test (A-type coupon). Left: Crude temperature-time evolution at some locations during the last plateau (with a pulse illumination) and during the catastrophic rupture. Right: infrared image taken after the pulse and showing the locations chosen for the analysis.*

Time analysis of the thermograms (normalization, log-log plot…), using the procedure and relationships proposed in (Balageas et al., 1987) for defect identification by pulsed stimulated thermography permits to assess that during the last plateau a delamination was already present at location 5 and that the rupture origin is at locations 4 and 5.

The paper will analyze several tests performed with the two types of coupons and will compare the thermographic results to strain-gage measurements, to X-ray examination and to theory. It will be concluded that, although the experimental conditions were not ideal (very thin skins, catastrophic type rupture, relatively low frame rate used – 100 Hz-), it was possible to demonstrate how thermography can be very useful for achieving a better understanding of the material behavior.

References

Arnould O., Hild F., Bremond P., “Thermal evaluation of the mean fatigue limit of a complex structure”, *Thermosense XXVII*, 2005, SPIE Proc. vol. 5782, paper 33.

Balageas D.L., Déom A.A., Boscher D.M., "Characterization and non destructive testing of Carbon-epoxy composites by a pulsed photothermal method", Materials Evaluation, vol. 45, n°4, 1987, pp. 461-465.

Brémond P., “La thermography infrarouge pour voir les contraintes”, *Mesures*, vol. 673, mars 1975, pp. 53-56.

Chrysochoos A., Belmahjoub F., “Thermographic analysis of thermomechanical couplings”, *Archives of Mechanics*, vol. 44, N°1 (1992), pp. 55-68.

Chrysochoos A., “Infrared imaging and thermomechanical behaviour of solid materials”, Quantitative InfraRed Thermography 5, Akademickie Centrum Graficzno-Marketingowe Lodart S.A., Lodz (Poland), 2000, pp. 22-27.

Krapez J.-C., Pacou D., Gardette G., “Lock-in thermography and fatigue limit of metals”, Quantitative InfraRed Thermography 5 (QIRT’2000), Akademickie Centrum Graficzno-Marketingowe Lodart S.A., Lodz (Poland), pp. 277-281.

Maldague, X., “Theory and practice of infrared technology for non destructive testing”, Wiley series in microwave and optical engineering, 2001.

Mountain D.S.S, Webber J.M.B., “Stress Pattern Analysis by Thermal Emission (SPATE)”, *SPIE Proc. vol. 167*, 1978, pp. 189-196.

Vavilov V., “Thermal non destructive testing: short history and state-of-the-art”, *QIRT 92*, ed.D. Balageas, G. Busse, J.M. Carlomagno, EETI, Paris 1992, pp. 179-189.

ENERGY DISSIPATION IN MEDIUM AND HIGH CYCLE FATIGUE OF METALLIC AND COMPOSITE MATERIALS

G. Meneghetti*, M. Quaresimin°
*Department of Mechanical Engineering, University of Padova
via Venezia, 1, 35131 Padova, Italy
°Department of Management and Engineering, University of Padova
Stradella S. Nicola, 3, 36100 Vicenza, Italy

Experimental estimation of the fatigue limit of metallic materials on the basis of temperature measurements is well documented in the literature [1]. Typically, infrared cameras are adopted in order to monitor surface temperature of specimens and components subjected to fatigue tests, thus leading to the so called “thermographic method”. In summary, the thermographic methodology is sketched in fig. 1. When a force-controlled, constant amplitude fatigue test is running, temperature measured at the specimen surface is seen to increase at the beginning of the test and then, after a certain number of cycle N, stabilises so that it is possible to identify a stable temperature increase ΔT_{stat}. The higher the stress amplitude σ_a the higher the stable temperature increase, as depicted in fig. 1a. Since fatigue failure is caused by microplastic strains which initiate a small fatigue crack, then temperature increments have been qualitatively interpreted as the manifestation of energy dissipation due to plastic hysteresis energy. A quantitative evaluation is reported in [2]. By plotting the stable temperature increments as a function of the applied stress amplitude, one can extrapolate the ΔT_{stat} versus σ_a curve, as shown in fig. 1b. By so doing, one can estimate the fatigue limit $\sigma_{0,th}$ of the material, according to the thermographic method presented in the literature (for example [1,3] and references quoted therein).

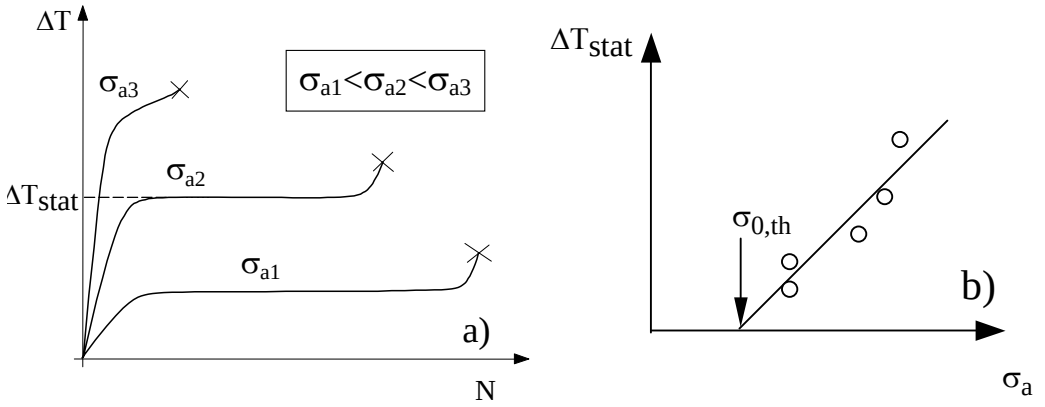

Figure 1. Observed temperature evolution during constant amplitude fatigue tests on metallic and composite materials (a), estimation of the material fatigue limit according to [1] (b).

Anyway the specific energy Q dissipated as heat in a unit volume of material per cycle seems to be a more promising parameter for fatigue characterisation. In fact, thermal increments for a given material undergoing a fatigue test depends on applied stress amplitude, test frequency, load ratio, specimen geometry and thermal boundary conditions which determine the rate of heat extraction from the material in the form of conduction, convection and radiation. Conversely, the specific energy dissipated as heat is a material parameter in constant amplitude fatigue tests, which depends only on the applied stress amplitude and load

ratio. In particular it does not depend on the specimen geometry so that it seems reasonable to extend the laboratory test results obtained from specimens to real components having an arbitrary geometry. Recently it has been shown that the specific energy Q can be estimated by means of a simple experimental technique [4]: if the fatigue test is suddenly stopped after that temperature has reached its stable value, then the specific energy Q can be estimated from the cooling rate observed after test stopping:

$$\frac{\rho \cdot c}{f} \cdot \left. \frac{\partial T}{\partial t} \right|_{t=(t^*)+} = -Q \qquad (1)$$

where f is the test frequency, ρ is the material density and c is the material specific heat. Aim of the present work is to show that the energy parameter Q, derived from temperature measurements by means of an infrared camera, is able to rationalise the fatigue strength of specimens having different geometries. Fig. 2 shows the results of fatigue tests obtained from two different series of specimens made of AISI 304L stainless steel (yield stress σ_y=300 MPa, ultimate tensile stress σ_u=650 MPa) having different geometries, i.e. a smooth geometry and a plate containing a central hole with a diameter of 20mm. Fatigue tests were conduced with a nominal stress ratio R (ratio between the minimum and the maximum applied nominal stress) equal to 0.1. Fig. 2 shows that results can be summarised in terms of specific energy dissipation independently of the specimens geometry. Such an experimental technique will be extended also to a short fibre reinforced plastic. Material will be a PA66-GF35 short glass fiber polyamid composite.

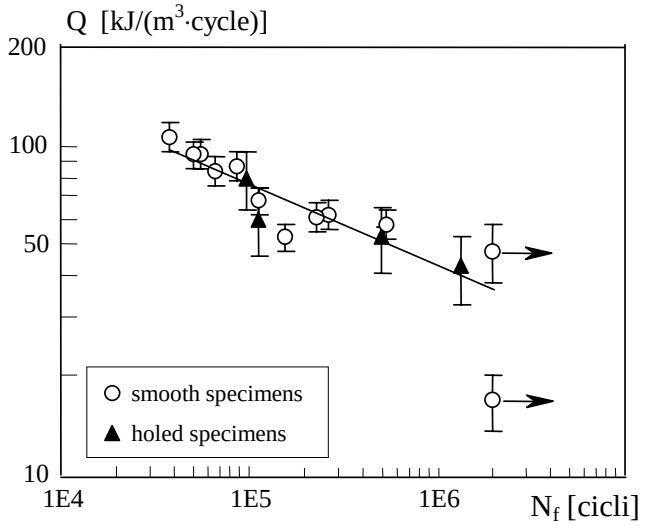

Fig. 2: fatigue behaviour of AISI 304L stainless steel in terms of specific energy dissipation.

Two series having different geometries will be fatigue tested at a nominal stress ratio equal to 0.1 and during fatigue tests surface temperatures will be measured by means of an infrared camera. Then by means of eq. (1) the experimental data will be processed in order to plot the fatigue lives in terms of specific energy Q and to verify if Q is a unifying energy parameter even for this class of materials .

References

[1] G. La Rosa, A. Risitano, Thermographic methodology for rapid determination of the fatigue limit of materials and mechanical components, Int. J. Fatigue, **22**, 65-73 (2000).

[2] J. Kaleta, R. Blotny, H. Harig, Energy stored in a specimen under fatigue limit loading conditions, JTEVA, 19(4), 326-333 (1990).

[3] M.P. Luong, Fatigue limit evaluation of metals using an infrared thermographic technique, Mechanics of Materials, 28, 155-163 (1998).

[4] B. Atzori, G. Meneghetti, Energy dissipation in low cycle fatigue of austempered ductile irons, 5th Int. Conf. on *Low Cycle Fatigue*, Berlin (Germany), 2003, pp. 147-152.

Combined thermoelastic and thermographic data for the evaluation of crack growth in industrial components

U. Galietti, D. Modugno

Mechanical and Management Engineering, Politecnico di Bari
Viale Japigia 182, Bari-Italy

galietti@poliba.it, dmodu@poliba.it

ABSTRACT:

The application of infrared thermography as a non-destructive method to detect the occurrence of damage and to investigate the fatigue process of materials has become popular and has been widely investigated in literature. Thermography has clearly shown to be a powerful tool for the characterization of structural material properties such as fatigue limit. Many previous works from literature have gone into the relation between the damage in the material and the temperature arising as result of internal energy dissipation.
On the other hand, thermoelastic stress analysis has become in the last years a well established technique for the determination of the stress field in mechanical components, even with an high geometrical complexity.
The present work starts from the observation that damage in the material results both in a change in superficial temperature and in a change of the stress field. A differential infrared camera, DeltaTherm 1560 by Stressphotonics, has been used to acquire both thermographic and thermoelastic data from industrial mechanical components subjected to a fatigue cyclic load.
Infrared signal from the samples has been acquired with a time gap of few minutes, in order to have a continuous monitoring of the crack growth in the sample under investigation until the occurrence of the failure. A comparison of thermographic and thermoelastic data shows that the change in temperature field is strictly related with the change in the pattern of the stresses distribution due to the evolution of the damage in the material.
Experimental data are provided from welded joints and samples in composite material.

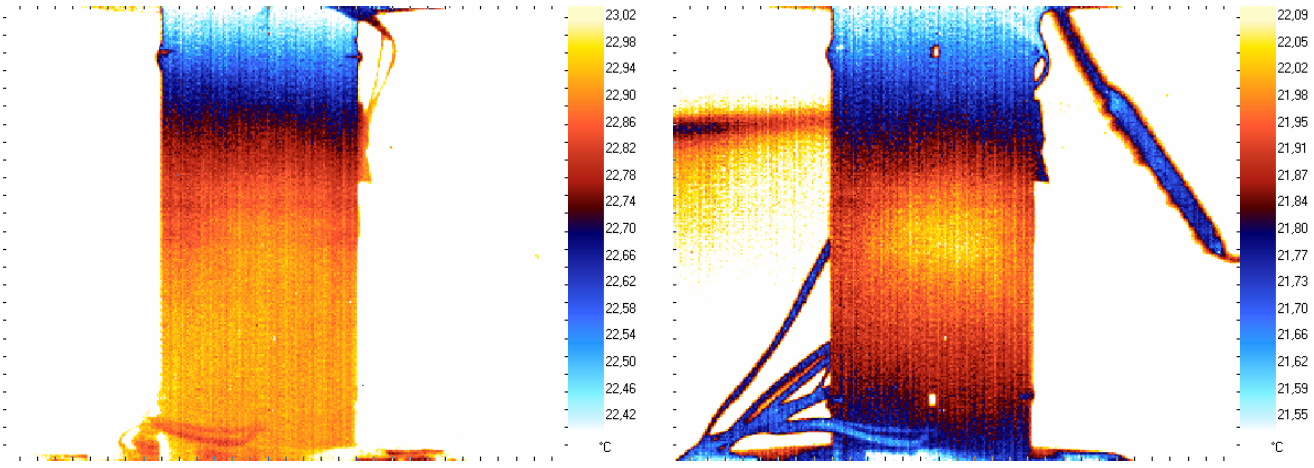

Figure 1- Thermographic image of a welded joint, (on the left) at the beginning of the test, (on the right) just before the occurrence of the failure.

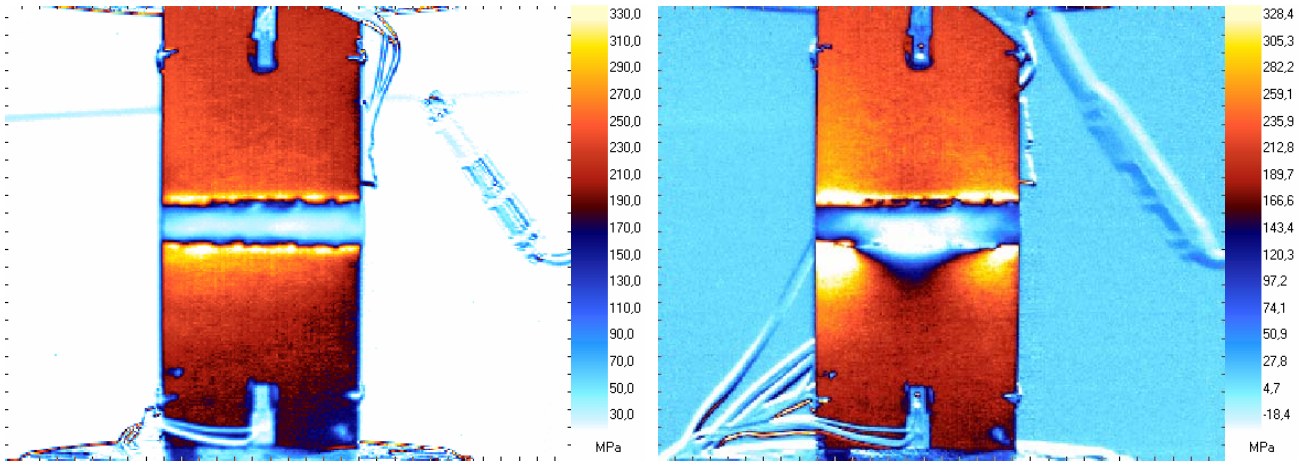

Figure 2- Thermoelastic image of a welded joint, (on the left) at the beginning of the test, (on the right) just before the occurrence of the failure.

REFERENCES

[1] M. P. Luong, “Fatigue limit evaluation of metals using an infrared thermographic technique”, Mechanics of Materials, 28, 1998, p. 155-163 (Journal).
[2] G. La Rosa, A. Risitano, “Thermographic methodology for rapid determination of the fatigue limit of materials and mechanical components”, International Journal of Fatigue, 22, 1, 2000, p. 65-73 (Journal).
[3] J.C. Krapez, D. Pacou and G. Gardette, “Lock-in thermography and fatigue limit of metals”. Quantitative infrared thermography 5: QIRT'2000.
[4] A. Chrysochoos, H. Louche, “An infrared image processing to analyse the calorific effects accompanyng strain localisation”, International Journal of Engineering
Science, pp. 1759-1788, 38, (2000).
[5] A.E. Morabito, “Analisi termomeccanica degli effeti termoelastici e dissipative associati al comportamento a fatica della lega di alluminio 2024 T3”, PHD thesis, Universita’degli Studi di Lecce, 2003, *in italian*.
[6] Stanley, P., Chan, W.K., "Quantitative stress analysis by means of the termoelastic effect", Journal of Strain Analysis, Vol. 20 (3), 1985, pp. 129-137
[7]. Maldague, X.P.V., *“Theory and practice of infrared technology for nondestructive testing”*, 2001 John Wiley & Sons Inc., ISBN 0-471-18/190-0.
[8]. Harwood, N., Cummings, W.M., "Thermoelastic Stress Analysis", Adam Hilger IOP Publishing.
[9] DeltaTherm user manual.

QIRT associated to Digital Image Correlation to perform thermomechanical analysis of the yield behaviour of a semicristalline polymer.

Jean-Michel Muracciole, Bertrand Wattrisse, Yves El Kaïm, André Chrysochoos
Mechanics and Civil Engineering Laboratory, Montpellier II University, France
muraccio@lmgc.univ-montp2.fr

ABSTRACT: This paper first presents the characteristics of a new experimental set-up using digital image correlation and infrared thermography. The kinematical data are used to track the temperature variations of material surface elements. They are then combined to construct local energy balance. To illustrate the interest of such an approach, the paper then describes the calorimetric effects accompanying the propagation of necking in a PolyAmide 11. A thermodynamic analysis of cyclic loading finally aims to show the existence of an entropic elastic effect generally associated with rubber-like materials.

INTRODUCTION

Ever since 2000 we have developed an experimental approach to the material behaviour characterization which combines Digital Image Correlation (DIC) with InfraRed Thermography (IRT). The DIC techniques give access to the measurement of displacement and deformation fields while the thermal images enable us, under certain conditions, to estimate the distribution of heat sources induced by the deformation process. Those thermal images were recorded using an IRFPA camera (Cedip Jade 3) and a specific "pixel per pixel" calibration method described in [1]. A specialized electronic system was performed to get a simultaneous recording of speckle and infrared images. A combined treatment of kinematics and thermal data then allowed to track the temperature of material surface element and to construct local energy balances. This opportunity is particularly interesting to study the thermomechanical behavior of materials even if localization mechanisms occur at the observation scale imposed by the optical lenses. Applications to steel and polymer were already carried out for monotonic quasi-static loadings [2, 3]. In what follows, after having recalled the main characteristics of the experimental arrangement, we show the protocol defined to compute the heat source taking into account the existence of localization zones. To illustrate this we consider tension tests on Polyamide 11 samples. For this kind of material the necking zone spreads out during monotonic tensile test. Using thermal and kinematic data we will first show that the heat transfers by matter transport are not negligible in the moving necking lips. Then, we will analyse the thermomechanical coupling effects that appear in the necking zone during a cyclic loading around a given tension state.

MAIN CHARACTERISITCS OF THE SYNCHROCAM SYSTEM

The experimental setup implements a visible CCD camera and an IRFPA camera which film both sides of thin, plane specimens. We developed a special electronic master-slave system to ensure a perfect synchronization of the frame grabbing of the two cameras equipped with external trigger. Moreover, the SYNCHROCAM system enables to record simultaneously various analogical signals (force, crosshead displacement, etc.) provided by the testing machine. It also sets the data capture frequency. The performances of the system are the following: the rate of the master camera can vary –insofar as the camera allows it – from 1 frame per hour to 500 frames per second. The rate of the slave camera can vary in this same range after application of a division or multiplication factor ranging between 1 and 512. Finally the acquisition time accuracy is better than 10^{-4} s. which is sufficient for classical mechanical tests.

EXPERIMENT AND RESULTS

Space-time charts were constructed with the abscissa axis (bottom) representing the time and the ordinate axis (left) being the longitudinal sample axis (see Figure 1). The conventional stress-time diagram was superimposed to give the reader a familiar landmark to link the local pattern of the measurements to the loading state of the sample (right and top). For such a diagram we have plotted in white the conventional stress classically defined by $\sigma_c = f/S_0$, where f is the loading force, S_0 the initial cross-section and the time t. In these charts, the evolution of the longitudinal profiles of heat sources during the loading are represented using the colormap set at the right of the figure. The path of the bad pixels clearly shows that this representation takes account of the matter convection.

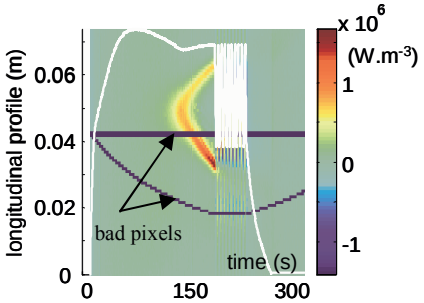

Figure 1.a.: $w_{ch}^{\bullet}$ profiles on a PA11 sample

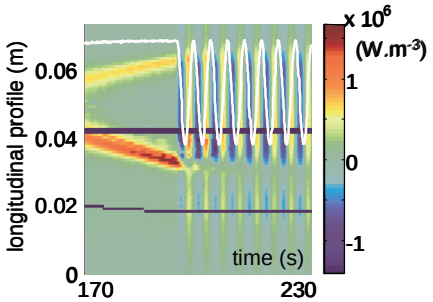

Figure 1.b.: $w_{ch}^{\bullet}$ profiles during the last load-unload cycles

RUBBER COUPLING EFFECTS

Some polymers can undergo very large strains in a reversible way. This remarkable behaviour is often called rubber (or entropic) elasticity. The fundamental hypothesis of the molecular theory of rubber elasticity is that the variation of internal energy is proportional to the variation of the absolute temperature [4]. The analogy with ideal gases leads to an internal energy independent of the elongation, the stress being attributed to a so-called configuration entropy. As in classical elasticity, temperature T and strain ε are chosen as state variables and no intrinsic dissipation occurs. It was shown in [5] that the free energy is of the form:

$$\psi(T,\varepsilon) = T\xi(\varepsilon) + \eta(T) \tag{1}$$

As shown in Eq.(2), the heat sources involved during a mechanical test are, in this case, only associated with the rubber coupling effects, and they are equal to the rate of mechanical energy $w_{ext}^{\bullet}$ [4-5]. This coupling is in phase with the mechanical loading, in contrast with the classical thermoelastic effects which are in phase opposition with the loading.

$$w_{ch}^{\bullet} = \rho T \frac{\partial^2 \psi}{\partial T \partial \varepsilon} \dot{\varepsilon} = w_{ext}^{\bullet} \tag{2}$$

ANALYSIS OF RESULTS

The Figure 1.a. shows that, at the beginning of the test, the overall heat sources are homogeneous along the profile and negative. These heat sources correspond to the classical thermo-elastic effect. The macroscopic softening is associated with the progressive localization of positive heat sources preceding the inception of the two necking lips. There, the convective terms are not negligible as they account for more than 25% of the overall heat sources [3]. The Figure 1.b. represents the heat distribution during the last unload-load cycles. We observe that the heat sources are quasi homogeneous and that they are in phase with the load. As the observation scale is not, in this application, adapted to the realisation of local energy balances in the necking lips, we have chosen to perform a global energy balance on the whole sample (see Figure 2). The amplitude of heat sources is smaller to the one of the external energy-rate. The symmetry of both mechanical and calorimetric energy rates during the cyclic loading can be interpreted as a non dissipative competition between the classical thermoelasticity and the rubber effects.

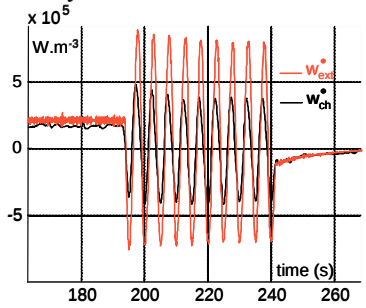

Figure 2: energy-rates $w_{ext}^{\bullet}$ and $w_{ch}^{\bullet}$ during a cyclic loading

CONCLUSION

The synchrocam system allows to record simultaneously images (in the infrared and the visible spectrum) and analogical signals which are necessary to construct local energy balances during “heterogeneous tensile tests”. Using this set-up during cyclic tests performed after the necking of a PA11 specimen, we have shown the existence of an entropic elastic coupling competing with a classical thermoelastic coupling. This kind of behaviour was already evidenced in rubber material [6-7]. The natural continuation of this work will be to analyse more locally, using adapted infrared and visible optical lenses, the competition between these two effects within and outside the necking zone.

REFERENCES

1. Honorat V., Moreau S., Muracciole J.-M., Wattrisse B., Chrysochoos A. (à paraître) , *Calorimetric analysis of polymer behaviour using a pixel calibration of an IRFPA camera*, QIRT Journal.
2. Chrysochoos A., Wattrisse B., Muracciole J.-M. (2000), *Experimental analysis of strain and damage localization*, Symposium on continuous damage and fracture, Ed. A. Benallal, pp.41-51.
3. Wattrisse B., Muracciole J.-M., Chrysochoos A., (2001), *Thermomechanical effects accompanying the localized necking of semi-crystalline polymers*, Int. J. of. Therm. Sci, 41, pp.422-427.
4. Chadwick P. and Creasy, C.F.M., (1984) *Modified entropic elasticity of rubberlike materials*, J. Mech. Phys. Solids, 32, p 337-357
5. Ogden R. W., (1992) *On the thermoelastic modelling of rubberlike solids*, J. of thermal stresses, 15,4, p 533-557.
6. Saurel J-L. (1999) *Etude thermomécanique d'une famille d'élastomères thermoplastiques*, PhD thesis of Montpellier University. 6.
7. Honorat V. (2006) *Analyse thermomécanique par mesures de champs des élastomères*, PhD thesis of Montpellier University.

Analysis of Thermal Stress in Fatigue Fracture Specimen using Lock-in Thermography

by Won-Tae Kim (1), Man-Yong Choi (2), Jung-Hak Park (2)

(1) Dept. of Bio-mechanical Engineering, Kongju National University, Chungnam, Korea, 340-702
(2) Life Measurement Group, Korea Research Institute of Standars and Science, Daejeon, Korea, 305-600

Abstract

This paper aims to describe the thermal stress analysis using Lock-in thermography as a nondestructive testing (NDT) method with real time. Due to the first and second principles of thermodynamics, there is a relationship between temperature and mechanical behavior laws. Applying the IR thermographic measurement to fatigue testing would significantly reduce the necessary specimens and testing duration. As this technology is based on the thermal elastic effects, however, it can be used only under dynamic loading conditions, but not under static loading conditions. Further studies should be undertaken to resolve this limitation. Using a lock-in thermography system, this study examined the distribution of stresses in specimens by applying the principle of thermal elasticity. The analysis of the linear relationship between the strength and stress found in this study also implies that the changes in temperature caused by the measured stresses from the thermography camera were consistent with the applied loads.

Keywords: Infrared (IR) Thermography, Thermal Stress, Nondestructive Testing(NDT), Fatigue Fracture, Loading Condition

Thermal transient mapping systems for integrated semiconductor devices and circuits.

Lucio Rossi, **Giovanni Breglio***, Andrea Irace, Paolo Spirito
Università degli Studi di Napoli Federico II,Dipartimento di Ingegneria Elettronica e delle Telecomunicazioni, via Claudio 21, 80125 Napoli, l.rossi@unina.it

Abstract

Aim of this paper is to present two systems for the acquisition of dynamic thermal maps of ICs, developed at the University of Naples "Federico II", Department of Electronic Engineering and Telecommunication (DIET).
First of the two is a system completely automated that measures the infrared radiation emitted by a device or an electronic system subjected to a periodic electro-thermal transient.
In order to guarantee the speed needed to follow the thermal dynamics of an IC device a fast single cooled Cd-Mg sensor have been used. With this device it is possible to achieve a time resolution lesser than 2 μs. Moreover, since the spatial resolution of the system is also of main concern, the sensor is mounted in a microscope optical chain with an equivalent spot size of about 10 μm.
The controlled reproduction of the thermal transient along with the in-plane translation of the DUT under the microscope spot performed by two 0.1 μm linear positioning stages, gives us the possibility to acquire the temperature transient information on a DUT surface as wide as 5x5 cm^2 using only one single point IR sensor.
A 5MS/s 12bit A/D converter card performs the acquisition of the radiometric waveforms which are later elaborated and pre-filtered by an acquisition software developed under a MatLab environment.

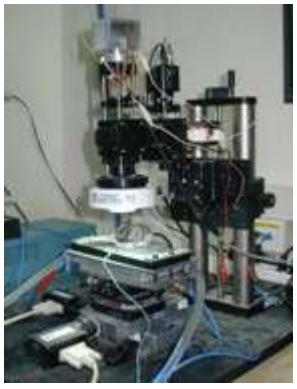
(a)


(b)

Fig.1 (a) The IR acquisition system.
(b) The thermoreflectance acquisition system

This software, not only performs the averaging procedure of pre-filtering necessary to increase the signal to noise ratio, but also controls all the single parts of the system and carries out the preliminary characterization step which is necessary to measure the target emissivity coefficient. It is important to point out that, since the surface of any IC device is composed by a variety of different materials, it would be impossible to recover the absolute thermal information without this preliminary characterization.
The second system on the other hand exploits the thermo-optic effect, which consists in a variation of the reflection coefficient of reflective materials, to recover an estimate of the superficial temperature.

Since this effect is substantially different from the infrared emission of a warm body, in this case it is possible to work with wavelengths smaller than those falling into the IR spectrum, giving a not negligible improvement on spatial resolution.
The radiation reflected by the surface of the DUT is acquired by a high-speed silicon PIN photodiode with a bandwidth in excess of 1 GHz on a 50Ω load. As in the case of the IR system the DUT is translated in a x-y plane by means of two stepper motors providing a 0.1 μm minimum incremental motion over a 5x5 cm^2 square area.
A graphic user interface developed under a MatLab environment again, provides the overall system control and the elaboration of the signals with the possibility of displaying 2D animated temperature maps.
In order to recover the absolute temperature information, and for the same reasons pointed out above, in this case a parameter called thermo-reflectance coefficient, which relates the variation of temperature with the relative variation of reflectance, is measured preliminarily point by point.

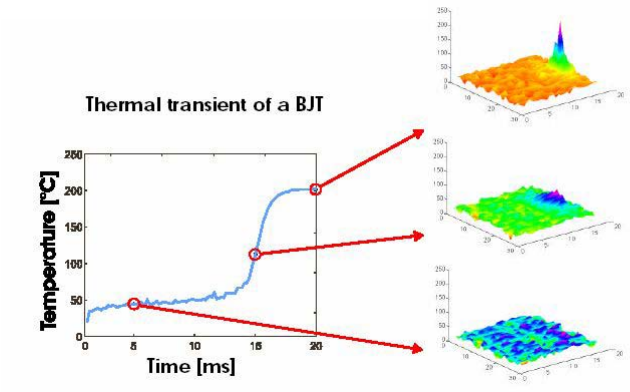

Fig.2 Example of Dynamic thermal map of a power BJT device obtained by means of the first system.

REFERENCES
[1] O. Breitenstein, M. Langenkamp "Lock-in Thermography" Springer 2003, ISBN 3-540-43439-9
[2] G. Breglio, P. Spirito, "Experimental detection of time dependent temperature maps in power bipolar transistors", MicroElectronic Journal, vol.31/9-10, pp. 735-739, 2000
[3] G. Breglio, N. Rinaldi, P. Spirito, "Thermal Mapping and 3D Numerical Simulation of New Cellular Power MOS Affected by Electro-Thermal Instability", MicroElectronic Journal, vol. 31/9-10, pp. 741-746, 2000
[4] D'Arcangelo, E; Irace, A; Breglio, G; Spirito, P; "Experimental characterization of temperature distribution on power MOS devices during Unclamped Inductive Switching" MICROELECTRONICS RELIABILITY 2004 SEP-NOV VL 44 IS 9-11 Pp 1455 1459

KEYWORDS: 2D Thermal Mapping Systems, Fast Acquisition systems, Power Semiconductor Devices

***CORRESPONDING AUTHOR:** E-mail: breglio@unina.it, Ph: 0817683128*

THERMOGRAPHIC INSPECTIONS ON MINI EVAPORATORS TO EVALUATE PERIODIC BOILING HEAT TRANSFER COEFFICIENTS

S. Filippeschi, G. Salvadori
Department of Energetics "Lorenzo Poggi" – University of Pisa
Via Diotisalvi 2, 56100 Pisa, Italy
tel. +39-050-2217153 fax +39-050-2217150
s.filippeschi@ing.unipi.it ; g.salva@ing.unipi.it

ABSTRACT

A particular two-phase thermosyphon able to operate even against gravity is the Periodic Two-Phase Thermosyphon (PTPT. A PTPT prototype for thermal control miniature applications for electronic equipment cooling has been realised at the Department of Energetics "Lorenzo Poggi" (University of Pisa).
This device is similar to a loop two-phase thermosyphon because it is characterised by two main elements (evaporator and condenser) interconnected by two separated pipes: the vapour line and the liquid line. But a PTPT is characterised by a periodic heat and mass transport inside the loop, so that it operates with periodic difference of temperature and pressures along the loop and a natural circulation even against gravity is realised.
In a such device the evaporator is, therefore, periodically filled and empted of working fluid and the heat transfer regime change periodically during the operation. The critical heat transfer regime that influences very much the global thermal resistance of mini PTPT cooling device is relative to the heat transfer between the hot surface near to chip and the working fluid. In a previous experimental analysis this heat transfer coefficient have been experimentally measured in time during periodic operation with an approximate original method.
One of the main problem of this approximate method has been to analyse the uncertainties in the measurements. For this aim an infrared thermo analysis of the evaporator has been carried out.
This paper presents how the thermographic instruments can be used to evaluate the errors during the periodic boiling heat transfer coefficients measurements In order to understand the experimental method and the themographic analysis carried out a simple description of the experimental apparatus must be made.
The evaporator case of the experimental apparatus is made of aluminium. The electronic components has been simulated by an electric themo-heater that is connected with the evaporator case by a copper dissipator. A PTFE ring thermally disconnects the aluminium case of the evaporator and the upper portion of the copper dissipator. The lower portion of the dissipator is in contact with the environmental air. The lower portion of the copper dissipator can be observed with an infrared thermo-camera as shown in Figure 1. A section of the evaporator and the cylindrical copper dissipator is reported in Figure 2.
The periodic boiling heat transfer coefficient has been experimentally determined by measuring the temperature T_W of the dissipator with the thermocouple, located 2 mm under the heat transfer wall, by measuring the temperature T_S of the vapour inside the evaporator and the heat flux supplied to the dissipator with a frequency of 0.33 Hz.
The transient heat transfer coefficient h(t) in the evaporator is therefore calculated by the following thermal power balance:

$$\dot{Q}_e = \dot{Q}_d(t) - \dot{Q}_a(t) - \dot{Q}_{env}(t) \qquad (2)$$

where Qe is the electric power that is constant on time, $Q_a(t)$ is the heat stored by the dissipator for each time increment and $Q_{env}(t)$ is the power loss in the environment. If the power loss through the PTFE ring is considered negligible, $Q_{env}(t)$ is equal to the power dissipated in the environment by the lower portion of the copper dissipator.
The thermo-camera allows T(r,z) to be measured in the portion of the copper dissipator that has no thermal insulation with a frame frequency of 30 Hz. The surface observed is semi-cylindrical, with a diameter of 0.038 m and a height of 0.01 m, while the image of the copper dissipator is a rectangular area divided into 1575 pixels of 6·10-5x6·10-5 m. In this way 25 pixels are in direction z and 63 pixels in direction x (where $x = r \cdot \cos(\theta)$).
If the temperature relative to 20 more external pixels, 10 on the right and 10 on the left, are not taken into account, the temperature can be considered constant for each z level, with an error lower than 5 % with respect to their mean value.
In this way a temperature profile of 14 points in z-direction has been obtained every 0.03 s. The thermal balance of every 14 nodes has been carried out and the heat losses into the environment are so determined in time.
In conclusion, in order to calculate the power Q_d in time by eq.(2), $Q_a(t)$ has been evaluate by approximating the function T(r,z,t) in the copper dissipator, with a transient finite difference method. The main results of this analysis are shown in Fig. 3-4. Fig. 3 and Fig. 4 show the evolutions of the heat transfer coefficient h, in the case of different values of VT, for Q_e =30 and 40 W, respectively.
In the case of large volumes (>$64 \cdot 10^{-6}$ m^3), the maximum heat transfer coefficient is about 11000 $W/m^2 \cdot K$, while for volumes lower than $3.5 \cdot 10^{-6}$ m^3 the maximum heat transfer coefficient is approximately 5000 $W/m^2 \cdot K$. The minimum

heat transfer coefficient is similar for all volumes and it is about 1100 W/m^2·K. As a result, the heat transfer coefficient decreases down to 20% of the maximum for small liquid pool volumes (<3·10^{-6} m^3) or down to 9% for large liquid pool volumes (>64·10^{-6} m^3).
The temperature distribution T(r,z,t) determined with the transient finite difference method which supplies the exeriental coefficient shown in figure 3 and 4 has been compared with the temperature distribution measured with a thermal resolution of 0.15 K by the micro bolometric thermocamera. Figure 5 shows some thermal profile measured by the thermocamera in time. This comparison joined with a detailed analysis o the experimental accuracy of measurements allows the accuracy evaluation of the experimental method.

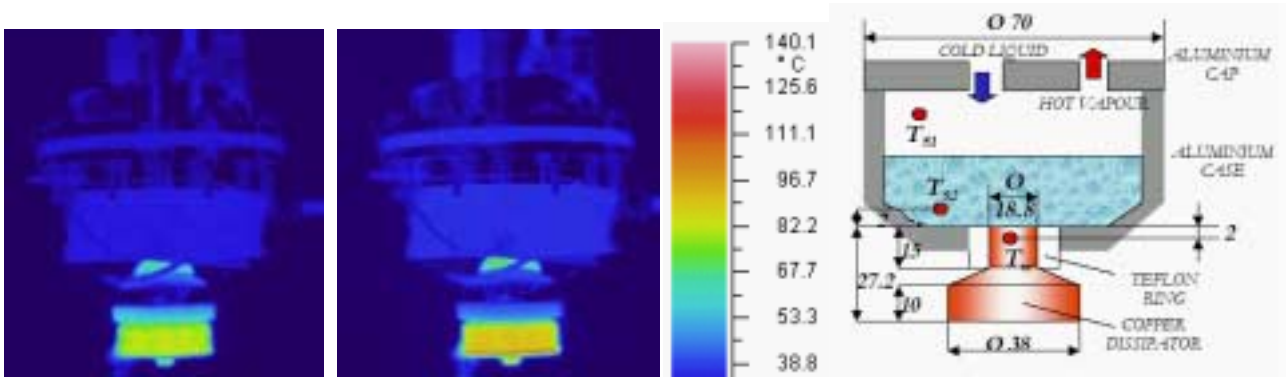

t= 0 s t = 240 s

Figure 1– Infrared images of the evaporator at different times and its scheme (q_d=10.83·10^4 W·m^2 e V_T = 25·10^{-6} m^3)

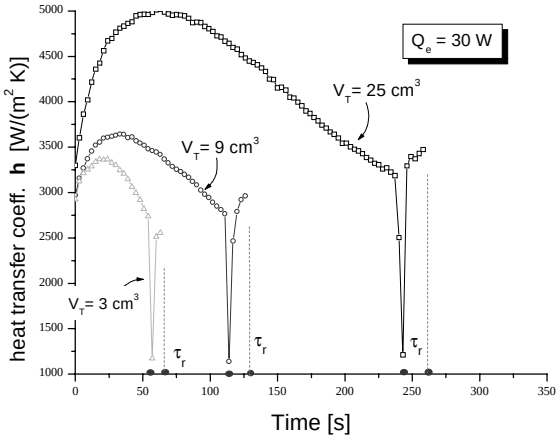

Figure 2 – Evolution of heat transfer coefficient h for Q_e=30 W)

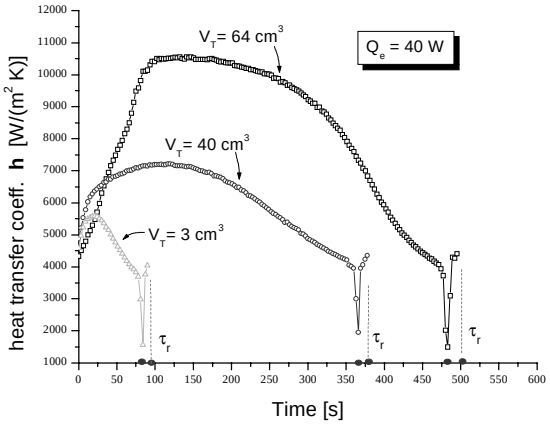

Figure 3 – Evolutions of heat transfer coefficient h for Q_e=40 W

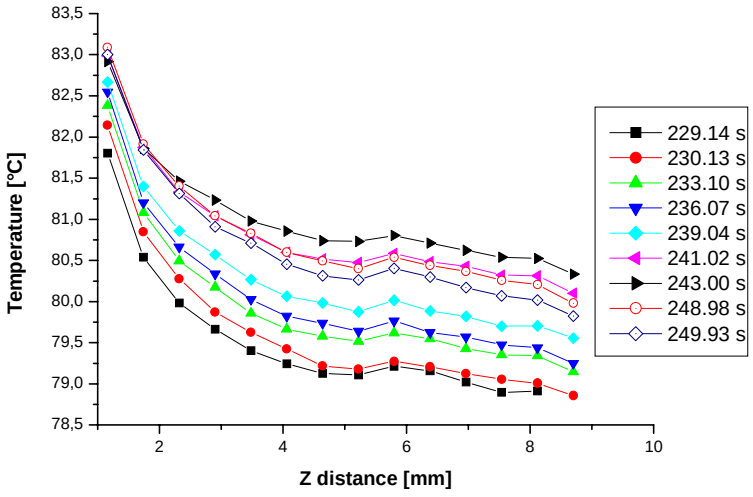

Figure 4 – Evolutions of the Ti (1<i<10) for Q_e=30 W, V_T=25·10^{-6} m^3

COMBINED CFD AND INFRARED THERMAL ANALISYS OF A WOOD REFUSE AND DI-METHYL-ETHER CO-FIRED FLAME

Authors: ***Tudor Prisecaru****, Lucian Mihaescu, Constantin Dumitrascu, Malina Prisecaru, Nicolae Panoiu, Elena Popa, Ion Oprea*

Affiliation: Politechnica University of Bucharest, Romania
313 Splaiul Independentei, Bucharest, Sector1, Faculty of Mechanical Engineering. E-mail: tudor_prisecaru@mail.com
Tel./Fax. + 40 21 318 1019

Key words: ***CFD, InfraRed Thermography, Co-firing, Bio-regenerable fuels***

Oral presentation

INTRODUCTION

This paper presents theoretically and experimental study of possibilities to incinerate different kinds of wood refuse, using di – methyl – ether (CH_3OCH_3) as a supporting fuel.
Trying to improve both the flame's characteristics and the furnace general assembly of performances, 3D CFD simulations together with infrared analysis of the flame have been carried out, as they are further described.

GENERAL CONDITIONS AND ASSUMPTIONS

Several wood types of refuse (such as sawdust, wood pieces, etc.) have been considered to be burned, in order to be able to realise a continuous significant main fuel flow rate for the incinerator and di-methyl-ether as a supplementary fuel in case of starting up and other transition periods. This type of incinerator has been designed to operate in the neighbourhood of the Prahova Valley in Romanian Sub-Carpathians region, where a lot of oil refineries are in operations to offer C_2H_6O as a by-product, together with a strong wood local industry.
Present research has as principal purpose to establish the best possibilities to co-fire both wood refuse and di-methyl-ether in order to a maximum reduction of NOx and mechanical heat losses.
Results have been obtained concerning the minimum supplementary di-methyl-ether flow rate and the best place to be injected in order to realize a constant regime of the flue gas at the end of the furnace, when changing the main fuel.

PROCEDURES

First some numerical simulations of the burning process of co-firing have been performed with FLUENT 6.1 in order to reduce the costs of experiments; in this way the best places of di-methyl-ether injections have been identified on the experimental 2MWt furnace of the Politechnica University of Bucharest. At the same time a special burner for di-methyl –ether has been created in order to create an extended core of the flame to touch as much as possible the cloud of the wood refuse.

After the new burner construction experiments have been operated on the pilot furnace already been up-mentioned.
Using a ThermaCAM SC 1000 in a common installation with a HORIBA PG 250 S flue gas analysis and ThermaGRAM 95 Pro analysis software the co-firing process a lot of interesting results have been obtained.
First, only small impacts of the di-methyl-ether injections have been detected when transient regimes of main fuel have been operated, as it can be seen in the fig.1 and 2.

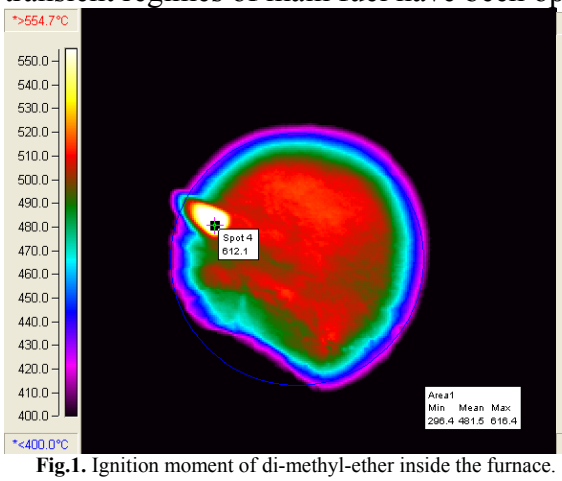

Fig.1. Ignition moment of di-methyl-ether inside the furnace.

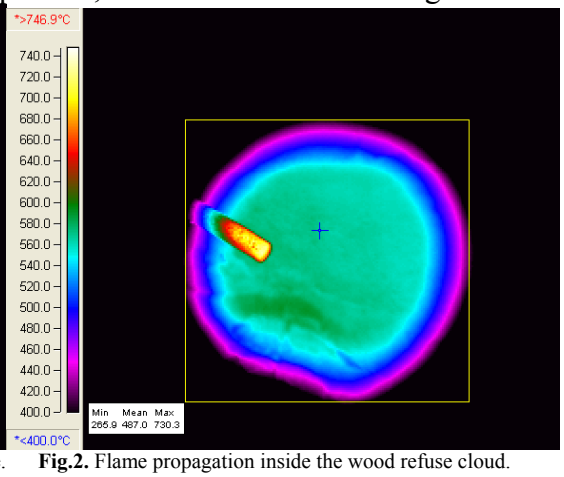

Fig.2. Flame propagation inside the wood refuse cloud.

As it can be seen the flame has a small influence and it is not sufficient at all to sustain the whole process (a flue gas temperature coloured scale has been attached to the pictures).
After some more similar injection places have been placed in the furnace, according to the CFD results, a better situation has been achieved, as it can be seen in the fig.3.

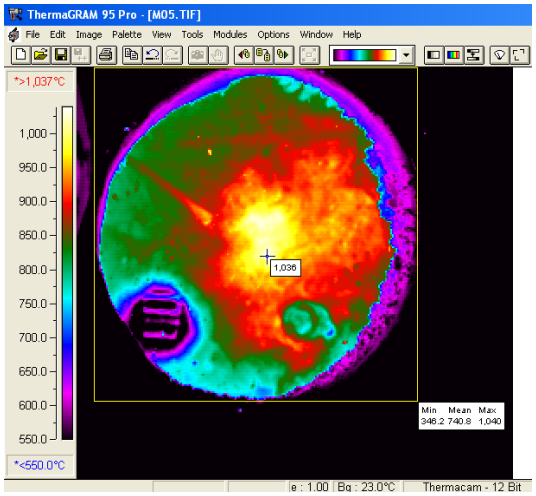

Fig.3. The new improved aspect of the co-fired flame.

At the first sight, a better flue gas temperature distribution can be observed inside the combustion chamber, due to the fact that di-methyl-ether has been injected through a more complex burner (it can be seen in the down left corner of the picture) and due to the fact that the air circulation has been strongly modified after the first experiments.
Some more aspects of impulse injections of di-methyl-ether are also developed in the paper, concerning prevention of temperature field decay, due to the variable humidity content of the solid wood refuse.

BIBLIOGRAPHY (selective)

1. **T. Prisecaru,** ***Numerical Simulation of Solid and Gaseous Fuels' Burning Process***. BREN Ed. Bucharest, 2001, 176 pp, ISBN 973-8143-76-4.
2. **A. Mihai**, ***Infrared Thermography***, Ed. Tehnica, Bucharest 2005, 360 pp.
3. **N. Panoiu, a.o.** ***Some possibilities to use di-methyl-ether for power production purposes***. The IV National Conference of Thermal Equipment, Proceedings, Politechnica University of Bucharest 2005, ISBN 973-7984-41-2.

RESEARCH AND TESTING OF FUEL OIL COMBUSTION, USING FLAME INFRARED THERMOGRAPHY

byVictor V. Ghiea (Research Professor, Dr. Eng.)

Polytechnic University of Bucharest, Thermo-Mechnical Engineering Dep., 313 Splaiul Independentei, Sector 6, Bucharest, Romania, E-mail: ghiea_victor@yahoo.co.uk, phone 4021/6743276,fax: 4021 346 43 70

Summary*: Infrared thermography used in combustion processes research, generates an original method for combustion testing of fuel oil (FO) droplet flame. Above all, by flame infrared thermography are obtained, valuable data on the laminar diffusion process development of gas oils, according to the measured apparent temperature (T_a), and new criteria for determination of their combustion quality Also resulted a complex graphologyc – thermographyc method for research and testing of fuel oil droplet combustion, with many efficient industrial applications. The method is founded on laboratory imagining processing of experimental results by combustion oscillogram (COS) and infrared thermogram (IT) of a FO burning droplet flame, using in a simulator the emitted radiation in spectral visible and infrared band. This radiation was converted into electrical signals stored in the memory of a electronic computer, especially to determine the radiation-combustion-ignition (RCI) characteristics and T_a .As edifying example of the method efficiency, is detailed the improvement of combustion with additived air (CWAA) of inferior fuel oil (IFO) at boilers for environment pollution decrease and fuel savings increase..*

The main fuel oils are considered: heavy (HFO) and intermediate (IFO) fuel oil together with gas oil (GO). HFO and *IFO*, especially are produced by mixing in different proportions of the residues obtained from crude petroleum treatment (atmospherically distillation, vacuum distillation, thermal cracking, catalytical cracking...etc.) and light products. As *IFO* are considered HFO and inferior IFO. Infrared Thermography (IT) for droplet combustion research uses the accumulated experience by the research and particularly advantageous applications of fuel oil droplet combustion graphology which concerns especially with the graphic transposition of fuel oil droplet combustion processes. Thus, using a combustion simulator, experimentally are established the RCI characteristics, also including the laws that govern their changes, depending on combustion conditions and fuel oil quality. Similar, we can create and develop the droplet combustion thermography, which at the beginning is used for fuel oil droplet flame research, and combustion testing. In addition valuable new data on combustion process development can be obtained, according to the T_a variation, presented in a flame infrared thermogram (FIT) of the burning fuel oil droplet. The used simulator with an un-heated combustion chamber permits the burning at T_e environmental air temperature of individual fuel oil droplets, with the initial mean diameter d_0 having temperature T_0. Was used an infrared camera (IRC) type ThermaCam PM 350 operating in the wavelength infrared band $\Delta\lambda$=3.4-5μm, in order to obtain the IT with thermal images. This IT gives the fields of apparent temperatures T_a of burning droplet at a real - time of the combustion process development. The values of T_a are function especially of: d_0 diameter , t time and FO characteristics. These characteristics establish the combustion droplet fuel quality which determine the droplet combustion process development with droplet flame T_a for his emissivity ε. From the IT initial analyze has resulted that for a given fuel oil the apparent temperatures are greater when d_0 is greater and the t time is nearer of value corresponding to the droplet flame maximum volume (DFMV) which is the reference value. Using an appropriate IRC, the mean real temperature T_r corresponding to T_a, can be significant characterize the *FO* combustion process development. But T_r temperature results when is know the emissivity ε in direction of normal incidence of xAy plane of IT picture, within the $\Delta\lambda$ band. The droplet symmetry center is specified by point A. Theory and practical experience show that in the IT points of droplet flame, the emissivity ε is variable in function of numerous parameters. These are especially: concentration in flame of soot fine particles (which is the most important parameter), content of CO_2 and H_2O gases which are released in combustion process, gaseous layer thickness and temperature of gases. But these parameters are variable in the time of droplet burning. For this reason it is impossible to determine with precision, even by special methods, the variable value of ε. In laminar diffusion flames, the soot forms on fuel rich side of the reaction droplet envelope formed by burning of yielded volatiles matters. To obtain a small variation of ε in normal direction at x'x axe for the interval of burning droplet liquid, with a reduce difference between T_a and T_r , it is necessary to burn in ambient air relative large droplet releasing abundant soot by diffusion combustion and the environment giving a very low emissivity. Thus, the released fine particles of soot are rich and spectral emissivity ε(λ) varies slowly with wavelength λ, for some droplet flame zones, being similar as for solid objects. In normal direction to xAy plane surface for the point A, where the released soot is larger, and the liquid droplet represent a background screen, the emissivity ε for an industrial fuel oil in diffusion combustion, has a great

value which can approach to blackbody emissivity. Apparent temperature T_A for the point A is computed according to radiation energy of the referent flame layer thickness with abundant soot, and the burning fuel oil droplet liquid. In direction from droplet towards the droplet flame ended, the emissivity decreases especially due soot concentration and gaseous layer thickness decrease, but increases with temperature diminution. IRC can automatically realizes the correction for emissivity ε, but for the whole IT. Thus for ε_1 the apparent temperature is T_{a1} , and for ε_2 the apparent temperature $T_{a2} = (\varepsilon_1 / \varepsilon_2)^{0.25} T_{a1}$, but the influence of ε variation is much less important as temperature T_a variation in the validity field of Stephan Boltzmann's law. For this reason, the analysis and comparison of T_a temperature fields from IT, according to ε estimation give valuable qualitative informations on diffusion combustion process development, very dependent on T_r temperature. Also by use of the proposed method, analyzing IT obtained by experiments performed in the same initial combustion conditions of droplets, for a tested fuel oil, and a standard fuel oil, new criteria of the fuel combustion quality determination, are established. Thus to characterize and compare, the GO combustion quality at DFMV, where defined criteria: T_{mx} – average of flame apparent temperatures in normal direction on the xx' axe and xAy (picture) plane, ^oC; T_t – average of total flame apparent temperatures in normal direction on xAy plane obtained by conversion of total radiation energy in Δλ band, from the burning droplet; T_A – apparent temperature in normal direction on the xAy plane, for the point A. Also can be established secondary qualitative selection criteria in connection with the shape of curves for apparent temperature corresponding to xx' and yy' axes, namely T_{ax}=f(x) and T_{ay}=F(y). Experimental researches and testing were effected using the presented combustion simulator, and different types of GO, IFO and *IFO*, in the same initial conditions, characterized by: temperatures of environmental combustion air T_e and fuel oil T_o; natural draft for combustion air feeding; cylindrical un-cooled combustion chamber; and initial mean diameter of droplet d_o. It was necessary the realization of a special device for precise droplet calibration at diameter d_o to obtain the same volume for every type of *FO*. Also a special igniter was used. During the majority of *FO* testing, variation of above mentioned criteria, for ε = 1, was: T_{mx} =295 - 357 ^oC; T_A =387 - 447 ^oC and T_t =263 - 293 ^oC. The conclusion of numerous experiments and according theory shows that as for *the GO quality at combustion intensification is better, the criteria T_{mx}, T_A and T_t have larger values.* For an IFO or *IFO*, are very important the volatile matter combustion time t_v (combustion with flame), chemosphere combustion time t_c, together with the self-ignition time t_i. These especially characterize the fuel quality and easily can be obtained using the graphologycal method, using a combustion simulator having a heated combustion mini-furnace. In addition, can be determined others specific characteristics concerning combustion and radiation (for example, maximum radiation intensities in t_v and t_c, namely I_v^m and I_c^m). This method consists in the ignition and burning into the incandescent mini- furnace, under initial standard conditions, of a calibrated droplet. The radiated energies E_v and E_c of the burning droplet in times t_v and t_c are received and transformed by a photocell, into electrical signals in wavelenght band Δλ=0.35─1.3 μm. The experimentally obtained data are acquired, processed and stored in the memory of a computer, and then they are represented on a computer display under the form of combustion oscillogram curve, drawed in a rectangular system of co-ordinate axes (having the time t in abscissa and the radiation intensity I of the burning droplet, in ordinate). The main RCI characteristics in case of CWAA are: t_{ia}, t_{va}, t_{ca}, I_{va}^m, I_{ca}^m, Eva, Eca, having the above meaning. The flame radiated energy Eva is determined by the area Ava between Iva=fa(t) curve and Ot axe, and the energy radiated by the burning cenosphere Eca is determined by the area Aca between Ica=Fa(t) curve and Ot axe.

Numerous experiments, showed that for an industrial high efficient additive it is necessary to be simultaneously accomplish the conditions: tia<ti; tv; $I_{va}^m > I_v^m$; $I_{ca}^m > I_c^m$; Ava>Av; Aca>Ac These seven relations represent new scientifically criteria to select the variants of additivation, for obtaining the optimal economic solution at industrial boilers .

Key figures: Fig.1- Simulator for FO miniaturized combustion research and testing using IR. Thermography; Fig.2- FIT for GO and IFO droplets; Fig.3- Research-testing graphic representation of droplet combustion in cases: a) schematic IT of superior GO droplet at DFMV and b) COS of *IFO* droplets using CWAA and without air additivation.

The Application Of Principal Component Analysis Using Fixed Eigenvectors To The Infrared Thermographic Inspection Of The Space Shuttle Thermal Protection System

K. Elliott Cramer and William P. Winfree
National Aeronautics and Space Administration
Langley Research Center
3b East Taylor St.
Mail Stop 231
Hampton, VA 23681 - USA

Abstract:

The Nondestructive Evaluation Sciences Branch at NASA's Langley Research Center has been actively involved in the development of thermographic inspection techniques for more than 15 years. Since the Space Shuttle *Columbia* accident, NASA has focused on the improvement of advanced NDE techniques for the Reinforced Carbon-Carbon (RCC) panels that comprise the orbiter's wing leading edge. Various nondestructive inspection techniques have been used in the examination of the RCC, but thermography has emerged as an effective inspection alternative to more traditional methods. Thermography is a non-contact inspection method as compared to ultrasonic techniques which typically require the use of a coupling medium between the transducer and material. Like radiographic techniques, thermography can be used to inspect large areas, but has the advantage of minimal safety concerns and the ability for single-sided measurements.

Principal Component Analysis (PCA) has been shown effective for distinguishing damaged regions from undamaged regions. Figure 1 shows how PCA, when applied to flash thermographic data from an RCC impact test specimen, highlights the location subsurface delaminations. A common implementation of PCA is when the eigenvectors are generated from the data set being analyzed. This implementation of PCA is a powerful tool for enhancing the visibility of defects in thermal data, however is computationally intense and time consuming when applied to the large data sets typical in thermography. Additionally, this implementation yield ambiguous results when very large defects are present (defects that dominate the field-of-view), since the calculation of the eigenvectors is now dominated by the defect responses, not the nominal material response. To increase the processing speed and to minimize the negative effects of large defects, an alternative implementation of PCA utilizes a fixed set of eigenvectors to process the thermal data from the RCC materials. These eigenvectors can be generated either from an analytic model of the thermal response of the nominal and flawed material, or experimental data acquired from test specimens.

Figure 2 shows the results of a one-dimensional analytic model that has been developed and the agreement with experimental results. This paper will provide the details of the analytic model; an overview of the PCA process; as well as a quantitative signal-to-noise comparison of the results of performing both embodiments of PCA on thermographic data from various RCC specimens.

Details of a system that has been developed to allow *insitu* inspection of a majority of shuttle RCC components will be presented along with the acceptance test results for this system. Additionally, the results of applying this technology to the Space Shuttle Discovery after its return from flight will be presented.

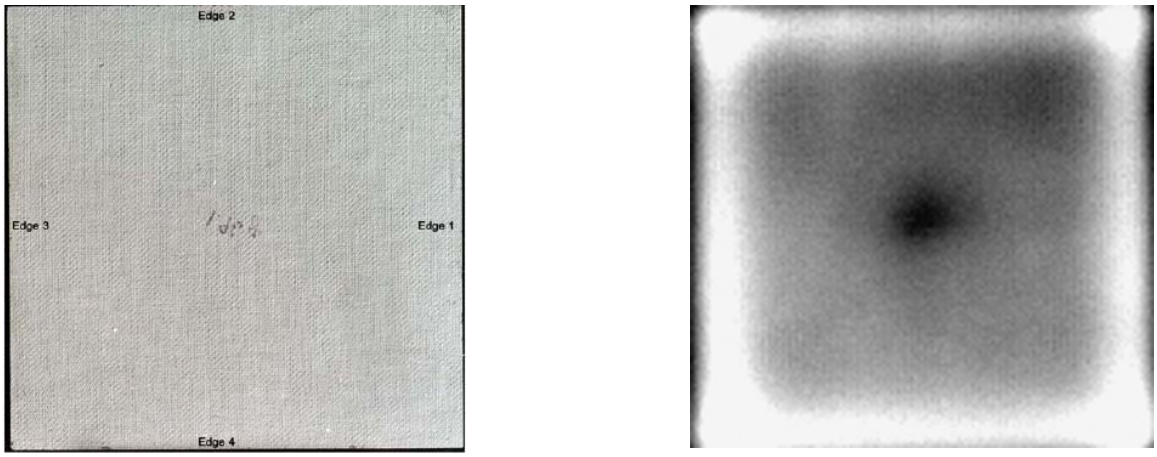

(a) (b)

Figure 1 – (a)Photograph of an RCC impact test specimen and (b) PCA processed flash thermography image showing the extent of damage from the impact.

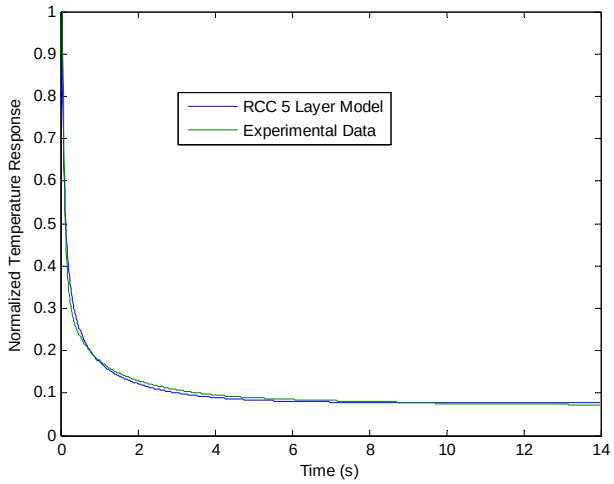

Figure 2 – Comparison of the results of a 5 Layer one-dimensional thermal model of the response of RCC material to flash heating with experimental data.

Defect Quantification with Thermographic Signal Reconstruction and Artificial Neural Networks *

By Hernan Benitez[1], Clemente Ibarra-Castanedo[2], Humberto Loaiza[1], Eduardo Caicedo[1], Abdelhakim Bendada[2], Xavier Maldague[2].

[1]hbenitez, hloaiza, ecaicedo@univalle.edu.co
Universidad del Valle, Colombia, Phone: (57) 2 3391780,Fax:57 2 3392361

[2] bendada, IbarraC, maldagx@ gel.ulaval.ca
Université Laval, Canada, Phone: (418) 656-2962, Fax: (418) 656-3594

***Oral presentation is preferred, poster presentation is acceptable.**

***Keywords*:** Artificial Neural Networks, Defect Characterization, Thermal Signal Reconstruction, Infrared Thermography

Introduction

Thermographic Signal Reconstruction (TSR) is a processing technique that makes use of the one dimensional heat diffusion equation describing the surface temperature evolution in a semi-infinite sample after it has been thermally stimulated with a Dirac pulse [1]:

$$T = \frac{Q}{e\sqrt{\pi t}} \quad (1)$$

where *t* is the time, *e* is the material effusivity and *Q* is the input energy. This relationship can be rewritten in a double logarithmic form so that the time dependency of a pixel can be approximated with a polynomial having the following form [2]:

$$\ln[T(t)] = a_0 + a_1 \ln(t) + a_2 \ln^2(t) + ... + a_n \ln^n(t) \quad (2)$$

TSR provides good qualitative results [3] allowing the detection of defects, the reduction of data for processing and the filtration of high frequency noise. TSR can also be used for quantitative characterization since the logarithmic behaviors of the pixels that correspond to a defective area depart from the pseudo-linear behavior at a particular time that is correlated to the depth of the defect. TSR inversion capabilities can be improved by using Artificial Neural Networks (ANN) given their easiness of implementation, low sensibility to noise and abilities for learning and generalization [4], [5], [6], [7]. To illustrate this concept several Multilayer Perceptron (MLP) ANN were trained with the coefficients acquired after the application of the TSR to the thermogram sequences of several simulated glass plastic fiber samples with air defects. Simulated samples were designed using *ThermoCalc* software from Innovations Inc [8]. To train the ANN we used 20 samples of dimensions: 0.1m x 0.1m x 0.002 m, with defects dimensions: 8mm, 16mm and depths ranging from 0.3 to 1.7 mm. The polynomials degrees selected to train and validate the ARN were: 5, 6 and 7.

Results and discussion

Figure 1 shows the results of testing the trained ANN with a sample whose defects A, B, C, D, E have depths 0.1, 0.4, 0.7, 1, 1.3 mm, respectively. Figure 1a shows the validation results without noise, for this case 90.24 % of sound pixels and 92.9 % of defective pixels were correctly classified. Figure 1b corresponds to a validation set that was contaminated with Gaussian noise $\sigma = 0.039$ [4, p 88]. The results for this case show that noise strongly affects the ANN response producing erroneous estimations of defect depths. Moreover, increasing the *pd* (polynomial degree) makes the calculated coefficients more sensitive to noise. However, if reconstructed logarithmic temperature curves are used for training and validation instead of the polynomial coefficients, noise has a lesser impact on the results given the noise filtering capabilities of the polynomial fitting. Furthermore, data reduction is still possible since it is only necessary to keep the time vector and the polynomial coefficients obtained with TSR to generate the training and validation data sets. In addition, it is observed in figure 2b that the correlation between a defective pixel placed in the border of a defect (defect E, depth = 1.3 mm) and a sound pixel is smaller in the first time intervals (when the impact of thermal lateral diffusion is not so strong) for logarithmic temperature curves than for raw temperature curves. Figure 2a shows the validation results of an ANN trained with logarithmic temperature curves extracted from one sample whose defects A, B, C, D, E have depths 1.6, 1.7, 1.0, 1.8, 0.8 mm. Finally, in the paper this presentation will be also validated with experimental data.

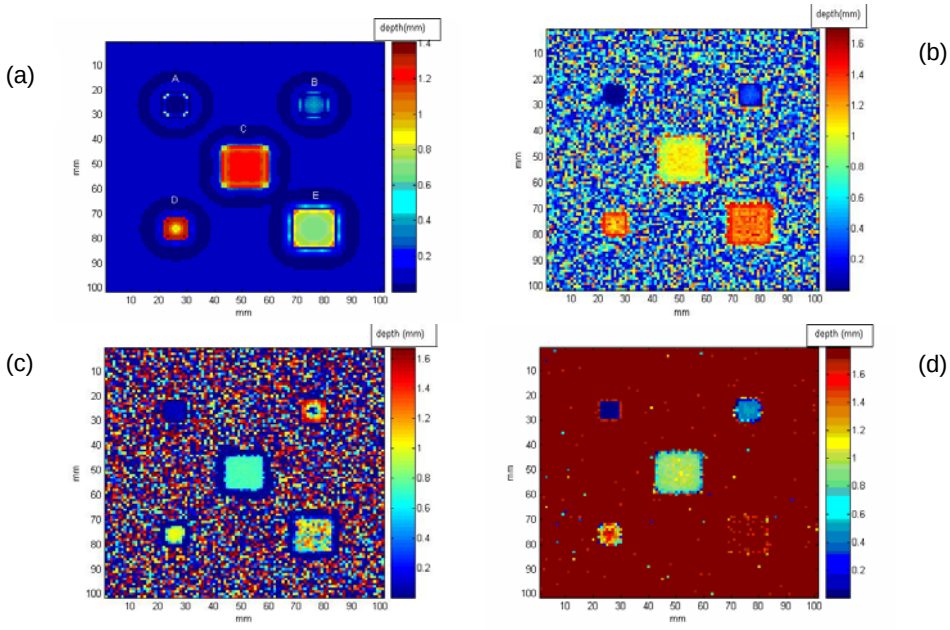

Figure 1 (a) ANN response to noiseless data (trained with pd = 5) (b) ARN response to noisy data pd = 5 (c) pd=6 (d) pd= 7

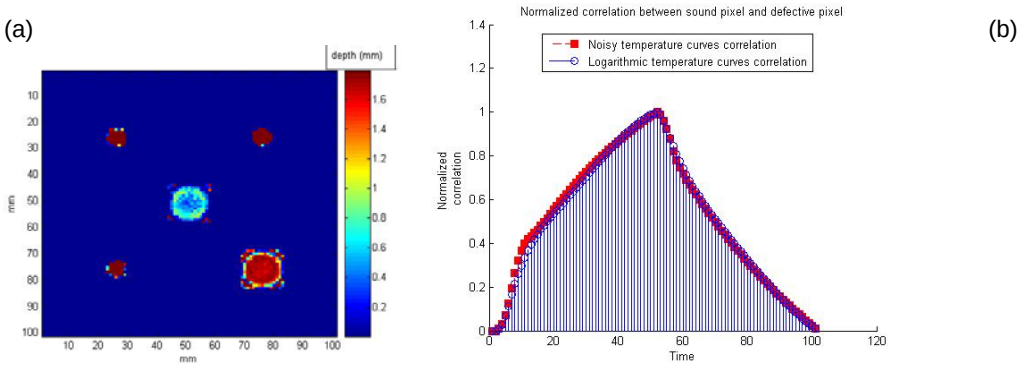

Figure 2. (a) Response of an ANN trained with logarithmic temperature curves to noisy data. Defect depths = 1.6, 1.7, 1.0, 1.8, 0.8 mm (b) Normalized correlations between a sound pixel and a defective pixel.

References

[1] Carslaw HS, Jaeger J C, "Conduction of Heat in Solids," Oxford University Press, 2nd edition, 1959.
[2] Steven M. Shepard, “Advances in pulsed thermography”, p. 511-515, Thermosense XXIII; Mar 2001.
[3] C. Ibarra-Castanedo, D. Gonzalez, M. Klein, M. Pilla, S. Vallerand, X. Maldague, ” Infrared image processing and data analysis “ Infrared Physics and Technology 2004.
[4] Darabi and X. Maldague, “Detection and Estimation of Defect Depth in Infrared Thermography Using Artificial Neural Networks and Fuzzy Logic”, PhD Thesis, Université Laval, 2000.
[5] Trétout .H et al ’An evaluation of artificial neural networks applied to infrared thermography inspection of composite aerospace structures’, Review of Progress in Quantitative Nondestructive Evaluation, Vol 14, 1995
[6] Santey M.B and Almond, M.B ”An artificial neural network interpreter for transient thermography data” NDT & E International Vol 30 No 5 pp 291-295, 1997.
[7] Bison P.G,Marinetti S, Manduchi G, Grinzato E, Improvement of Neural Networks performances in thermal NDE, in Advances in Signal Processing for Nondestructive Evaluation of Materials, 3rd Quebec Workshop(1997), Quebec 1998.
[8] Vavilov V – *ThermoCalc* Manual, 2004.

A neural approach for thermographic image analysis

T. D'Orazio[a] , M. Leo[a], A. Distante[a], V. Pianese[b], G. Borzacchiello[b], G. Cavaccini[b]

[a]CNR-ISSIA via Amendola 122/D-I, 70126 BARI ITALY

[b]Alenia Aeronautica v.le dell'Aeronautica, 80038 Pomigliano D'Arco (Napoli) ITALY

Keywords: Infrared thermography, internal defects, neural networks, defect classification

Preference: ORAL PRESENTATION

The problem of guarantying reliable and efficient safety checks has received great attention in recent years in aeronautic contexts: the maintenance operations, especially those applied on in-service aircraft, have to be reliable but also have to be performed at low cost in order to meet frequent schedules. In particular non destructive testing and evaluation (NDT&E) techniques are necessary to detect damage in high stressed and fatigue-loaded regions of the structure at early stage. Some of these NDT&E techniques are based on analysis of the transmission of different signals such as ultrasonics, acoustic emission, thermography, laser ultrasonic, X-radiography, eddy currents, shearography, and low frequency methods [1].

Transient thermography is a very promising technique for the analysis of aircraft composite materials [2]. It is a non-contact technique which uses the thermal gradient variation to inspect the internal properties of the investigated area: the materials are heated by some external source (lamps) and the resulting thermal transient is recorded using an infrared camera. Some research has been presented in the literature on the use of thermography to investigate aircraft components [3,4,5]. They have demonstrated the effectiveness of thermography in detecting internal defects and show excellent results on all the investigated samples.

Different qualitative approaches have been developed by many researchers to investigate the effects on thermographic images of a number of parameters such as: specimens of materials, defect types, depths of defect, size and thickness [6,7,8].

Quantitative approaches are attractive in the analysis of thermographic images because of the possible diagnosis capabilities that they introduce. They involve the solution of the direct problem, that is the computation of the expected response from known sound and defect materials, and the inverse problem, that is the evaluation of defect characteristics from a known response. Due to the nonlinear and non-univocal nature of these mapping problems, the solution is rather complex. For this reason some attempts using neural networks have started to emerge in the last few years [9,10,11].

In this paper we address the problem of developing an automatic system for the analysis of sequences of thermographic images to help the safety inspector when elaborating his diagnosis. Starting from the observation that composite materials have different behaviors during the transient phase of the thermographic inspection, we devised a neural approach that learns the main characteristics of these thermic evolutions and then uses them to classify the investigated area as a defective or sound area. The neural network classifiers were found to be particularly effective since they can easily implement the non linear mapping from an input feature space to an output space.

In this work three different composite materials were considered: they have a sandwich structure that differs both on the materials that compose the external and internal layers and for the geometrical form of the cell that is periodically repeated in the inner structure. When these materials are irradiated with high power lamps their surfaces have variable thermic gradients that can be recorded with a thermo-camera. The reflectivity time evolution of each pixel of the image differs between the three types of composite materials; but they also differ when some regions of the same material contain inner defects due, for example, to water intrusion or holes caused by impact. A supervised learning method was used to train the neural network to analyze the variations of these mono dimensional signals and to extract the main characteristics associated to different regions of the same materials. To reduce the effects of noise, a denoising algorithm has been applied to the initial signals. The neural network was trained to recognize different defects by using a sample set of image points. The whole system was tested on all the image pixels. Experimental results on the three composite materials demonstrate the effectiveness and the potential capabilities of the proposed approach. Besides varying light conditions have been simulated in order to demonstrate the ability of the proposed approach to generalize the results to different acquisition conditions. In figures 1,2 and 3 the results obtained on the three composite materials considered are shown.

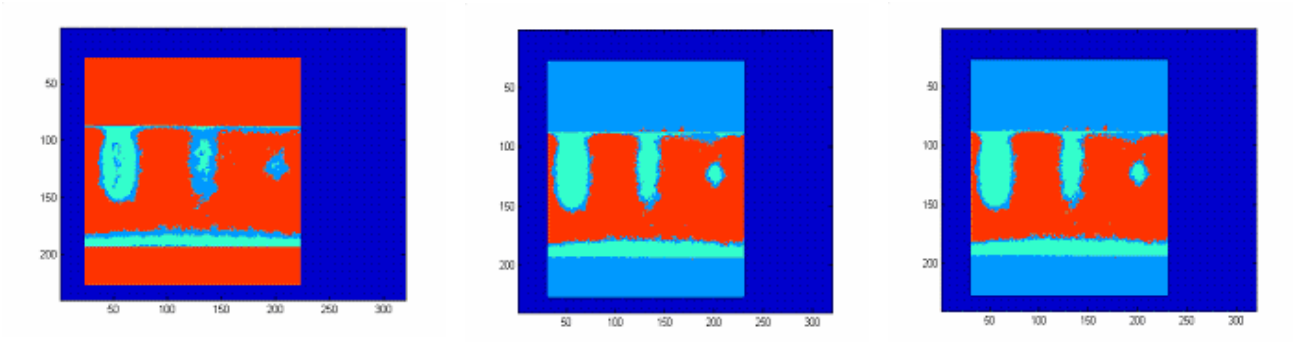

(a) **(b).** **(c)**

Figure 1- Nomex: (a) The classification results without any preprocessing (b) with a low pass filtering (c) with a normalization step.

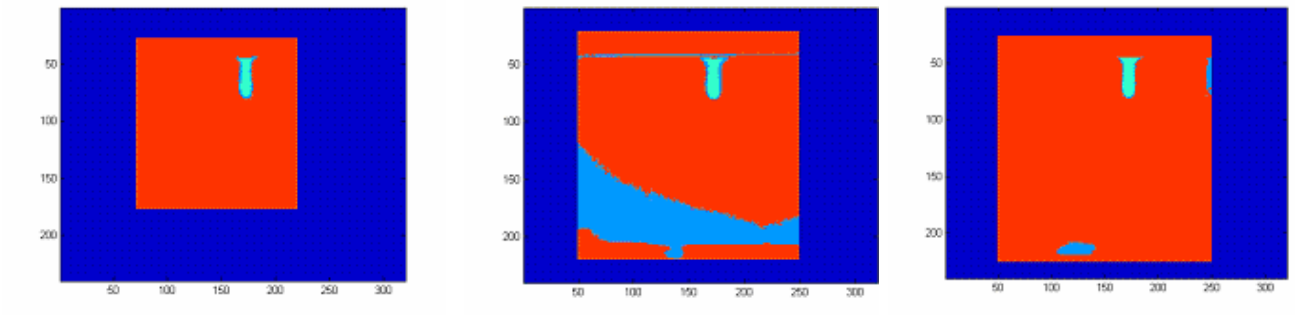

(a) **(b).** **(c)**

Figure 2- Syncore: (a) The classification results without any preprocessing (b) with a low pass filtering (c) with a normalization step.

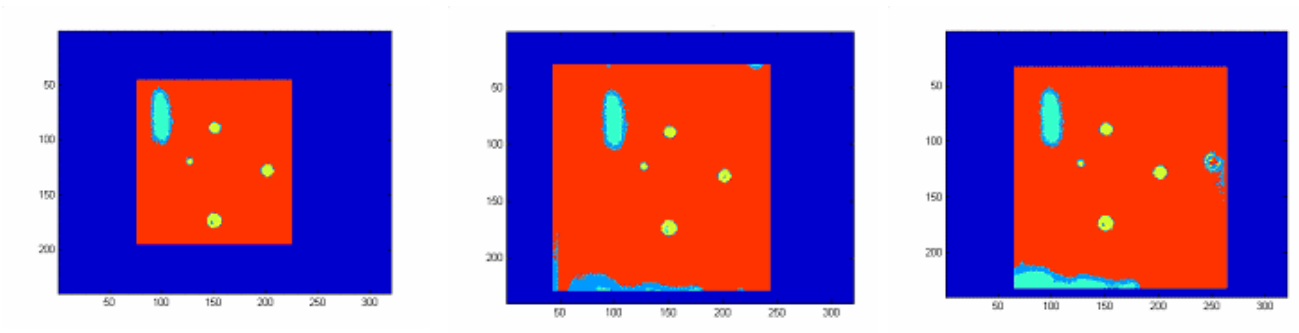

(a) **(b).** **(c)**

Figure 3- Honeycomb: (a) The classification results without any preprocessing (b) with a low pass filtering (c) with a normalization step.

References

[1] Y.D. Huang, L. Froyen, M. Wevers Quality Control and Nondestructive Test in Metal Matrix Composites. Journal of Nondestructive Evaluation, 2001; 20 (3): 113-132

[2] G. Gaussorgues, Infrared Thermography. Champan& Hall, 1994

[3] T.S. Jones, Infrared Thermographic evaluation of marine composite structures, SPIE Vol. 2459; 1995.

[4] N.P.Avdelidis, B.C. Hawtin, D.P. Almond. Transient thermography in the assessment of defects of aircraft composites. NDT & E Int. 2003; 36: 433-439.

[5] D.Wu, G. Busse. Lock-in thermography for nondestructive evaluation of materials. Rev. Gen. Therm. 1998; 37, 693-703.

[6] T. Sakagami, S. Kubo. Applications of pulse heating thermography and lock-in thermography to quantitative nondestructive evaluations. Infrared Physics & Technology. 2002; 43:211-218.

[7] G.Giorleo, C. Meola, A. Squillace, Analysis of Detective Carbon-Epoxy by Means of Lock-in Thermography. Res. NonDestr. Eval 2000, 241-250

[8]T. Inagaki, T. Ishii, T. Iwamoto On the NDT and E for the diagnosis of defects using infrared thermography. NDT & E Int. 1999; 32:247-257.

[9] X. Maldague, Yves Largouet, J.P. Couturier. A study of defect using neural networks in pulsed phase thermography: modeling, noise, experiments. 1998; 37:704-717.

[10] J.Y. Marin, H. Tretout. Advanced technology and processing tools for corrosion detection by infrared thermography. AITA- advanced Infrared Technology and Appliation 1999, 128-133.

[11] M.B.Saintey, D.P:Almond. An artificial neural network interpreter for transient thermography image data. NDT & E Int. 1997; 30(5):291-295.

Enhanced Reconstruction of Thermographic Signals for NDT

S.M. Shepard, Y.L. Hou, J.R. Lhota and T. Ahmed
Thermal Wave Imaging, Inc., 845 Livernois, Ferndale, MI 48220 USA
sshepard@thermalwave.com

Since its introduction in 2000, several independent investigations have confirmed the increased sensitivity and depth ranging capability of the Thermographic Signal Reconstruction (TSR) technique. In various studies, it has been applied to data from pulsed, pulse phase and modulated heating experiments, and in each case, the TSR results have outperformed raw or conventional processing results. Recent enhancements to the basic technique have resulted in further performance improvements. In particular, the enhanced TSR technique has optimized to accommodate data from noisy and nonlinear sources, such as uncooled IR cameras. The improvements also allow much higher measurement accuracy, and compensation for flash effects and residual heating. The high repeatability and predictability of TSR processed signals has also facilitated the development of true automated, non-visual processing, and decision-making based on individual pixel behavior in time, rather than image contrast.

With the TSR approach, the time history of each pixel is replaced by a low-order series approximation based on a least-squares fit after an appropriate scaling operation is performed (the particular scaling operation depends on the type of excitation that has been applied to the sample). In pulsed thermography, natural log scaling of both time and temperature result in a monotonically decreasing curve that approximates a straight line with slope –0.5, and deviates gently from linear behavior in the presence of a subsurface feature. A low order polynomial can be used to fit the logarithmic temperature curve to achieve an excellent replica of the original time history, with the added benefit of near-complete elimination of temporal noise and an order of magnitude reduction in the size of the data structure. Close comparison of an original image from the cooling sequence and its TSR replica reveals that the images are nearly identical, with the only difference being high spatial frequency noise that is not discernible to the eye of most observers. In other words, elimination of temporal noise, which seems like a worthy goal, may improve signal-to-noise, but does not necessarily improve the detectability (i.e. target to background contrast) that is most significant for NDT applications. Thus, simple viewing of reconstructed data is unlikely to result in any significant improvement in results for NDT applications.

The true significance of the TSR technique lies in the use of the time derivatives of the reconstructed logarithmic signal. The behavior of the 1^{st} and 2^{nd} derivatives is invariant with respect to variations in input energy, emissivity or typical gradients in excitation energy. Timing of the derivatives may be used to measure thermophysical properties, and the shape of the curves allows one to determine whether a point on the sample surface represents an intact or defective subsurface without referring to adjacent points (in fact, no image is required at all).

Abstract QIRT 2006:

Thermography applied to the evaluation of non-uniform deformation heat of metals.

J.Wullink, F.D. van den Berg, P.van Liempt.

Corus Research, Development &Technology
po box 10.000
1970CA IJmuiden, The Netherlands

Introduction

This report deals with digital filtering techniques to separate heat sources and heat diffusion effects in subsequent infrared images during plastic deformation of metals. Information about the deformation heat as a function of position and time of a sample under plastic deformation potentially indicates the degree of (non-) uniformity of the deformation process itself and of the metal microstructure after rolling and heat treatment. However, the raw, unfiltered infrared images suffer from blurring effects due to heat diffusion and therefore deformation heat effects are hard to distinguish. To overcome this problem, digital filters based on the heat diffusion equation have been implemented in Matlab®, which takes raw, 14 bit IR image sequences as input. The filter procedure is tested on a steel sample during plastic deformation with constant strain rate. The initiation and propagation process of deformation bands are clearly observed.

Background theory

The momentary local heat generated during plastic deformation is expressed in terms of stress and strain rate:

$$\dot{Q} = s\ \dot{e} \qquad [1]$$

The stress is a function of time and will be considered constant over the position on the sample, while the strain rate is generally a function of time and position. The infrared camera generates temperature data as a function of position and time. We can consider this as a 2 dimensional heat diffusion phenomenon as described by the partial differential equation:

$$\frac{\partial T}{\partial t} = \frac{k}{r\,C_p}\nabla^2 T + \frac{1}{r\,C_p}\dot{Q} \qquad [2]$$

Q= heat production per unit of volume.

The first two terms of [2] can be deduced from the IR measurement of T(x,y,t), hence the third term can be calculated, yielding a distribution of the locally produced heat density $\dot{Q}(x,y,t)$. A similar procedure on aluminium was reported in [1], with the exception that the nabla term was not taken into account.

Measurement set-up

The steel samples were mounted vertically in a tensile testing machine. The width is 20 mm and the surface was coated with a thin layer of ordinary flat black paint from a spray can in order to increase the amplitude of the infrared signal. The strain rate was set to 0.08 s^{-1} and frame rate of the infrared camera was set to 100 Hz. The spatial resolution in this set-up is 2 pixels/mm and the camera's integration time 1ms.

[1] "Some aspects of Portevin- Le Chatelier plastic instabilities investigated by infrared pyrometry", N.Ranc, D.Wagner, Materials Science&Engineering,2004.

Results

Figure 1 represents the result of the filtering of the series of infrared images. The left part is the raw temperature data (^{o}C), the right part shows the dQ/dt (W/m^{3}) images. The time step between the individual images in this series is 200 ms.

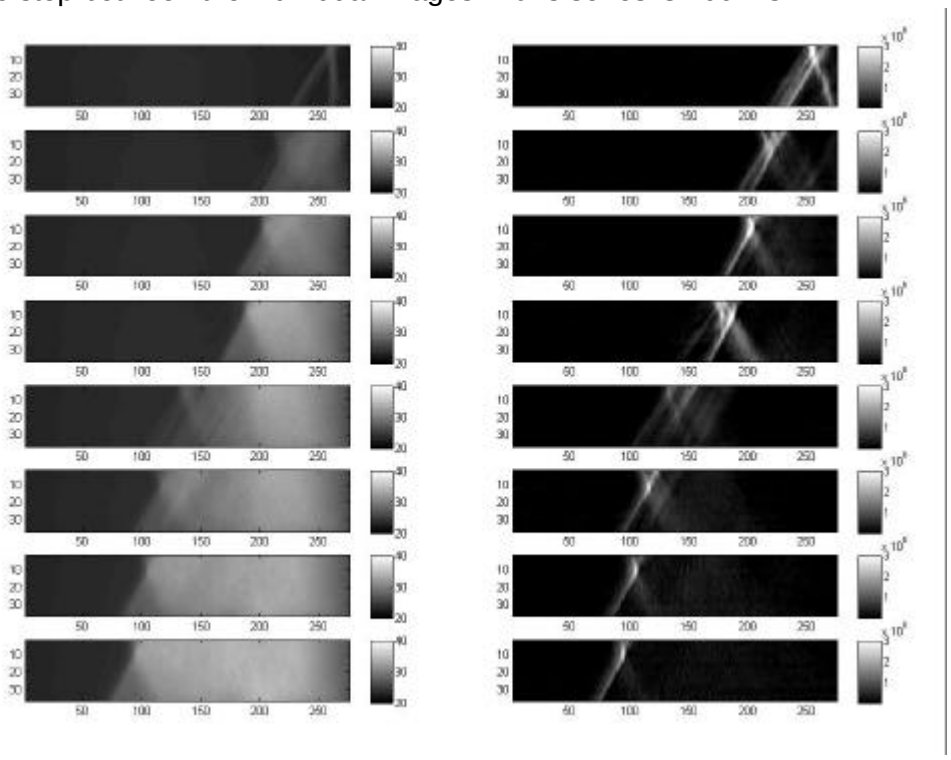

Figure 1: consecutive infrared images of the original (left) and the filtered (right).

From the filtered data, the position of the maximum value of dQ/dt as function of frame can be derived, as represented in figure2. From this curve 4 stages can be distinguished i.e. frame 0-110 (high average front speed), 110-270 (lower front speed), 270-340 (homogeneous deformation) and 350-450 (collapse of sample).

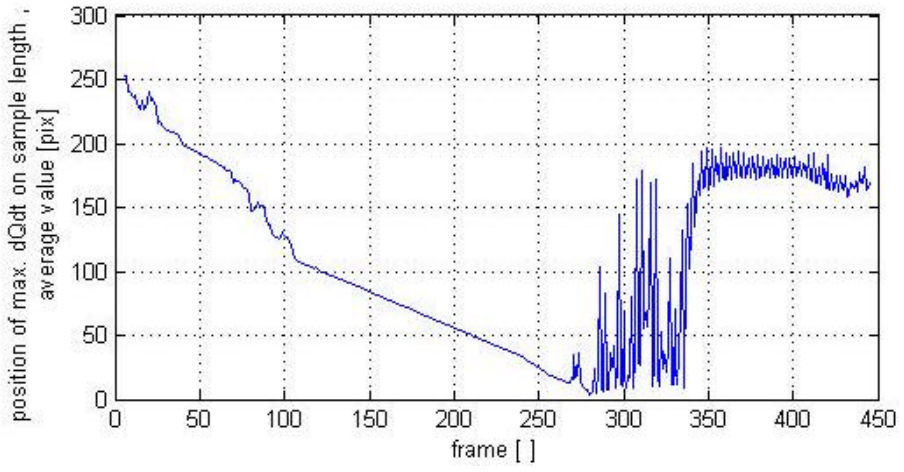

Figure 2: position of dQ/dt on the sample length as function of frame.

The degree of localization can now be computed from the maximum energy rate dQ/dt ,measured with IR camera and from the mechanical energy rate, measured by the tensile testing machine.

Phase contrast using Differentiated Absolute Contrast Method *

By Mirela Susa[1], Hernan Benitez[2], Clemente Ibarra-Castanedo[1], Humberto Loaiza[2], Xavier Maldague[1]

[1] msusa, IbarraC, maldagx@ gel.ulaval.ca

[2]hbenitez, hloaiza@univalle.edu.co

Université Laval, Canada, Phone: (418) 656-2962, Fax: (418) 656-3594

Universidad del Valle, Colombia, Phone: (57) 2 3391780,Fax:57 2 3392361

*Oral presentation is preferred, poster presentation is acceptable.

***Keywords*:** Pulsed phase thermography, Fast Fourier Transform, Differentiated Absolute Contrast Method, Defect Characterization, Infrared Thermography

Introduction

Pulsed Phase Thermography (PPT) [1] is a well known and established approach in active thermography that combines pulse stimulation thermography with the Fast Fourier Transform (FFT) to obtain phase and amplitude images. As proposed in [2], the blind frequency f_b, *i.e.* the maximum frequency at which the defect still can be seen from the phase contrast diagrams, can be used for defect depth extraction by means of the following equation derived form the thermal diffusion length, $\mu=(\alpha/\pi f)^{1/2}$:

$$z_{def} = C\sqrt{\frac{\alpha}{\pi \cdot f_b}} \tag{1}$$

where z_{def} is the defect depth, C is a correlation constant estimated from the experimental data and α is the diffusivity of the material.

Even though non-uniform heating, emissivity variations, reflections from the environment and surface geometry have less impact on phase than in raw thermal data [2], the difficulties regarding the proper choice of the sound area and the corresponding result uncertainties are still present, although at a lower degree than the thermal contrast-based counterparts. The Differential Absolute Contrast (DAC) method was proposed in [3] to avoid the need of a sound area definition. This technique is based on the well known 1D solution of the Fourier diffusion equation describing the surface temperature time evolution of a semi–infinite body after an energy Dirac pulse Q, has been applied:

$$T = \frac{Q}{e\sqrt{\pi t}} \tag{2}$$

where t is the time, $e=(k\rho c_P)^{1/2}$ is the material effusivity and Q is the input energy. Taking the thermogram obtained at the time t' right before the first defect becomes visible on the surface, and assuming that the injected energy over specimen is changing relatively smoothly, local values of Q/e can be extracted from

$$\frac{Q_{[i,j]}}{e_{[i,j]}} = \sqrt{\pi t'} \cdot \Delta T_{[i,j]}(t') \tag{3}$$

where $\Delta T_{[i,j]}(t')$ is the distribution of the sound area temperature at time t'.

Sound area temperature can be then calculated using Eqs. (2) and (3) from:

$$\Delta T_{s[i,j]}(t') = \sqrt{\frac{t'}{t}} \cdot \Delta T_{[i,j]}(t') \tag{4}$$

In order to avoid the impact of the sound area choice on the final results, we propose using the surface temperature distribution calculated from (4) as the ideal sound area temperature. PPT can then be applied to experimentally obtained temperature curves as well as on the calculated ideal sound area temperature. Phase images obtained from PPT for both thermal sequences can be now subtracted yielding in a phase contrast curves representing the difference in phase values in the frequency domain between the defective and non-defective sample area.

Results and discussion

Figure 1 shows an example of the data analysis obtained for a Carbon Fiber Reinforced Plastic Specimen, with the defect depths ranging from 0.2 to 1.0 mm and the defect size in range from 3 to 15 mm. The phasegram at frequency of 1.26Hz is shown. The sequence of acquired thermograms was obtained at the rate of 157 Hz with the 6.6 s of the overall acquisition time. Figures 2 (a) and (b) show the phase evolution in frequency domain, using the proposed method of calculating the sound region temperature distribution to obtain the phasegrams and applying the contrast analysis afterwards, and the standard phase contrast obtained from the same data, respectively. The phase curves of the defective area are shown in red, the non-defective areas are in black and their corresponding contrasts are in blue.

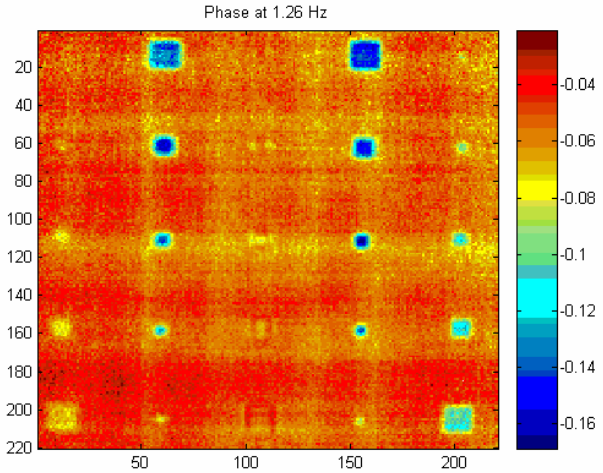

Figure 1. Phase diagram obtained from the acquired thermogram sequence for frequency of 1.26 Hz

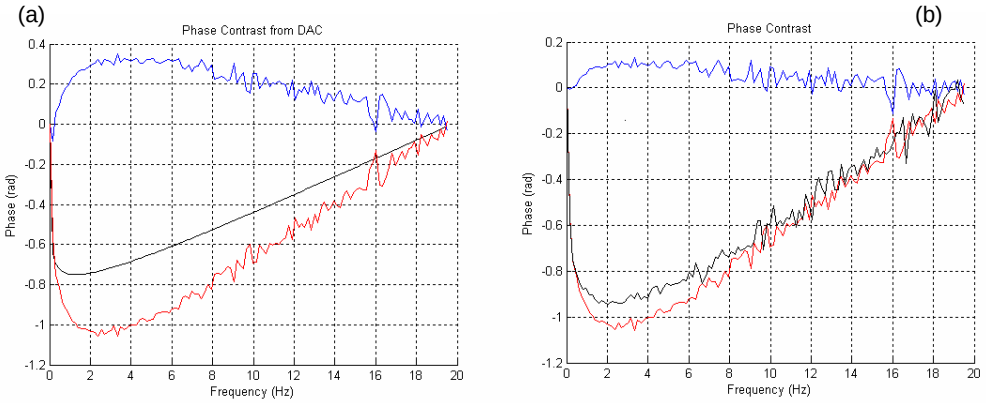

Figure 2. (a) Phase contrast diagram obtained using the FFT on the data obtained from Differential Absolute Contrast Method approach, (b) Phase contrast diagram for the same defective pixel using the standard Phase Contrast method

References

[1] Maldague X., Marinetti S.: *Pulsed phase infrared thermography*, Journal of Applied Physics, 79[5], 1996, 2694-2698

[2] C. Ibarra-Castanedo, "Quantitative Subsurface Defect Evaluation by Pulsed Phase Thermography: Depth Retrieval with the Phase", PhD Thesis, Université Laval, 2005

[3] M. Pilla, M. Klein, X. Maldague, A. Salerno, " New Absolute Contrast for Pulsed Thermography", Proc. of QIRT 2002, 53-58

[4] C. Ibarra-Castanedo, D. Gonzalez, M. Klein, M. Pilla, S. Vallerand, X. Maldague, " Infrared image processing and data analysis " Infrared Physics and Technology 2004.

[5] D.A. Gonzalez, C. Ibarra-Castanedo, M. Pilla , M. Klein, J.M. López-Higuera, X. Maldague, " Automatic Interpolated Differentiated Absolute Contrast Algorithm for the Analysis of Pulsed Thermographic Sequences", QIRT 2004

[6] Steven M. Shepard, "Advances in pulsed thermography", p. 511-515, Thermosense XXIII; Mar 2001.

A method to integrate thermographic data and 3D shapes for Diabetic Foot Disease

S. Colantonio[1], G. Pieri[1], O. Salvetti[1], M. Benvenuti[2], S. Barone[3], L. Carassale[4]

[1] Institute of Information Science and Technologies, ISTI-CNR, via Moruzzi 1, 56124 – Pisa, Italy
[2] TDGroup S.p.A., via Traversagna 48, 56010 – Migliarino Pisano (PI), Italy
[3] University of Pisa, Dept. of Mechanics, Nuclear and Production Engineering, via Diotisalvi 2, 56126 – Pisa, Italy
[4] Scansystems s.r.l., Via Giuntini 25, 56023 – Cascina (PI), Italy

Summary

Following the needs for a comprehensive visual analysis of objects under investigation and aiming to exploit two different technologies, like thermal imaging and three-dimensional model reconstruction, a specific project was carried on. In particular this project aimed at the reconstruction, visualisation, and data management of three-dimensional infrared volumes. The project was conducted within the frame of a collaboration between TD Group S.p.A., ISTI-CNR, University of Pisa, and the Diabetology Dept. at the “San Giovanni di Dio” Hospital in Florence.

Introduction

The goal of the project was the development of an integrated system for both the acquisition and processing of thermal images, as well as the modelling and three-dimensional reconstruction of objects. The system is aimed to be a support tool for the diagnosis and prognosis in the biomedical field. In particular the attention is focused on pathologies producing ulceration and laceration, for example that caused by an advanced diabetes condition like the Diabetic Foot Disease (DFD).
The analysis of absolute and relative temperature values can be a valuable support for an early diagnosis and the follow-up monitoring of diabetic patients. It is relevant that, when diabetes is well controlled it should be possible to avoid these foot problems, which can otherwise bring to the lower extremity amputation.
The designed system involves the realization of an acquisition tool for thermal images [1], and a tool for the visualization, registration, and management of three-dimensional reconstructed volumes.
In particular the 3D thermal image contains both the surface structure data, and surface temperature distribution. Both these characteristics support the evaluation of the ulceration, and the identification of anomalies or pathologic conditions.

Materials and Methods

The designed and implemented system is composed of three main parts:

- Multi-source (visible and infrared) image acquisition
- 3D reconstruction and registration of the acquired images, with the integration of the thermal data associated
- Data and images management, for the visualization of images and the addition of specific identification data

The acquisition system is composed of two stereo visible cameras, a synchronized thermocamera, and a structured light projector. The acquisition from the two stereo visible cameras allows a 3D reconstruction, obtaining a cloud of 3D points, which is obtained using well known reconstruction

algorithms. Furthermore a consistent triangular mesh is built, yielding the object surface in real colours [2].

Once the object is reconstructed an integration model is used to correctly classify each point of the 3D reconstructed mesh with its correct radiance value, acquired through the thermocamera. Thus a global 3D model of the investigated object is obtained, represented both with real colours, and synthesized colours obtained from the exact radiance values.
Following single 3D reconstructions, algorithms for multiple volumes registration are used to obtain a complete 3D object representation, the most possible close to the real object. This is very important to allow physicians to have a global look at the inspected object, in such a way that an optimal diagnosis or prognosis can be performed (e.g. all around views of the patient's foot).
Finally, a data management system allows the insertion and management of information related to the specific object under investigation (e.g. detailed patient identification data), together with the storage of previously reconstructed 3D volumes.

Results

A prototype of the system has been realized and final tests with 3D reconstruction integrated with the radiance values performed. Furthermore the registration of multiple acquisitions, from different points of view, of the same subject has been processed, and some very interesting results are shown (see Figure 1).

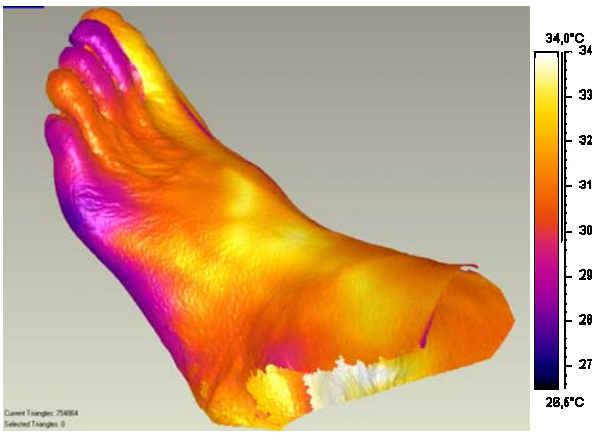

Figure 1: Example of 3D reconstruction integrated with thermal data.

The physicians confirmed that this prototype tool can be a valuable support in their work improving the quality of disease diagnosis and follow-up.

Acknowledgments

The authors would like to thank Dr. Cristiana Baggiore, head of the Diabetology Dept. at the Hospital "San Giovanni di Dio" in Florence, for her valuable help and assistance during the entire project and in particular during all the tests performed on case studies.

References

1. S. Colantonio, M.G. Di Bono, G. Pieri, O. Salvetti, M. Benvenuti, "Object tracking in a stereo and infrared vision system", Proceedings of the 8th Advanced Infrared Technologies and Applications Conference – AITA (Rome, Italy, 7-9 September), pp. 113, 2005.
2. C. Rocchini, P. Cignoni, F. Ganovelli, C. Montani, P. Pingi, R. Scopigno, "The Marching Intersections Algorithm for Merging Range Images", The Visual Computer, 20 (2-3), 149 – 164, 2004.

Quantitative 3d-Thermography

Wilhelm Satzger [1)], Günter Zenzinger[2)], Volker Carl[3)]

Key word: thermography, 3d-point cloud, texture, measurement

Presentation: Poster

Abstract: Thermography becomes increasingly important for industrial quality assurance. Until now thermography gives only coloured 2d – images. The colours indicate the temperature on the specimen's surface. However industry needs quantitative geometric data (position, size, etc. of defects). A thermographic image as every picture inevitably distorts geometric features since the third dimension is missing. For geometrically complex parts it is difficult or impossible to get reliable data of positions and sizes of defects etc. out of thermographic images alone.

The idea to get correct data is to fuse thermographic data and 3d – measurement data taken on a surface contour. The 3d – measurement delivers a so called point cloud, which represents (on a PC) in three dimension the specimen's surface without distortion. Standard 3d -software for point clouds can derive geometric entities like positions, length, areas, angles etc.

With such a fusion thermographic interesting areas can be marked on the point cloud and numerically processed.

The crucial step for this fusion is to put the thermographic camera into the 3d-scene and to measure the position and specimen together. In this way the metrical relation between the thermographic camera and the specimen is derivable. With this relation a kind of ray-tracing is possible, carrying the thermographic information at each pixel onto the point cloud.

To establish this metrical relation it is necessary to know photogrammetric features of the thermographic camera, the so called internal and external orientation. Till now these orientations are calculated / measured only for optical camera and it is by no means trivial that it works in the infrared regime. The internal orientation addresses distortion of the objective, principal point of objective, position of image (chip) plane, external orientation addresses position and orientation of the camera in space.

The 3d – measurement is done with fringe projection technique which generates a point cloud of a surface contour with approximately 500 000 3d-points in 30 seconds. Since not all pixel rays of the thermographic camera hit such a 3d-point interpolating steps are necessary.

The technique of texturing point clouds is not restricted to one point of view of the specimen. Different thermographic images can also be mapped back onto the point cloud. To do this without contradiction in an overlapping region normalized thermographic images are employed.

With the quantitative 3d-thermography it is possible to calculate the area of curved surfaces (e.g. turbine vanes) with a precision of 0.4 mm^2. It also turns out to be very helpful, to have a 3d- visualisation of the thermographic indications.

1) Wilhelm Satzger,
MTU Aero Engines GmbH,
Dachauer Str. 665
D-80995 Muenchen

Phone+ 49 89 14894693
Fax +49 89 14896414
e-mail wilhelm.satzger@muc.mtu.de

2) Günter Zenzinger,
MTU Aero Engines GmbH,
Dachauer Str. 665
D-80995 Muenchen

Phone+ 49 89 14895072
Fax +49 89 14896414
e-mail guenter.zenzinger@muc.mtu.de

3) Volker Carl,
T-ZfP V.Carl Messtechnik
Magnusstrasse 18
D-46535 Dinslaken

Phone+ 49 2064 603512
Fax +49 2064 603527
e-mail carl@t-zfp.de

Thermal characterization and kinetics analysis of reaction microfluidic medium by Infra-Red Thermography.

C. Pradère*, M. Joanicot*, J.C. Batsale**, J. Toutain**, C. Gourdon***

* Laboratoire du futur (LoF), FRE 2771 : CNRS-Rhodia, 178 avenue du Docteur Schweitzer, 33608 Pessac.
** Laboratoire interétablissements Transferts Ecoulements Fluides et Energétique (TREFLE), UMR 8508 : CNRS-ENSAM-UB1, Esplanade des Arts et Métiers, 33405 Talence.
*** Laboratoire de génie chimique (LGC), UMR 5503 : CNRS-INP-UPS, BP 1301, 5 rue Paulin Talabot, 31106 Toulouse Cedex 1.

One of the new ways of research is the use of infra-red camera to obtain the local field of microfluidic temperature of the system to deduce some from the thermophysical cartographies of properties. One of the first aspects of this work consists in developing an experimental device likely to measure the fields of temperature and/or flux of microfluidic systems for various type of flow: co-flows or droplets. The idea is to be able to provide quickly, for a given concentration and an imposed flow, the profiles space and temporal of the source term in the case of chemical reaction.

Manufacture of the micro systems (*figure 1*). A micro system is seen in the case of reaction medium as a means to carry out micro reactors where the chemicals products are under flow. The description of the manufacturing process using an elastomer (polydimethylsilexane, PDMS) is detailed [1]. This is a simple and inexpensive means of manufacture of microfluidic chip. Moreover, it is significant to stress that the photolithography allows a great diversity in term of manufacture of micro network. Characteristic dimension of the micro channels used goes from 10 to 1000 µm of depth and width. That generates volumes going of 1 nl to 10 µl per centimeter of channel.

Experimental device (*figure 2*). The device is simple; it is a question of placing in front of the camera and at the good focal distance the microfluidic chip (*figure 1*). The latter is fed in chemical (here acid-bases) using growths syringes making it possible to deliver flows going from 0.01 µl/h to 10 ml/min. The infra-red camera (CEDIP) is equipped with a InSb detector (1.9-5.3 µm, 7.8mm²) and with a germanium objective (focal distance 25 mm).

First results (*figure 3*). A first series of measurements was carried out on the microfluidic chip (*figure 1*) with a chemical reaction between a strong acid (HCl) and a strong base (NaOH) proportioned with 0.5 M. The dimension of the microreactor is: width 250 µm, thickness 50 µm and length 32 cm. The flow is co-flow type, i.e. the mixture is carried out by molecular diffusion. Various flows were imposed on the system and the field of permanent temperature speed range was measured (*figure 3*: *a, 100 µl/h, b, 500 µl/h and c, 2000 µl/h*). The results obtained show that with low flow, the reaction is quasi instantaneous (beginning at the injection) and that for the most important flow (2000 µl/h) a zone of mixture by diffusion clearly appears. In all the cases, a very intense zone (more or less significant) where the reaction develops is highlighted. And finally, a zone where the reaction (or source term) dies out is also visible. Thus, knowing the space distribution of the source term as well as the rate of the flow, it is possible to go up with the kinetics of the chemical reaction. However, the convection between the fluid and the walls must be studied as a preliminary, this is why a measurement consisting in exciting locally (laser beam or Joule effect) of water circulating with various flows and measuring the response in temperature and under development.

Simple image processing. One of the interests of this kind of experiment is to be able to estimate the heat flux spatial distribution from the temperature observation. With this simple assumption (adiabatic channel) the relation ship flux and temperature gives: $\rho C V \frac{dT(x)}{dx} \pi R^2 = \Phi(x) - 2\pi R h\left(T(x) - T_0\right)$

Such expression is easily related to the time evolution of chemical reaction.

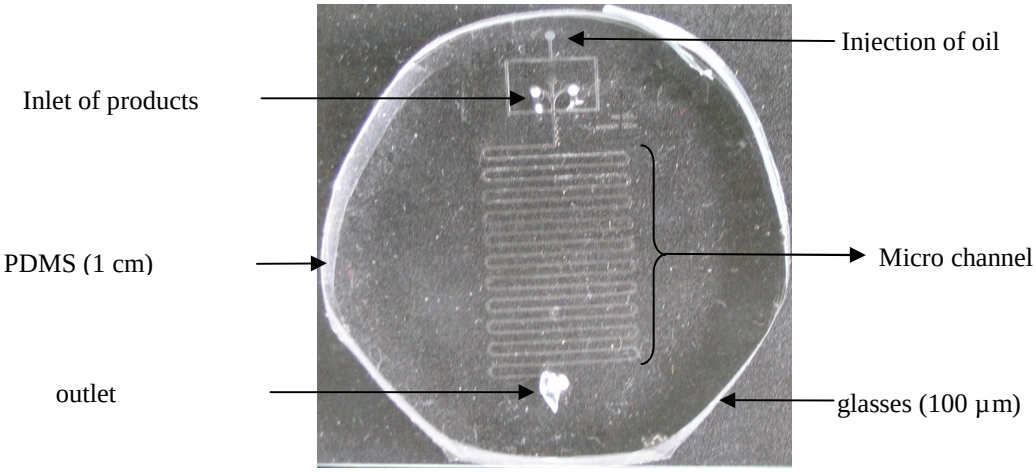

Figure 1 : Photography of microfluidic system

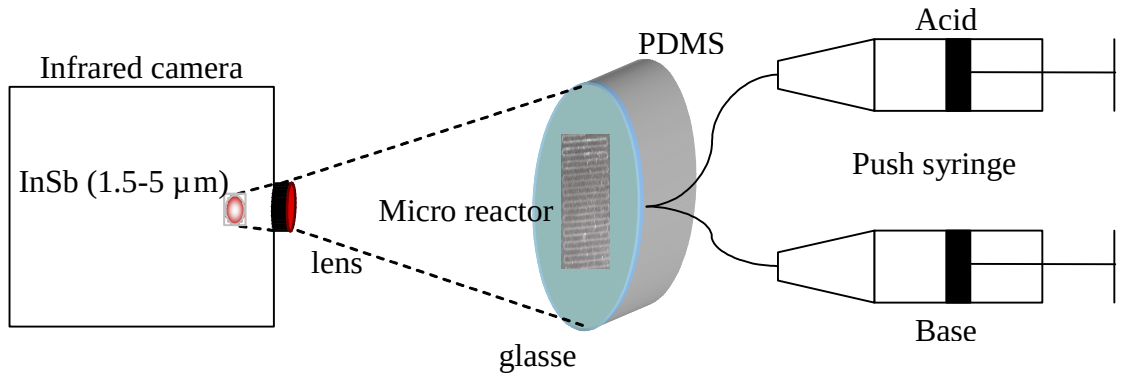

Figure 2 : Scheme of experimental device

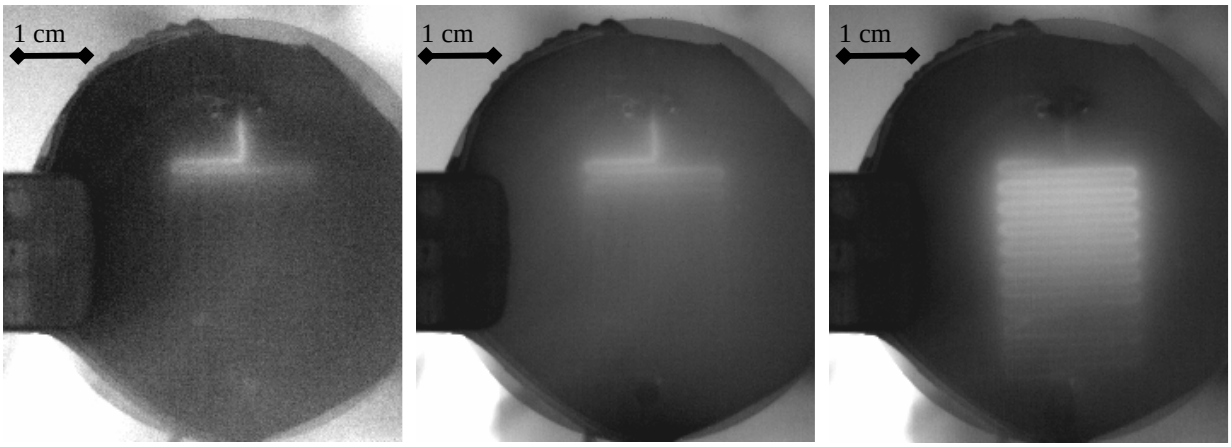

Figure 3 : acide-base reaction in co-flow at various rate ; (a) 100 µl/h, (b) 500 µl/h, (c) 2000 µl/h

[1] D.C. Duffy, J.C. McDonald, Olivier J.A. Schueller, George M. Whitesides, Anal. Chem., 70, p 4974-4984, 1998.

Experimental study of the Heat Transfer Coefficient distribution in a single finned tube model: effect of fin spacing and flow velocity

M. Sanhaji, D. Bougeard, A. El abbadi, M. Nacer bey, S. Russeil, B. Baudoin.

Ecole des Mines de Douai, Département Energétique Industrielle,
941, rue Charles Bourseul, B.P 838, .59508 DOUAI, Cedex, France,
e-mail: sanhaji@ensm-douai.fr

Abstract. This study presents a confrontation between the flow structure and the related heat transfer over single finned tube heat exchangers. We analyze both flow velocity and fin spacing effects on local heat transfer coefficient distribution around a single finned tube. A large number of experimental works has been performed for both flow structure and heat transfer around a finned tube [1][2][3][4]. However, the flow structure and its impact on the heat transfer characteristics are still needed to be investigated. This has motivated the present study. Both horseshoe vortices upstream the tube and the wake developed downstream it were investigated. The thermal results are confronted to dynamic data.

The fluid mechanics features upstream, around, and downstream the tubes are investigated using a PIV techniques [4]. Quantitative infrared measurements of convection heat transfer coefficient using an inverse method [5] are carried out. Results are analyzed and correlations are highlighted in order to understand convection heat transfer mechanisms in such configurations.

The infrared set-up consists in a small wind tunnel with a single finned tube test model. The method deduces the heat transfer coefficient by means of the local time variation of surface temperature of the fin.

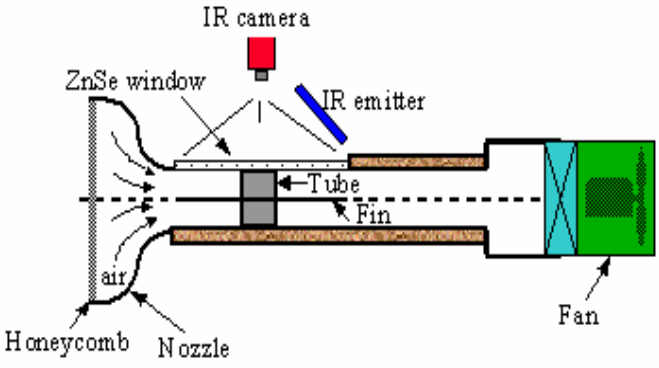

Fig 1. Experimental bench for local heat

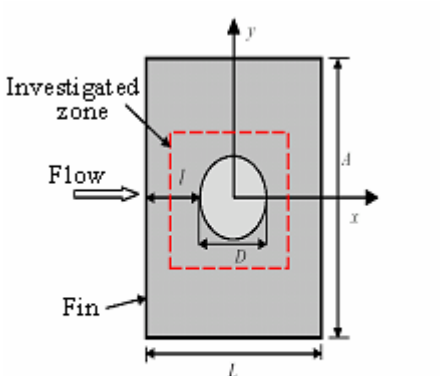

Fig 2. Geometry tested : Top view of a plate-finned Tube

The plate-finned tube model, same as in[4], consists of a single tube passing trough two spaced parallel fins (figure 2). First of all, the fin spacing E/D was fixed equal to 0.2 and flow measurements were performed for Reynolds numbers between 410 and 2740. Thereafter, distance between the fins was varied for a constant Reynolds number of 2270. Four fin spacings were investigated, E/D = 0.13, 0.2, 0.27 and 0.34.

Typical results are shown in figure 3 where local heat transfer coefficient field was confronted to M.N.Bey [4] results as shown in figure 3, in order to explain h_{cv} variations upstream and downstream the tube.

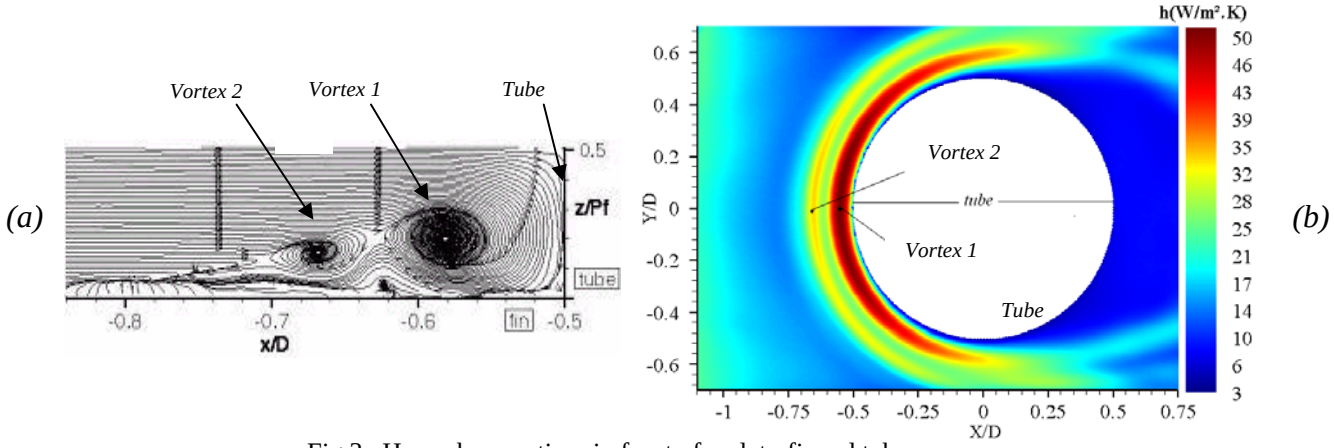

Fig 3. Horseshoe vortices in front of a plate-finned tube.
(a) lignes de courant, (b) Heat transfer coefficient

References :

[1] U. Bossel and F.V. Honnold. On the formation of horseshoe vortices in plane fin heat exchangers. Archives of mechanics, 28 : 773-780,1976.

[2] G. Schüz and V. Kottke. Visualization of flow, heat and mass transfer on finned tubes in cross flow. 4th Int. Symposium Paris, pages 637-642, 1987

[3] Z.Q. Chen and J.X. Ren. Effect of fin spacing on the heat transfer and pressure drop of a two-row plate fin and tube heat exchanger. Int. Journal Refrigeration, 11, November 1988.

[4] M.N.Bey. Etude expérimentale des caractéristiques des structures tourbillonnaires se développant dans les échangeurs de chaleur à tubes et ailettes planes continues. Thèse de Doctorat, Université de valenciennes, Ecole des mines de Douai, 2004

[5] A. El abbadi, D. Bougeard et B.Baudoin. Local Heat Transfer Coefficient Measurements, Using a Transient Imaging Method With an Inverse Scheme , 7th International Conference on Quantitative Infrared Thermography, (QIRT'2004), Von Kármán Institute, Belgique, juillet 2004

Infrared thermography for shear stress field measurements in flows

J. Pirisinu, G. L. Rossi

Dipartimento di Ingegneria Industriale – Università di Perugia
Via Duranti, 1 – I 06125 PERUGIA - ITALY

Abstract

Keywords: boundary layer, infrared thermography applications, subsonic flows, passive technique, shear stress measurement

In thermo-fluid-dynamics, it is known the important role played by boundary layer. Therefore, the present paper wants to dwell on the possibility to enlarge the application of infrared measurement technique, in particular for subsonic flows analysis. Subsonic flows point out important problems of measurement for the low energy content. In order to overcome this drawback, a high thermal resolution camera has been chosen and used. Moreover it has been experimentally characterized in order to define its modulation transfer function and to provide a tool for data restoration. Tests have been carried out in a subsonic no-cooled closed circuit wind tunnel. That is, during the start-up of facility, a natural air heating is produced by exchange with fan. However, the latter is not localized and equal to few degrees during the whole run. In this way, problems own of active technique are avoided and measurement can be performed in subsonic flows in a way called passive technique. A new theoretical model has also been defined to correlate superficial body temperature maps to convective coefficient distribution and therefore to shear stress field. It has been pointed out for semi-infinite slab in thermal transient conditions and for a continuous convective exchange between air and body. As test case of the proposed measurement methodology a Fokker airfoil was used. Results are presented in this paper for zero angle of attach.
In all aerodynamic aspects, the boundary layer plays a fundamental role. It affects the performances of each body immersed in a fluid in terms of drag and lift. Firstly boundary layer inspection was performed in supersonic vehicle optimization. Later, the growth of fuel prizes moved the interest towards new aspects as the possibility to enhance performances for a power plant or to reduce the flight fuel consumption. Nowadays, the horizons are changed and widened again and some of the aims could be represented by a faster race car or less time for travelling in train. In order to set up an experimental tool, able to analyse the boundary layer, many efforts have been done and some advanced measurements techniques have been developed. Possible experimental chains make use of traditional or advanced methods.

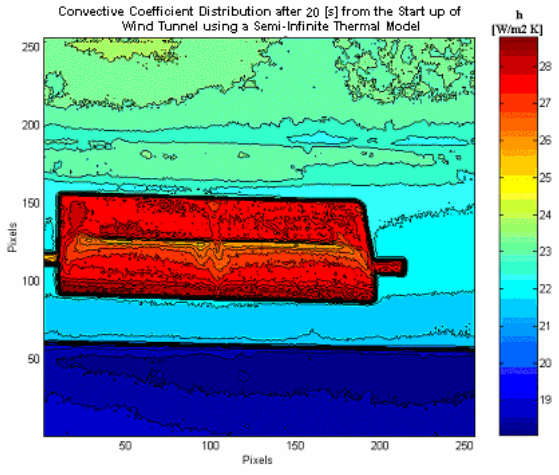

Figure 1: A typical convective coefficient map obtained

The formers, as with Stanton tubes, are very intrusive and they point out only punctual information. Moreover, their application in turbulent fields is quite inaccurate and it does not produce reliable data [1]. Otherwise, advanced techniques make use of pressure sensitive paints (PSP) [2], temperature sensitive paints (TSP) [2], shear sensitive liquid crystals (SSLC) [3] or oil film interferometry [4]. They are non-intrusive and carry out bi-dimensional maps, but they are very time-consuming and difficult to be performed outside a controlled ambient, as in a laboratory. Since mid-sixties, the use of infrared thermography has started too. Primarily, this technique was used in space missions. Indeed it was fundamental to protect the space shuttle in the re-entry phase. Therefore, special materials were tested to verify their capability to resist to these mechanical and thermal stresses. Later, it became to be wider and wider applied in all the aforementioned sectors. Nowadays it is one of the most advanced measurements and fuses the positive aspects of traditional and advanced measurements; indeed it could be set in hostile ambient, if properly employed, no time-consuming and it performs a non-intrusive measurement of thermal surface distribution, caused by interaction between fluid and body [5]. These maps get information about boundary layer and can be reduced in convective coefficient distributions by an ad hoc thermal model or, using the following Reynolds' analogy, in any parameter of interest for aerodynamic aspects.

$$\frac{Nu_x}{Re_x \; Pr} = \frac{C_{fx}}{2} \quad (1)$$

In particular, as described in [6], assuming Pr = 1, eq. (2) gives rise to the following linear relationship between convective and skin friction coefficients.

$$C_{fx} = 2 \cdot \frac{\nu \cdot h_x}{c \cdot k} \quad (2)$$

An example of results obtained is given in fig 1. In the paper detail of the measurement and processing techniques used to obtain this kind of results are given.

References

[1] "Fluid Mechanics Measurements", R. J. Goldstein, 1983, Hemisphere Publishing Corporation.

[2] J. Sullivan, "Temperature and Pressure Sensitive Paint", Lecture Series on "Advanced Measurement Techniques", Von Karman Institute for Fluid Dynamics, 2001-01.

[3] D. C. Reda, M. C. Wilder "The Shear Stress Liquid Crystal Coating Method: Measurement of Continuous Surface Shear Stress Vector Distributions", Lecture Series on "Advanced Measurement Techniques", Von Karman Institute for Fluid Dynamics, 2001-01.

[4] D.M. Driver, "Oil Film Interferometry Technique for Measuring Skin-Friction", Lecture Series on "Advanced Measurement Techniques", Von Karman Institute for Fluid Dynamics, 2001-01.

[5] E. Gartenberg, A. S. Roberts Jr., "Twenty-Five Years of Aerodynamics Research with Infrared Imaging", Journal of Aircraft, Vol.29, No2, March-April 1992.

[6] E. Gartenberg, A. S. Roberts, Jr. Griffith, G. J. McRee, "Infrared Imaging and Tufts Studies of Boundary Layer Flow Regimes on a NACA 0012 Airfoil", CH2762-3/89/0000-0168, 1989 IEEE

[7] T. Astarita, G. Cardone, G. M. Carlomagno, C. Meola, "A survey on Infrared Thermography for Convective Heat Transfer Measurement", Optics & Laser Technology, Elsevier Science 2001.

Utilization of the infrared thermography to identify the convective heat transfer coefficient into a rotating cylinder with an axial airflow

S. SEGHIR-OUALI[1, 3], D. SAURY[1], S. HARMAND[1, 3], O. PHILLIPART[2], D. LALOY[2, 3]

[1] Laboratoire de Mécanique et Energétique Université de Valenciennes et du Hainaut-Cambrésis
Le Mont Houy, 59313 Valenciennes CEDEX 9 France

[2] FRAMATOME-ANP/Jeumont, F59573 Jeumont BP 189 France

[3] *CENTRE NATIONAL DE RECHERCHE TECHNOLOGIQUE - FUTURELEC 2*

Extended abstract :

The rotating electric machines are subject to very severe heating resulting from electric losses reigning in their different parts. To maintain the correct usage of a motor it is necessary to have perfectly designed cooling systems. In absence of cooling, materials used are unable to sustain, without damage, the temperature levels obtained during usage. Heating problems into such machines remain alarming in spite of numerous progresses made for their design. In order to avoid this warming, the cooling systems allowing to dissipate the heat flux in the ambient environment have to be take into account in the optimized design of such machines. Keeping this aim in mind, we present an experimental technique allowing to identify the convective heat transfer coefficient inside a rotating cylinder with an axial airflow. This empty cylinder models the rotor of the motor. The method used consists in heating the external face of the cylinder using infrared lamps, and acquiring the evolution of the external surface temperature with time using an infrared camera.

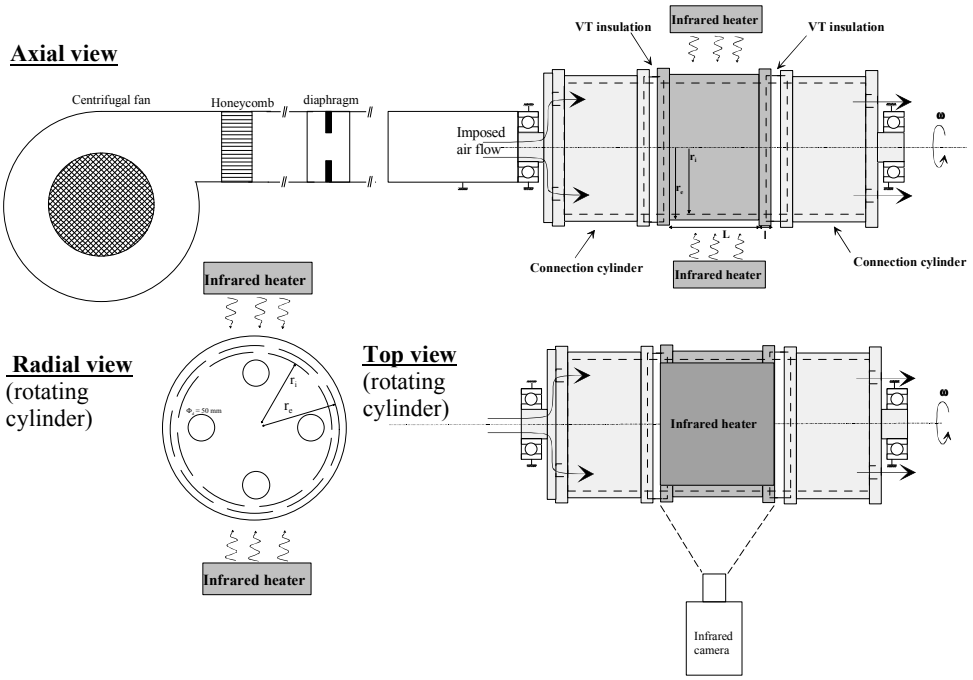

Figure 1: Scheme of the experimental setup

The figure 1 presents the experimental setup. The rotating part is composed of three cylinders made of steel and separated by an insulation in vetronite epoxy (VT) whose conductivity λ_{VT} is 0.3 W/m K. These cylinders are concentric and reamed together to obtain a perfect interior surface quality. The 198 mm length central cylinder corresponds to the studied area. The internal and external diameters of the studied cylinders are respectively 393 and 403 mm. The two 330 mm length cylinders surrounding the central cylinder are used to avoid the too disturbed phenomena at the inlet and the outlet, the insulation in VT being used to minimize the thermal losses of the studied zone towards the two cylinders of connection. The external face of the studied zone is heated with two fixed infrared transmitters located above and below the rotating part and connected to a power regulator. The power supply to the heat transmitters can be regulated manually between 0 and 4 kW. An electric motor associated to a variable speed transmission drives the cylinder up to 1000 rpm. The rotating part is connected to the static part with two ball bearings assembled in ball self-aligning bearing. The static part is composed by a centrifugal ventilator connected to the revolving part with a 1.3 m length pipe on which a diaphragm is placed. The ventilator imposes an air flow in the test bench from 0 to about 530 m^3/h. Upstream and downstream the diaphragm, two pressure tappings are placed and let know the air flow rate in the test bench. The airflow provides by the ventilator to the revolving part impacts on a flask tapped with 4 holes of 50 mm of diameter equally distributed. The impact zone is in a small plenum chamber. The air from the ventilator enters into the rotating part via the

plenum chamber, flows through the first cylinder used to homogenize the velocity profiles, then it flows through the studied area, and finally through the last cylinder before flowing by the outlet flask which is identical to the inlet flask.

Heat transfer coefficients are then identified using three methods. The first one is based on an inverse model, the second one assumes the wall of the cylinder as a thermally thin wall and the third one is based on an analytical method letting obtain the temperature field into the whole cylinder. Whatever the method used, they are all based on the knowledge of the temperature of the external surface of the cylinder. Infrared thermography is used to obtain this quantity. The surface temperature of the cylinder is obtained using a short wavelength infrared camera (2 to 5.4 µm) equipped with a 20° lens. This camera gives a signal I(T) for a black body surface at the temperature T observed through a transparent environment. During measurement, the camera returns a digital signal coming from an elementary surface of the flat plate. This signal is attenuated by the atmosphere. This signal also takes into account radiation of the environment which reflects itself on the cylinder. In order to improve the part of radiative heat flux emit by the cylinder, this plate is painted in black in order to increase its emissivity. The emissivity of the black painted surface, determined by calibration, is then 0.93±0.02. A second calibration allows to connect, in a real situation, the signal intensity I(T) to the real temperature of the cylinder. The temperature uncertainty is estimated to $\Delta T=\pm 0.3$ °C for a range of temperature varying from 30 to 130 °C. The air temperature in the test room is measured using two type K thermocouples. The absolute error on this temperature is about $\Delta T=\pm 0.5$ °C.

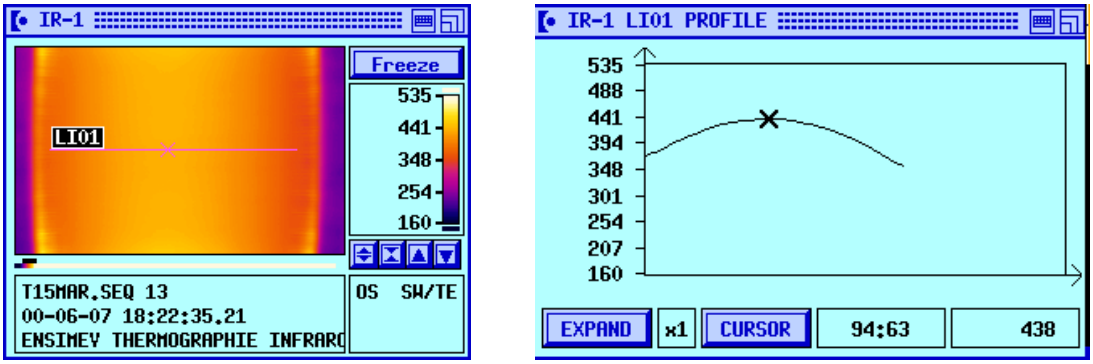

Figure 2: Example of profile obtained with the infrared camera

The experiments were carried out for a rotational speed ranging between 4 and 880 rpm corresponding to rotational Reynolds numbers varying from 1.6×10^3 to 4.7×10^5 and an air flow rate varying from 0 to 530 m^3/h which corresponds to an axial Reynolds numbers ranging from 0 to 3×10^4.

Figures 3 and 4 present respectively an example of temperature profile and its fitting obtained using infrared thermography and an example of the evolution of the internal convective heat transfer coefficient.

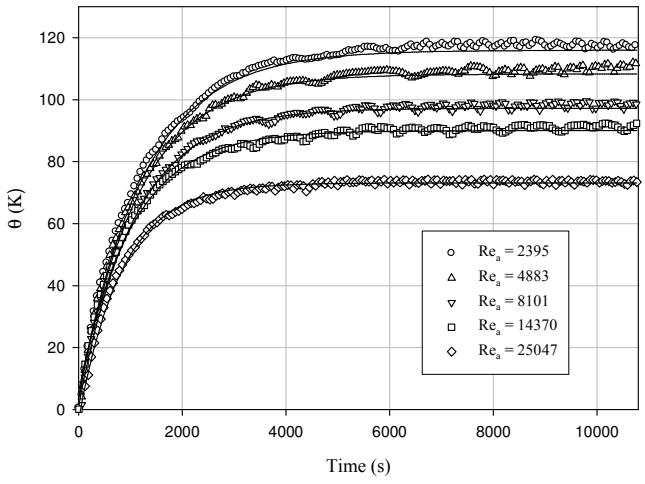

Figure 3: Evolution of the temperature on the external surface of the cylinder with the axial air flow

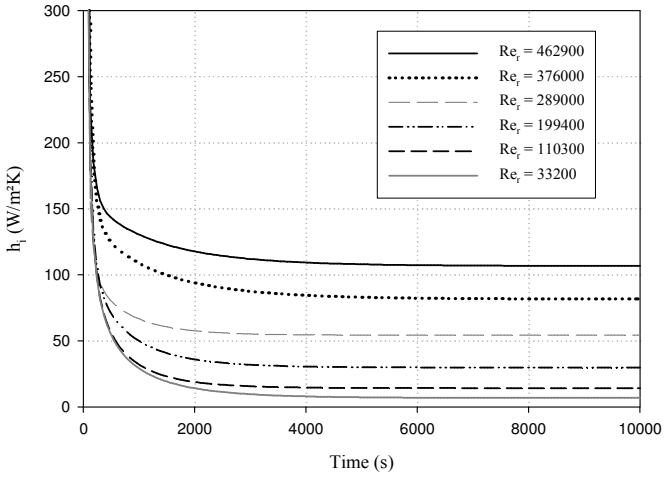

Figure 4: Evolution of the internal convective heat transfer coefficient

Heat Transfer Measurements in Rotating Channel

M. Gallo[*]*, T. Astarita, and G.M. Carlomagno*
University of Naples – DETEC
P.le Tecchio, 80 – 80125 Naples, ITALY
Tel. +39 81 7683389; Fax +39 81 2390364
[*]*Corresponding author. e-mail: maugallo@unina.it*

Keywords: Rotating channel, Infrared thermography, Gas turbine

Abstract

The thermal efficiency of gas turbine engines strongly depends on the gas entry temperature; the higher this temperature, the more efficient is the turbine thermal cycle. Present advanced gas turbines operate at gas entry temperatures much higher than metal creeping temperatures and therefore require intensive cooling of their blades especially in the first stages. A way of cooling turbine blades is by means of internal forced convection: generally, cooling air from the compressor is supplied through the hub section into the blade interior and, after flowing through a serpentine passage, is discharged at the blade trailing edge.

The serpentine passage is mostly made of several adjacent straight ducts, spanwise aligned, which are connected by 180deg turns. The presence of these turns causes flow separations and reattachments and induces secondary flows; the overall effect is that the convective heat transfer coefficient exhibits an increase associated with high local variations and with consequent increased thermal stresses in the blade wall.

The aim of this paper is the study of convective heat transfer coefficient distribution in a rotating channel by using Infrared Thermography and the *Heated Thin Foil* heat flux sensor. As shown in Fig. 1 a plexiglas channel with a sharp 180° turn is mounted on a revolving platform connected, by means of a transmission belt, to an electric motor; by using an inverter it is possible to vary in a continuous way the platform rotational speed. The channel cross section is 60*mm* wide and 60*mm* high. The length ahead of the 180deg turn, which is 1200*mm*, ensures an almost hydro-dynamically fully developed flow before the turn. The central partition wall, which divides the two adjacent ducts, is 12*mm* thick.

In order to use the *Heated Thin Foil* heat flux sensor one of the walls, in the test region, is made of a printed circuit board. The printed circuit is designed so as to achieve a constant heat flux over the whole surface (except beneath the partition wall) by Joule effect. The tracks are 5*mm* thick, 2.9*mm* wide and placed at 3*mm* pitches; the overall thickness of the board is 0.5*mm*. The length of the printed circuit board in the entrance duct (600*mm*) ensures an almost thermally fully developed flow before the turn. A stabilised DC power source supplies the electric current to the circuit and the power input is monitored by precisely measuring voltage drop and current across it. The external (to channel) surface of the printed circuit board, which is viewed by the infrared camera, is coated with a thin layer of black paint which has emissivity coefficient equal to 0.95 in the wavelength of interest.

Water, which is used as a working fluid, is aspirated from a tank by a pump, then passes through an orifice flow meter and then, after flowing in the test channel, is discharged again in the tank; the mass flow rate is regulated in continuous way by a by-

pass circuit and the water temperature is maintained constant by means of a control circuit and a heat exchanger.

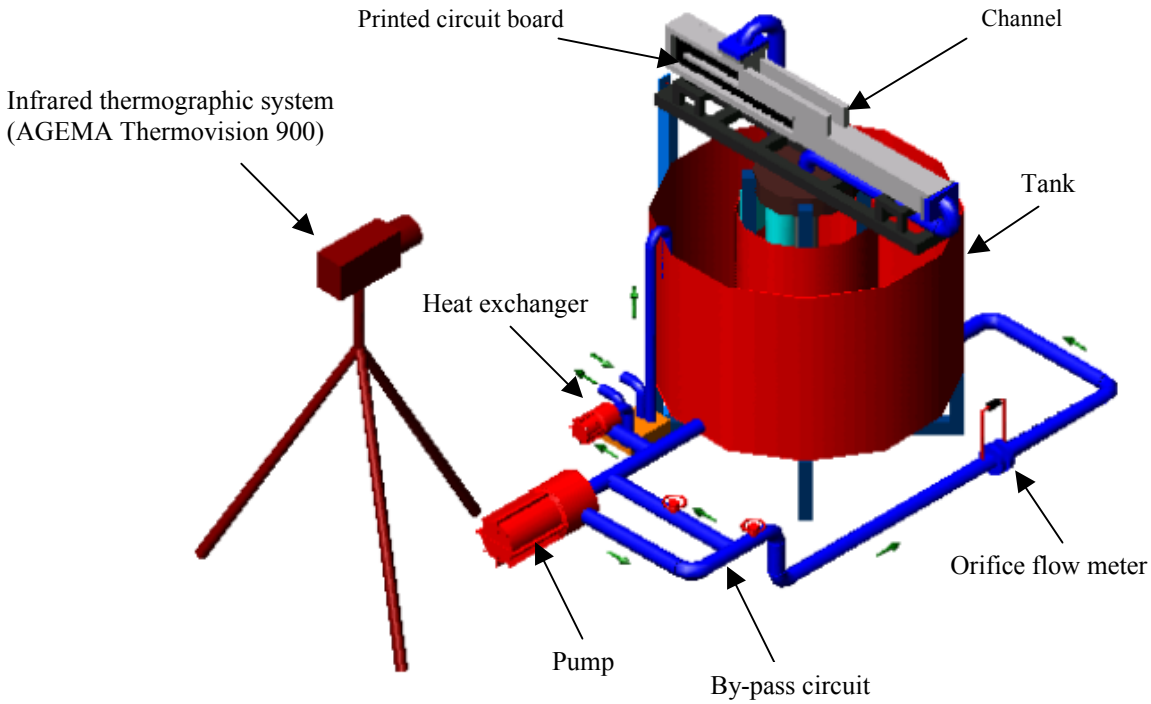

Fig. 1 *Sketch of experimental apparatus*

The infrared thermographic system employed is the AGEMA Thermovision 900. The field of view (which depends on the optics focal length and on the viewing distance) is scanned by the Hg-Cd-Te detector in the 8-12mm infrared window. Nominal sensitivity, expressed in terms of noise equivalent temperature difference, is 0.07°C when the scanned object is at ambient temperature. The scanner spatial resolution is 230 instantaneous fields of view per line at 50% slit response function. A 10°x20° lens is used during the tests at a viewing distance of 1.2m which gives a field of view of about 0.21x0.42m^2. Each image is digitised in a frame of 136 x 272 pixels at 12 bit. An application software can perform on each thermal image: noise reduction by numerical filtering; computation of temperature and heat transfer correlations.

Results are presented in terms of both normalised Nusselt number maps and averaged profiles for different values of the Reynolds and rotational numbers.

DETERMINATION OF HEAT TRANSFER INTENSITY BETWEEN FREE SREAMING WATER FILM AND RIGID SURFACE USING THERMOGRAPHY

S. ŠVAIĆ, I. BORAS, M. SUŠA
University of Zagreb, Faculty of Mechanical Engineering and Naval Architecture, 10000 Zagreb, Croatia; e-mails: srecko.svaic@fsb.hr, ivanka.boras@fsb.hr

The goal of the research was to find the relation for determining the heat transfer coefficient between a free streaming water film and metal corrugated surface. The relation between relevant parameters which determine the heat transfer coefficient was obtained by means of Wilson-plot method using data from the measurement.

The experiments were performed on experimental rig shown on figure 1., whose main part was the single plate heat exchanger. The primary water stream flows through the plate and the secondary water flows across the upper corrugated plate surface with effective layer thickness between 2 and 5 mm. The plate heat exchanger was inclined toward the horizontal plane.
All measurements were done with hot secondary and cold primary water stream having different mass flows and with plate inclination of 3 and 5 degrees. The temperatures of the water streams were measured by means of thermocouples type T, while the mass flows were determined by weighing the water quantities collected in certain period of time. The surface temperature distribution on the thin film surface of the secondary stream was recorded by IR camera FLIR SC2000. The goal of the thermographic measurement was to find if this method can be applied for measuring the temperature of the water stream film layer instead of using thermocouples which shows certain disadvantages.
The thermograms of the water film layer surface temperature distribution for two measurements are shown on figure 2. The obtained results give the satisfying results for the purpose of the analysis carried out. All measurements take place in stationary state.

The relation for determining the heat transfer coefficient obtained by Wilson-plot method is given in form:

$$\alpha = \mathrm{f}\,(v_{s,}\,\text{inclination})$$

where v_s (l/s) is a volume flow of the secondary (hot) water stream.

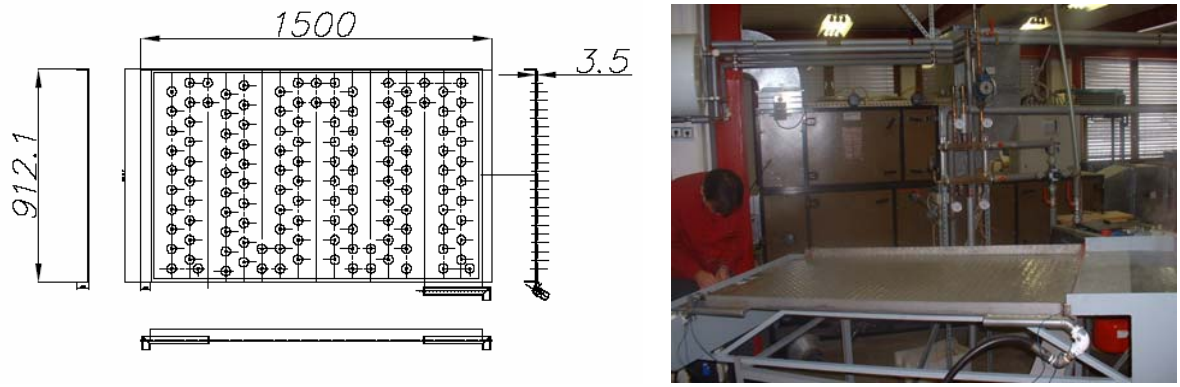

Fig.1 Experimental rig and dimensions of the plate heat exchanger

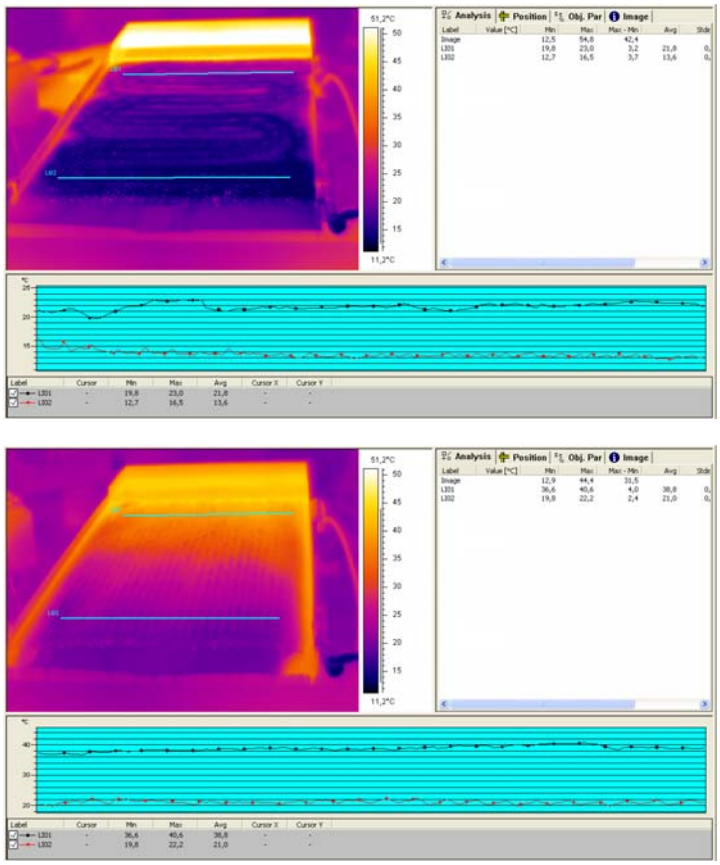

Fig.2 Thermograms of the temperature distribution on the surface of water film layer

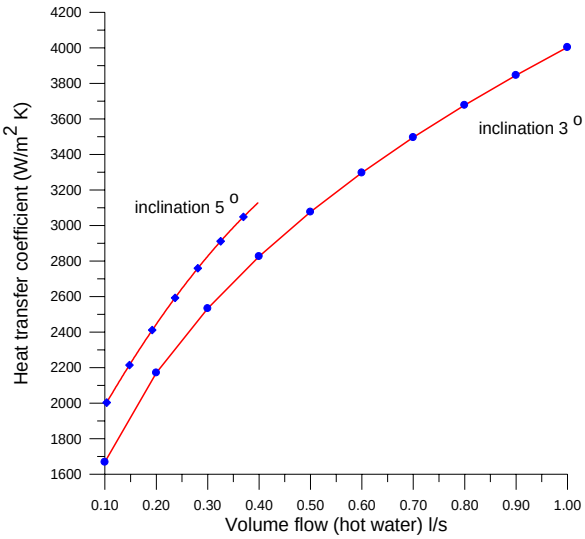

Fig.3 Heat transfer coefficient on the outer side (hot water) as a function of volume flow

Intensive cooling of large surfaces with arrays of jets

Carosena Meola[a], Giovanni Maria Carlomagno[b]

Department of Energetics Thermofluidynamics and Environmental Control (DETEC)
University of Naples Federico II, P.le Tecchio 80, 80125 Napoli, ITALY
[a] Tel. Fax ++390817683389, e-mail carmeola@unina.it
[b] Tel. ++390817682178, Fax ++390812390364, e-mail carmagno@unina.it

Keywords Impinging jets, convective heat transfer, infrared thermography

Jets of fluid are used in many industrial applications to dissipate heat generated by microelectronic circuits, to cool the leading edge of turbine blades, to heat the zones over aircraft that are critical for the formation of ice, to dry textiles and to temper glass. Many studies both experimental and numerical were performed but, despite the considerable amount of data present in literature, a general correlation is still not available. The main reason is that impinging jets may be arranged in a lot of different configurations that affect the convective heat transfer; on the other hands, the complex phenomena, which are associated with the jets fluid-dynamic, are still not completely understood.

The attention of the present study is mainly focused on the intensive heat removal within the objectives to add new pieces of information about impinging jets fluid-dynamics and to search for a data correlation. Different jets configurations are considered that involve variation of many factors:

- the geometry of the array of jets, which includes round and rectangular nozzles with variation of nozzles diameter and nozzle-to-nozzle spacing;
- the flow rate, which is varied to allow for the variation of the Reynolds number *Re*, based on the nozzle diameter, in the range 30000-80000;
- the impinging distance, which is varied between 4 up to 8.3 diameters.

The choice of round and rectangular nozzles is not made for only a merely variation of test parameters, but mainly to gain insights into the role played by the nozzles geometry on heat transfer. In fact, the use of rectangular nozzles, arranged on blades, offers some advantages over circular nozzles mainly owing to the spent air exhaust.

Infrared thermography applied to the *heated-thin-foil* technique is used to measure the convective heat transfer coefficient, *h*, which is calculated from the relationship:

$$h=\frac{\dot{q}-\dot{q}_l}{T_w-T_{aw}} \qquad (1)$$

with $\dot{q}$ the Joule heating and $\dot{q}_l$ the losses which are due to radiation, conduction and natural convection, T_w the wall temperature and T_{aw} the adiabatic wall temperature. The surface to be cooled is manufactured with a thin constantan foil, which is heated by passing an electric current through it. In particular, the foil is covered with a thin film of opaque paint of emissivity $\varepsilon = 0.95$.

Data are reduced in dimensionless form in terms of Nusselt number *Nu*, which is averaged in two different ways owing to two different correlations described in literature. In particular, one correlation, proposed by Gardon and Cobonpue (1962), involves the Nusselt number based on nozzles spacing Nu_s and the Reynolds number based on the arrival velocity u_a (Taylor, Grimmett and Comings, 1951) and nozzles spacing.

The other correlation instead, proposed by Martin (1977), involves *Nu* and *Re* calculated in the classical way (nozzles diameter and exit velocity) but the Nussel number is averaged over the relative nozzle area f which is given by the ratio of nozzle exit cross section to the area A of the square, or the hexagon, attached to it.

The suitability of both the above described correlations is analysed within the obtained experimental data. It is found that the correlation proposed by Gardon and Cobonpue (1962) works better than the correlation developed by Martin (1977). A modified Martin correlation is found which well correlates the data obtained for all the tested conditions.

Acknowledgements The authors are grateful to Mr. Giuseppe Sicardi for setting up the experimental apparatus and for his technical assistance during experimental tests.

References

1. Gardon R. and Cobonpue J. Heat transfer between a flat plate and jets of air impinging on it in *International Developments in Heat Transfer* ASME New York, pp.454-460, 1962.
2. Taylor J.F., Grimmett H.L. and Comings E.W. Isothermal free jets of air mixing with air *Chemical Engineering Progress*, vol. 47, pp. 175-180, 1951.
3. Martin H. Heat and mass transfer between impinging gas jets and solid surfaces in *Advances in Heat Transfer* ed. J.P. Hartnett and Th.F. Irvine, Academic Press New York vol. 13, pp.1-60, 1977.

Paint effects on the advanced quantitative infrared thermography applied to jet impacts

Reza Mehryar, André Giovannini, Sébastien Cazin
Institute de Mécanique des Fluides de Toulouse,
Allée du Prof. camille soula, 31400 Toulouse, France
Tel: 00 33 (0)561285932, fax: 00 33 (0)561285992
Reza.Mehryar@imft.fr

oral presentation

Key words: jet impact, heat transfer coefficient, infrared thermography, paint effects

In a global research of jet impact ,the infrared thermography was utilized for obtaining the heat transfer coefficient of single or multiple jets impact with electronic cooling applications. In a part of this work, the effect of the paint layer on the measured heat transfer coefficient was studied. A very thin steel plate of $50\mu m$ of thickness, heated by joule effect, is cooled by the flow of jet in one side, and the temperature field is visualized by an infrared camera on the other side. The visualized side of the thin hot plate is covered by a spray of black paint. The emissivity of this paint is guarantied greater than 0.92 if one uses three layers of the paint on the plate. For calculating the heat transfer coefficient, the measurement are accomplished in the steady state and transient cases. In the latter case, jet flow exists but the impingement plate is heated suddenly. In the figure 1, the temperature field, measured by the infrared camera, is shown for the case of nine jets.

In the time of the data analysis, it was observed a very important noise about the lateral conduction term that was obtained by the second derivative of the measured temperature. In the first part of this paper, the origin of this noise is investigated and few solution are proposed. The effect of the camera-plate distance and the heat generation power in the plate are shown in figure 2 and figure 3 respectively.

By the thermal unsteady measurement, it was observed that the calculated heat transfer coefficient was very high initially and it decreased exponentially after several seconds.

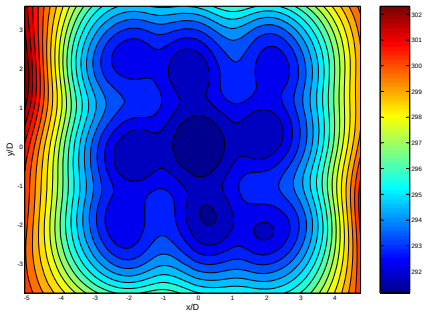

FIG. 1 – temperature field for nine jets

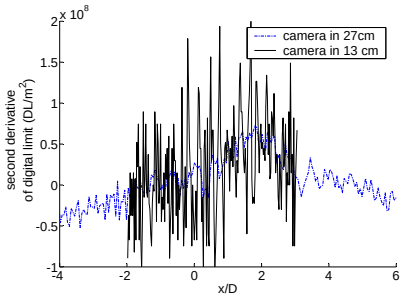

FIG. 2 – effect of the camera-plate distance about the noise of the second derivative

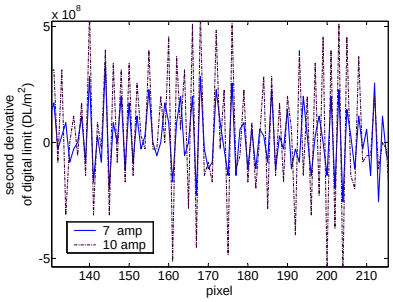

FIG. 3 – effect of the current intensity about the noise of the second derivative

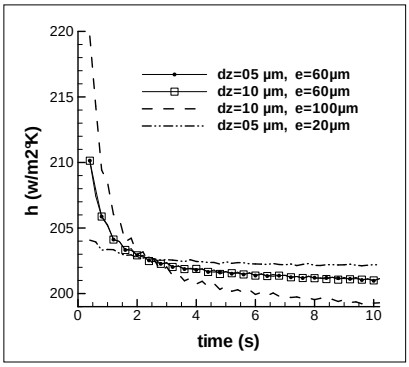

(a) at stagnation point x/D=0

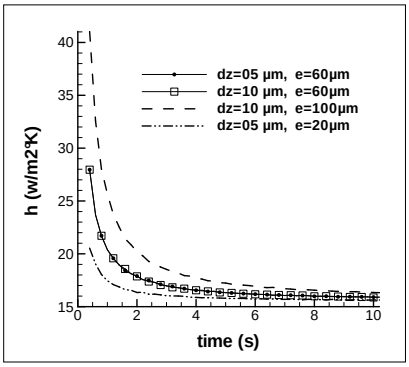

(b) at x/D=5

FIG. 4 – paint thickness effects for calculation of heat transfer coefficient by the measured data

As these variations had no meaning physically, a numerical program was prepared for investigating the obtained results. This program solves a three dimensional heat conduction in a several layer materials by the alternative direction implicit method with different boundary condition.

Utilizing this program, at the first step, the 3-D temperature field was calculated with a mixed boundary condition corresponding to the single jet impact and at the second step, the imposed distributed jet heat transfer coefficient was recalculated by the obtained temperature field on the paint surface. The results of this modeling are shown in the figure 4.

Results :

-the paint is caused a deviation on the calculated heat transfer coefficient in the thermal steady case and a more important one in the transient case.

-paint thickness increases not only this difference but also the time constant for arriving a steady calculated heat transfer coefficient.

-if the camera is near the plate, the effect of paint particles will not be negligible, although they are not distinguished by the eyes.

THERMOGRAPHIC ANALYSIS OF ACOUSTIC DISTOURBANCE EFFECTS ON LAMINAR SEPARATION BUBBLE

Renato Ricci °, Francesco Angeletti *, Sergio Montelpare *, Alessio Secchiaroli *

* Dipartimento di Energetica - Università Politecnica delle Marche.
° PRICOS - Università di Chieti-Pescara.

This research is aimed to evaluate the laminar boundary layer destabilization on a small wing section by means of acoustic perturbation; this phenomenon is observed by using an infrared thermography and the thin heated foil technique. The main purpose of this work is the reduction of the laminar separation bubble that usually occurs in airfoils operating at low Reynolds numbers.
These airfoils are normally used in sailplanes, unmanned aerial vehicles, small wind turbines blades etc..., and the effects of the local boundary layer separation phenomena on the performances of airfoils consist in the reduction of the lift coefficient and in the increase of the drag coefficient.
The experimental tests were conducted in an open circuit subsonic wind tunnel having the subsequent overall dimensions: length 165 cm; width 65 cm; height 38 cm. The tested wing section, based on E205 airfoil, span the entire wind tunnel height and was previously coated with a brass sheet 25 micrometer thick. An alternating electric current is supplied by a variable voltage generator in order to increase the airfoil surface temperature over environment temperature. By this way the infrared camera may detect the fluid-dynamic phenomena over the airfoil surface as local temperature variations.
A sound source is placed before the wind tunnel inlet section and is controlled by an amplifier that generates a pure sinusoidal tone. The frequency of the acoustic perturbation is changed in the range 50 Hz-1000 Hz.
Preliminary the power spectral distribution over the cross section of the wind tunnel was measured by varying the frequency of the incoming disturbance. Measures are carried with and without the wing section. The sound pressure level generated by the external source was fixed at lest at 25 dB over the background level, in order to avoid the effect of the fan noise.
Once characterized the test section, thermographic measures at different wind flow angle of attack ($\alpha = 0° \div 8°$) and Reynolds number (Re=60000 and Re=100000) was carried out. For every angle and Re disturbances at different frequencies were investigated in order to identify the ones that produce the best effects on the bubble reduction. The acoustic analysis was conducted either in 1/3 octave band and 1/24 octave band and the power of the sound source was kept constant during all tests.

The thermographic images were post-processed with a custom made MatLab procedure that implements a finite difference scheme to take in account the energy balance of the infinitesimal element of the metallic coating. This software produces the Stanton number distribution along the chord length. An analysis of this distribution may evidence the characteristic points of laminar separation bubble: separation, transition and reattachment point

The results show an evident influence on the bubble behavior for a restricted range of the disturbance frequency and a dependence on the sound power level of the source is also observed. The parameter that seems mainly influenced is the laminar bubble reattachment point.

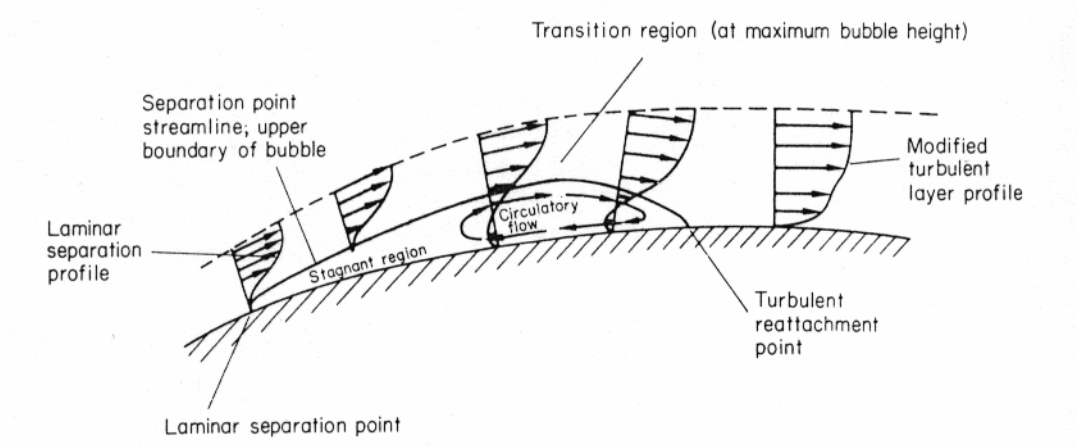

laminar separation bubble phenomenon over an airfoil

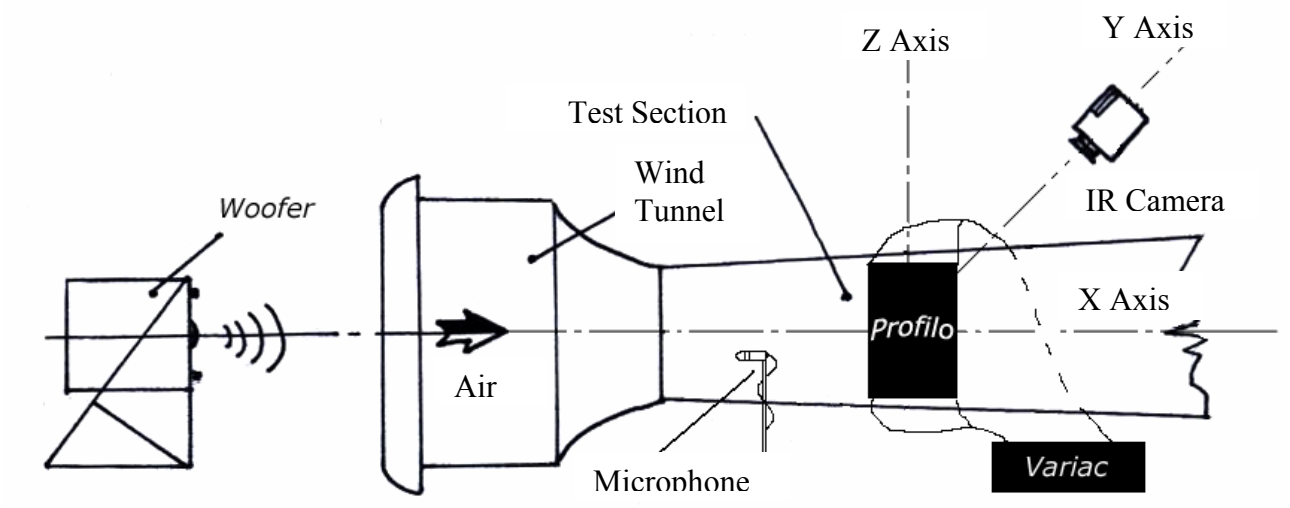

Test Facility configuration

Wing section with metallic coating

Wing section painted with measured emissivity paint

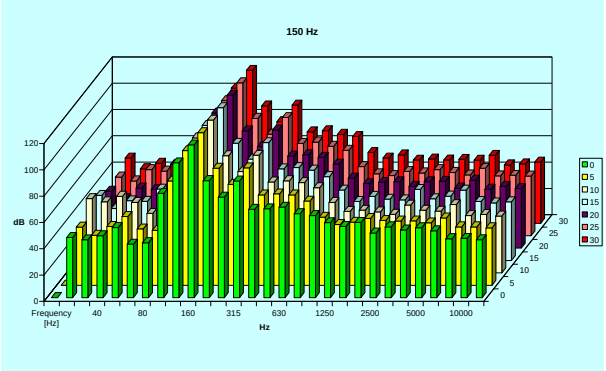

Sound emission spectrum

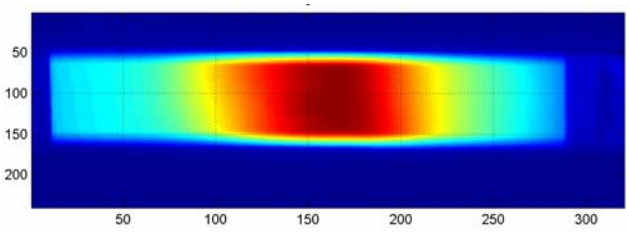

Thermographic Image

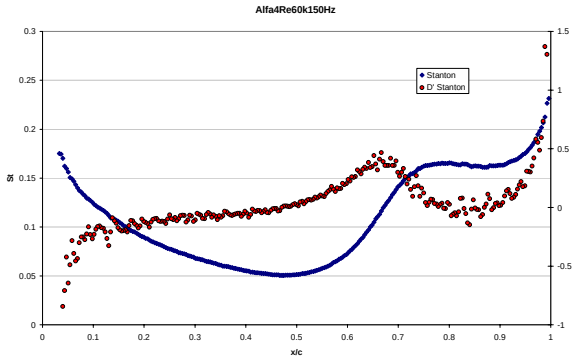

Stanton number and its first derivative versus chord length

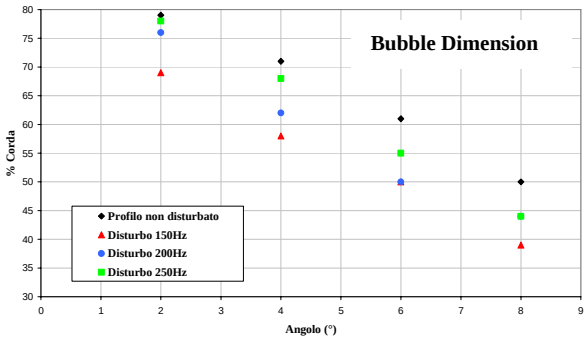

Bubble dimensions varying sound disturbance frequency

EVALUATION OF THE CONVECTIVE HEAT TRANSFER COEFFICIENT IN ELECTRONIC COOLING

Mourad REBAY[1, *], Rejeb BEN MAAD[2], Sadik KAKAÇ[3] and Jacques PADET[1]

[1] UTAP - Lab de Thermomécanique (EA 3082) Faculté des Sciences, 51687 Reims, France
[2] LETTM, Faculté des Sciences de Tunis, 2092 Manar II, Tunisia
[3] Turkish Academy of Sciences, Department of Mechanical Engineering, University of Miami, Coral Gables FL 33124, USA
([*] mourad.rebay@univ-reims.fr)

As the electronic industry pushes towards microprocessors and integrated circuits to be faster and smaller, the heat flux that must be evacuated becomes higher. Thus, the electronic cooling becomes more than ever a critical task to develop faster and miniaturized electronic components. To cope with the increase of cooling requirement, several theoretical and experimental studies have been carried out to understand convective heat transfer in micro sized systems. Because of the high heat capacity and thermal conductivity of liquid, many studies have been focused on single phase flow of liquid or on phase change from liquid state to vapour state. In the same time and due to the advantages of the maintenance facility and of the relatively low cost in cooling with air flow, considerable attention has been given to thermal control and management techniques with this fluid.

As contribution to the development of the thermal management of the cooling of electronic devices, we present here the measurement results of the thermal field on a main electronic card used in personal computer. A method for the determination of the convective heat transfer coefficient between the microprocessor and its environment is also presented. In the direction parallel to the card, the former is exposed to an air flow generated by a fan and passing through a rectangular diffuser.

The evolution in time of the cartography of the thermal field on the whole electronic card is obtained by a short-wave infrared camera with a sample rate of 50 Hz. The details of the temperature field around one selected component may be given by a 100 μm macro-objective. After starting the personal computer, a simple computational program on DOS is executed in order to reach the steady state working conditions of the electronic components. When the steady state is reached, a sudden deposit of the luminous energy with fixed duration on the front face of the card is given. The analysis of the induced temperature elevation allows the calculation of the heat transfer coefficient between the air flow and the surface of the microprocessor. This transient non-destructive method for the heat transfer rate evaluation, called pulsed photothermal radiometry method, is based on the flash one that was introduced by Parker and al. for the measurement of thermophysical properties such as the thermal diffusivity.

For the examination of the experimental thermograms on the microprocessor, a semi-infinite conduction model is used. In the model, the heat loss by the air flow on the microprocessor is characterized by a constant value in time of the convective heat transfer coefficient. The Duhamel's theorem gives the theoretical elevation of temperature from the initial state for a finite duration pulse. The evaluation of the convective heat transfer coefficient thus obtained by the use of 0-order temporal momentum of the thermogram. The measurements are performed for three air velocity and for two dispositions of the electronic card.

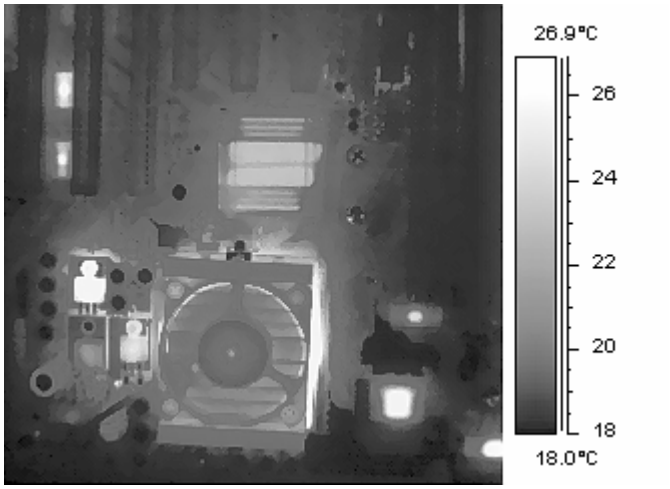

Figure 1 - Infrared photography of the main electronic card

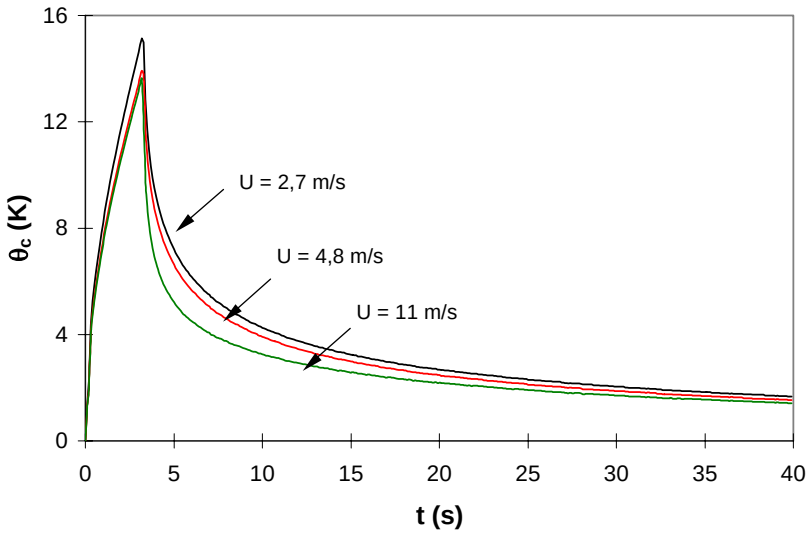

Figure 2 - Thermograms on the surface of the microprocessor with 3 seconds excitation

CHARACTERIZATION OF THE EXPERT VEHICLE CONTROL SURFACES BY MEANS OF IR MEASUREMENTS

Gennaro Cardone* and Antonio Del Vecchio+

**University of Naples"Federico II", DETEC Department, p.le Tecchio, 80127 Naples (Italy), email: gcardone@unina.it*
+CIRA – Italian Center for Aersopace Research - Via Maiorise, 81043 Capua (Italy), email: a.delvecchio@cira.it

The aim of the present work is to designs the IR tests to be performed in the CIRA plasma wind tunnel "Scirocco" in the frame of technology project CLAE. The objective of this project is the characterization of the EXPERT vehicle control surfaces. In particular, model configuration and plasma test conditions have been selected in order to duplicate either the shock wave boundary layer interaction occurring around the body-flap, either the associated mechanical and thermal loads on the control device encountered in some EXPERT capsule re-entry flight conditions. Within this Project frame, at first, two tests on the same model at two different aero-thermodynamic conditions have been planned. These tests are focused on the aero-thermodynamic behaviour of the flow on the control device. In a subsequent phase other tests are foreseen to analyse the different materials of the control surface behaviour.
The SCIROCCO arc-jet facility presents some peculiarities that make it unique in the world. In particular, the arc heater length and diameter are respectively of 5500*mm* and 110*mm* and its maximum power is 70*MW*. Briefly, the SCIROCCO facility is a typical segmented constrictor Arc-Jet Wind Tunnel (AWT). The gas used for the tests is dry compressed air with mass flow variable from 0.1 to 3.5*kg/sec*. It accelerates through a convergent-divergent conical nozzle with interchangeable exit diameters up to 1950*mm*. The flow velocity at the nozzle exit can reach a value of 7000 m/s. A powerful Vacuum System working via the act ion of twelve steam ejectors is located downstream of the test chamber. During a test, after the stable flow condition is, in the test chamber, attained and confirmed by probe sensor, t he testing model is put into the flow by the support system with characteristic time of 2-5*sec.* The thermocamera used is the Agema Thermovision THV900LW. It is equipped with a Cd-Te-Hg detector scanning and its field of view holds in the IR waveband 8-12μm with a frame of 136 not-interlaced lines in 1/15*s*. The thermal image is digitized with a resolution of 272x136 pixels that, in combination to a 10°x20° IR lens (or 5°x10°) placed at the distance of about 4*m* from the test sample, results in a spatial resolution of about 1*cm/pixel (*0.5*cm/pixel)*. The thermocamera is mounted in a protected box on a robotized remotely controlled gear, in order to avoid any disturbance from ambient radiation. In front of the thermo camera a ZnSe IR windows with a special coating to reduce the band pass wavelength region to the proper values of about 8-10*mm* is installed.
The model geometry that will be tested is show in fig. 1. The leading edge is a water cooled copper alloy cylinder. The upper part of the model is covered by a metallic panel of PM1000, equipped of pressure and heat flux sensors (RAFLEX) along the surface. A flap covered by a C/SiC panel is installed with an angle of 20° with respect to the PM1000 panel, in order to deflect the flow of 20°

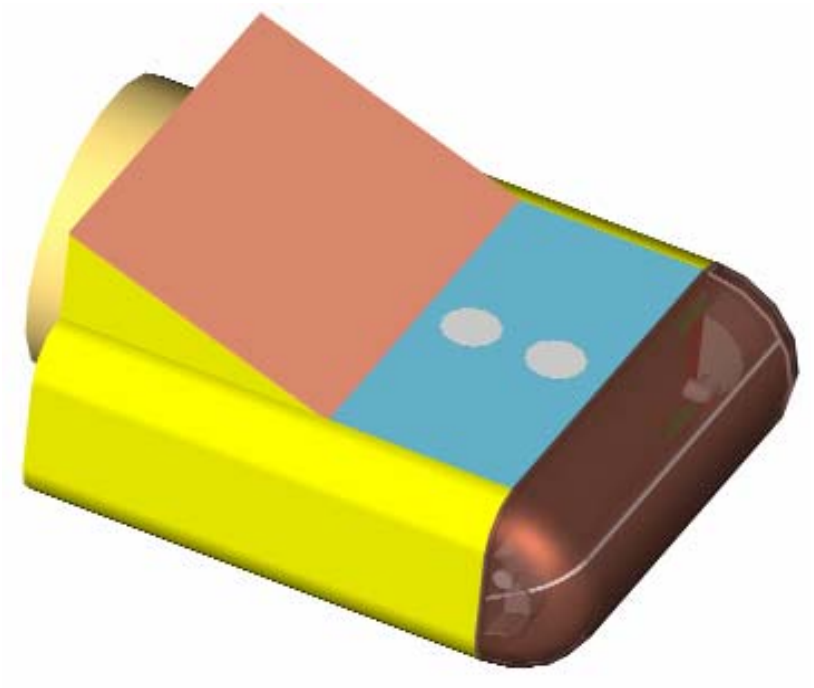

Fig. 1 Model geometry

Such a model is conceived to be applied for several types of tests. All the components of the test article are easily removable, in order to be replaced by others, for the same scope or different. Those characteristics make such a model to be very flexible for different types of applications. This is a very important aspect of the test article that will not be used only for the scope of this work, but also for other applications, very different from this one.
In order to obtain information of flow field around the control surface (size of the re-circulation induced by the shock wave boundary layer interaction, peak heating position, re-attachment front of the boundary layer etc.) the time sequence of temperature map that will be acquired during the tests will be processed be means of ad hoc developed heat flux sensor (based on classical thin film sensor) but taking in account the 3D model effects. The IR tests will be also used to evaluate and understand the effects of different surface material properties (catalysis, emissivity) on the flow past the flap. IR measurements will be also compared with heat flux measurements performed with standard heat-flux sensors and thermocouples.

Title:

Two channels NIR camera system to detect foreign matter in cotton

Authors:

Stephan Böhmer, Helmut Budzier, Volker Krause, Gerald Gerlach, Thomas Pusch*
Dresden University of Technology, Institute for Solid State Electronics, *Institute for Textile and Clothing Technology

Address:

TU Dresden
Institut für Festkörperelektronik
Dipl.-Ing. Stephan Böhmer
Helmholtzstraße 18
01062 Dresden
Tel. 0351 4633 4098
Fax 0351 4633 2320

Email: boehmer@ife.et.tu-dresden.de
URL: http://ife.et.tu-dresden.de

Oral Presentation

Abstract

Up to now the cotton industry uses camera systems in the visible range of light to detect foreign matter like packaging material. These systems are limited to colored materials since they can not detect white or transparent foils. In this paper a two channels NIR camera system capable to recognize these types of extraneous substances is presented.

The newly developed camera system is based on two InGaAs line-scan sensors operating in the near infrared range. Both are installed in one single camera head. A beam splitter is used to partition the detected radiation into two parts, one for each sensor. A 1520nm/1720nm filter pair makes each sensor selective for a specific spectral line within the NIR absorption spectrum that is characteristic for the materials to be detected. The signals measured by the two sensors are than processed in terms of evaluating a two-dimensional sample space. The different materials (PVC/ Metal/ Cotton) create significant clusters within the sample space and can thereby be recognized.

The camera system operates at 5 kHz with a resolution of 512 pixels per channel. The two sensors have to be aligned exactly to ensure that both channels scan the same spatial points. The high data rates of about 40 Mbit/s per channel require an interface fast enough to handle those rates. Therefor the camera head is equipped with a CameraLink interface to transfer the measured data to a PC.

The PC has a frame grabber plug-in board and performs the entire necessary signal processing including fixed pattern noise correction, dead pixel correction, spatial and temporal filtering and the evaluation of the sample space for each pixel.
All this has to be done in real time to keep up with the process. An external unit connects the system to the process control that separates the detected extraneous matter from the cotton.

Changes in the process conditions like cotton quality, cotton tint or illumination result in changes in location and size of both the clusters representing the “no-trash” region and the clusters representing the “trash” region within the sample space. The system has to be adapted to those changes by teach-in procedures.

The camera system has a robust housing and is suitable for use in harsh industrial environments. First results for the use of this system will be presented.

Key words: infrared systems; NIR spectroscopy; IR application; extraneous matter recognition

SPATIAL RESOLUTION AND ACCURACY IN TEMPERATURE OF A THERMAL FOCAL PLANE ARRAY CAMERA : EVALUATION OF ERROR IN TEMPERATURE FROM SLIT RESPONSE FUNCTION AND CALIBRATION CURVE

Olivier RIOU, Dominique PAJANI, Jean Félix DURASTANTI

The problems of the spatial resolution of the thermal scanner cameras were largely treated in the work [2]. We will present here the subject with a very pragmatic approach for the focal plane array camera.

A fine analysis of the process of formation of the images will show the limits of the spatial resolution present in a standard optical system ; a study of the scattering spot is given and it indicates a very strong sensitivity with the optical number N of the camera and its spectral band.

Applied to a FPA camera, the scattering spot is associated to the bidimentional impulse response D(x,y) of a detector. In this frame, we will review the interpretation of the signal provided by the observation of a slit presenting a thermal contrast (Slit Response Function or SRF).

The SRF will be detailed in connection with the concept of accuracy in temperature and one will point out the characterization of Distance To Spot Size Ratio very used in pyrometry but new in thermography.

In this article, one will call upon the french standards of thermography [3] ; nevertheless, FPA cameras being posterior to the standards, those became incomplete and sometimes unsatisfactory. The metrological aspects will be treated in the respect of the International Vocabulary from Metrology, or VIM [4]. The metrological considerations are essential to decide relevance of the criteria recommended for on site measurements.

TABLES AND FIGURES

Table 1. Optical scattering angle for a simple lens

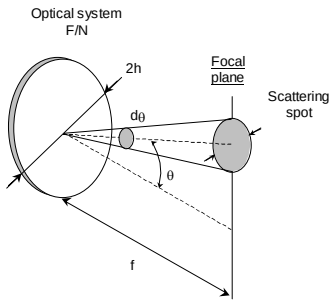

aperture number $N = \frac{f}{2h}$

(focal length f, lens diameter 2h)

Diameter of scattering spot $\approx f \times d\theta$

Diffraction (rad)	Chromatic aberrations (rad)	Spherical aberrations (rad)		Coma (rad)	Astigmatism (rad)
$d\theta = 2{,}44\ N \frac{\lambda}{f}$	$d\theta = \frac{1}{2N\nu}$	n=4,0	$d\theta \approx 10^{-3} \times \frac{8{,}7}{N^3}$	$d\theta = \frac{\theta}{16(n+2)N^2}$	$d\theta = \frac{\theta^2}{2N}$

Table 2. Evaluation of scattering spots for a Germanium lens (FOV : 12°, focal length : 100 mm, diameter 2h = 50 mm)	spectral Band 3-5 µm		spectral Band 8-12 µm	
	Scattering angle (mrad)	Scattering spot (µm)	Scattering angle (mrad)	Scattering spot (µm)
Diffraction	0,194	19,4	0,488	48,8
Chromatism (constringence)	2,84 (88)	284	0,225 (1112)	22,5
Spherical aberration	1,087	108,7	1,087	108,7
Coma	0,26	26	0,26	26
Astigmatism	2,5	250	2,5	250

Scattering angle except coma and astigmatism	4,12 mrad	1,8 mrad
Achromatic lens	1,3 mrad	1,6 mrad

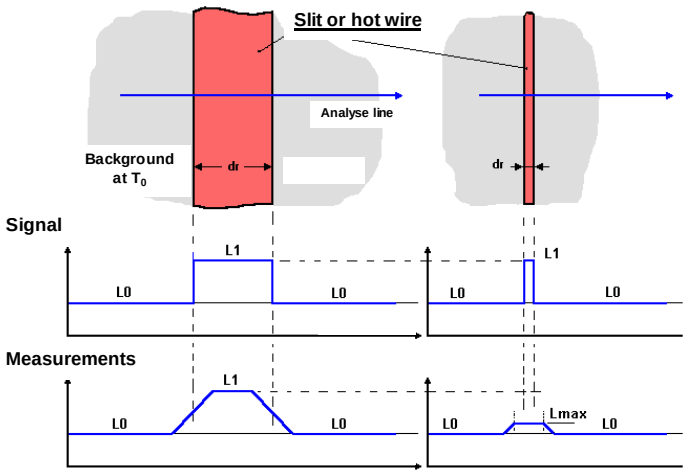

Figure 1. Variation of maximum of intensity versus opening slit dr according to the line analyzed in the thermal scene (input) and result on the thermal image (output measurements)

Table 2. Theorical evaluation of the relative maximum value of the signal given by a slit (σ : mean scattering spot diameter ≈ IFOV)				
$I_{max}(dr)$	0,5	0,8	0,9	0,99
dr / σ (mrad)	0,96	1,8	2,32	3,64

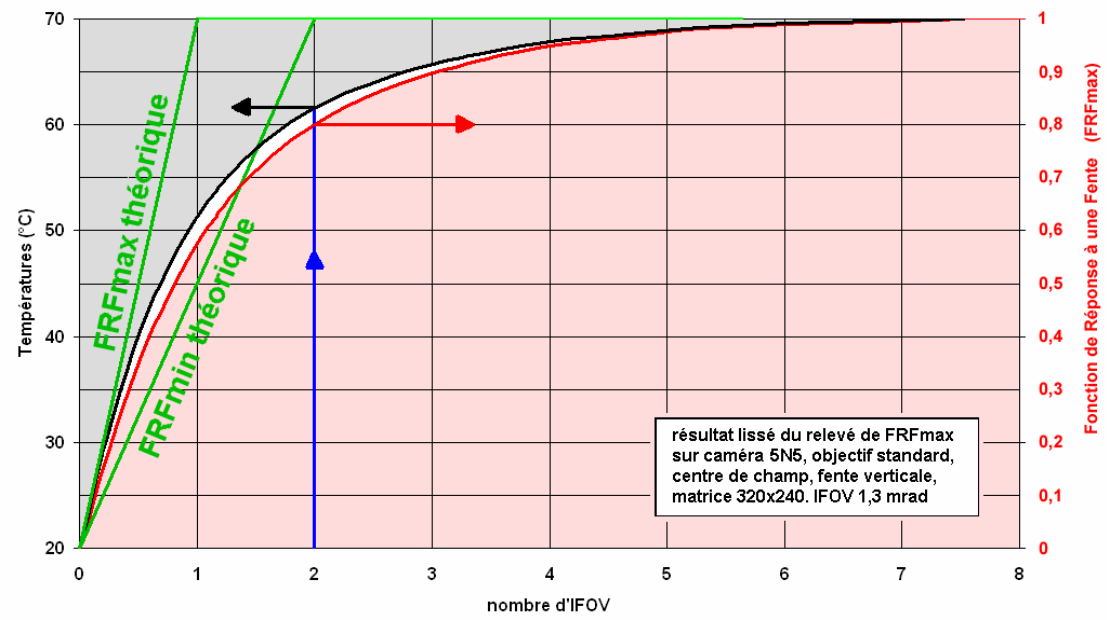

Figure 2. FRF with vertical slit of a camera 8 to 12 µm and corresponding curve of the apparent temperature measured for the temperatures limit 20°C and 70°C. The theoretical curves of FRFmax and FRFmin are also indicated.

BIBLIOGRAPHIE

[1] Réflexions thermographiques : état de l'art et perspectives. PAJANI D. Conférence à la Journée Thermographie de l'EXERA. Octobre 1995.

[2] Mesure par thermographie infrarouge. PAJANI D. ADD Editeur. 1989. 450 p.

[3] NF A 09-400. Thermographie infrarouge. Vocabulaire. Décembre 1991. NF A 09-420. Thermographie infrarouge. Caractérisation de l'appareillage. Avril 1993. NF A 09-421. Thermographie infrarouge. Méthodes de caractérisation de l'appareillage. Avril 1993.

[4] NF X 07-001. Vocabulaire international des termes fondamentaux et généraux de métrologie. Décembre 1994.

Near Infrared Thermography with Silicon Focal Plane Arrays - Comparison to Infrared Thermography

Y. Rotrou[a], T. Sentenac[a] and Y. Le Maoult[a],
P. Magnan[b] and J. Farré[b]

[a]Ecole des Mines d'Albi-Carmaux, Route de Teillet, 81000 ALBI, FRANCE
[b]SUPAERO-CIMI, 10 avenue Edouard Belin, 31055 Toulouse, FRANCE

1. PRESENTATION PREFERENCE

"Oral Presentation".

2. ABSTRACT TEXT

After monodetectors (pyrometers and scanning detectors), multi-detectors focal plane arrays have been developped to improve the spatial resolution, and to tend to infrared thermography with video characteristics. (see [Pajani]) So the *ideal* thermographic camera could be defined as a system which would provide, whatever the experimental conditions, an excellant image quality with high spatial and thermal resolutions, and 25 or 50 frames per second. Furthermore, it should be easy to use, with integrated electronics, low power consomption and without cooling of the detector. The better spatial resolution is provided by video CCD cameras, with Silicon detectors. That's why we propose to realise temperature measurements using these kind of cameras, in the Near Infrared (NIR) spectral range ($\lambda < 1.1\mu m$ due to Silicone properties). Furthermore CCD cameras are low cost compared to IR ones, compacter... and permits to realise *both* thermal/dimensionnal field measurements ([Sentenac 02]), that presents interest in some industrial applications.

In this paper, we focus on thermal *measurements* using a CCD camera in the NIR spectral range, and we compare its performances with two commercial IR cameras.
[Moore 98] still considered such a system to realise temperature *visualisation*, and some other articles (for exemple [Meriaudeau 95] or [Saunders 96]) reported applications of measurement with low cost CCD cameras related to higher temperatures (over $800°C$). We presently show that we can realise temperature *measurement* with CCD cameras on the $300 - 1000°C$ temperature range.

The first part deals with the radiometric model of our system, which determine the relation between the temperature T of an ideal blackboby source and the digital camera signal output I_D. In introduction, we discuss the classical model used with SWIR and LWIR cameras. To perform measurements on a large temperature range, we have to use differents f-numbers,and to consider one parameters set for each f-number. With our system, we prefer to adapt the integration time. That permits to track *on line* the temperature evolution. Considering the fact that we can use a great number of integration times (from $0.1ms$ to $16s$), we propose a model with only a single parameters set, for all integration times. This implies to take into account possible non-linearities of the photoresponse ([Rotrou 05]).
Otherwise, with a mutiple detector array, we need to correct the non uniformities of the array (Fixed Pattern Noise and PhotoResponse Non Uniformities) to obtain *identical* responses for all pixels. Then we correct "ghost" reflections and smearing to obtain *independant* responses.
Finally we build *step by step* a model with a single parameters set, and we link each of these steps to the specific near infrared operating spectral range. Then we consider models used in pyrometry and based on effective wavelenghts depending on the temperature ([Kostkowski 62], [Saunders 97]). Using this progressive method, our work of modelisation appears to be general and can be applied to any radiometric model.

In the second part, we compare our system with commercial ones in term of blackbody temperature measurements. We study three cameras : our NIR system based on the Sony XCD SX910, the SWIR ($3 - 5\mu m$)

For further information : Email: rotrou, sentenac, lemaoult@enstimac.fr. fax : +33 (0)5 63 49 32 42.
magnan, farre@supaero.fr

camera 782 SW AGEMA with a monodetector in InSb, and the $8-12\mu m$ camera 880 LW AGEMA, with a monodetector in HgCdTe. We evaluate different criteria as NETD or sensitivity (figure 1) for each of the three systems.

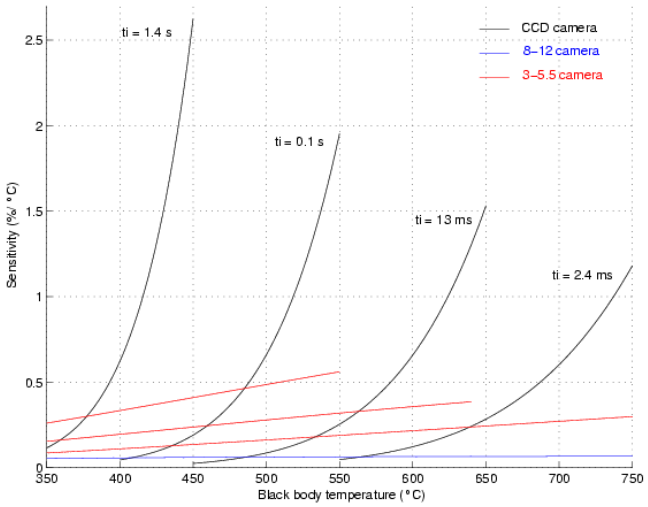

Figure 1. Comparaison of sensitivities for different systems

In the third part, we consider true temperature measurement. We qualitatively compare the performances of NIR, SWIR and LWIR systems. We show that we are less dependant to the emissivity of the observed material in the NIR (figure 2), insensitive to the radiative ambiant temperature in the NIR, and that LWIR measurement are less deteriorated by the solar or artificial light.

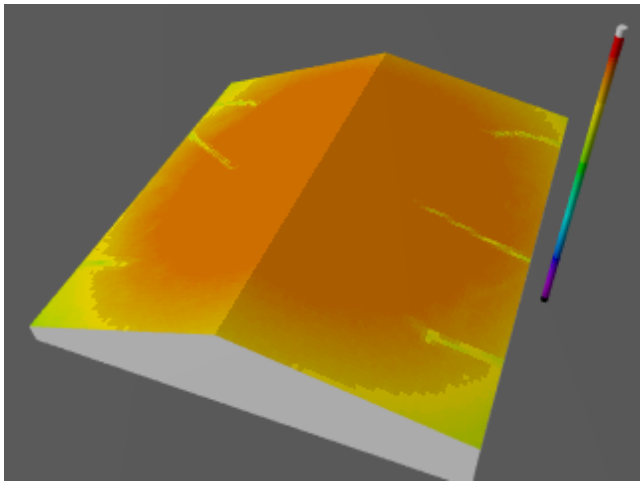

(a) NIR image : we see temperature, not emissivity variations

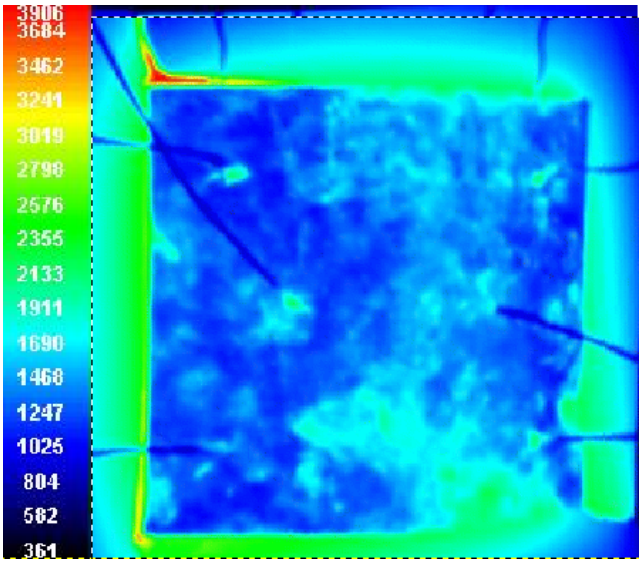

(b) LWIR image : we see the emissivity map more than the thermal one

Figure 2. Sensitivity to the non uniformity of the emissivity on the surface

3. KEYWORDS

Radiometric Model, Temperature measurement, Silicon detector, near infrared camera, Emissivity

References

[Kostkowski 62] H.J. Kostkowski & R.D. Lee. Theory and Methods of Optical Pyrometry. Reinhold Publishing Corporation, **1962**.

[Meriaudeau 95] F. Meriaudeau, E. Renier & F. Truchetet. *Visualisation de température proche infrarouge à l'aide d'une caméra CCD.* In 7e congrès International de Métrologie, volume 1, pages 189–194, **1995**.

[Moore 98] P. Moore & F. Harscoet. *Low cost thermal imaging for power systems applications using a conventional CCD camera.* In Energy Management and Power Delivery. Proceedings of EMPD '98., volume 2 of *ISBN : 0-7803-4495-2*, pages 589–594, **1998**.

[Pajani] Dominique Pajani & Luc Audaire. *Thermographie : Technologies et applications.* In Techniques de l'Ingénieur, traité Mesures et Contrôle.

[Rotrou 05] Yann Rotrou, Thierry Sentenac, Yannick Le Maoult, Pierre Magnan & Jean Farré. *Demonstration of near-infrared thermography with silicon image sensor camera.* In SPIE, editeur, Thermosense XXVII, volume 5782, pages 9–18, **2005**. ISBN 2-9511591-3-7.

[Saunders 96] P. Saunders & T. Ricolfi. *The characterisation of a CCD camera for the purpose of temperature measurement.* In TEMPMEKO'96 - International Symposium on temperature and thermal measurement in industry and science, pages 329–334, Torino, Italy, **1996**.

[Saunders 97] P Saunders. *General interpolation equations for the calibration of radiation thermometers.* Metrologia, vol. 34, pages 201–210, **1997**.

[Sentenac 02] Thierry Sentenac. *Surveillance de scènes dynamiques avec une caméra CCD dans le proche infrarouge : application à la détection couplée de feu et de déplacements d'objets.* PhD thesis, Institut National Polytechnique de Toulouse, **2002**.

CALIBRATION AND PERFORMANCE EVALUATION OF AN UNCOOLED INFRARED THERMOGRAPHIC SYSTEM

Sara Rainieri, Fabio Bozzoli and Giorgio Pagliarini
Department of Industrial Engineering – University of Parma
Parco area delle Scienze 181/A 43100 Parma – Italy
Fax +39 0521 905701
e-mal: sara.rainieri@unipr.it

ABSTRACT

The efforts made in the last decay in the field of infrared detectors technology are mainly devoted to the development of systems of high sensitivity and performance characterized, at the same time, by low cost and simple maintenance. These goals are hardly achieved with photon detectors which, in spite of the high sensitivity and signal-to-noise performance, need to be cooled in order to operate correctly. Therefore they are often integrated in heavy and expensive instruments because of the cryogenic or thermoelectric cooling device required. For this reason, a big revolution has been achieved with the development of uncooled IR arrays, like the thermistor bolometer which is nowadays applied in most of infrared system available on the market [1]. Until the nineties this kind of thermal detector had not been exploited extensively neither in civil nor in military applications since its performance was believed to be rather poor in terms of sensitivity, time response and stability. The possibility to operate at room temperature and to offer low cost thermographic systems has instead acted as a stimulus for the applied research in this field to expend vigorous effort in order to develop new strategies to compensate the disadvantages of this kind of infrared detector. The market of infrared cameras has followed this trend, by offering as main product low-cost instruments based on the microboleter IR detector technology. The production of instruments based on the mature technology of cooled photon IR detector has instead been limited and directed to a specific market sector (mainly military or research) by causing a significant rise in their cost. This aspect may represent a problem for many research laboratories which may encounter some difficulties in purchasing high sensitivity and performance instruments.
The object of the investigation here presented is to consider these aspects by means of an experimental analysis aimed to the assessment of the performance of an infrared camera having a 160 × 120 array of microbolemetric detector. The potential capability of the instrument have been verified by means of measurements taken by observing an isothermal plate of uniform emissivity in the temperaure range 10-80°C. Some representative results regarding the data acquired by viewing the plate kept at a uniform temperature of 40°C are shown in figure 1. The frequency histogram of the signal is reported both for a single image and for the image obtained by averaging 200 images acquired at a frequency of 50 Hz. The response of a single pixel in instead reported as function of time in figure 2.
The application field to which the instrument performance test is addressed is quantitative measurements in the field of heat transfer. In particular the measurements are intended for anpplication of the infrared system to the estimation of the local heat transfer coefficient on thin surfaces. Regarding this specific field, Rainieri et al. [2-3] have successfully developed an optimal data processing procedure, based on the Wiener filter technique, to be applied to infrared thermographic temperature maps in order to recover the heat transfer coefficient distribution on thin metallic surfaces. In this experimental investigation these Authors use an infrared camera, having a Focal Plane Array of photoemissive PtSi detectors working in the 3-5 nm spectral range and cooled to a temperature of 77 K by a Stirling cycle incorporated in the instrument, namely the PRISM DS infrared camera by Flir Systems. The same Authors have proved that a basic step in order to apply successfully the infrared thermographich technique to this specific research field, and in general in

quantitative application in the heat transfer research filed, is an accurate calibration of the detectors' array to be possibly made *in situ* [4-6]. The object of the investigation here presented is to test the capability of a new technology uncooled infrared microbolometric detectors (namely the ThermoVision A20-M by Flir Systems), in terms of signal to noise ratio, sensors' stability and uniformity, and to compare it with the performance achieved with the cooled Focal Plane Array infrared camera in the above referenced investigation.
The main outcome is an adequate instrument's calibration and signal processing procedure for quantitative measurements in heat transfer application.

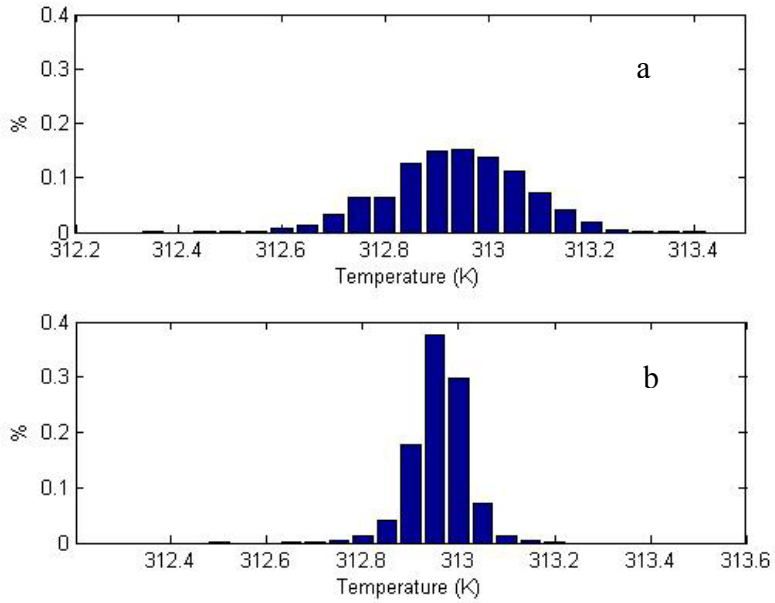

Figure 1: Frequency histogram of the signal: a) signal of a single image b) signal averaged over 200 images

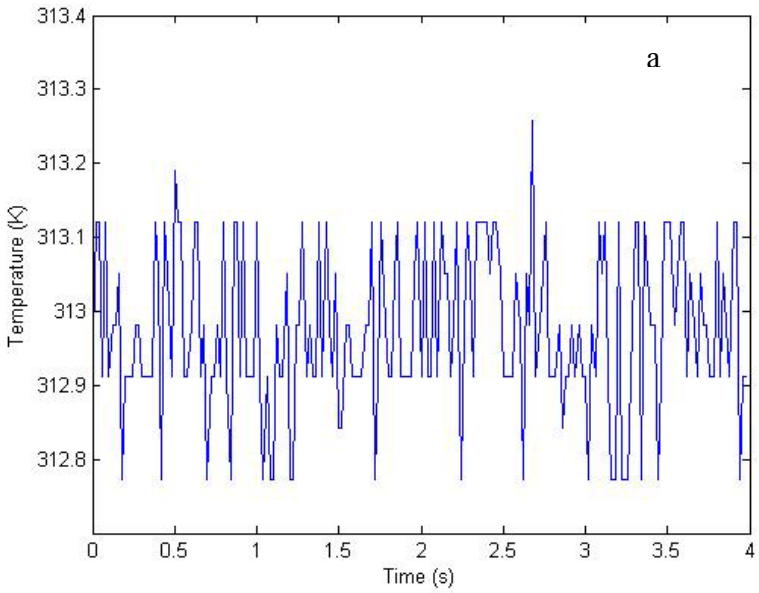

Figure 2: Response of a single pixel versus time

BIBLIOGRAPHIC REFERENCES

1. Rogalski A., "Infrared detectors: an overview", *Infrared Physics and Technology*, Vol. 43, pp.187-210, 2002.
2. Rainieri S. and Pagliarini G., "Data Filtering Applied to Infrared Thermographic Measurements Intended for the Estimation of Local Heat Transfer Coefficient", *Experimental Thermal and Fluid Science*, Vol. 26, pp.109–114, 2002.
3. Rainieri S., Bozzoli F. and Pagliarini G., "Wiener Filtering Technique Applied to Thermographic Data Reduction Intended for the Estimation of Plate Fins Performance", *Experimental Thermal and Fluid Science*, Vol. 28, Issue 2-3, pp.179-183, 2004.
4. Rainieri S. and Pagliarini G., "Calibrazione di un Termografo a Matrice di Sensori per Applicazioni nel Settore dello Scambio Termico", *Atti del XVI Congresso Nazionale sulla Trasmissione del Calore*, Siena 18-19 Giugno 1998, Vol. 2, pp.795-806, 1998.
5. Rainieri S. and Pagliarini G., "Data Processing Technique Applied to the Calibration of a High Performance FPA Infrared Camera", *Infrared Physics and Technology*, Vol. 43, Issue 6, pp. 345–351, 2002.
6. Rainieri S. and Pagliarini G. "Thermographic Image Processing Intended for the Estimation of Local Heat Transfer Coefficient in Channel Flow Configuration", *Proc. 4th European Thermal Science Conference, Birmingham 2004.*

Proposed abstract for
QIRT 2006

Abstract submission deadline: November 28th

Thermal imaging for enhanced foreground-background segmentation

Louis St-Laurent[1], Donald Prévost[2], Xavier Maldague[1]

[1] Université Laval, Département de génie électrique et informatique, Québec, Québec, Canada
[2] Institut National d'Optique, Québec, Québec, Canada

Over the last decade, we saw the appearance of video monitoring in numerous applications. To make apart foreground and background pixels is the first step of any automated video monitoring system aiming at object tracking, event detection or scene interpretation. Still today, this basic task is challenging when the monitoring takes place in uncontrolled environments.

Most solutions proposed for moving object extraction are based on the visible spectrum. Actually, in brightly illuminated scenes, standard color cameras still provide the best information for object segmentation. However, in outdoor applications, darkness and other environmental conditions such as fog, rain and smoke strongly decrease the efficiency of standard cameras.

In many applications, the achievement of zero false negative rate is a critical requirement and the investment in more powerful imaging systems is justified. This opens the way to video systems that would combine thermal and color cameras. In this work, we demonstrate that the addition of LWIR cameras (8-12μm) can significantly improve the robustness of foreground-background segmentation in uncontrolled environments.

As a starting point, and for comparison purposes, we selected a state-of-the-art foreground-background segmentation technique based on color video. This approach, recently presented in [1], use codebook background subtraction. In short, a quantization/clustering technique is used to generate a compressed form of background model on a pixel-by-pixel basis. The method can handle scenes containing moving backgrounds or illumination variation. Moreover, the algorithm allows foreground objects in the scene during the initial training period. The codebook representation is more efficient than other background modeling techniques, including approaches based on Mixture of Gaussians, in term of processing time and memory requirements.

Our original contribution lies in the addition of criterions based on thermal information in the foreground-background segmentation technique presented by [1]. As is widely known in the field of image fusion, the combination of thermal and visible images is not trivial. For this reason, we propose to combine thermal and color information rather than performing image fusion.

The addition of thermal data increases the challenge related to real-time processing of most monitoring systems. Our work also addresses this problem. In order to minimize the processing operations needed for image registration, we developed an approach to register both fields of view at hardware level. Such design also allows to support applications requiring large effective depth-of-field, an advantageous characteristic comparatively to set-ups with parallel or convergent optical axis.

For performance evaluation, qualitative and quantitative assessments were achieved. A Perturbation Detection Rate analysis was performed to objectively measure the impact of the addition of thermal data to the color-based algorithm. A comparison of processing time is also presented.

Reference:

[1] K. Kim, T. H. Chalidabhongse, D. Harwood and L. Davis, “Real-time foreground-background segmentation using codebook model”, *Real-time Imaging*, in press, 2005.

Keywords (5): **Video monitoring, Foreground-background segmentation, LWIR imaging, Thermal-color data fusion, Codebook model.**

SIMULATION AND EVALUATION OF NEW THERMOGRAPHIC TECHNIQUES FOR THE INDUSTRIAL DEPLOYMENT IN THE AUTOMOTIVE INDUSTRY

U. Siemer[a,b]
[a]) Volkswagen AG, Wolfsburg, Germany
[b]) Fraunhofer Institute for Non-Destructive Testing IZFP, Saarbrücken, Germany

Keywords: thermography, non-destructive, simulation, automotive, joining technology

Abstract: To control the joining quality of automotive body structures, there are still many destructive testing methods like chisel testing, metallographic examinations (microsections) or other similar evaluation techniques in use. However, for example for the process control of resistance spot welds, ultrasonic pulse-echo techniques are already successfully adopted. A great potential is also expected by establishing new fuzzy logic techniques that are surveying several process parameters of manufacturing machines to characterise the joints. Due to a reliable non-destructive testing method that ensures the joint quality and is suitable for a process control, the production costs could be reduced enormously, even if we just focus on the discarded body structures scrapped after the destructive tests. For laser welded car bodies a thermographic non-destructive testing method starts to establish itself. So far, for a restricted application range, the applied thermographic impulse technique with flash light excitation is sufficiently robust for the utilization under production line conditions. It represents a reliable testing method for a half automated sampling inspection of laser welded body structures. Consequently, the intention to enhance these potentials and to expand thermography particularly with regard to spot weld evaluation is obvious.

The experimental procedure was designed to evaluate the joining quality of resistance spot welds and the sensitivity of thermographic testing methods under laboratory conditions. The test assembly was optimized using different excitation sources and evaluation methods.

For parameter variations and the analysis of disturbances finite element calculations are conducted. After the validation of the simulation data with experimental results it can be transferred to complex car body structures. Thus, an estimation of the testing feasibilities is possible. The applicability of the testing techniques as well as the minimum device requirements (e. g. temperature resolution, frame rate) is already available in an early development stage. Significant advantages result from the simulation of the heat transfer processes during the thermographic testing. Additionally, by knowing the theoretical temperature response from the specimen, an optimized evaluation can be carried out.

THERMAL ANALYSIS AND THERMOGRAPHIC MEASUREMENTS OF PIEZOELECTRIC TRANSFORMERS

K. Tomalczyk, B. Wiecek

Technical University of Lodz, Institute of Electronics
Wólcza_ska 223, 90-924 _ód_, Poland
e-mail: ktom@p.lodz.pl, wiecek@p.lodz.pl

SUMMARY

The paper deals with the problem of thermal effects in piezoelectric transformers. Very high mechanical quality factors of piezoelectric materials allow to obtain power density and efficiency levels high above the possibilities of traditional magnetic-core transformers. However, the high transformation efficiency is obtained only if the working frequency is strictly controlled and held within the narrow range around one of the resonant modes of the transformer. A slight variation of frequency is needed to control the transformation ratio, but it also has an influence on the overall efficiency. Even in high efficiency operation (at above 90%), thermal effects caused by energy loss can have a considerable magnitude due to small size of the piezoelectric structure.

The main aim of this work was to determine the distribution of heat generation within the piezoelectric material in order to find the source of energy loss in a working transformer. A new type of ring-shaped, multi-layer piezoelectric transformer was examined for various load, input voltage and frequency values. Other aspects like vibration damping due to improper fixing technique were also considered. The results presented in this paper will create a background for proper thermal management in the design of piezoelectric transformer based power converters.

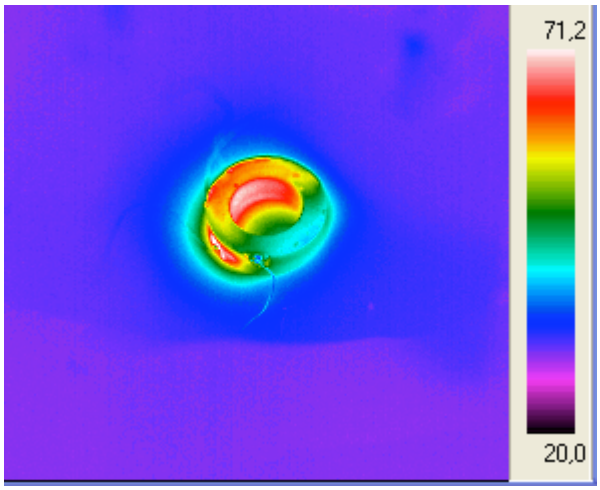

Example thermal image of a ring-shaped piezoelectric transformer under efficiency test

Optimization of electronic devices placement on printed circuit board cooled by forced convection

by M. Felczak and B. Wi_cek

Technical University of _ód_, Wólcza_ska 223, 90-924 Lód_, Poland

Keywords: genetic algorithm, convection

Abstract

Power densities generated in today's electronic components arise very quickly. Electronic components such as VLSI (Very Large Scale Integration) are placed on Printed Circuit Boards (PCB). Optimal placement of the devices on the board plays very important role for dissipation of power to the ambience. Each electronic component, as a heat source, thermally interacts with other ones.

Work includes optimization of electronic devices placement on printed circuit board. Devices are placed along a bottom surface of a duct fig. 1 and cooled with forced convection by air stream with velocity v. Optimization method includes genetic algorithm as an engine searching near optimal placement of electronic devices and thermal solver which calculates temperature distribution in two dimensions. Optimization was carried out in a view of maximal temperature on each of the components.

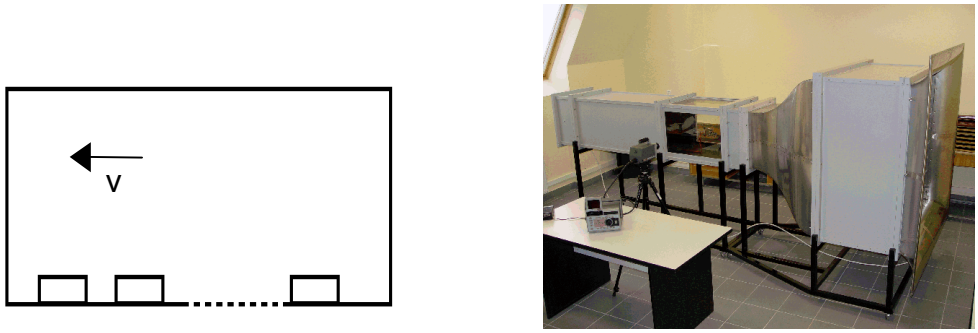

Fig. 1. *Duct with the electronic devices cooled by forced convection*

The investigations are verified by thermographic measurements in the low speed wind tunnel designed especially for application in electronics (Fig. 1).

REFERENCES

[1] A.K. da Silva, S. Lorente, A. Bejan. Optimal distribution of discrete heat sources on a plate with laminar forced convection, International Journal of Heat and Mass transfer 47 (2004) 2139-2148.

[2] Nestor V. Queipo, Joseph A. C. Humphrey, and Alfonso Ortega, Multiobjective Optimal Placement of Convectively Cooled Electronic Components on Printed Wiring Boards

[3] B.A. Jubran, A.S. Al- Salaymech. Thermal wakes measurement in electronic modules in the presence of heat transfer enhancement devices, Applied Thermal Engineering 19 (1999) 1081-1096

[4] Anderson, A.M., 1997, "Comparison of Computational and Experimental Results for Flow and Heat Transfer from an Array of Heated Blocks," Journal of Electronic Packaging, Transactions of the ASME, Vol. 119, pp. 32-39.

Proposed oral presentation

APPLICATION OF INFRARED THERMOGRAPHY IN INVESTIGATION OF ROLLING OF STEEL WITH TRANSVERSAL ROLLS MOVEMENT

TOMASZ S. WISNIEWSKI[1], JACEK PAWLICKI[2], ANNA DRUŻYCKA-WIENCEK[3], FRANCISZEK GROSMAN[2] AND KRZYSZTOF J. KURZYDŁOWSKI[3]

[1] Institute of Heat Engineering, Warsaw University of Technology, ul. Nowowiejska 25, 00-665 Warszawa, POLAND, ph.: (+4822) 6605250, fax: (+4822) 8250565, e-mail: tswis@itc.pw.edu.pl
[2] Department of Process Modeling and Medical Engineering, Silesian University of Technology, ul. Krasinskiego 8,Katowice, POLAND, ph.: (+4832) 6034401 fax.: (+4832) 6034416 e-mail: grosman@plast.polsl.katowice.pl , jpawlicki@polsl.katowice.pl
[3] Materials Science and Engineering Faculty, Warsaw University of Technology, Wołoska 141, 02-507 Warszawa, phone: (+48 22) 849-99-29, fax:(+48 22) 660-85-14, e-mail: doku@inmat.pw.edu.pl

Key words: infrared thermography, rolling, metal forming

In recent years several techniques based on severe plastic deformation (SPD), leading to generation of nanostructures in metals and alloys have been developed. These are cyclic extrusion compression (CEC), hydrostatic extrusion (HE), equal channel angular pressing (ECAP) or high pressure torsion (HPT). These severe deformations involve thermal effects associated with mechanical work done on the deformed material.

In the case of rolling with transversal rolls movement relatively large deformation per pass (true strains of an order of 10) is achieved. It is accompanied by significant thermal effect leading to increase of the extruded product temperature. Temperature is one of the dominating factors which controls the structure and mechanical properties of metals and alloys during their plastic deformation. Therefore, in some cases, it is important to monitor 'on line' and control the temperature rise within the deformed product. Ability to predict the temperature increase during plastic deformation of metals and alloys is crucial for control and design of the structures and properties in final products. The magnitude of the thermal effect depends on the deformation parameters and material properties and can increase the product temperature even by hundreds degrees.

The rolling with transversal rolls movement is performed with use of special patented device that allows for change of rotational speed of rolls, range of their transversal movement and its frequency (Fig. 1). This kind of rolling process was applied to 316LVM austenitic steel that is used, for example, for medical implants.

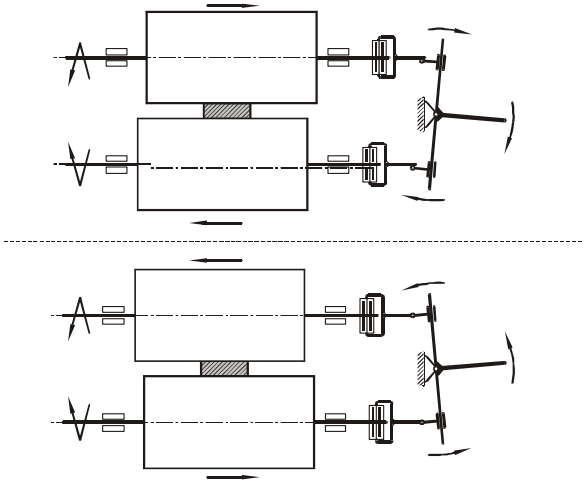

Figure 1. Principle of rolling with transversal rolls movement

Proposed oral presentation

Due to considerable deformation and movement of the rolled samples infrared thermography seems to be the only possibility of temperature changes measurements during this dynamic process (Fig. 2). The measurements were performed with use of ThermaCAM SC 2000 infrared camera together with the high speed recording interface and ThermaCAM Researcher 2001 software. The images of rolled products were recorded with frequency of 50 Hz.

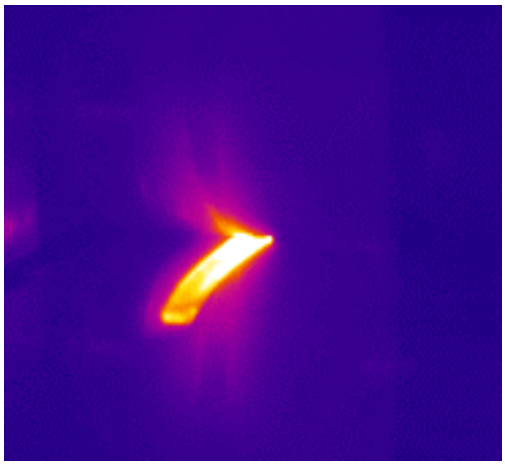

Figure 2. An example of the IR image of rolled 316LVM steel

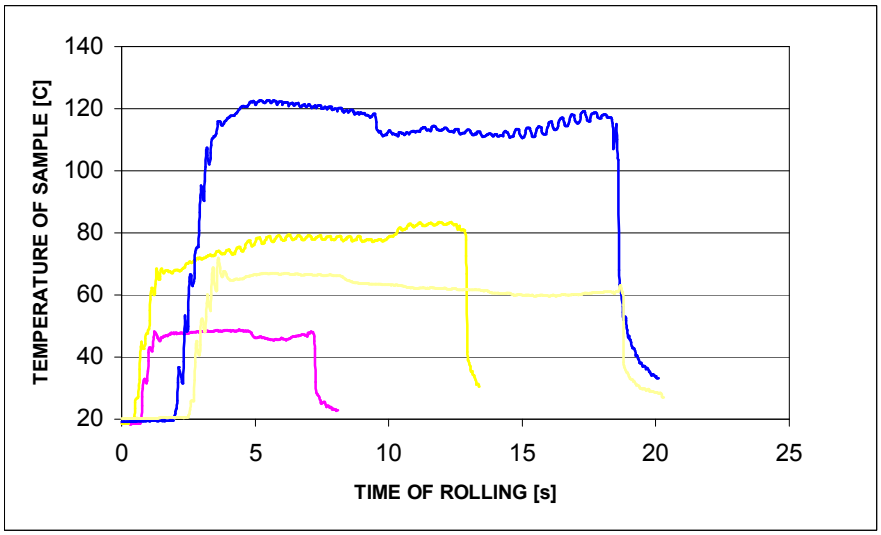

Figure 3. Temperature rise during rolling of 316LVM austenitic steel with transversal rolls movement; examples for processes conducted at different parameters

References

[1] Kong L.X., Lin L., Hodgson P.D.: Material properties under drawing and extrusion with cyclic torsion. Materials Science and Engineering, A308, 2001, pp. 209-215.

[2] Grosman F., Pawlicki J.: Concepts of technological applications in controlled deformation of materials. Acta Metallurgica Slovaca, R.8, 1/2002, pp. 178-182.

[3] Bochniak W., Korbel A.: KOBO Type Forming: forging of metals under complex conditions of the process. Journal of Materials Processing Technology, vol. 134, 2003, pp. 120-134.

[4] Grosman F., Pawlicki J.: Concepts of technological applications in controlled deformation of materials. Procedings of the 7th International Conference on Technology of Plasticity, Advanced Technology of Plasticity, Yokohama, Japan, vol.1, 2002, pp. 1219-1224.

QIRT 2006 extended abstract

Finding of the mechanical power distribution in an horizontal ring mill using infrared thermography.

by

G. Zannis*, M. Founti, P. Makris

National Technical University of Athens
Mechanical Engineering Department
Zografou Campus, Athens - 15780, Greece

*Author for Correspondence: PhD Candidate G. Zannis
National Technical University of Athens
Department of Mechanical Engineering,
Laboratory of Machine Design,
Heroon Polytechniou 9, Zografou Campus,
Athens – 15780, Greece
e-mail : gzannis@central.ntua.gr
Tel. (+301) 7723886,
Fax. (+301) 7723663

Comminution is an extremely energy consuming process with efficiency factor around 1%. This factor is defined as the quotient of the mechanical energy necessary for the creation of new surface in the grains of the material to the mechanical energy which enters the mill. That means the energy entering the mill is converted almost entirely to thermal energy resulting the increase of the temperature of the working parts of the mill e.g. rings in the ring mill balls in the ball-mill rod in the rod-mill etc as well as the temperature of the produced material.

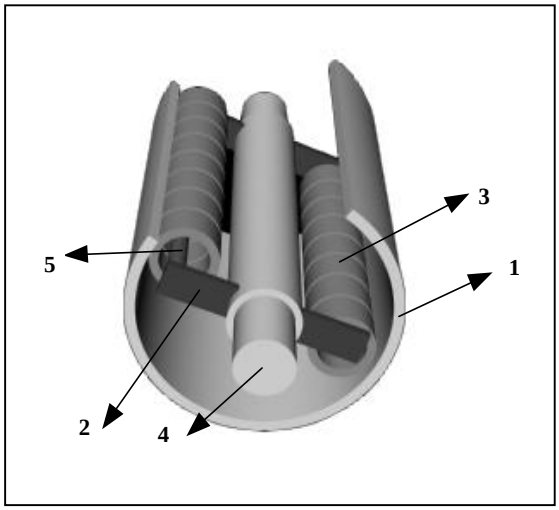

Fig 1. Components of the ring-mill

The aim of present work is the finding of regions with intense release of thermal power in order to be better understood the comminution process along the horizontal ring mill (Fig. 1) Observation of the internal fast rotating parts of the mill during the operation and measurement of the local temperature with conventional methods (thermocouples) is impossible due to lack of access and problems with the wiring inside the mill. For this reason the temperature distribution on the mill shell was revealed with the aid of infrared thermography. An infrared camera (FLIR PM595) is used and the thermographs have been post processed with the appropriate software in a PC.

Figure 1 shows the main components of the ring mill. A cylinder (1) forms the main body of the mill. A rectangular metal frame is positioned along the principal axis of the cylinder and is attached to the main shaft (4). The main shaft can be rotated with the help of an electric motor. The rectangular metal frame comprises two arms (2) which are held parallel with the help of two ring-connecting rods (5). A variable number of annular metal rings (3) is inserted along each connecting rod. Each ring is allowed to move freely along and around each rod. During rotation of the orthogonal metal frame the metal rings, due to centrifugal forces, are compressed against the inner surface of the cylinder of the pulverizer. Simultaneously frictional forces are developed between the metal rings and the inner surface of the machine. Thus, the rings rotate freely around their symmetry axis and simultaneously

slide along the arms of the frame and roll on the inner surface of the cylinder. The particles are ground in the space left between the inner surface of the mill and the annular metal rings.

The experiment was conducted in an horizontal ring mill grinding olivine which is a material with high hardness (ca. 7 on the MOSH hardness scale) and demands large amounts of energy for it' s comminution. The operating parameters –rotational speed and raw material through-put- are kept constant during the experiment. The initial temperature of the mill is 30°C while the final is 62°C. The duration of the experiment is 270 s.

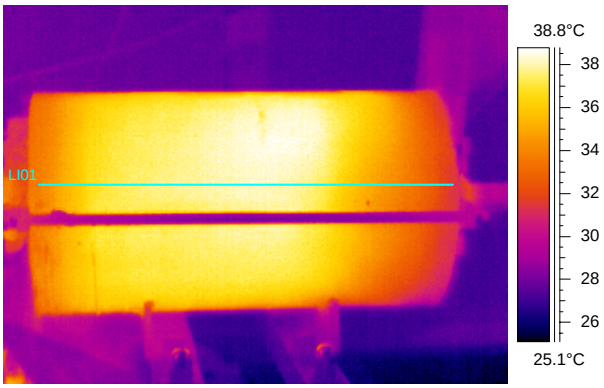

Fig. 2. Thermograph of the mill with the temperature line L01

Fig. 2 is the thermograph of the mill external surface after 60 s of operation in which is seen the temperature line along which are extracted the temperatures presented in Fig 3 every 30 seconds. This line is a feature of the software for the processing of the thermographs. It is observed that during the whole duration of the experiment the distribution of the temperature is not uniform. The maximum value is on the 1/3 from the entrance of the material. It is concluded from this that the maximum absorption of power from the material takes place in this area meaning that the operation of the mill is optimum for the granulometry in this area but also increased wear of the rings. As the material is moved to the exit it's temperature is decreased indicating reduced mechanical power.

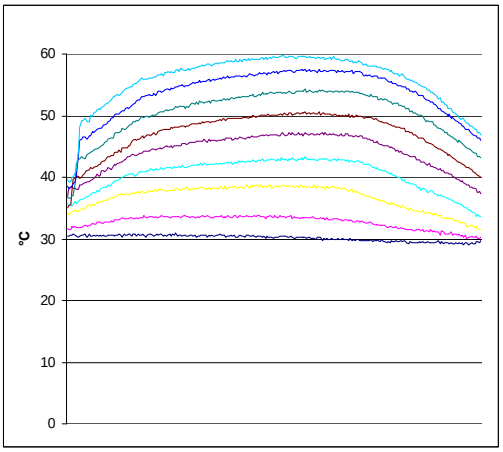

Fig. 3 Temperature distribution along the mill in relation with time.

The results are taken into account for the dimensioning of the mill for specific production requirements and for the cooling system of the mill surface.

References

1. Zannis, G. Founti, M., Makris P., "Estimation of the grinding efficiency of a horizontal ring mill with the use of IR-thermography", 6th International Conference on Quantitative Infrared Thermography, QIRT 2002, Dubrovnik, Croatia, September 2002.

2. M. Founti, G. Zannis, E. Tsolis, P. Makris "Influence of design parameters on the energy balance of a horizontal ring mill", Engineering Design Conference 2002, London, July 2002.

DETECTION OF ROLLING BEARING DEGRADATION USING INFRARED THERMOGRAPHY

Atef MAZIOUD, Jean-Félix DURASTANTI, Laurent IBOS, Evelyne SURUGUE
CERTES (EA 3481), University Paris XII, France

Key-Words-: *Temperature measurement by IR thermography; Vibratory analysis; defect of movement;*

Summary

Our study deals with the detection and the diagnosis of spalling in rolling bearings. Our idea is to show the correlation which exists between the outside temperature of the spalling and the vibratory level generated by increasing appearance of the defect.

This study is based on thermal modeling of the heat transfer between the rolling elements and the spalling outside border on one hand and on modeling of the spalling vibratory answer on the other hand.

We led an experimental study on a test rig which allows the creation in a progressive way, of a spalling defect on the external ring of a rolling bearing. On this test rig, we measure simultaneously the mechanical vibration in radial direction (by means of a piezoelectric accelerometer) and the landing external surface temperature (by means of an infrared camera). Then, we show the correlation existing between theses two phenomena.

The methodology is described below (see also figure 1):

- Periodic impacts are generate by a spalling zone located between one of both rings of the rolling bearing (an impact in every passage of a rolling on the spalling zone).
- These periodic impacts are going to excite the system mechanical structure (movement, connection with the frame of the machine…).
- The whole landing is thus going to vibrate in its own frequency of echo.
- The vibrations generated have a sinusoidal shape. The amortization has the effect to transform a part of this vibratory energy into heat.
- This heat loss induces a rise of the ring temperature, and more particularly of its outside surface.

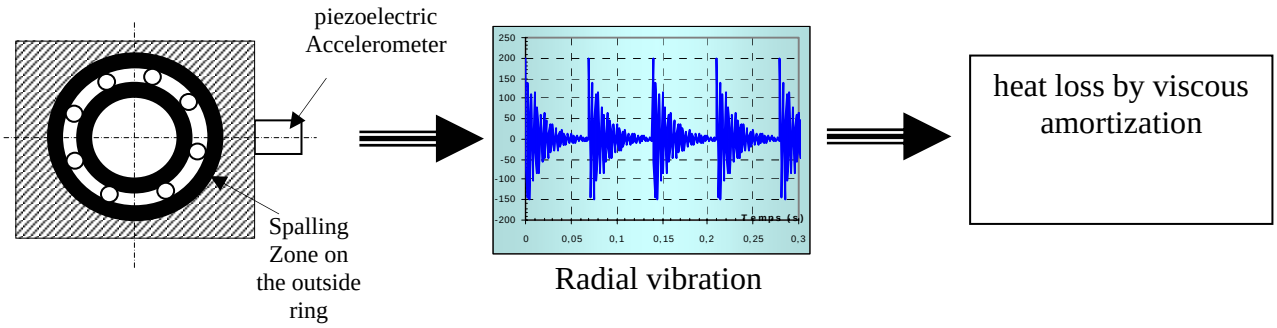

Figure 1. Rise of temperature of the rolling bearing due to the presence of a spalling zone on the outside ring.

Our laboratory has a turning machine (fig. 2) which main characteristics are:

- AC motor: 1.5 kW, maximum turning speed 1500 rpm
- Rolling bearing type : angular-contact ball bearing (SKF 7206)

Various defaults can be simulated on this test rig. The default analyzed in this paper concerns a spalling on the inner face of rolling bearing.

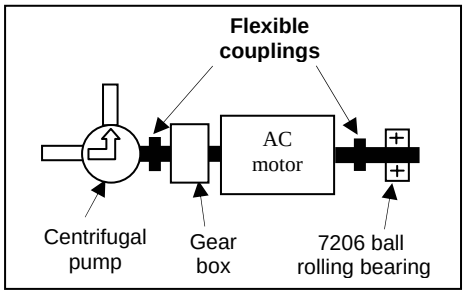

Figure 2. The experimental setup

To summarize, we think that the measurement of this temperature rise might allow us to estimate the vibratory energy quantity generated by the periodic impacts, and therefore to estimate the level of rolling degradation.

This objective is naturally ambitious, and we shall present here only the first part of our study. It is essentially based on an experimental study of the temperature rise of the external ring bearing, and on the influence of the evolution of the spalling default.

The results obtained in this first stage are encouraging concerning the objectives which were fixed. Indeed, on one hand, the vibratory defect caused by the movement leads to a quantifiable heating of the surface; on the other hand, the numeric modeling shows a correlation between vibratory defect and heat production but also allows us to quantify the involved streams.

THERMOGRAPHY IN THE INVESTIGATIONS OF THE THERMAL DEFORMATIONS IN NC MACHINE TOOL BODIES

Roman Staniek
Poznan University of Technology, Institute of Mechanical Technology
ul. Piotrowo 3, 61-138 Poznan
E-mail: Roman.Staniek@put.poznan.pl Tel. ++4861 665 27 58 Fax ++4861 665 22 00

Key words: NC machine tools, thermography, thermal deformations, compensation methods

The essence of thermal phenomena occurring in NC machine tools as well as their influlence on the thermal deformations has been described in the paper. The influence of the thermal deformations upon the NC machine tool accuracy has been also discussed. There have been pointed out sources and flow ways of the heat streams in the system of NC machine tool – environment by means of radiation, convection and conduction. There have been discussed the influence of the structure and design upon the machine tool thermal properties and on the machine tool deformations.

The paper presents the role and significance, which are contemporary played by the thermographic investigations of the thermal states and effects by means of an infrared camera (Fig. 1 and Fig. 2). There is presented their vital importance in the area of diagnostics the sources and intensity of heat, as well as the influence on the positioning accuracy.

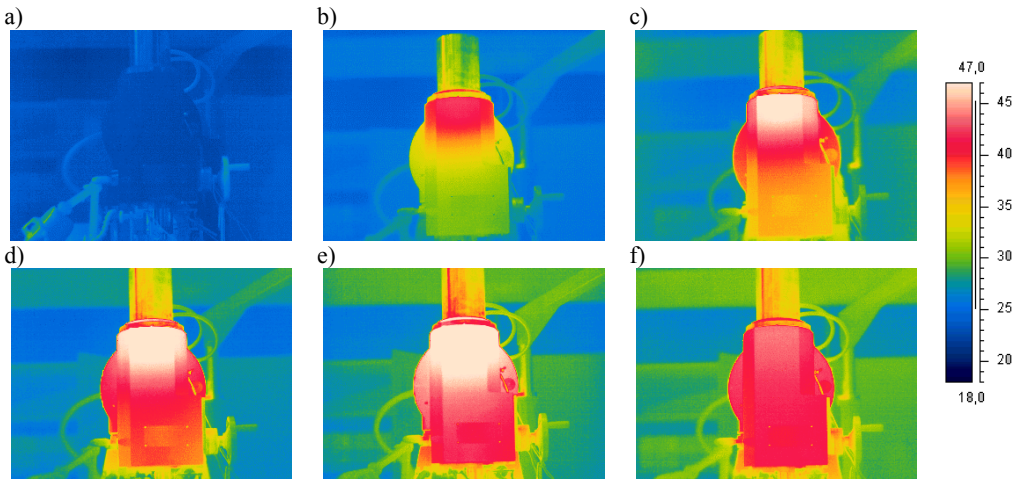

Fig.1. Thermograms of the face surface in the spindle head of the milling machine working in idle run performed after: a - 0 min, b - 60 min, c - 120 min, d - 180 min, e - 240 min and f - 300 min of work

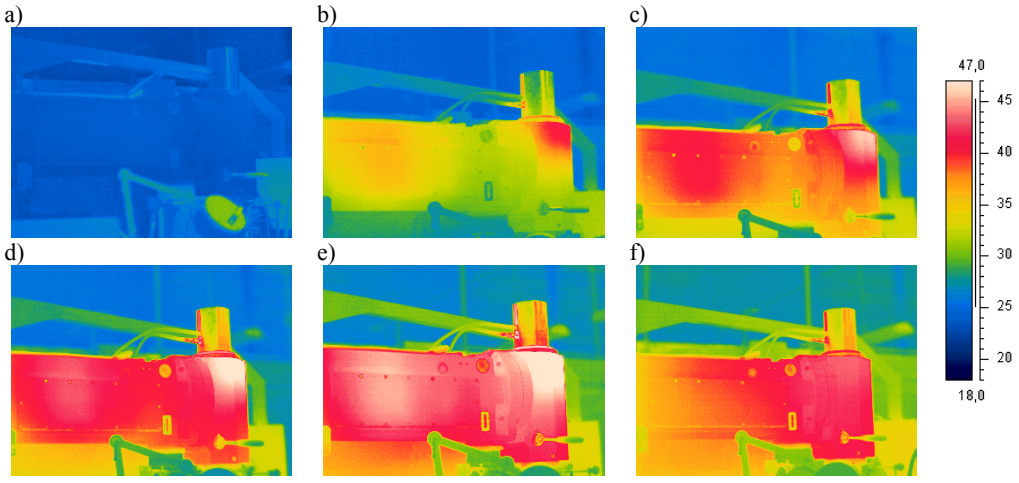

Fig. 2. Thermograms of the side surface in the beam of the milling machine working in idle run performed after: a - 0 min, b - 60 min, c - 120 min, d - 180 min, e - 240 min and f - 300 min of work

Describes the measuring system of thermal displacements. Experimental investigation results of the linear deformations according to the ISO 230/3 standard demanding in three axis and angular deformations in two axis of the NC milling machine have been presented (Fig. 3 and Fig. 4).

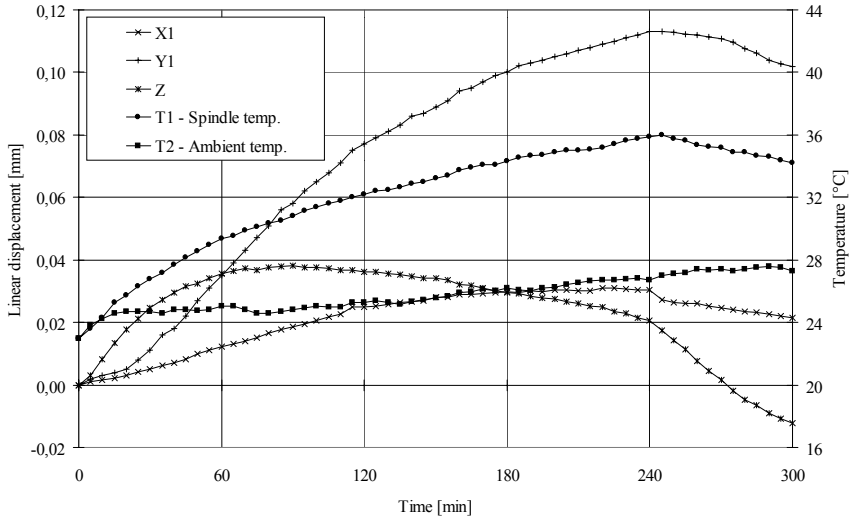

Fig. 3. Linear displacements of the spindle end in X, Y, Z axis and temperature courses (ambient and spindle) in idle run of milling machine

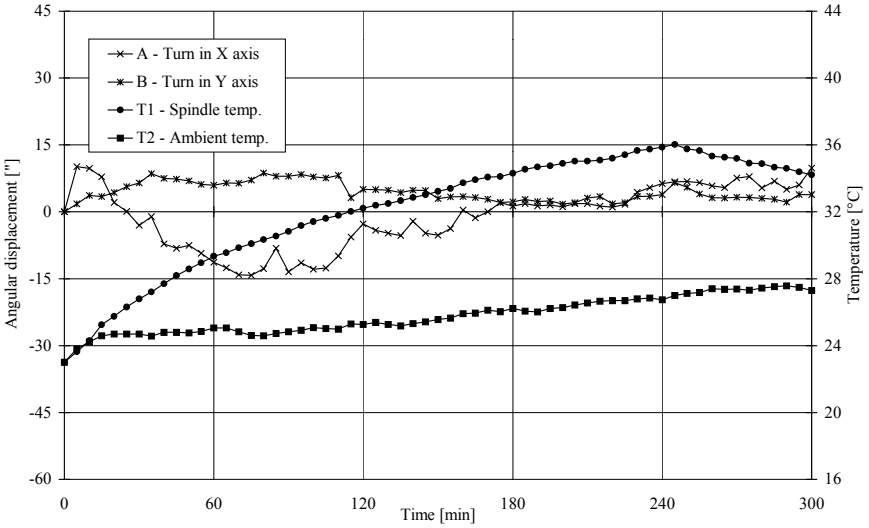

Fig. 4. Angular displacements of spindle head in X and Y axis and temperature courses (ambient and spindle) in idle run of milling machine

Describes the compensation methods of thermal deformations in machine tools connected with linear and angular displacements and their effectiveness. The effects of the compensation have been also presented.

Title of Abstract:
On-Line Thermal Barrier Coating (TBC) Monitor for Real-Time Failure Protection and Life Maximization

Dennis H. LeMieux, Materials Engineering / Non-Destructive Testing,
Siemens Westinghouse Power Corporation
4400 Alafaya Trail, MC Q3-031, Orlando, FL 32826, USA
Phone: +1 407 736 5137
e-mail: dennis.lemieux@siemens.com

Vinay Jonnalagadda, Materials Engineering / Non-Destructive Testing,
Siemens Westinghouse Power Corporation
4400 Alafaya Trail, MC Q3-031, Orlando, FL 32826, USA
Phone: +1 407 736 6810
e-mail: vinay.jonnalagadda@siemens.com

Abstract:
Monitoring of mission critical engine parts during gas turbine operation is now possible by combining innovative access port design, high-speed infrared imagery, a tailor-made overall control and image evaluation system, and related TBC lifing models. The need for such monitoring has become more critical in recent years as engine firing temperatures have risen and the potential impact of part failure has grown. In particular, the need to guard against the loss of TBC has become an important factor for maximizing turbine availability and for minimizing commercial risk. This On-Line TBC Blade Monitor will not only help insure the safe operation of a gas turbine, but also provide the opportunity to extend the life of blades beyond the nominal operating hours, based on real-time and historical images that clearly prove the integrity of the thermal barrier coating.

This paper will present an overview of an On-Line TBC Blade Monitoring system, which is able to capture two-dimensional quantitative infrared images of row-1 blades during full engine operation. This system, which was successfully tested on our 200 MW class gas turbine at full load, was developed by a team of Siemens Westinghouse Power Corporation Engineering and Diagnostics experts in cooperation with Siemens Corporate Research under the sponsorship of the U.S. Department of Energy's National Energy Laboratory.

Keywords:
Infrared Thermography, Thermal Barrier Coating, Gas Turbine Engines, Condition Monitoring, Image Evaluation

The Thermal Wave Method for Investigations of Textile Properties

by M. Michalak[1], B. Wi_cek[2], I. Kruci_ska[1] M. Felczak[2]

[1]*Department of Textile Metrology, Technical University of _ód_. Poland*
[2] *Institute of Electronics, Technical University of _ód_, Poland*

The results of investigations of new method for textile thermal parameters determinations are presented. In the papers [1-3] the original solution with using IR mirrors for registration of temperature distribution on opposite surfaces of flat textile product were presented. This make possible to investigate heat transport in throw direction of product. In the paper [4] the thermal wave method was applied and the possibility of heat transport determination along surfaces of product was shown.
In this paper the authors trial connect thermal wave method with IR mirrors method.
The thermal measurement setup is presented on figure 1.

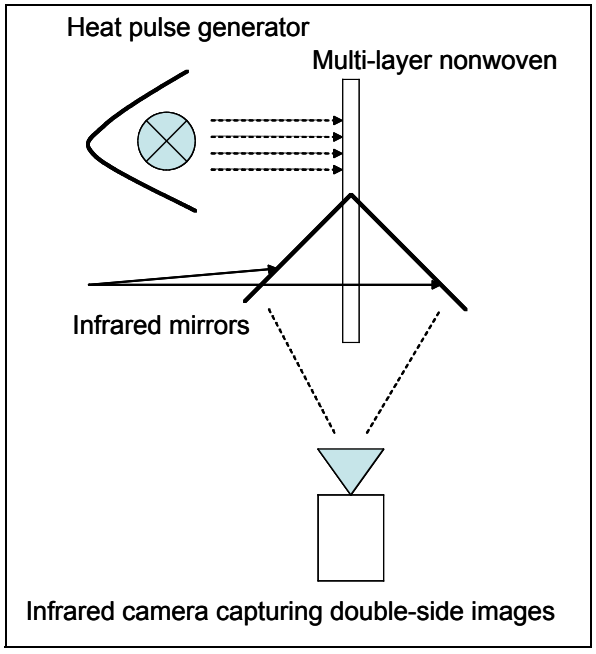

Fig. 1. Thermal measurement setup

The surface of one half of the sample was exposed to the thermal wave generator. The heat flux was transferred along the surface and then to the opposite side of the not heated area of the sample. On the line between the heated and not heated part of the sample, two specially prepared mirrors were placed, at an angle of 90^o to each other (Fig. 1). They were located in such a way, that registration of thermograms from the two opposite surfaces, was possible at the same time. The thermovision camera was placed on the line of the longitudinal axis of the sample. Signal from the camera was transmitted to the computer. In this way, it was possible to register temperature distribution on both surfaces of the sample - heated and not heated.

The exposure process was periodic with frequency 1 Hz. During the measurements, thermal images were registered at the frequency of 2 frame/s and transferred to the computer memory and then analyzed. A sequence of 300 thermograms was acquired.

The map of temperature distribution reflected in IR mirrors was registered, that means that the temperature distributions on radiated and nonradiated site of sample was analyzed. The amplitude and phase analysis were carried out. For determination of thermal parameters the additional investigations on standard uniform flat material with known thermal properties were provided.

The nonwoven structures manufactured from polypropylene and electroconductive fibers were investigated. The morphological, electro-physical and comfort properties of produced textiles were studied, in parallel with thermographic measurements.

1. M. Michalak, M Zimniewska, I. Kruci_ska, B. Wi_cek. The Study of Thermal Properties of Linen/PES Fabrics using Thermovision methods. The 3^d AUTEX Conference “World Textile Conference”, Gda_sk, Polska, 25-27 czerwiec 2003, s. 385-393.
2. M. Michalak, B. Wi_cek, I. Kruci_ska, M.Lis: “Thermal Barrier Properties of Nonwovens Multilayer Structures Investigated by Infrared Thermography”. VIIth Quantitative Infrared Thermography – QIRT 2004, Brussels, Belgium, 5-8 July, 2004.
3. M. Michalak, B. Wi_cek, I. Kruci_ska: „Badanie warstwowych uk_adów w_ókninowych now_ metod_ termowizyjn_”, IV Krajowa Konferencja TTP-2004, Ustro_, 6-8 listopada 2004r.
4. M. Michalak, M Zimniewska, I. Kruci_ska, B. Wi_cek. The physical properties of the surface of apparel made from flax and polyester fibres. 1st International textile, clothing & design conference – Magic World of Textiles, Dubrovnik, Croatia, October 2002

Thermographycal Analysis of the coking oil-products degree

Vladimir Zaharenko

Rendering and graphic analysis of the infrared fields on the technological equipment surfaces actualize new informing possibilities for the purpose of inspecting the technological processes. The high thermographic control informativeness is connected first of all with the rendition of energetical transformation in the control objects, as far as the energy transformation process is in most cases connected with release or absorbency of the warm and these alternations rendering makes it possible to follow the very energetical transformation's dynamics.

The work at the termographic control systems, adapted for the purposes of the ceaseless termographic inspecting of different technological processes in the conditions of the main technological equipment's exploitation is carried out in Omsk State Technical University since 1993, and especially for the purpose the inspecting of the temperature fields of whirling furnaces producting cement, haydite, oil-coke, lime burning, bake-out in aluminum industry.

The main demands for such system are conditions of temperature fields control in the range $(100 – 600)^0$ C with absolute accuracy $(3\text{-}5)^0$C, working ability while medium thermal change from – 40 ^{0}C to +60 ^{0}C, high operation reliability, providing continuous work of the system during some years, solving the problem of measurement assurance.

In this work, the coking degree control is supposed to be indirect, according to the temperature gradient along vertical forming external surface of the coke cell. The statement of the connection of the temperature gradient $\triangle$T on the reactor surface with the phasic conversion dynamics inside the reactor is based on the following notions of the coking processes. The fresh breeze, warmed to 470..490 ^{0}C, chuted through the inferior reactor neck, fills the space above the formed coke. At certain temperature and pressure, the coking processes proceed with fluid products releasing. At reactions` process coke takes the inferior part of the reactor, and fluid takes the superior, above the liquid layer. The thermal transmission density between the

reactor`s panel and products, being in fluid, liquid, and solid stages, will be different. The most intensive thermal transmission will be on the liquid layer degree, the lest – in the zone of fluid and solid phases. Besides, as far as the transit from liquid to fluid phase has endothermal character, there appear conditions for gradient temperature increase. At the same time, reactions of condensation, compression, and coking take place with thermal release, that also promotes increase of the temperature differential on the liquid and coke border. So, the derivatives -△T/△h (h – coordinate of the reactor's height) above the liquid layer and under it will have different signs. Negative -△T/△h above the liquid layer, and with the sign "plus" on the liquid and solid phases border.

The functional scheme of the coking degree control is attached.

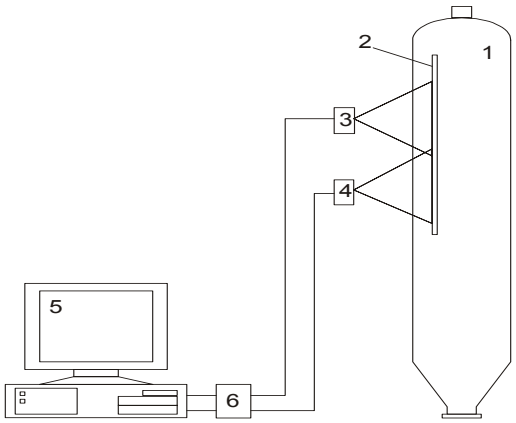

The system represents an appliance, consisting of one or several scanning pyrometric transducing apparatus 3 and 4, IBM-computer 5, channel adapter 6, programming provider refinement and visualization of the temperature fields. In the thermal insulation layer of the reactor 1 there is a 0,1m wide shelter 2.

Emissive Properties of Materials and its Relation with Roughness

Leszek Rozanski
Poznan University of Technology, ul. Piotrowo 3, 60-965 Poznan, Poland, phone: +4861 6653595,
fax +4861 6653570, e-mail: leszek.rozanski@put.poznan.pl
Michal Wieczorowski
Poznan University of Technology, ul. Piotrowo 3, 60-965 Poznan, Poland, phone: +4861 6653569,
fax +4861 6653570, e-mail: wieczoro@sol.put.poznan.pl

Key words: surface topography, emissive properties, IR thermography

Appropriate characterization and description of object emissivity has a crucial influence on accuracy of IR system for remote temperature measurement, e.g. IR thermography or pyrometry (the value of the measured signals of the IR systems is a function an object temperature and, among others, is also function an object emissivity [1],[2],[3],[4]). Therefore, to measure the temperature accurately with IR system, it is necessary to know this parameter. Generally, emissivity is not a constant, as it depends on several parameters: temperature, viewing angle, wavelenght, contamination or roughness. All totoal radiative properties of materials can only be regarded as fuction of veiwing angle and temperature. Spectral emissivity $\varepsilon(\lambda)$ as a function of wavelenght λ decreases for metals, increases for dielectrics and is band-like for gases, liquids and same solids. The chemical and physical changes of the emitting body caused by temperature, time and pressure influence its emissivity. A general characteristic, independent of the kind of material is the variability of emissivity according to surface roughness [5]. Emissivity increases with the increase of roughness. In particular the emmisivity of metal, which is usually low, can considerably increase with roughness. An analysis of the emissivity as a function R_q (root-mean-square-roughness) demonstrates that a treatment of the surface in terms of R_q is absolutely insufficient to predict radiative properties of materils [6].

Most of commercially available IR thermal instruments need the effective emissivity $\varepsilon_{eff}(\lambda)$ of the tested object as an input parameter. The effective emissivity of the IR system, in spectral band from λ_1 to λ_2, is defined as the mean value of the function of spectrally variable emissivity $\varepsilon(\lambda)$ weighted by the product of function of the spectral object luminance $L(T_{ob},\lambda)$ at the temperature T_{ob}, the detector relative sensitivity $s(\lambda)$ and the optics transmittance $\tau_o(\lambda)$ [4]. At present, longwave 7.5 -13 μm IR thermograpic systems with the uncooled microbolometric arrays (FPA) are most popular in the industry and the science. To do the test, measurement of the effective emissivity specially prepared steel samples with modern IR system was made (fig. 1)

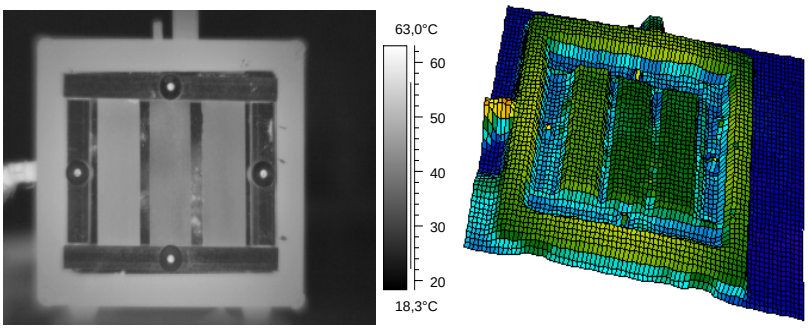

Fig. 1 *Thermal imagings of the steel test sample (sand blasted surfaces)*

Surface profilometry is for many years a well-known method of topography inspection. Based on multiprofile representation or spiral sampling [7],[8],[9] gives a three-dimensional image of the surface. It is also possible to evaluate topography parameters and it is a proven fact that they represent surface properties much better. Among surface parameters there are the ones representing vertical, horizontal and hybrid properties, as well as functions describing surface behaviour.

Basing on knowledge concerning emission a number of topography parameters were chosen for possible relation with emissive properties. First parameters from material ratio curve were used. Second a developed area and its relation with sampling area were chosen. Third there was an idea to use isotropy. For periodic surface which in our case was a milled surface two very different examples were chosen. One surface was relatively smooth while the other was very rough. Though difference in asperities is about ten times we can see practically no difference in emissive properties. Also all the parameters connected with material ratio and developed area do not show any correlation with emissive properties. The only parameter that can reflect these properties in this case is isotropy. A different situation can be observed at isotropic surface e.g. a sand blasted one (fig. 2, fig. 3). This surfaces are different from milled ones and isotropy cannot be used to describe heat emission

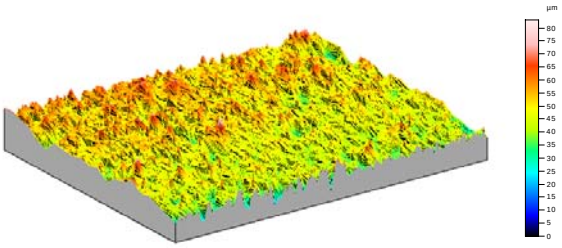

Fig.2 *Axonometric view of sand blasted surface*

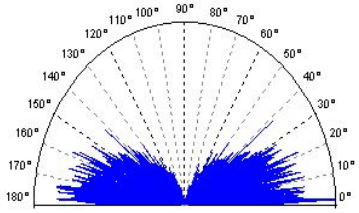

Fig.3 *Isotropy graphs for sand blasted surface*

from the surface. A question emerges why isotropy is not suitable for surfaces of that kind. In our opinion this is due to the fact that shape of asperities is very different from milled surface what effects in a different heat transfer and emission. Asperities are much sharper and holes caused by sand direct heat rays very randomly, what can be seen from isotropy graph (fig. 3). As in our case all the tested specimen were flat this element was a plane. Values of roughness parameters were calculated after polynominal filtering.

Surface topography is one of the features influencing on emissive properties. For periodic surfaces isotropy seems to be a good measure of theoretical emissive properties. Here even big changes in amplitude parameters do not significantly change emissive properties. On the other hand for random surfaces a ratio of mean spacing and Sz seem to be a much better measure of emissive properties. As all the asperities are random and cause random direction of heat rays, isotropy does not give a good image of emission.

References

[1] A. OTSUKA, K. HOSONO, R. TAAKA, K. KITAGAWA, N. ARAI. „*A survey of hemispherical total emissivity of the refractorymetals in practical use*", Energy, N^o 30, 2005, pp. 535–543.
[2] X. MALDAGUE. *"Theory and Practice of Infrared Technology for Nondestructive Testing"*, John Willey & Sons, Inc., ISBN 0-471-18190-0, 2001.
[3] S. POLOSZYK, L. ROZANSKI. „*Thermographic Diagnosis Station of Machines"*. 7th International DAAAM Symposium. Vienna 1996, pp. 351-352.
[4] K. CHRZANOWSKI. „*Problem of Determination of Effective Emissivity of some Materials in MIR Region"*. Infrared Phys. Technol. Vol 30, N^o 3, 1995, pp. 679-684.
[5] A. SALA. "*Radiacyjna wymiana ciepla"* WN-T, Warsaw, ISBN 83-204-0367-7, 1982.
[6] W. SABAGA, R. TODTENHAUPT. „*The Effect of Roughness on the Emissivity of Precious Metals Ag, Au, Pd, Pt, Rh and Ir"*. High Temperatures – High Pressure. Vol. 33. N^o 3, 2001,pp. 261-269.
[7] M. WIECZOROWSKI. *"Spiral sampling as a fast way of Data Acquisition in Surface Topography Measurements"*, International Journal of Machine Tools & Manufacture, 41, 2001, pp. 2017-2022.
[8] T. TSUKADA, T. KANADA. *"Evaluation of two- and three- dimensional surface roughness profiles and their confidence"*, Wear, 109, 1986, pp. 69-78.
[9] M. WIECZOROWSKI, A. CELLARY, J.CHAJDA. "*Parameters for three dimensional surface texture character analysis"*, Proceedings of the Third International Symposium on Measurement Technology and Intelligent Instruments ISMTII'96. Hayama, Japan 1996, pp. 209-216.

Can reflections strongly modify the measured surface temperature of plasma facing componants in experimental fusion reactors like Tore-Supra, JET and ITER ?

D. Guilhem

CEA-Cadarache, 13108 Saint Paul Lez Durance (France)

In fusion experimental reactors, heat flux deposition measurements on the main plasma facing components are a crucial issue when the safety of the elements is looked at [1]. Using modelling and extensive electron beam tests on size one elements, a relation between the surface temperature and the impinging heat flux, is established. On the other hand, any actively cooled plasma-facing component has its own critical heat flux limit, which depend on the geometry, flow velocity and temperature. This limit must not be overpassed, otherwise a breakthrough of the leak tight water pipe is observed and a water leak into the main vessel is taking place.

Usualy the luminance coming from the observed object is the sum of different contributions. One has to be able to unfold them so that only the luminance coming from the Planck radiation of the observed object is accounted for when converting into surface temperature through the calibration tables of the thermography system. The weight of the different contributions has to be estimated so that any non-relevant contribution is wiped out when possible. This is of the most importance in nuclear fusion tokamak since these contributions depend strongly on the material used to build theses palsma facing componants. For example in today tokamaks, the main plasma facing components material is Carbon Fibre Composite (CFC) having an emissivity (~0.9) which is not very dependant on surface temperature and wavelength, which makes thermographics measurements relatively reliable. On the other hand, it is planned to have limiters made of Tungsten (Tg) in the European JET tokamak, actually in activity at Culham (GB) and in the world (China, Europe, Japan, Korea, Russia, United States) future fusion reactor ITER being implemented in Cadarache (France). For tungsten material the emissivity (~0.2) is strongly dependant on the surface temperature, as well as on wavelength of observation.

The main limiter is heated by large heat fluxes up to 20Mw/m² (70MW/m² at the surface of the sun) and so their surface temperature are relatively high between 1000°C and 1500°C. Such a hot limiter is radiating toward the inner wall of the vessel (radiation N°1 figure-1), which usually is made of metal (stainless steal, inconnel or berylium). Such a closed metalic volume can be compared to a radiating sphere, used to calibrate detectors in laboratories. Integrating spheres are optimized to have a large flux multiplicator factor ($10<M<100$), meaning that the output flux can be much larger than the input flux. Does this effect could make a large difference when such a radiation is reflected by the limiter surface, radiation N°2 figure-1. If the surface of the limiter is a good reflector then the reflected flux generated at the surface of the inner wall (constant bacbground temperature of the inner wall) where eventually a hot spot is present (radiation N°3 figure-1) may also pose problems.

To be able to weight these different contributions, we will first present briefly the theory of the integrating sphere, to be able to extrapolate the results to the case of the metal torus shaped tokamak. Then we will takle two other situations. The first one is when the surrounding wall of the main limiter (where the incident heat flux is maximum) is at a constant temperature (actively cooled wall) , the one of the water cooling loop. This tempertaure is set to 120°C for Tore-Supra, 200°C for the JET and finally to 100°C for ITER. The camera captures the reflected luminance coming from this wall by the limiter. The second situation takes place when the optical instrument gathers the specular reflected radiation from a hot spot.

We show that on the one hand, the effect of the “integrating torus” is completely negligeable both for CFC limiter machines like Tore-Supra as well as for the metalic limiter machines like JET and ITER. On the other hand, the reflected luminance of a known temperature wall is easily accouted for, but the specular reflected radiation issued from a hot spot, cannot be accounted for in metalic machines (but can be neglegted in CFC machines) unless we have an independant direct measurement of the surface temperature and emissivity of the hot spot. This is a very demanding and challenging issue for JET and ITER thermographic diagnostics. Active methods [2] are studied to be able to get as much as possible information on the emissivity/reflectivity of the observed object as well on the hot spot zones which may play a significant role in the determination of the surface layer properties. An example of the influence of a hot spot in the tokamak Tore-Supra during a real shot is presented.

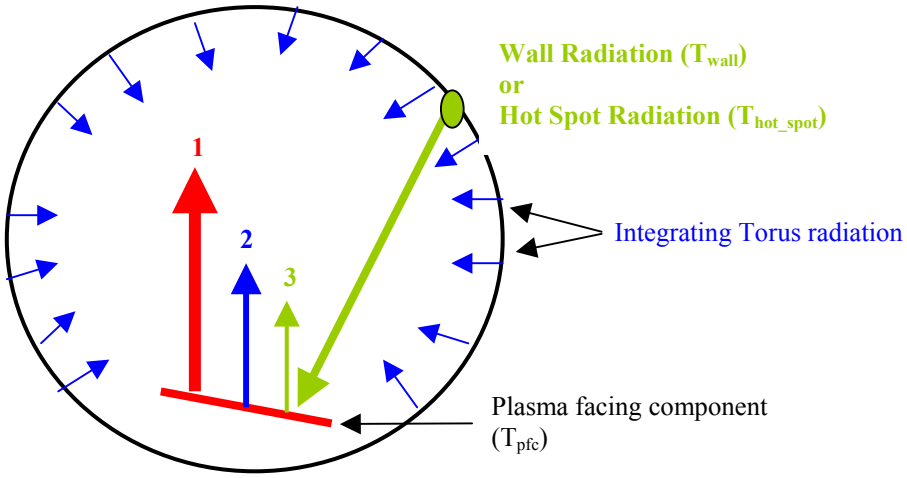

Figure-1 : Poloidal section of a Tokamak showing one plasma facing component. The camera detector captures the radiations 1, 2 and 3 at the same time. N°1 is coming from the plasma facing component at temperature T_{pfc}, radiation N°2 is similar to the one coming from an integrating sphere and finally N°3 is issued from one part of the wall at a low and constant temperature T_{wall}, or from a hot spot at temperature T_{hot_spot}, both captured after one specular/diffuse reflection on the plasma facing component under observation.

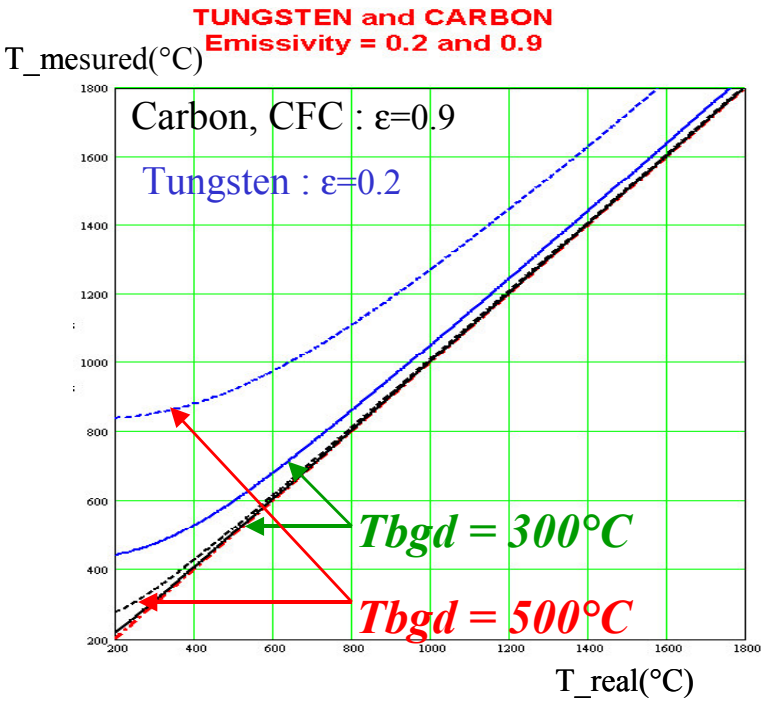

Figure-2 : Mesured surface temperature as a function of the real surface temperature. The effect of the specular/diffuse reflectivity of the observed material has a strong influence on the measured temperature. The hot_spot/background temperature has also a strong influence.

Re

[1] "Infrared surface temperature measurements for long pulse operation, and real time feed-back control in Tore-Supra, an actively cooled tokamak", D.Guilhem and al., QIRT Journal, Volume 2 – N°1/2005, pages 77 to 96

[2] "Bicolor pyroreflectometer using an optical fiber probe", D.Hernandez and al., Rev. Sci. Instruments 66 (12), December 1995

Corresponding author:
Dominique GUILHEM
DRFC / SIPP Bat. 507 CEN-Cadarache
F-13108 Saint Paul Lez Durance Cedex, France
dominique.guilhem@cea.fr

Calibration of incremental temperature fluctuations at high temperatures

Marija Strojnik[1] and Gonzalo Paez[2]
Centro de Investigaciones en Optica, Apartado Postal 1-948
C. P. 37000 León, Gto., México
mstrojnik@aol.com and gpaez@cio.mx

Abstract

We present experimental procedure to measure small and rapid temperature variations at elevated temperatures, traceable to National Institute of Standards.

Key Words: calibration, small temperature changes, high frequency

Poster presentation

Summary

Temperature distribution over a target surface may be effectively measured as a function of time with an IR camera. This may be very convenient when the temperature distribution varies slowly compared to the IR camera scan rate. This is not adequate in the case when a laser beam at a 1 Khz rate irradiates a surface pixel at 1 kHz rate. A radiometer calibrated for the required temperature range, speed of response, and field of view is needed. Three experimental setups are required to measure the temperature profile of the pixel temperature: the calibration setup, the temperature measurement setup, and the temperature fluctuation measurement setup. A cooled, single-element mercury-cadmium-telluride (HgCdTe) detector sensitive in 8 μm to 12 μm wavelength interval measures temperature and its ripple.

The calibration step, shown schematically in Fig. 1, measures the response of the detector to a high temperature blackbody simulator, traceable to the NIS (US National Institute of Standards) reference sources. The output of the square wave radiation chopper is used to trigger the oscilloscope time base. The detector output voltage is shown as a function of temperature in Fig. 2.

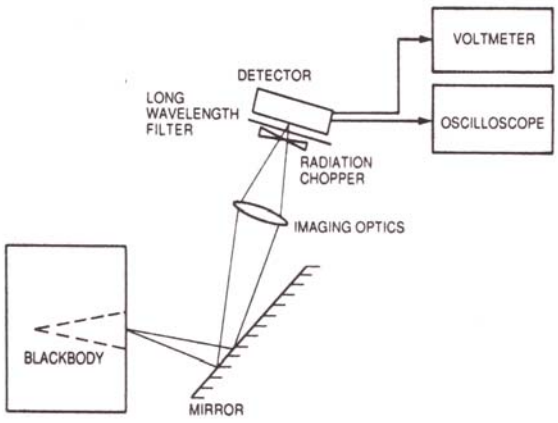

Fig. 1. Detector calibration in the temperature ripple measurement.

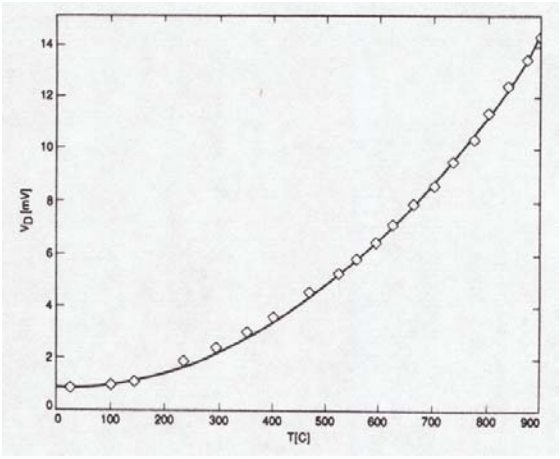

Fig. 2. The detector output voltage as a function of reference temperature.

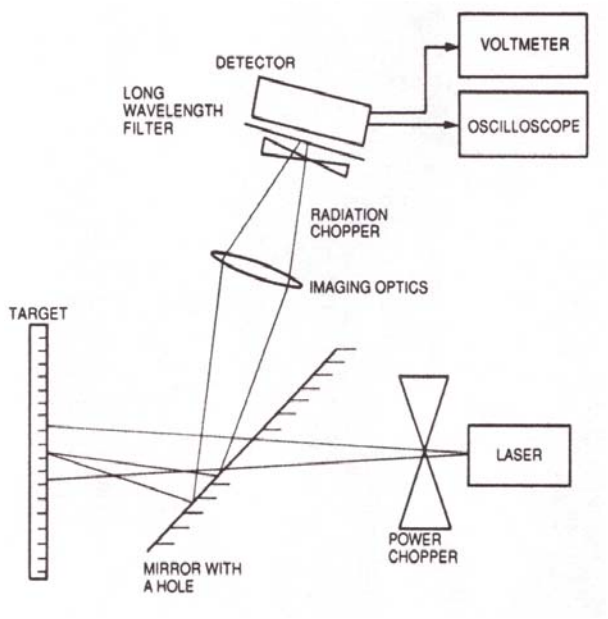

Fig. 3. Setup to measure target temperature.

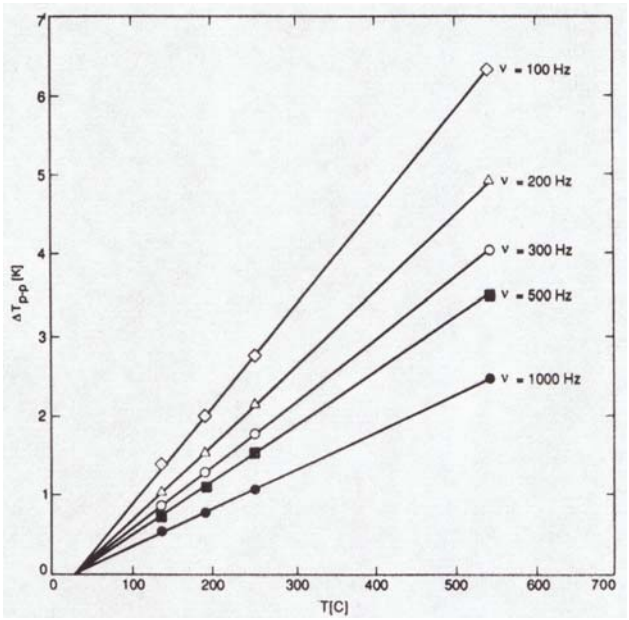

Fig. 4. Temperature peak-to-peak fluctuations as a function of temperature of the surface element.

The setup to measure the temperature is presented in Figure 3. The peak-to-peak voltage and the RMS voltage of the first harmonic measured with the lock-in amplifier are related upon visualization of the temperature waveform at high-temperatures. Temperature peak-to-peak fluctuations are shown as a function of surface element in Figure 4. The frequency of irradiation is a parameter, varying from 100 Hz to 1000 Hz. The amplitude increases linearly with temperature of the surface and decreases logarithmically with frequency.

References

1. J. Merchant, "Interframe image processing," *Thermal Imaging*, Proc. SPIE 636 (1986).
2. M. D. Kelly, L. D. Abney, "Fast times at high temperatures," *Thermosense VII*, Proc. SPIE 520 (1984).
3. R. Fourier, R. A. Buckwald, D. Cabib, E. Sapir, "Microprocessor-based radiation sources and radiometers for testing thermal imaging systems," *Thermosense VII*, Proc. SPIE 520 (1984).
4. J. M. Milne, W. N. Raynolds, "Non-destructive evaluation of composites and other materials with thermal pulse video thermography," *Thermosense VII*, Proc. SPIE 520 (1984).
5. J. Hopper, S. Bauman, N. Faust, R. Smith, M. Weathersby, "A digital infrared imagery data collection and analysis system," *Thermal Imaging*, Proc. SPIE 636 (1986).
6. C. L. Wyatt, "Radiometric linearity calibration,"·*Infrared Technology XI*, Proc. SPIE 572 (1985).
7. M. S. Scholl, "Measurement of small temperature fluctuations at high average temperature,"·*Infrared Technology XI*, Proc. SPIE 972, 409-415 (1988).
8. M. S. Scholl, *Simulation of spectral radiance of a dynamic IR source*, Ph. D. Dissertation, University of Arizona, Tucson, Arizona (1979).

Measurement and calibration of temporal and spatial temperature differences of 100 K

Gonzalo Paez[1] and Marija Strojnik[2]
Centro de Investigaciones en Optica, Apartado Postal 1-948
C. P. 37000 León, Gto., México
gpaez@cio.mx and mstrojnik@aol.com

Abstract

We present experimental procedure to measure large and rapid temperature gradients of 200 K/mm and 100 K/s, traceable to National Institute of Standards.

Key Words: calibration, high heating rate, temperature measurements, high gradients

Poster presentation

Summary

Temporal and position temperature measurements are performed with an IR camera with 30 frames per second and pixel resolution projected on the object space of 1 mm. Three experimental setups are required to measure the temporal profiles of several adjacent pixels upon heating with high power IR laser beam: measurement of the incident laser power density on the pixel(s), shown in Fig.1; the irradiation of pixels and measurement of their temperature as a function of space and time, indicated in Fig. 2; and the calibration of the infrared camera using a black-body simulator, indicated in Fig. 3.

Camera incorporates a cooled, single-element mercury-cadmium-telluride (HgCdTe) detector sensitive in 8 μm to 14 μm wavelength interval. It measures scene temperature upon scanning. The nominally 100-W Nd:YAG laser has been described previously.[1] The Barnes Engineering 11-200T blackbody simulator operates at 200 C – 1000 C.

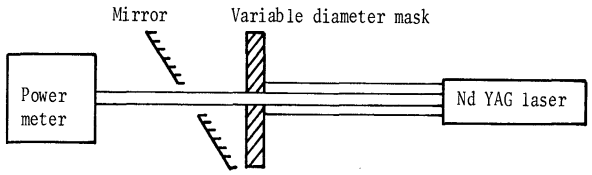

Fig. 1.Experimental setup to measure the laser power density incident on the target surface.

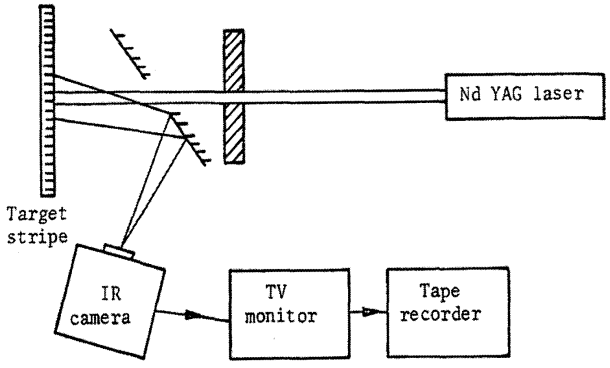

Fig. 2. Experimental setup to irradiate target pixels and measure their temperature as a function of space and time.

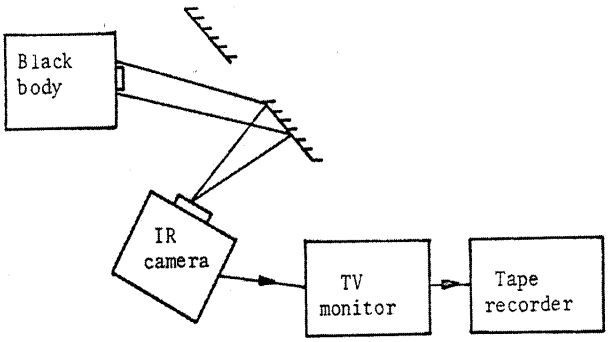

Fig. 3.Experimental setup to calibrate the infrared camera using a black-body simulator.

A thin, black plate with a smaller hole decreases the effective cavity opening, nominally 12.5 mm diameter. Its temperature range of operation has been extended below 200 C, by using a thermocouple and an independent voltage source in this interval.[2] We consider target surface divided into small 1 mm by 1 mm pixel elements due to historical reasons.[3] Then we consider a 3 mm heated spot as consisting of 3 heated pixels (Left Hot Spot, Central Hot Spot, Right Hot Spot) as illustrated in Figure 4. The first pixel to the right is Right Neighbor 1, followed by Right Neighbor 2. Object-pixel heating rate of over 100 K/s is demonstrated for 3 heated pixels on a glassy carbon slab in Figure 5. Figure 6 demonstrates that high temperature gradients of over 200 K/mm are maintained between heated pixels and their neighbors. Figure 7 illustrates the high heating rate of the irradiated spot as a function of heating power during the first two seconds.

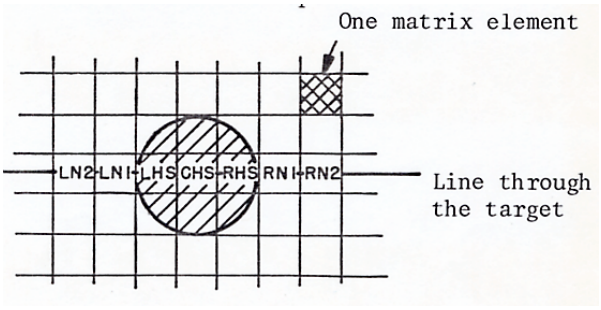

Fig. 4. Definition of pixels on the surface of the target.

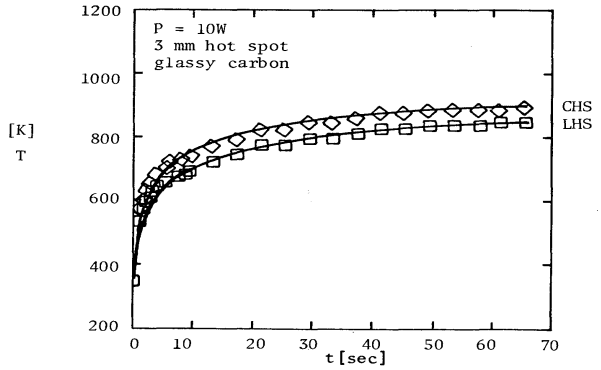

Fig. 5. Object-pixel heating rate of over 100 K/s is measured for 3 heated pixels on a glassy carbon slab.

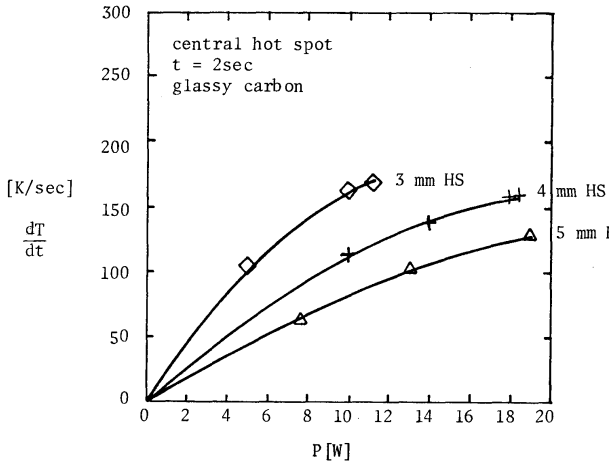

Fig. 7. Heating rate of the irradiated spot as a function of heating power during the first two seconds.

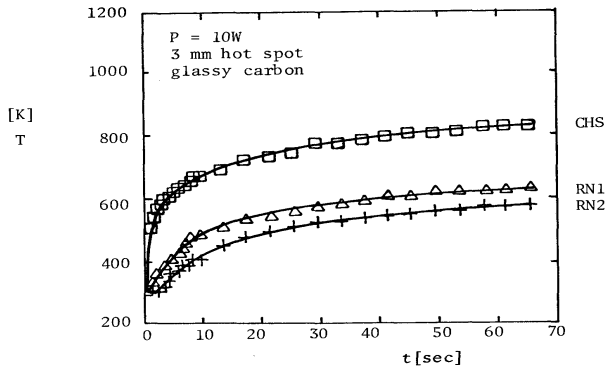

Fig. 6. High temperature gradients of over 200 K/mm are measured between heated pixels and their neighbors.

Bibliography

[1] M. S. Scholl, "Measured Spatial Properties of the CW Nd-YAG Laser Beam," *Appl. Opt.,* **19** (21), 3655-3659 (1980).

[2] M. S. Scholl, "Temperature Calibration of an Infrared Radiation Source," *Appl. Opt.,* **19** (21), 3622-3625 (1980).

[3] M. S. Scholl, W. L. Wolfe, "An Infrared Target Design - Fabrication Considerations," *Appl. Opt.,* **20** (12), 2143-2152 (1981).

New measurement methods for the thermal emissivity of semi-transparent and opaque materials

By Didier Demange, Michel Bejet, Bertrand Dufour

ONERA - DMSC - Fort de Palaiseau, Chemin de la Hunière 91761 Palaiseau, France CEDEX
Tel: 33 (0) 1 69 93 61 23, Fax: 33 (0) 1 69 93 61 25, E-mail: demange@onera.fr

In order to take into account the internal or surface thermal radiation in computer prediction codes for heating in isolating structures, or in metallic systems where thermal radiation is of primary importance, a new experimental system was developed (fig. 1). The system makes possible the measurement of spectral thermal emissivity of semi-transparent materials using a laser as a heating source, or of directional spectral thermal emissivity of opaque materials by contact between the specimen and one of the faces of a heating cylinder.

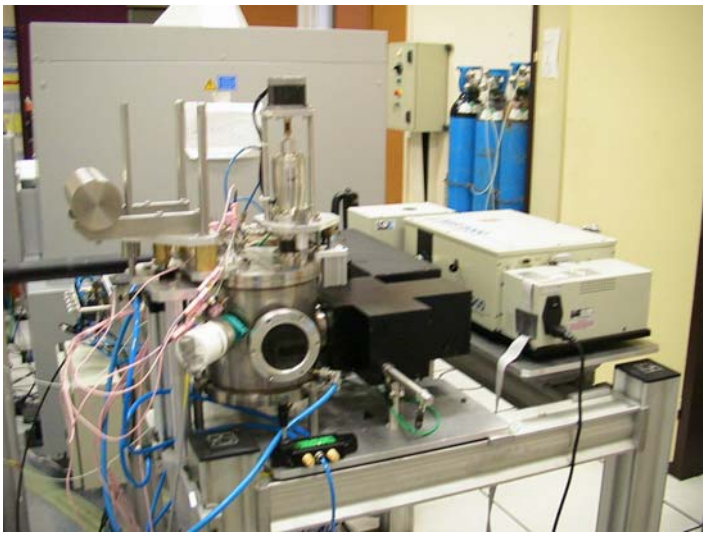

Figure 1 – Overview of the test system

To ensure correct measurements on semi-transparent materials, one must avoid all spurious radiation such as black body radiation from a furnace for instance. The use of a laser source emitting at 10.6 μm allows one to heat the sample without any stray radiation. The method used is to rotate a cylindrical sample about its axis and to expose a section of it to a high-power laser beam. The radiation emitted by the opposing section is then analysed by an FTIR spectrometer.

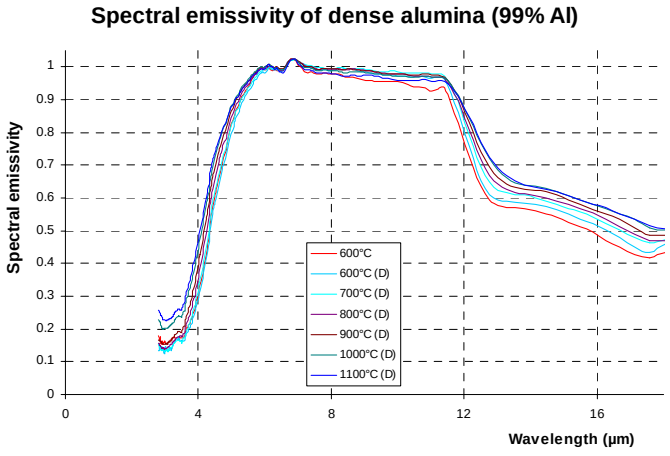

Figure 2 – Spectral emissivity of alumina

The area observed is in this way free of spurious radiation (no furnace), and the rotation of the sample ensures lateral homogenisation of the specimen (external heating of the specimen). Use of a multimode laser ensures fairly good longitudinal homogeneity of the specimen. The measurement of absolute temperature is made possible by a thermocouple positioned in the centre of the cylinder. A sample result is illustrated in figure 2.

For the characterisation of metals or more generally of opaque materials, a more standard apparatus has been set up.

Heating of the specimen is carried out by a micro-furnace with electrical resistance. The samples are put into contact with one of the faces of a heating cylinder, and the whole apparatus is put into a testing enclosure under a secondary vacuum (10^{-5} torr) to avoid all oxidation during the measurement. The non-polluting micro-furnace is put into the enclosure and brings the sample to the measurement temperature (figure 3).

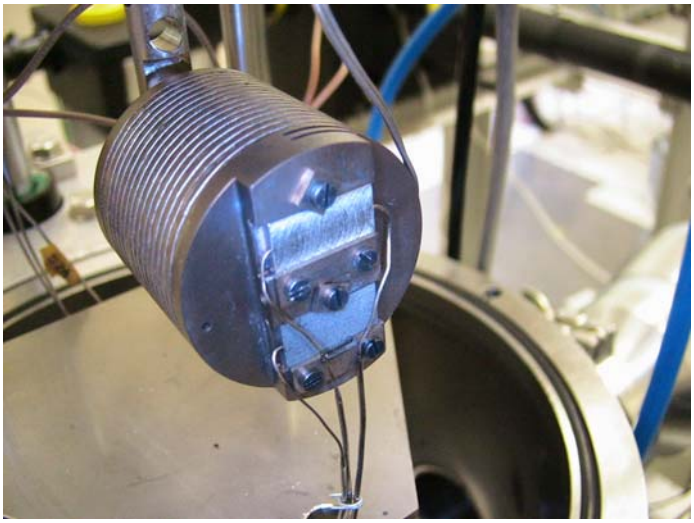

Figure 3 – Heating apparatus – View of the samples

The measurement of the surface temperature is made by an N-type thermocouple placed in the centre of the sample, with a possible correction made to take into account the internal thermal gradient within the material. This system provides values of directional spectral emissivity, with computer software then determining from raw measurement data the spectral hemispheric emissivity and the total hemispheric emissivity.

Total hemispheric emissivity is calculated with the following formula: $\varepsilon_{\theta,\varphi}=\frac{\int_0^{\infty}\varepsilon_{\lambda,\theta,\varphi}L^0_{\lambda T}d\lambda}{\int_0^{\infty}L^0_{\lambda}d\lambda}$.

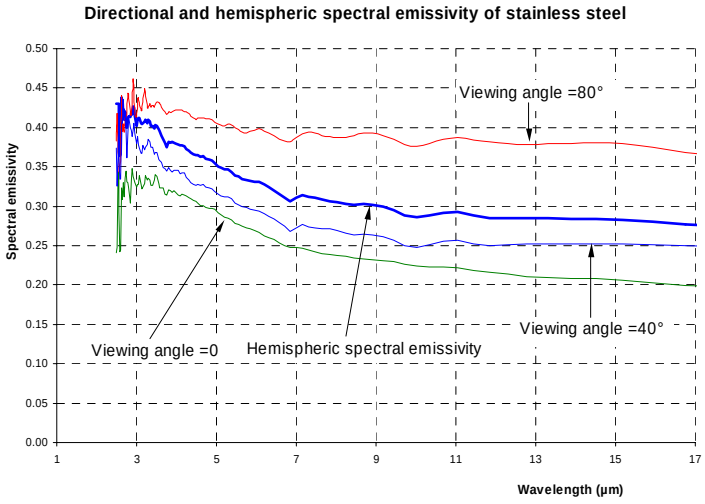

Figure 4 – Directional and hemispheric spectral emissivity of stainless steel at 550°C

Then the spectral hemispheric emissivity is obtained by the equation:

$\varepsilon_{\lambda,T}=\frac{1}{\pi}\int_{\Omega}\varepsilon_{\lambda,\theta,\varphi}\cos\theta\, L^0_{\lambda}d\omega$, as well as the total hemispheric emissivity which is equal to:

$$\varepsilon_{\lambda,T}=\frac{\frac{1}{\pi}\int_{\lambda=0}^{\infty}\int_{\Omega}\varepsilon_{\lambda,\theta,\varphi}\cos\theta\, L^0_{\lambda}d\omega d\lambda}{\sigma T^4}.$$

A sample result for stainless steel at 550°C is shown in figure 4.

For instance, these two methods were used to characterise thermal thresholds for turbine blade roots and materials likely to be used in an HTR (High Temperature Reactor).

Defect detection in ceramic materials by quantitative infrared thermography.

Gian Marco Revel, Simone Rocchi

Dipartimento di Meccanica, Università Politecnica delle Marche
via Brecce Bianche, 60131 Ancona, Italy
e-mail: gm.revel@mm.univpm.it, phone: +39 071 2204441; fax: +39 071 2204813.

Keywords: ceramics, non-destructive testing, thermography.

Preference: oral presentation.

Abstract

In the ceramic industry rarely testing systems was employed on-line to detect the presence of defect in the ceramic tiles; some applications of thermographic systems can be found in literature [1] [2] regarding the detection of big delaminations on green ceramic tiles. In fact till the tile is in a green state, the ceramic material is completely recyclable and then an inspection to the whole production can be very useful.

In this paper infrared measurement techniques [3] [4] [5] were applied for defect detection on ceramic materials. Defects on ceramics are generally characterized by delaminations, inclusion of heterogeneous material or agglomerates; each one of these subsurface features can be detected thanks to temperature differences, still observable in the surface by an infrared camera.

Thermal measurement have been done by a long wave infrared camera equipped with a FPA of uncooled microbolometers, with spectral range from 7.5 to 13 μm and accuracy in temperature measurement of 2 °C or 2% of the reading. The measurement setup is completed by a thermographic test bench realized in aluminum, to reduce the irradiation of the bench during tests; it is capable to deposit a sufficiently uniform amount of energy (for a sample large 0.4×0.4 m) in a controlled time period by four IR lamps, with an overall power of 4 kW.

As the first stage, with the aim to properly test the capability of the proposed method, many tiles samples was realized in the labs of a ceramic industry, inserting intentionally some defects of different size and depth. Then thermographic tests have been accomplished acquiring either heating and cooling phase of the tile placed in the bench and subjected to a thermal pulse excitation of variable duration.

As rarely defects appear directly in the IR acquisition, a post-processing stage has been necessary to highlight the thermal effect generated by every defect or material in-homogeneity.

Good results was achieved employing thermal tomography (TT), pulsed phase thermography (PPT), principal component analysis (PCA), techniques of image balancing and trend removing.

Thermal tomography is based on measurement of the surface temperature of the component under inspection after the initial thermal heating; assuming an uniform heating of the component surface, areas of the specimen having uniform thermal properties will cause the maximum thermal contrast to occur in the same time window in the timegram. On the contrary, defect or delaminations having different thermal properties exhibit different values of that parameter and consequently different time values in the timegram; this makes defect detection possible (see Fig. 1). Pulsed phase thermography consists of pulse heating the specimen briefly and recording the surface temperature decay curve with an infrared camera. The temperature of material changes rapidly after the initial thermal perturbation; the presence of any defect reduces the diffusion rate so that defects appear as areas of different temperature with respect to a surrounding sound area. Extraction of the frequency content of the thermal response exhibited by the tile is performed by application of the FFT algorithm on the thermal history of each pixel. As results of this processing, amplitude and phase images are reconstructed at different frequencies and, since phase images are less affected by heating non-uniformities, experimental constraints about positions of thermal sources are relaxed (see Fig. 1).

In defect detection methods based on analysis of thermographic images, the image background hold an important role; in fact, because of heating non-uniformity effects, the borders of the tile in an IR image tend sometimes to be hotter than the other parts.

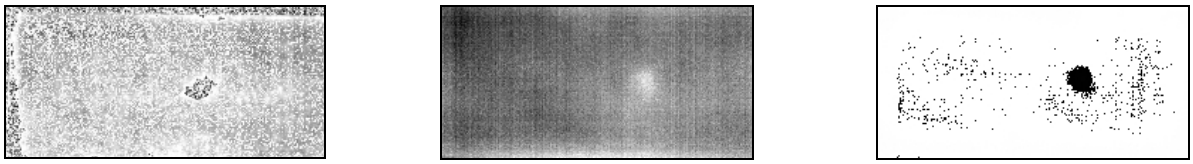

(1) (2) (3)

Figure 1 – (1): TT, maximum contrast image; (2) and (3): PPT, amplitude and phase images.

This situation engenders some problems when an automated threshold algorithm is applied to a thermal image because on the tile there is not a good separation between defects and background.
To solve this problem a procedure of trend removal has been and applied to single IR images where some defect are localized. In this procedure a synthetic image was produced from the original image by making use of a polynomial fitting algorithm to obtain, after subtraction of the synthetic image by the original image, an uniform background on which defects appear more clearly; then an automatic threshold technique was applied to separate the two modes (defects and background).
Alternatively to the previous processing, the image balancing treatment was implemented in order to remove the effect of a non-uniform heating on the tile surface and to automatically threshold the final image with good characterization of the defect (see Fig. 2).
Moreover utilisation of the PCA was oriented to reduce the data set provided by the PPT algorithm (sequence of phase images at different frequencies) and to obtain an unique map containing information about a complete IR acquisition.
Finally a quantitative analysis of the influence of measurement noise on the detection capabilities has been performed. This allows to evaluate NDT performances in relation to the measurement environment, the sensor inherent noise, the uncertainty propagation into algorithms, etc.

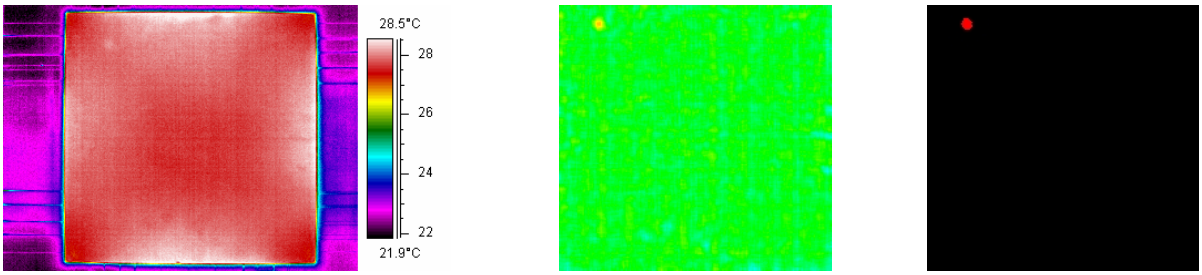

a) Original IR image **b) Balanced image** **c) Thresholded image**

Figure 2 – Image Balancing and Thresholding procedure.

Bibliography

[1] De Andrade R.M., Paone N., Revel G.M., *Non Destructive Thermal Detection of Delamination in Ceramic Tile*, Proc. ENCIT 98, Rio de Janeiro, 727-731, 1998;

[2] De Andrade R.M., Esposito E., Paone N., Revel G.M., *Non-destructive Techniques for Detection of Delamination in Ceramic Tiles: a Laboratory Comparison between IR Thermal Cameras and Laser Doppler Vibrometers*, Proc. SPIE Vol. 3585, p. 367-377, Non-destructive Evaluation of Aging Materials and Composites III, George Y. Baaklini; Carol A. Lebowitz; Eric S. Boltz; Eds, 1999;

[3] Maldague, Xavier P.V., *Theory and Practice of Infrared Technology for Non-destructive Testing* , John Wiley & Sons, New York, NY, 2001;

[4] Maldague X., Marinetti S., *Pulse Phase Infrared Thermography*, J. Appl. Phys, **79**[5]: 2694-2698, 1996;

[5] Marinetti S., Grinzato E., Bison P.G., Bozzi E., Chimenti M., Pieri G. and Solvetti O., "Statistical analysis of IR thermographic sequences by PCA", *Infrared Physics and Technology*, **46** [1, 2], Elsevier, 2004;

Qirt 2006 Padua

TITLE

Acoustic thermography using an un-cooled high speed camera and low power ultrasonic excitation: test system and its application to impact flaw detection in CFRP

AUTHOR LISTING

Lothar Haupt[1], Uwe Hoffmann[2], Helmut Budzier[2], Norbert Meyendorf[1], Bernd Köhler[1]

[1]Fraunhofer Institute for Non-Destructive Testing, Dresden branch
Krügerstrasse 22, 01326 Dresden, Germany

Lothar Haupt
E-mail: lothar.haupt@izfp-d.fraunhofer.de
Phone: +49 (0) 351-264 82-43
Fax: +49 (0) 351-264 82-19

[2]DIAS Infrared GmbH
Gostritzer Str. 63, 01217 Dresden, Germany

Uwe Hoffmann
E-mail: uwe.hoffmann@dias-infrared.de
Phone: +49 (0) 351 871 7227
Fax: +49 (0) 351 871 7230

Keywords: Infrared, thermosonics, acoustic thermography, imaging, tomography, CFRP

PRESENTATION
Oral

ABSTRACT

Acoustic thermography is a new method for NDE of material flaws, based on thermo graphic detection of dissipated ultrasonic energy. The test system presented is using an un-cooled high-speed camera and low power ultrasonic excitation. This technology is characterized by low system costs, since no nitrogen or stirling cooling is necessary. Low power applications are facilitated by efficient ultrasonic coupling, hence taking care of sensitive objects.
A camera has been developed which uses a 384 x 288 pixels micro-bolometer array as sensor and may record up to 100 frames per second.

The advantages of this system are demonstrated on a set of carbon fiber reinforced plastic plates damaged by impacts of various strengths. The impact flaws consisting of fiber fractures and delaminations can be detected while transmitting low ultrasonic energy of about 1.3 W to the specimen.

COMPARATIVE STUDY BETWEEN INFRARED THERMOGRAPHY AND LASER DOPPLER VIBROMETRY APPLIED TO FLAWS INDENTIFICATION IN COMPOSITE MATERIALS

[1]Daniel Pedro Willemann, [2]Sinthya Gonçalves Tavares, [1]Paolo Castellini, [2]Roberto Márcio de Andrade
[1] Dipartimento di Meccanica – Università Politecnica delle Marche, Ancona, Italy, Phone: +39-071-2204508,
Fax: +39-071-2204801, e-mail: a.agnani@mm.univpm.it
[2] Departamento de Engenharia Mecânica da Universidade Federal de Minas Gerais,
Belo Horizonte, MG – Brazil, Phone: +55-31-3499-5140,
Fax: +55-31-3499-5140, gtavar@terra.com.br

Keywords: NDT techniques, Thermography, laser Doppler vibrometry, composite materials, mathematical model

ORAL PRESENTATION

There are many NDT techniques available but only a few allow in situ analysis. Thus, the requirements for non-destructive evaluation are continuing to be driven by the need for lower cost methods and instruments with greater reliability, sensitivity, user friendliness and high operational speed as well as applicability to increasingly complex materials and structures [1]. Both infrared termography and laser Doppler Vibrometer accomplish these characteristics and, for this reason, are widely employed in the NDT sector.

In this work, a comparative study between laser Doppler vibrometry and infrared thermography applied to the damage detection in composite material is presented. A mathematical model was implemented in order to validate the results obtained experimentally through the thermographic technique. The thermal measurements uncertainty and the noise of the LDV system, which are limitations of each methodology, are also discussed.

The experimental procedure was carried out in the Mechanical and Thermal Measurements laboratory of the Mechanical Engineering Department of the Università Politecnica delle Marche. The honeycomb panel used in this work has its four layered top part made with a combination of glass-fibre fabric type RE 200 and E277 epoxy resin. Three wax inclusions were inserted in certain positions among the layers during its manufacturing process in order to create the flaws. After, by warming, the wax inclusions were eliminated from the panel to simulate real delaminations. Figure 1 shows the geometry and the position of the 20 mm circular defects in the upper part of the honeycomb panel.

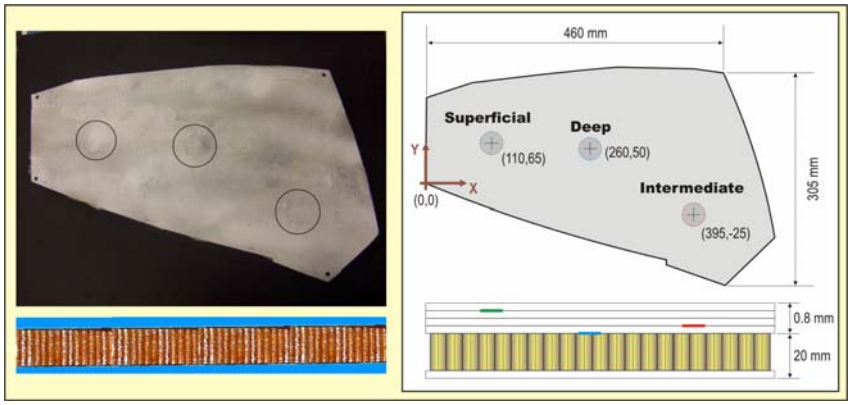

Figure 1 – Honeycomb Panel

In the mathematical model employed for the numerical validation of the thermographic investigations, the Fourier equation has been used, considering a transient regimen, without heat generation, in three-dimensional cartesian coordinates. During the investigations, the lateral sides of the sample have been isolated which allowed to consider the heat flow as one-dimensional. For the Fourier equation solution, numerical technique with formularization in finite volumes has been employed. A program, written in FORTRAN®, has been developed for the solution evaluation. The number of control volumes has been defined from mesh test and criterion of convergence based on the comparison between the numerical and analytical solutions for the temperature reached at each point (only differences smaller than 10^{-5} had been accepted). In the analytical solution, the panel has been considered as a semi-infinite solid.

Both pulsed and modulated Thermography were employed and the testing procedure suggested in [3] has been followed. Regarding the uncertainty analysis, the methodology indicated in [4] and [5] has been used and more details will be given in the final paper.

The Figure 2 shows, for the maximum contrast, two temperature maps: (A) obtained by the infrared camera and (B) obtained by means of MATLAB program. Both maps use pulsed thermography.

Images analysis allowed the identification of the flaws since the temperature difference between the unflawed and flawed areas was twice greater than 0.8°C that is the maximum uncertainty for the measurement set. The two deepest flaws are better defined by means of modulated Thermography.In the final work, further maps obtained by means numerical solutions using FORTRAN® program and modulated Thermography will be shown.

The analysis of the numerical results for the more superficial fail indicate the validation of the experimental datas because the temperature difference between the fail and their neighborhood is lesser than the uncertainty of measurement. Figure 3 shows the experimental and numerical surface temperature decay for the area with and whitout flaw.

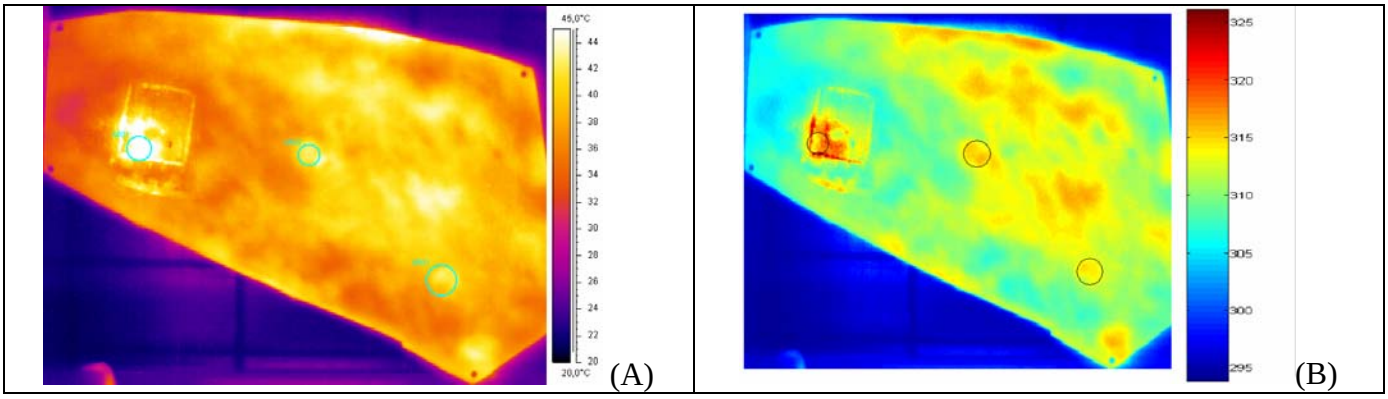

Figure 2 – Temperature Maps: Infrared camera (A) and MATLAB (B)

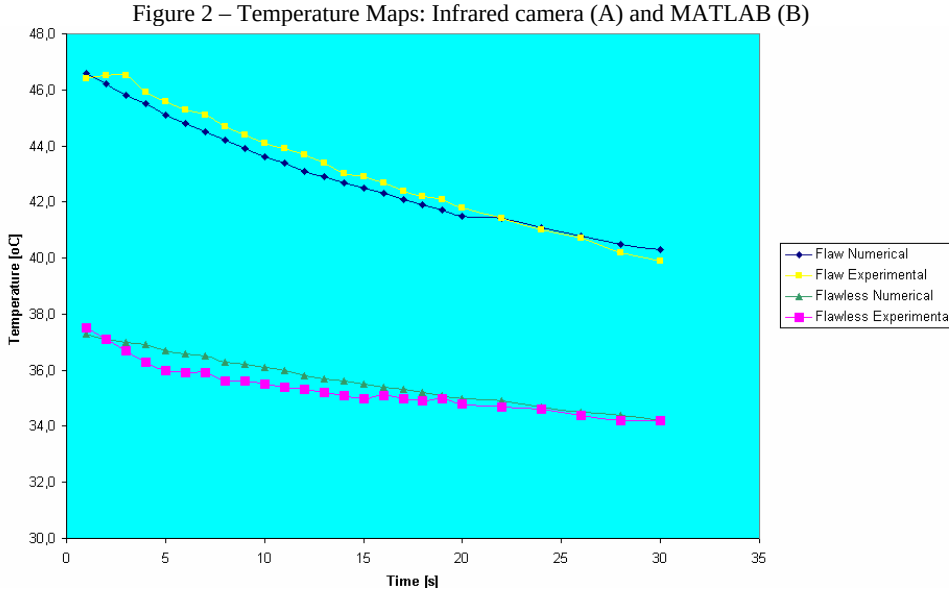

Figure 3 – Temperature decay

The dashed circles in Figure 4 show different maps highlighting the delaminations present in the panel: (A) in a RMS velocity map at 11.15 kHz and (B) in a PCA (Principal Component Analysis) map. Both maps were obtained from a measurement performed by a scanning laser Doppler vibrometer. In this case, a speaker driven by white noise signal has been used as excitation device and 20 kHz of measurement bandwidth and 1600 spectral lines were employed during the measurements. A detailed discussion of the results will be done in the final paper.

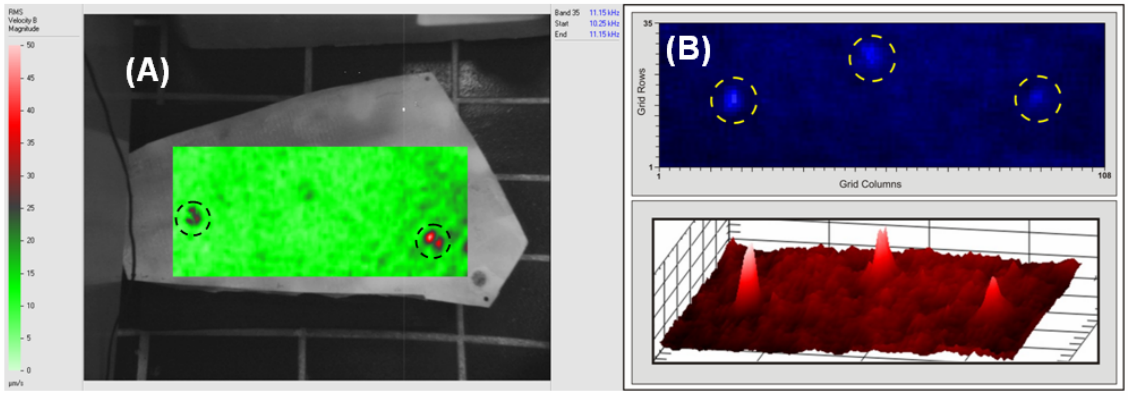

Figure 4 – Laser Doppler Vibrometry Measurements: RMS Map (A) and PCA Map (B)

References

(1) Meola, C., Calomagno, G. M., Giorleo, L., “The use of infrared thermography for materials characterization”, Journal of Materials Processing Technology, Vol. 155-156, pp.1132-1137, 2004.

(2) Tavares. S. G., Andrade, R. M., “Metodologia de ensaio e análise de incerteza na aplicação da termografia”, 2003, Anais do III Congresso Brasileiro de Metrologia, Recife, PB, Brasil.

(3) Tavares, S. G., Cunha, A. M., Andrade, R. M., “Metodologia Experimental para Aplicação da Termografia em Ensaios Térmicos não Destrutivos”, 2004, Proceedings of the 10th Congress of Thermal Sciences and Engineering – ENCIT 2004, Brazilian Society of Mechanical Sciences and Engineering, ABCM, Rio de Janeiro, Brazil.

(4) Chrzanowski, K., Fischer, J., Matyszkiel, R., “Testing and evaluation of thermal cameras for absolute temperature measurement”, 2000, Journal of Optical Engineering vol. 39, no 9, pp. 2535-2544.

Induction-Lockin-Thermography and Induction-Burst-Phase Thermography for NDE Applications

G. Riegert, G. Busse

Institute of Polymer Testing and Polymer Science, Department of Non-Destructive Testing (IKP-ZFP), University of Stuttgart, Pfaffenwaldring 32, D-70569 Stuttgart, Germany, Tel.: +49-711/6852572, Fax: +49-711/6854635, Mail: riegert@ikp.uni-stuttgart.de

Keywords: Lockin-Thermography, Induction Heating, Eddy Current, Defect Selective NDT

Presentation: Oral

Induction-Lockin-Thermography (ILT) uses resistive losses inside the sample for periodical heating. This is possible due to a contact free induction coil inducing eddy currents in conductive materials. Modulation of the eddy current amplitude produces thermal waves which interact with thermal boundaries.

While conventional eddy current testing has only a limited depth range in metals due to the skin effect, the depth range of ILT is extended by the thermal penetration depth as thermal waves are involved.
An infrared camera monitors the modulation of the temperature field on the surface as a response to the coded excitation thereby allowing for fast imaging of defects in larger areas without the need of slow point-by-point mapping as in conventional eddy current techniques. The thermal response of the sample is extracted from the temperature image sequence by a Fourier analysis performed at each pixel at the modulation frequency. The information consisting of amplitude and phase of local temperature modulation is then displayed as an amplitude image and a phase image.

ILT has significant advantages as compared to inductive heating with only visual inspection of the thermographic sequence where only single images of the cooling down are evaluated: Phase angle images are independent of most artefacts like reflections, variation in emission coefficient, or inhomogeneous heating (Figure 1). Also the signal-to-noise ratio of the amplitude and phase images is significantly better than in single temperature images due to the performed band-width reduction achieved by Fourier analysis of the temperature image sequence (Figure 1).
Induction heating is confined to conductive materials. However, it is applicable not only to metals but also to carbon fibre reinforced laminates (CFRP). The example (Figure 1) shows that the probability of defect detection (POD) is much higher with phase images than with simple temperature images taken from a sequence.

Image of highest contrast
650 ms after burst

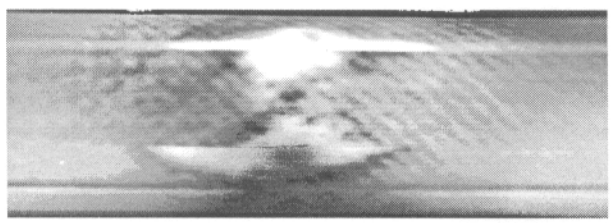

ILT phase at 0.1 Hz

Figure 1: CFRP – tube with impact damage. Left: Image of highest contrast 650 ms after excitation burst (transient thermography): only surface damages are visible. The image shows also high temperature gradients due to inhomogeneous heating.

Right: Phase image of ILT: the temperature gradients are suppressed and the signal-to-noise ration improved. The phase image shows fibre cracks and delaminations due to the impact. Also the fibre orientations of the outer layers are visible.

Induction-Burst-Phase Thermography (IBP) uses short induction bursts for sample excitation. The spectral components of the cooling down period after burst excitation provides information similar to the lockin method (amplitude and phase) but much faster since a burst consists of a frequency spectrum which is used for Fourier transformation. One single IBP measurement replaces several subsequent ILT measurements at different lockin-frequencies.
The advantages of IBP over transient thermography are the same as in ILT: suppression of artefacts like inhomogeneous heating or reflections and a better signal-to-noise ratio as compared to single temperature shots (Figure 2).

Image of highest contrast
360 ms after burst

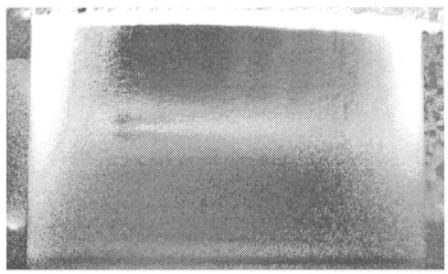

IBP phase at 0.5 Hz

Figure 2: The transient thermography result on a steel plate with two inclined slots on the rear side is compared to the result of IBP. Left: Image of highest contrast 360 ms after excitation burst shows only inhomogeneous heating. Right: Phase image of IBP shows parts of the slots milled into the rear side. This example shows the improved depth range of phase thermography as compared to conventional transient thermography.

The presented examples for applications of ILT and IBP on different materials and different kinds of defects will show the potential and restrictions of these new non-destructive and remote inspection methods.

Improved ultrasound activated Lockin-Thermography by frequency analysis of material defects

A. Gleiter, C. Spießberger, Th. Zweschper, G. Busse

Institute of Polymer Testing and Polymer Science, Department of Non-Destructive Testing (IKP-ZFP), University of Stuttgart, Pfaffenwaldring 32, D-70569 Stuttgart, Germany, Tel.: +49-711/6852694, Fax: +49-711/6854635, Mail: gleiter@ikp.uni-stuttgart.de

PRESENTATION PREFERENCE: Oral Presentation

There is an increasing demand in industry for non-destructive testing methods which should be reliable and fast. Ultrasound activated Lockin-Thermography is such a defect selective NDT-technique. In ultrasound activated Thermography an intense acoustic wave propagates into an imperfect solid. Hysteretic internal friction in defect areas results in a local temperature raise. To enhance the sensitivity of detection of such faint heat sources, the lock-in approach is being applied by using a low-frequency amplitude modulation of acoustic excitation (Ultrasound-Lockin-Thermography).
A new way of detecting damaged regions is to analyze the frequency dependence of heat production: Defects like cracks in metal show characteristic frequencies of maximal mechanical losses. At these frequencies the temperature increases and can be measured by thermography. By modulating the frequency of ultrasound instead of its amplitude many defects are activated simultaneously at their specific frequencies. Thereby frequency modulation is turned into an amplitude modulation of local temperature. Compared to amplitude modulated Lockin-Thermography at one single frequency, the signal to noise ratio is improved because different defects receive an equal amount of power. Standing wave patterns of ultrasound, arising form the sample geometry are also suppressed. Intact regions of the material do not change their properties significantly with frequency. Therefore a defect selective result is obtained.

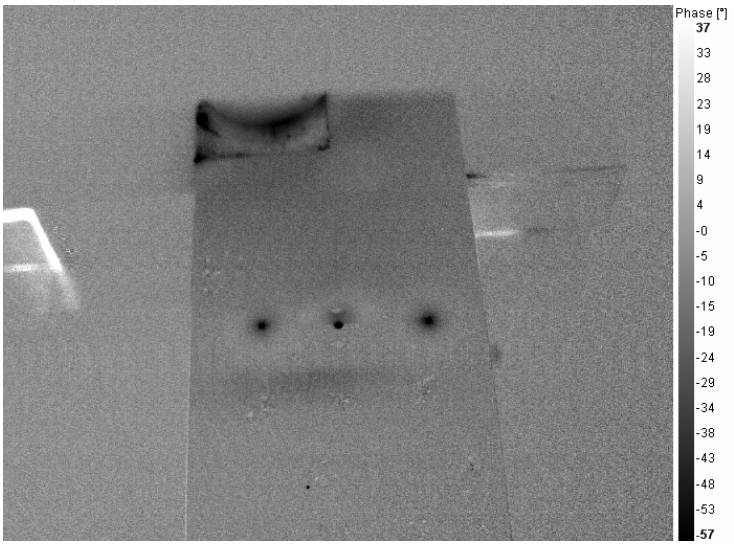

Figure 1: Phase image of a steal sample containing cracks. Frequency modulation at 0,3 Hz.

KEYWORDS: Lockin-Thermography, Frequency analysis, Ultrasound Thermography, Attenuation Mapping, Defect Selective NDT

MEASUREMENT OF IMPACT-DAMAGED AREAS IN COMMINGLED E-GLASS/POLYPROPYLENE LAMINATES VIA THERMOGRAPHIC IMAGES ANALYSIS

Carlo Santulli
University of Reading, School of Construction Management and Engineering
Whiteknights, Reading, RG6 6AY, United Kingdom
telephone +44-118-3788564, fax +44-118-9313327 e-mail: c.santulli@rdg.ac.uk

Keywords: automotive composites; 3-D fibres; impact-damaged area; transmission transient thermography
Poster Presentation

The presence of fibres oriented in the direction of thickness has always being regarded as detrimental for the impact resistance of polymeric composite materials. However, in the particular case of commingled laminates, which are widely used in the automotive sector, a small percent of 3-D fibres can reduce the effect of damage at crossovers and possibly improve the resistance of these laminates to delamination. A drawback of the introduction of 3-D fibres is however that they present more complex impact damage patterns and influence of defects can be larger than in 2-D commingled laminates (Figure 1). This adds to the importance of correctly characterising impact damage, including a reliable measurement of impact-damaged areas. This is particularly crucial in that these composites can occasionally show backface damage for impact energies well below penetration energy (Figure 2). As a general point, the local properties of these laminates, hereinafter defined as 3-D commingled, have particular importance, and present a decisive influence in allowing prediction of penetration energy value.

Commingled E-glass/polypropylene laminates with 1-2% through-thickness fibres (60%wt. glass fibre content) have been impacted at energies up to penetration on a Rosand IFW5 impact tower using a 12.7 mm. diameter impactor. After impact, the damaged area was observed using an Agéma Thermovision 900 SW thermographic camera, thermo-electrically cooled, with a spectral response 2-5.4 micron and a sensitivity 0.1ºC. The camera was fitted with a 25 mm lens, so that images of the specimens could be focused at a minimum distance of 480 mm. Thermographic images were averaged over a period of 30 seconds immediately following a 3-second heating phase obtained with a 500 W infrared lamp, by averaging each pixel on a sequence of 10 images, each one acquired every 3 seconds. Heating yielded on the laminate surface a maximum temperature of 45°C. After 30 seconds, the maximum temperature difference across the sample surface decreased to less than approximately 3.2°C, and therefore at that moment the signal/noise ratio was deemed no longer sufficient for impact damage characterisation. The adoption of transmission transient thermography for studying impact damage in these laminates has been suggested by the fact that this method allowed a better control over temperature in the initial part of the transient.
The impacted face and backface thermographic images at impact energies between 15 and 45 Joules have been analysed to obtain a reliable measurement of impact-damaged area on the surfaces and possibly across the thickness of the samples. Since previous studies have shown that commingled 3-D laminates typically present an elliptical impact damage area with some preferential directions of propagation, usually along the x-axis, a rectangular area of 40x32 mm was selected for analysis.

The method selected for image analysis involved using thresholding techniques by comparing the grey level histograms of the region of the samples including the impact area with the histograms of the remaining part of the laminate image (Figure 3). A suggested modification included transforming the images on the greyscale and then calculating pixel-by-pixel image differences between average images taken at every impact energy so to measure the ratio between impacted areas at the minimum energy (15 Joules) and at higher energies.

The analysis shows that the combined application of the two methods leads to measurement of the apparent impact-damaged area within a few percent from what observed using thresholding on

optical microscopy generated images, with the advantage of not needing the sectioning of the samples under observation. It is also important to consider that this is a particularly difficult case for the usually non-uniform "whitish" colour of the samples and their low conductivity, so that the results appear promising for further applications.

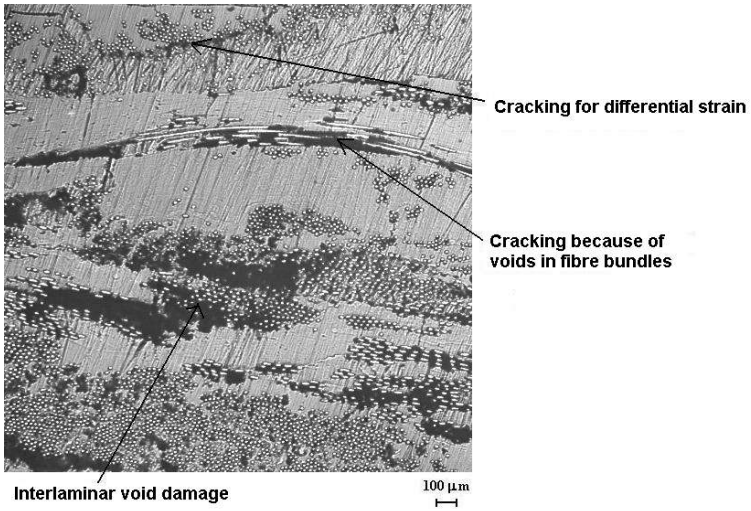

Figure 1 Different types of defects triggering impact damage in 3-D commingled laminates

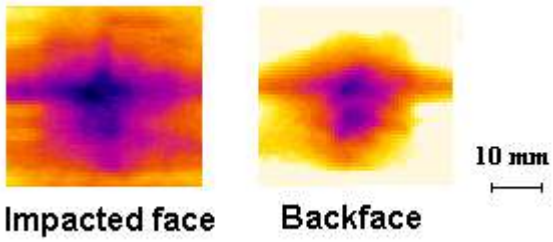

Figure 2 Impacted area in a 3-D commingled laminate (energy = 15 Joules)

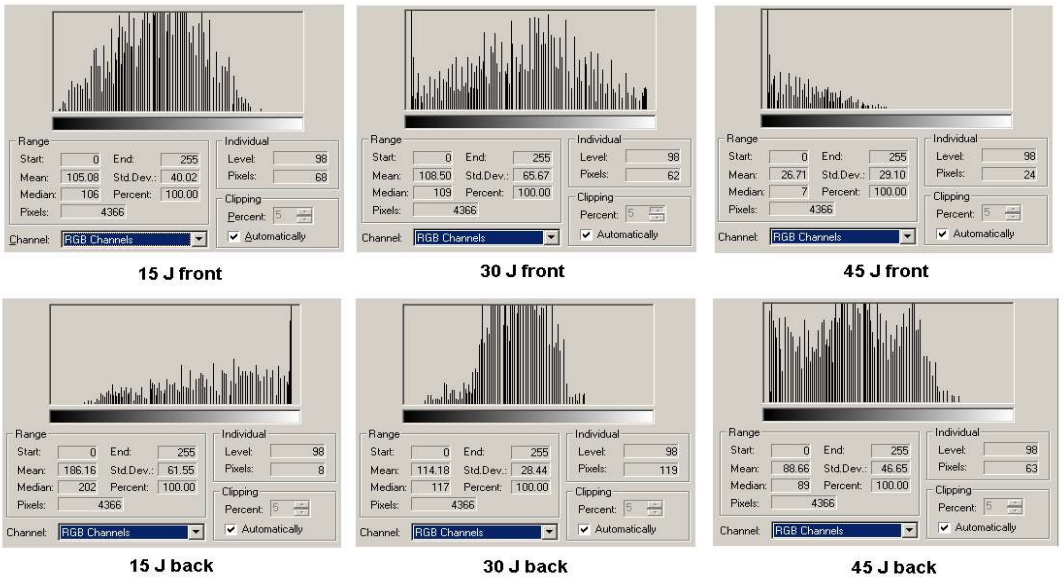

Figure 3 Grey level histograms for thermographic images (area 40x32 mm) of impacted 3-D commingled laminates

Pulsed Thermography in the assessment of composites for defect detection and analysis

N P Avdelidis, S Kenny

NDT Group, TWI Technology Centre in South Wales, ECM2, Port Talbot, SA13 2EZ, United Kingdom

Abstract

Thermographic approaches, particularly active and/or transient ones, could be used successfully in the detection of different types of defects (i.e. delaminations, adhesive bonds, impact damage, porosity) in composites. Nonetheless, there are limitations depended upon the thermography approach used, as well as on the materials thermal, optical and physical properties. In this research work, pulsed thermography (PT) was used for the investigation of composite materials. Different types of GFRP composites were investigated; defected pipes, various types of impact damaged composite plates, as well as plates with sub-surface defects. All specimens were examined by using an integrated pulsed thermographic evaluation system. In some instances, with the intention of avoiding reflection and thus increasing the emissivity of such surfaces, since GFRP is usually transparent material, the specimens were processed accordingly. Samples were either painted with black colour water based paint or even polished by applying a silver polishing substance (i.e. silvo). Quantification analysis was also implemented; temperature - time plots, as well as thermal contrast curves. The results of this study show that PT is a prompt thermal NDT & E approach that could be used successfully in the investigation for the assessment of composite components.

Reliability Testing on the Printed Circuit Board of Mobile Phone using Infrared Thermography

by Hoon Joo(1), Won-Tae Kim(2), Man-Yong Choi(3)

(1) IR Wave Corp., Seoul, Korea
(2) Dept. of Bio-mechanical Engineering, Kongju National University, Chungnam, Korea, 340-702
(3) Life Measurement Group, Korea Research Institute of Standards and Science, Daejeon, Korea, 305-600

Abstract

In this paper, reliability testing using infrared thermography is performed to investigate the failure and abnormal sympton of mobile phone in operation. As roles of the presented work, IR system for the analysis of PCB reliabilty was set-up to be appled as nondestructive testing method. From IR thermographic images obtained, following results are reviewed. First, prior confirmation and forecast for troble points by intensive control for the IR thermal profile. Secondly, available aging test with long time under real temperature, Thirdly, by making database for past results, it was possible the history control and worth for comparison data. Also, using IR thermographic images detected already, audits for mixed board are analyzed under several operational signals. From this work, it was assumed that IR testing is capable of saving the test time and increasing the test accuracy by diverse costomized functions.

Keywords: Reliability Testing, Infrared(IR) Thermography, Nondestructive Testing(NDT), Mobile Phone, Thermal Profile

POLITECNICO DI MILANO - Dipartimento di Architettura e Pianificazione
Laboratorio di Analisi e Diagnostica del Costruito
via Garofano, 39 – 20133 Milano
Tel. +39 (0)2.23.99.94.47 - Fax. +39 (0)2.23.99.94.45 - email davide.delcurto@polimi.it

THERMO - HYGROMETRICAL SURVEYINGS and MICROCLIMATE MONITORING at the SAN BENEDETTO PO ABBEY (Mantova - Italy)

Authors: Davide Del Curto, Alberto Grimoldi
Politecnico di Milano – DIAP, Via Garofano 39 – 20133 Milano, Italy
Keywords: passive procedures, moisture, historical architecture, masonry texture, microclimate monitoring

The aim of this research is to develop IRT procedures for the monitoring of thermo – hygrometrical conditions of ancient buildings and surveillance of risk areas.
The greater part of degradation phenomena such as decay of plasters and frescoes, damaging of stone and wood elements, actually can be led back to moisture. Water acts both as enviromental humidity determining microclimate (RH - SH), both by bathing mansonry moreover as of capillarity.
The campaign of surveyings lead on San Benedetto Po abbey (Mantova) has been extended for 3 years with the aim to inquire the exchange dynamics between microclimate and masonry; surveyings have regarded thermo – hydrometrical data T, RH, SH, collected both for microclimate (internal enviroments), both for masonry.[1]
Particularly IRT has been employed to map thermal gradient on the masonry surfaces and has integrated in innovative way with the psycrometrical reliefs and quantitative tests of water content in masonry.
The localisation of the thermal gradients, particularly in colder areas on masonry surfaces where condensation may occour, is an important issue for early detection of damage.
IRT tests can be periodically repeated in passive way with low cost and without any damage for the wall; repetition of the test allows to find out variations of superficial temperature which is due to any unbalance between masonry and microclimate; it also constitutes an early alert for damages that will occur in case microclimate conditions do not change.

SAN SIMEONE CHIOSTRO
Photographic Image

SAN SIMEONE CHIOSTRO
Thermographic Image, date 25.07.2003, time 12:05, range 18.3 - 29.5°C

The evolutionary character of the processes of decay connected to moisture has determined the necessity to set up a long time program of surveyings in order to acquire data in the most various external conditions and to return them as a trend. To such aim 4 strucks have been carried out to intervals of 4 and 7 months, at the beginning and at the end of the warm season.
In order to the remarkable extension of San Benedetto abbey, the monitoring of the thermo - hygrometrical conditions of the masonry has been preceded from a program of preliminary surveyings in the parts of the abbey where the degradation was manifest and in the zones whose

[1] The campaing has been started by the Laboratorio di Analisi e Diagnostica del Costruito, Politecnico di Milano, in 2003. A. Grimoldi and E. Rosina.

constructive history could suggest the presence of meaningful alterations in the structural order and, above all, in the collection system and removal of meteoric waters.
During this phase of pre - diagnosis IRT has been placed side by side to traditional techniques of stratigraphical analysis and has supplied an important support in order to read the masonry texture under plaster and to map the surfaces interested by moisture and capillarity; particularly it has allowed to reduce the number of samplings (drilling tests) for the determination of the water content in the masonry by means of quantitative tests.
Like described for masonries, also for monitoring the enviromental microclimate, the diagnosis has been articulated on two levels of sharpening: first a thermo - hygrometrical monitoring of the enviromental microclimate has been made by means of fixed probes for every day recording (to hour interval) of T° and U.R. % in every parts of the Abbey; then a campaign of psychrometrical surveys has been carried out in the most valuable rooms and in zones with critical microclimatic conditions.
The psychrometrical relief consists in a series of thermo-hygrometrical surveys executed according to an orthogonal mesh and overlapped to the plan of every room; collected data concur to draw maps able to evaluate very easy the distribution of ITI, HR, SH, diagnosis of the imbalances (and their causes), dangerous both for historical surfaces of ancient buildings both for the objects conserved to their inside.

RESULTS

The results obtained from this surveyings denounce the presence of an increasing hygrometrical gradient from the inside to the outside of masonry and from the bottom to the high. Water content diagrams allow to put in evidence that the part where moisture level reaches dangerous concentrations for the conservation of the building does not exceed 70 cm height from the ground.
Comparative reading of data moreover has allowed to design some synthetic maps concerning the distribution of enviromental humidity and to identify areas with the higher probability of risk for structures.
The present resesarch has also permitted to develop IRT, as an important support for reading of the masonry texture under plaster, for stratigraphical analysis and, finally, for a complete historical description of an ancient building carried on with the method of the *Raumbuch*.

VAULT CEILING- Photographic Image

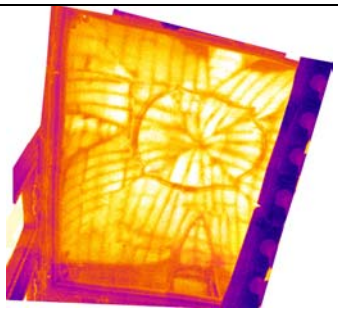

VAULT CEILING – Thermographic Image, date 23.07.2003, range 30.0 - 33.6°C

FURTHER RESEARCHES

The research has allowed to develop the potentialities of IRT in order to search and map the differences of temperature in the masonry and his connection with the other system in order to find, measure and control enviromental conditions of temperature and humidity.
The research will continue by monitoring microclimate during the start up of the new system of heating and air conditioning whose planning will be supported from the reliefs already made till today.

NON-DESTRUCTIVE TESTING OF BUILDING WALLS USING ACTIVE INFRARED THERMOGRAPHY

Laurent Ibos*, Mohamed Larbi Youcef, Atef Mazioud, Stefan Datcu, Yves Candau
CERTES, IUT de Créteil-Vitry, Université Paris XII Val de Marne,
61 avenue du général de Gaulle, 94010 Créteil, France
** Corresponding author: ibos@univ-paris12.fr; phone +33 1 45 17 18 43; fax +33 1 45 17 65 51*

Keywords: infrared thermography, non-destructive testing, thermal resistance, building thermal insulation

1. Introduction

This work concerns the development of a new method for the non-destructive testing of building walls. The final objective is to apply this method to the test of building thermal insulation. The method proposed uses active infrared thermography. We are more especially interested in the determination of the thermal resistance of multi-layered walls. In this paper, we will present the first results obtained concerning the determination of the experimental protocol and its application to the characterisation of a sample in laboratory conditions.

2. Experimental

The structure of the sample investigated is presented in figure 1. This sample is composed of two layers: one layer made of plaster and one made of expanded polystyrene. The thickness of the plaster layer is continuously varying along the horizontal direction from 0.5 cm (in the left part of the sample) to 2.5 cm (in the right part of the sample). The total thickness of the sample is equal to 5.5 cm. The bottom part of the plaster layer (front face of the sample) is coated using a black paint of known emissivity (0.97).

The experimental set-up is described in figure 2. The front side of the sample is heated using two halogen lamps of constant power P during a finite exposure time t_e. The sample front face temperature is measured using an infrared camera (model AGEMA 570) during the excitation pulse (heating) and also during the subsequent cooling.

3. Results

A thermal image taken at the end of the heating pulse (t_e = 1800 s) is presented on figure 3. The square points denoted AR01 to AR05 correspond to the areas where the front face temperature variations were analyzed. The analysis of these front face temperature variations was performed using two heat transfer models. For both models, we consider that heat transfer is mono-dimensional in the direction perpendicular to the sample front surface. Moreover, the heat transfers on the front face of the sample are modeled using a constant global heat exchange coefficient h, taking into account radiative and convective exchanges.

In the first model, we consider that the interface between the plaster layer and the polystyrene layer is adiabatic. In that case, by performing a least-square minimization (using the Levenberg-Marquardt method), we can identify three unknown parameters: the Biot number, the Fourier number (at $t = t_e$), and a temperature amplitude. From these parameters, we can compute the thermal resistance of the first layer, if the value of the front face heat exchange coefficient h or the power of the heating source P are known.

In the second model used, we consider that the sample is a semi-infinite body. In that case, the evolution of the front face temperature θ is given by:

$$\theta(0,t) = \alpha \cdot \left(1 - e^{\beta^2 \cdot t} \cdot erfc\left(\beta \cdot \sqrt{t}\right)\right) \tag{1}$$

with

$$\alpha = \frac{P}{h};\ \beta = \frac{h}{e} \tag{2}$$

The two parameters α and β can be identified by performing a least-square minimization. The identification procedure is performed for increasing measurement time, between $t = 0$ (beginning of the heating pulse) and $t = t_e$ (end of the heating pulse). The method used in that case is to follow the evolution of the identification residual norm upon measurement time. For shorter times, this norm is relatively small, indicating a good agreement between the measurement data and the semi-infinite model. For a measurement time longer than a characteristic time t_c, the residual norm increases dramatically. This indicates that the semi-infinite body assumption is invalidated. Moreover, this characteristic time t_c depends on the plaster layer thickness as different values are obtained for the five areas investigated (AR01 to AR05). Figure 4 shows the dependence of this characteristic time upon the real plaster layer thickness. We can notice a good correlation between these two parameters. An estimation of the layer thickness was also performed and is presented on figure 4. We note here a discrepancy between estimated and real value of the plaster layer thickness, especially for the smallest values.

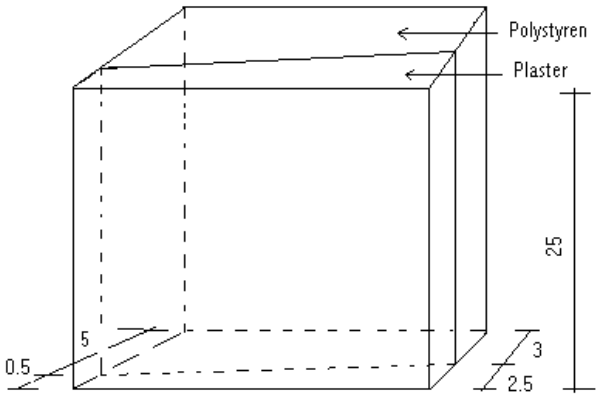

Figure 1. Structure of the investigated sample

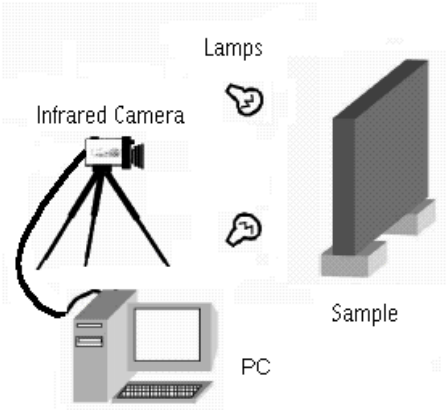

Figure 2. Experimental set-up

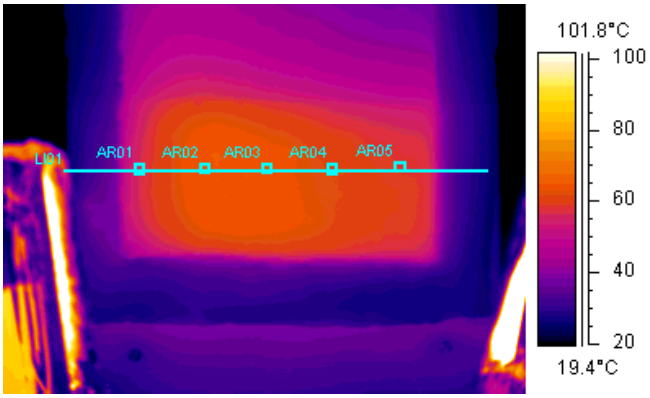

Figure 3. Thermal image of the sample front face at the end of the heating pulse

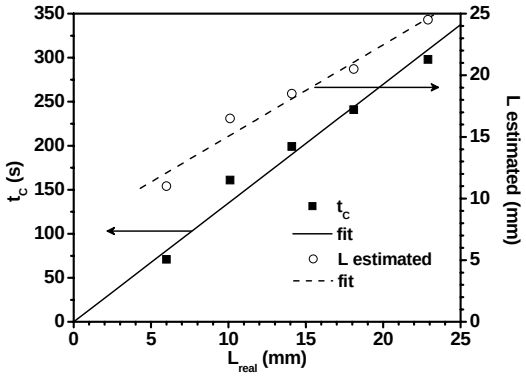

Figure 4. Dependence of the characteristic time and estimated thickness upon real plaster layer thickness

4. References

MANUEL, D., **OBLIN**, S., **RICHARD**, P.,Thermographie infrarouge appliquée à la détection de défaut d'isolation, Rapport final *CSTB, ENEA/SES 98.128R*, Paris, France, (2003).

DATCU, S., **IBOS**, L., **CANDAU**, Y.,Square pulsed thermography applied to thermal default characterization, QIRT 2004, Rhodes-St-Genèse, Belgium, (2004).

VAVILOV, V., Transient NDT : conception in formulae, QIRT, Paris, France, (1992).

RT 2000, Régles Th-U, Fascicule 2/5, CSTB, Paris, France, (2001).

TANG-KWOR E., Contribution au développement de méthodes périodiques de mesure de propriétés thermophysiques des matériaux opaques, Thesis University Paris XII Val de Marne, (1998).

Infra-red photothermal thermography: A tool of assistance for the restoration of murals paintings?

Jean Charles Candoré*, Gabriela Szatanik**, J.L Bodnar*, Vincent Detalle***, Philippe Grossel*

**Laboratoire d'Energétique et d'Optique, UFR Sciences Exactes et Naturelles, BP 1039, 51687 Reims cedex 02
* Restauratrice du patrimoine, 6 allée Pasteur, 78330 Fontenay le Fleury
*** Laboratoire de recherche des monuments historiques, 29 avenue du Paris, 77420 Champs sur Marne

Abstract

Delamination and air voids in renders are among the main sources of deterioration of mural paintings. Those decays are particularly dangerous because they are almost non visible, because underlying, but they can induce falls of parts of the artistic composition depending on their nature and the affected surface.
The traditional technique used by the restorers to localize delaminated areas is acoustic sounding. It consist in a systematic slight knocking of the painted surface with one hand, when the other hand stays in contact with the surface. The vibration induced by the knocking is then perceived both by hear and touch and allows an experienced restorer to determine the extent of the decay, on the basis of an empirical evaluation of the propagation of the vibration. This technique which is qualitative is very simple and does not necessitate any specific equipment, but the results are not very precise and their quality depend a lot on the skills of the restorer. For example, the thickness or the depth of an air void, cannot be detected, when they represent valuable information for the restorer to evaluate the real state of decay of the mural painting and as a consequence a key point for the choice of a suitable restoration technique.
Moreover, a contact with the mural painting, more or less long and powerful, is needed. It can be hazardous if the painting is powdering or weakened by scaling (as it was the case for the "*Saint Christophe*" of the Campana collection of the *Louvre* museum, before its restoration); or if the render is too thin (it then can collapse if the knocking is too powerful).
Finally, when the surfaces painted are wide, this operation can be long and laborious.

As infrared photothermal thermography has been successfully tested to localize and characterize decays such as delamination or cracking in several materials, it seemed interesting to evaluate its possible application in the field of historical monuments restoration, and in the specific case of mural painting as a complementary method of the empirical acoustic technique.
Infrared photothermal thermography is non-contact and quantitative technique, which allows rapid large surface examinations.
In this study, the performances of the technique in terms of precise localization and cartography of decays of the internal structure of mural paintings, invisible to the naked eye were evaluated. The tests were focused on the detection of renders detachment, and air voids situated in the underlying layers of the render, which are decays often generating weakened areas necessitating later consolidation.
The tests at first were performed on a fresco replica, and then the technique has been applied to the real "Saint-Christophe" wall painting which had been at the same time traditionally knocked.

As the spatial localization and the depth of the defects were coherent with both techniques, theses tests clearly show that stimulated infrared photothermal thermography is a suitable diagnosis technique for wall painting.
The association of both empirical and quantitative technique could provide valuable information for the restorer.

Figure 1: Studied replica

Figure 2: Detection of four defects in the studied replica

Figure 3: The studied fresco of the Saint Christophe

Figure 4: Detection of defects in the studied fresco of the Saint Christophe

keywords : Stimulated IRT, Cultural heritage, mural painting, defects detection.

COMPARATIVE STUDY BETWEEN INFRARED THERMOGRAPHY AND LASER DOPPLER VIBROMETRY APPLIED TO FRESCOES DIAGNOSTIC

[1]Sinthya Gonçalves Tavares, [2]Alexia Agnani, [2]Enrico Esposito, [2]Mara Feligiotti, [1]Roberto Marcio de Andrade
[1]Departamento de Engenharia Mecânica da Universidade Federal de Minas Gerais,
Belo Horizonte, MG – Brazil, Phone: +55-31-3499-5140,
Fax: +55-31-3499-5140, gtavar@terra.com.br
[2]Dipartimento di Meccanica – Università Politecnica delle Marche, Ancona, Italy, Phone: +39-071-2204508,
Fax: +39-071-2204801, e-mail: a.agnani@mm.univpm.it

Keywords: Non destructive thermal evaluation, laser Doppler vibrometry, frescoes diagnostic

ORAL PRESENTATION

In this work, a comparative study between the laser Doppler vibrometry and infrared thermography to damage detection in frescoes is presented. In order to validate the results obtained experimentally through both techniques, mathematical models were implemented which simulate the physical domains and conditions of the sample. The limitations of each methodology are also discussed.

The experimental procedures were carried out in the Mechanical and Thermal Measurements laboratory of the Mechanical Engineering Department of the Università Politecnica delle Marche. The sample has been made by the Spanish restorer Eudald Guillamet and represents the typical structure employed in the preparation of frescoes. The compact and resistant base of the sample has been fabricated in terracotta, a common material for the covering of old floors and walls. For the arriccio, a mixture of calcium and thick sand (granulometry of 1÷2mm) has been used with a ratio of 1:3. Also for the intonaco, has been used calcium and fine sand in the ratio of 1:2.5. Over the intonaco, a decorative geometric pattern has been painted. The defect has been simulated by a disc shaped delamination of approximately 2.5mm in thickness and 90mm in diameter, placed in a longitudinal position between the arriccio and intonaco layers. The void has been created by means of the same organic substance employed in the manufacture of ecclesiastical wafers, since the contact of this substance with the humidity, present in the arriccio and intonaco layers, provoked its partial dissolving, thus realistically simulating the flaw. Figure 1 shows a schematic view of the sample used in the tests which also represents the physical domain of the mathematical model.

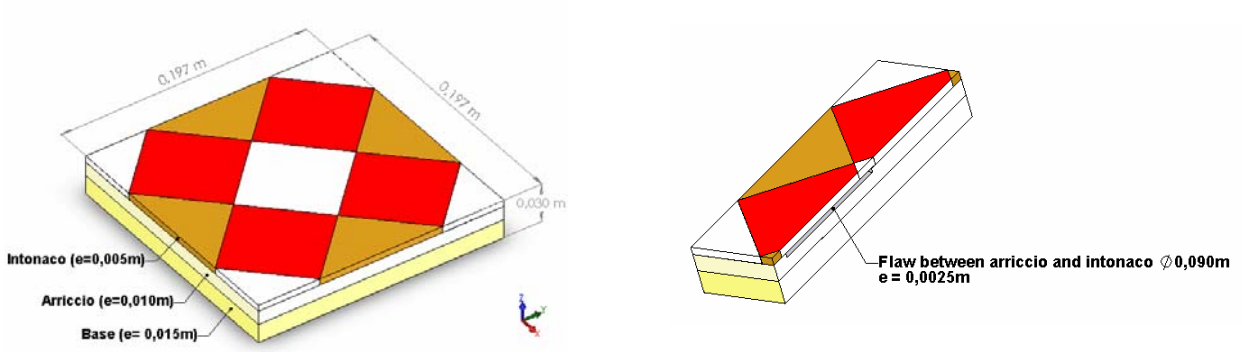

Figure 1 – Fresco sample.

The Fourier equation has been used for the mathematical model employed for the numerical validation of the thermographic investigations, considering a transient regimen, without heat generation, in three-dimensional cartesian coordinates. During the investigations, the lateral sides of the sample have been isolated which allowed the consideration of a one-dimensional heat flow in the z direction. This procedure also allowed to consider the physical domain as a semi-infinite solid. For the Fourier equation solution, numerical technique with formularization in finite volumes has been employed. The solution obtained by this technique supplies a perfect balance of energy for entire domain of calculation. A program, written in FORTRAN®, has been developed for the solution evaluation. The number of control volumes has been defined from mesh test and criterion of convergence based on the comparison between the numerical and analytical solutions for the temperature reached at each point (only differences smaller than 10^{-5} have been accepted).

The testing procedure suggested in [1] has been followed during the thermal experiments. Both pulsed and modulated Thermography were employed. Regarding the uncertainty analysis, the methodology indicated in [2] and [3] has been used and more details will be given in the final paper.

The numerical model of the vibrometric investigations has been constructed using Finite Elements Method (FEM) modeling; in this case, the main difficult task regarded the derivation of the proper values for the sample mechanical parameters (Young modulus, Poisson ratio and mass density). A new procedure based on the observation of Rayleigh waves propagation velocities allowed to acquire needed data. Comparison of experimental and simulated data and independent defect diameter measurement by echographic equipment, allowed to establish the confidence level and the discrepancies in the developed model. Operational limits of the vibrometric technique have been studied by acquisition of Signal-to-Noise ratio on different areas (pigments) of the sample. Regarding the acquisition of Signal-to-Noise ratio, the methodology indicated in [4] has been used and more details will be given in the final paper.

The Figure 2 shows, for the maximum contrast, two temperature maps: (A) obtained by the infrared camera and (B) obtained by means of MATLAB program. Both maps use pulsed thermography.

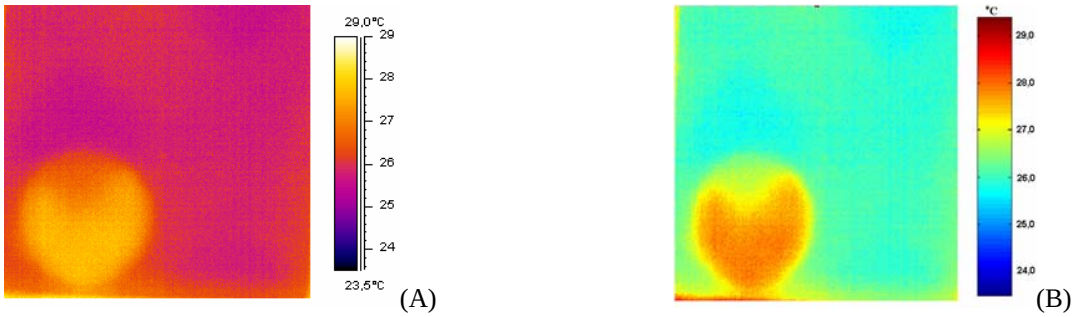

(A) (B)

Figure 2 – Temperature Maps: Infrared camera (A) and MATLAB (B)

In the final work, further maps obtained by modulated thermography will be shown and also compared to their numerical solutions using FORTRAN® program. Modulated thermography has allowed the best characterization of the defect since superficial emissivity difference problems are minimized.

Images analysis allowed the correct identification of the flaw since the temperature difference between the unflawed and flawed areas was twice greater than 0.6°C, i.e. the maximum uncertainty for the measurement set. Comparison of simulated and measured data has been quite favorable with discrepancies in the order of some tenths of a degree. Figure 3 shows the experimental and numerical surface temperature decay for the flawed and unflawed areas.

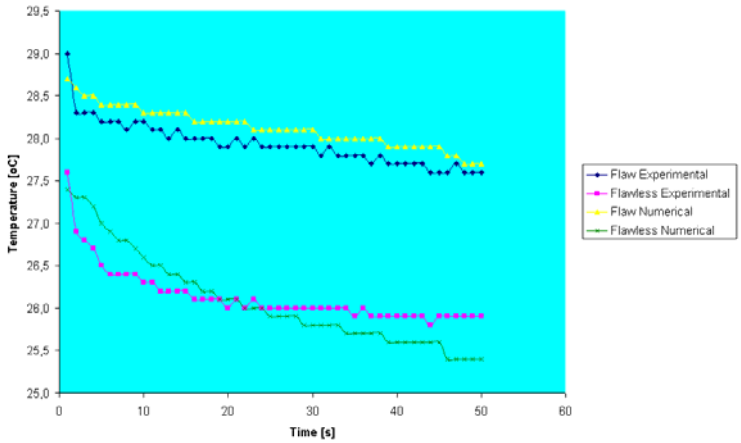

Figure 3 – Temperature decay

Finally, Figure 4 shows the resonance frequency of defect: (A) obtained by the vibrometric technique and (B) obtained by using Finite Elements Method (FEM) modeling. with a discrepancy of about 12%.

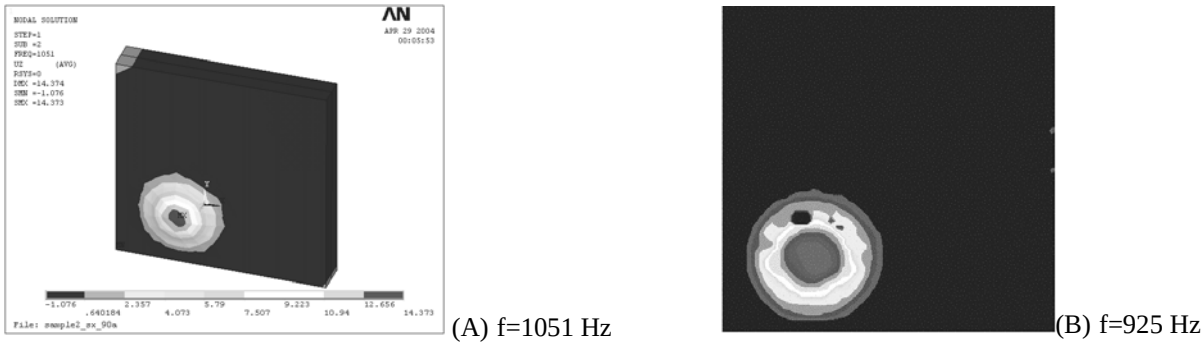

(A) f=1051 Hz (B) f=925 Hz

Figure 4 – Comparison of simulated (A) and measured (B) resonance frequency of defect.

References

(1) Tavares. S. G., Andrade, R. M., “Metodologia de ensaio e análise de incerteza na aplicação da termografia”, 2003, Anais do III Congresso Brasileiro de Metrologia, Recife, PB, Brasil.

(2) Tavares, S. G., Cunha, A. M., Andrade, R. M., “Metodologia Experimental para Aplicação da Termografia em Ensaios Térmicos não Destrutivos”, 2004, Proceedings of the 10th Congress of Thermal Sciences and Engineering – ENCIT 2004, Brazilian Society of Mechanical Sciences and Engineering, ABCM, Rio de Janeiro, Brazil.

(3) Chrzanowski, K., Fischer, J., Matyszkiel, R., “Testing and evaluation of thermal cameras for absolute temperature measurement”, 2000, Journal of Optical Engineering vol. 39, no 9, pp. 2535-254.

(4) Esposito E., Castellini P., Paone N.,. Tomasini E. P., “Laser signal dependence on artworks surface characteristics: a study of frescoes and icons samples”, Proc. of LACONA V, p. 327-332, Osnabrueck (D), 15-18 September 2003. Springer-Verlag Berlin Heidelberg, 2005, ISSN 0930-8989.

Thermal Patterns Due To Moisture Accumulation Within Exterior Walls

Antonio Colantonio, Garry Desroches
Public Works And Government Services Canada

ABSTRACT

In cold climates, air leakage is accompanied by moisture transport. When migrating through dew point temperatures, a considerable amount of moisture accumulation may occur depending on variables such as the duration of sub-zero exterior temperatures, building pressurization, wind effects and the level of interior relative humidity. Moisture accumulation may result in premature deterioration of wall assemblies and the formation of mold. When commissioning new building envelopes, or carrying out building condition inspections of existing building envelopes, it is imperative to differentiate the source of the moisture accumulation since the recommendation for remedial action will vary considerably. This paper will define the various types of thermal patterns created by surface penetration of water versus those patterns created by air leakage from the building interior in cold winter conditions. Various types of exterior building envelopes will be discussed along with their hygro-thermal performance characteristics and how these affect thermal patterns ring various inspection procedures.

Quantification of Voids and Delaminations in Real Concrete and Masonry Structures with Active Thermography: Case Studies

Ch. Maierhofer, R. Arndt, M. Röllig, R. Helmerich

Federal Institute for Materials Research and Testing (BAM), Berlin, Germany

A. Walther, B. Hillemeier

Department of building materials and building material examination, Technical University of Berlin, Germany

C. Rieck

Institute for Material Testing (MPA) Berlin-Brandenburg , Germany

Keywords: Impulse-Thermography, Pulse-Phase-Thermography, Non-destructive Testing in Civil Engineering, Concrete, Masonry

Introduction

As shown in recent publications [1], active thermography by inducing a non-stationary temperature distribution (e. g. impulse-thermography) in combination with the analysis of temporal data in frequency domain (e. g. pulse-phase-thermography) is very well suited for the visualisation of inhomogeneities and defects close to the surface (up to a depth of 10 cm) of building structures. For quantitative analysis of data recorded on-site, the main problems are manifold: the inaccessibility of most of the investigated structures, the changing environmental conditions, the inhomogeneity of the investigated surfaces and the relatively thick building structures in relation to the low thermal diffusivity of the building materials have to be considered. Although a lot of investigations of different measurement problems occurring in civil engineering have been carried out, most of the hitherto presented are results of laboratory measurements.

In this paper, the results of several case studies will be presented. These applications so far involve the investigation of the masonry structure behind plaster, the location of plaster delaminations, the location of delaminations of carbon fibre reinforced plastics (CFRP) for reinforcing concrete structures, the location of asphalt delaminations on concrete bridges and the location of voids below a stone pavement.

For performing on-site investigations, the measurement equipment has to be mobile, light, flexible, water resistant and easy to apply with a maximum of two operators. To overcome the obstacles given by the external conditions, different kinds of heating units including radiant and fan heaters, flash and halogen lamps in combination with a mobile computing unit for digital data recording in real time and a flexible infrared-camera for stationary and moved measurements were used (Inframetrics SC1000, 256x256 pixels in a wavelength range of 3-5 µm). Data analysis was performed in time domain (maximum contrast of defects or inhomogeneities) and frequency domain (pulse-phase-thermography). Quantitative information about the lateral geometry of defects was gained from lateral temperature distribution. Even more difficult is the analysis of the defect depth, which might be performed semi empirically (e. g. by determining the blind frequency in the phase images [2]) or by a comparison of experimental data to the results of numerical simulations [3].

Results

In the following, the results of two case studies are shown. More case studies and quantitative data analysis will be demonstrated in the full paper.

Location of voids below a stone pavement

For the detection of voids below a stone pavement consisting of granite tiles with a thickness of 1.5 cm, which were laid on mortar on a concrete floor, a whole area of 40 m^2 was investigated. Single areas of about 1 m^2 were heated up with a infrared radiator for about 3 min. The cooling down behaviour was recorded with the infrared camera. The voids could be easily detected with a temperature difference of about 2.5 K as shown in Figure 1. Here, the superpositioning of the photogrammetric equalised digital photo as well as of the equalised thermogram recorded 1.33 min after switching of the heating source is displayed.

Location of asphalt delaminations on a concrete bridge

On-site-investigations on a pre-stressed concrete bridge were carried out for the detection of voids or delaminations inside or below the top asphalt layer. The paving above the concrete plate consisted of up to 50 mm concrete for equalisation, 10 mm mastic for sealing and an asphalt layer with a thickness of 50 mm. Thermal images were taken at varying times after sunrise, thus using the sun as heating source.

Figure 2 shows a thermogram taken at 10:00 a.m. at a measured solar radiation of 800 W/m^2. Clearly distinguishable are areas of higher temperature which might be related to defects or delaminations. The largest of these areas in the middle of Figure 2 has a temperature difference of 3.5 K to it's surrounding.

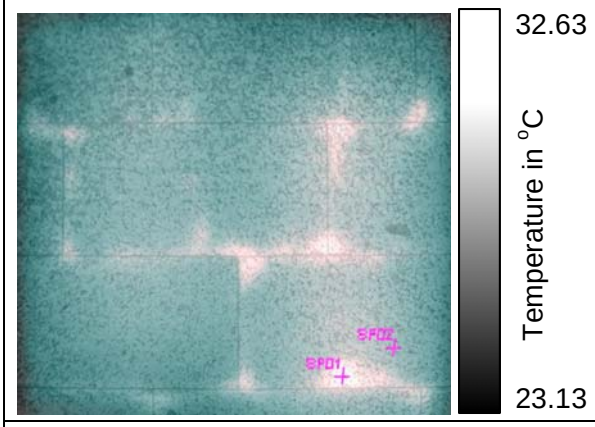

Figure 1: Superpositioning of an equalised digital photo and the related equalised thermogram of several granite tiles (1 x 1 m^2) recorded after a heating time of 3 min. The voids could be clearly detected as warmer (white) areas.

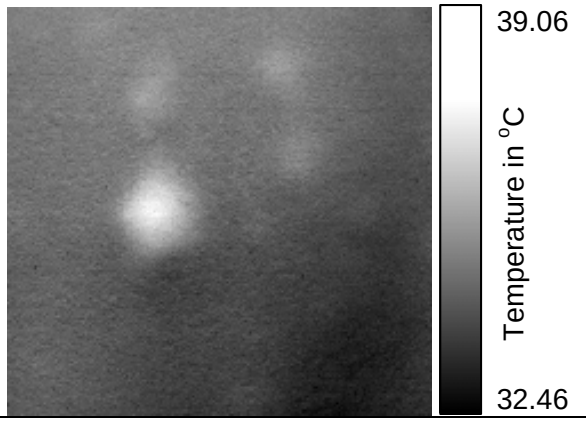

Figure 2: Thermogram recorded at 10 a.m. summer time, 2005-06-23, Sun, in Berlin of a 1 x 1 m^2 sized area of an asphalt layer on a concrete bridge. Again, the delaminations are clearly shown as warmer areas.

References

[1] Weritz, F., Arndt, R., Röllig, M., Maierhofer, Ch. and Wiggenhauser, H.: Investigation of concrete structures with Pulse-Phase-Thermography, Materials and Structures 38 (2005), pp. 731-737.

[2] Ibarra-Castenado, C., Maldague, X.: Pulsed phase thermography reviewed, Quantitative Infrared Thermography Journal, Volume 1, Nr. 1, Lavoisier, 2004.

[3] X.P.V. Maldague, Theory and Practice of Infrared Technology for Non-Destructive Testing. , John Wiley and Sons, New York (2001).

AN INFRARED EXPERIMENTAL APPROACH TO VISUALIZE THERMAL IRREGULARITIES IN HISTORICAL BUILDING MANSONRY WALLS

F. Fantozzi, S. Filippeschi, F. Leccese
Department of Energetics "Lorenzo Poggi" – University of Pisa
Via Diotisalvi 2, 56100 Pisa, Italy
tel. +39-050-2217153 fax +39-050-2217150
s.filippeschi@ing.unipi.it ; g.salva@ing.unipi.it

The infrared thermography represents a very useful non-destructive technique in the building diagnostics. In particular, the technical literature reports several "qualitative" criteria for the detection of thermal irregularities in building envelope are reported with regard to thermal insulation defects, air leakages and moisture effects.
In the last few years this technique has been widely used in the cultural heritage preservation field both with the solar heating (passive) and with heating devices (active). The flexibility of the passive infrared thermal method can depend, even significantly, on the environmental conditions (i.e. exposure of the walls of the building, climatic conditions, walls colours and decay).
On the other hand the most of the historical buildings under restoration are generally not occupied, not heated and in hard-decay situations, concerning both exterior envelope and interior partitions. In these cases a simple qualitative analysis can provide bad results and the operator's experience turns out to be crucial during the shooting procedure in situ.
All the quantitative analysis are based on the measurement of the temperature of sample over time and their successive images processing. The most of thermal quantitative methods reported in literature has been developed for industrial applications. In case of historical building the thermal properties of the materials are very different and the time of heating and thermal infrared observation is longer.
Moreover the materials found in historical walls are very different among them and, therefore, thay are different also by a reference case previously analysed in laboratory or reported in literature.
In literature a significant database containing experimental data deduced from images in situ is still lacking owing both to the recent application of these techniques to the specific field and to the difficulty in processing images according to standard procedures and in cleaning up the thermal signal by eliminating any measurement error (noises).
In this paper the authors show several experiences on infrared thermal tests of historical buildings in Tuscany realized by using a LW infrared camera with microbolometric sensor. The obtained thermographic images have been processed using the thermal contrast as referent parameter. The images have been corrected in order to taking in account the different angles of view.
In order to define the minimum thermal contrast that allows a good definition in the analysis of the texture. The images have been analyzed by proposing a quantitative analysis of active techniques (Step heating with oil burner) based on the comparison of the temperature evolutions of a wall experimentally measured and numerically simulated with simple algorithms.
The mathematical model is based on the idea that a portion of mortar and a portion of a stone, as a thermal radiation is supplied, show thermal evolutions that are not influenced by boundary and, therefore, a lumped capacitance method can be used. In particular have been neglected also the thermal diffusion in the plaster thickness.

The mathematical model has been developed in case of active heating, that in the experimental cases in situ has been realised by an oil burner heater. The most of heat supplied by the oil burn heat to the wall is in radiating mode, so that the natural convection can be neglected in the first hypothesis.
The mathematical model that have been compared with the experimental evolutions are three. The first method takes in account a wall made of a portion of mortar and a portion of another material (stone, whole brick, hollow brick, etc) both approximated as semi-infinitive medium. The second configuration add to the previous wall a thick of plaster which is approximated with a finite difference method both in space and in time.
This simple method has been compared with a wall made a layer of plaster and a layer of mortar and another material but this wall has been approximated with a finite difference method both implicit and explicit. These results have been compared with the experimental one. The mathematical model calculates the thermal contrast between the mortar and the other material which varies over time on the external layer of the plaster.
In figure 1 is reported the thermal evolutions of the thermal contrast for a wall made of whole bricks and the reference mortar. All the numerical results have been compared with in situ evolutions of walls.
The paper shows the numerical results of this calculations made with different material (different kind of stones, hollow and whole bricks, woods, etc.). Interesting considerations can be drawn on the time in which the different materials which made the wall "appear" on the external face of the wall. The "appearing time" is time for reaching a sufficient thermal contrast on the external face of the wall. The sufficient thermal contrast depends on the thermal resolution of the thermograhpic instruments.
The preliminary results on a sensibility analysis of the different parameters being able to influence the "appearing time" of different materials has been shown in this paper.

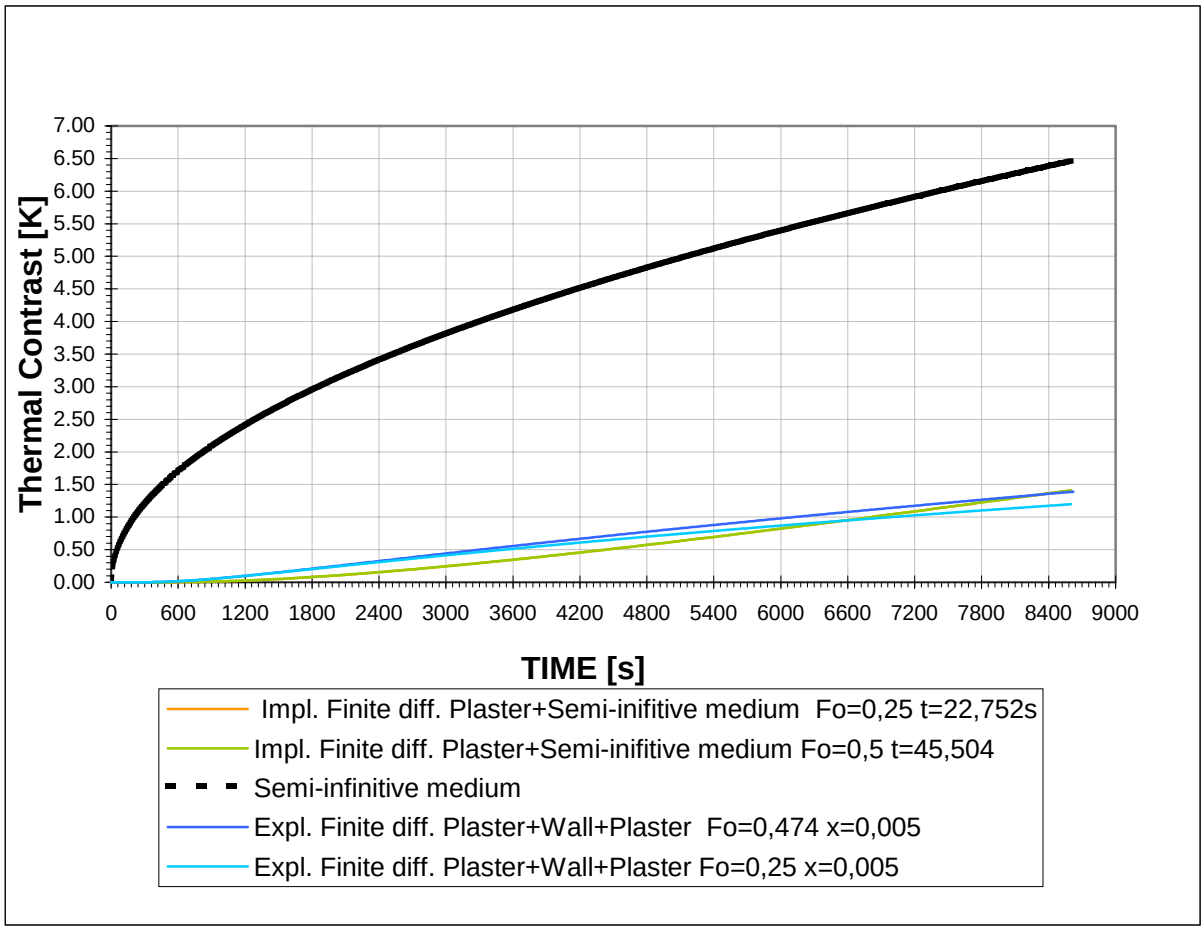

Passive and active thermography application for architectural monuments

by M. Poksinska*, B. Wiecek**

* Nicolaus Copernicus University, Faculty of Fine Arts, Poland, mapoks@art.uni.torun.pl
**Institute of Electronics, Technical University of Lodz,Poland, wiecek@p.lodz.pl

Keywords: Lock-in thermography, non-destructive testing, architectural monuments

The objective of the research is to solve problems concerning the chronology, conservation treatments and reconstruction of the oldest and the most valuable part of the middle-age castle complex in Malbork. Major stress will be put on non-destructive methods, especially on the use of thermography. Thanks to contactless measurements of temperature in the western wing of the castle, this method is expected to permit identification of the diversified structure and type of building and painting materials that were used in different historical periods.

The measurement system is composed of 4 halogen lamps set in two independent heating sections, each of 2 kW of power, connected to a driver. It enables lightening of the investigated objects with IR pulses of desired frequency, single pulses or a continuous light beam. Another autonomous part of the equipment is the image recording system. It is composed of two cameras: a wide range vision camera and a thermographic camera Reytheon Conrtoll IR 2000B. It also contains a grabber for catching and recording of images, with 3 analogue inputs: 2 video and one S-video. This enables simultaneous registration from a chosen input in PAL, SECAM and NTSC standards, with the resolution from 320x240 to 768x576 pixels. The whole device is equipped with the software systems – ThermoScope, which controls the heating lamps and records and processes of visual and thermographic images.

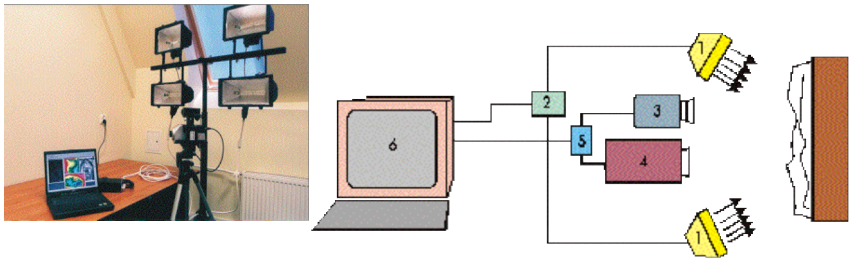

Fig.1. Multispectral imaging system for investigation on architectural monuments

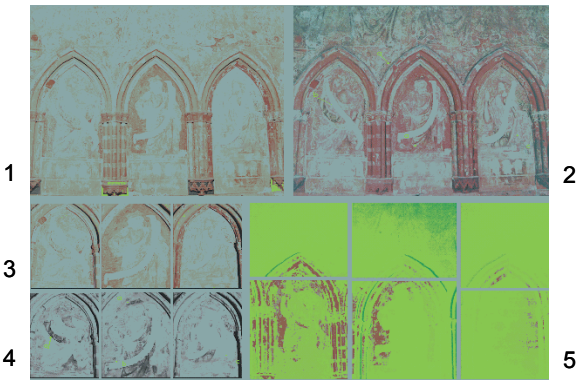

Fig.2. Images form the multispectral imaging system

The chosen results are presented in Fig. 2. The image of the whole in-door polychrome was recorded in the castle church, in various spectra of electromagnetic radiation. On the example of a chosen detail of the arcaded frieze on the northern wall, images recorded in different spectrum ranges have been presented.

Part 1- Image recorded in visible light. The state of preservation of the paintings.

Part 2 - Fluorescence in UV generated by radiation in the range 360-420 nm. Deteriorated areas became visible (a), over-paintings (b) and restoration treatments (c).

Part 3 - Image recorded in visible light.

Part 4 - Reflexography in IR, recorded by the thermo-optical device. Range is about 790 nm. The drawing is legible (a) as well as painting elements of the background (b) and restoration interventions (c).

Part 5 - Image recorded with a thermographic camera Raytheon Control 2000B. A clear differentiation of the image is probably due to variable depth of the plaster and paint layers. The possibility of identification of the brick plot (the third panel) is of great importance. Areas of previous restoration works are clearly visible.

Investigating heat engineering characteristics of building envelopes using infrared cameras

Oleg Lebedev[1], Vladimir Avramenko[1], Dmitry Kirzhanov[2] and Oleg Budadin[1]

[1]Technological institute of energetic surveys, diagnostic and nondestructive testing "WEMO", Russia, Moscow, 113162, Lusinovskaya st, 62, phone: +7 (095) 2377288, fax: +7 (095) 2376457, email: olegleb@gmail.com

[2]Mechanical Engineering Institute of Russian Academy of Sciences, Russia, Moscow, 101990, M. Haritonjevskij st, 4, phone: +7 (095) 9249800, fax: +7 (095) 2004239, email: kirzhanov@gmail.com

Keywords: building envelope, infrared survey, inverse heat transfer problem, heat engineering parameters

Preference for Oral Presentation

Different economical reasons force the world to produce more and more energetic efficient buildings. The building envelope's parameters are the mostly important parameters which define this efficiency. For several recent years some methods were created to monitor the envelope state using infrared methods. Such methods provide with the information about the current envelope consistency. Primarily this can be used to monitor defects on the surface of the envelope (figure 1, right). Such defects become obvious (figure 1, left) if the air is cold outside the building and the heating system operates inside the building. The defect looks like a zone with a temperature greater than one at the nearby zones.

Figure 1. Using an infrared image to detect thermal bridges.

When designing new buildings it is usually taken into account that the air of the building exploitation requires the building to preserve the heat efficiently. Dew to different reasons the heat engineering parameters of the construction's materials change with time. After several years of exploitation not only the envelope's structural defects determine the thermal resistance value. As the material is aging it the modified heat engineering parameters must be taken into account.

This way a more complicated problem must be solved. It can be solved using infrared camera together with several other measuring devices. The measurement procedure consists of two parts. At the first part a temperature recording devices are installed on the building coating in several points. As it has been shown previously when measuring several temperature time series for a rather large while one can calculate local heat engineering parameters of the envelope's point. The calculation is done by solving the inverse heat transfer problem.

This can be done using the plausibility functional method that can be reduced in this case to the square deviation of two functions: a measured one and a calculated one. This function is usually the temperature time series of the chosen zone of the envelope. To calculate the temperature time series it is needed to solve the direct problem of the heat conductivity. The mathematical approach usually provides the researcher with three values: the thermal conductivity of the insulator layer of the coating and the two values of the thermal emissivity coefficient at the both surfaces of the envelope.

$$R_0^r = \frac{F}{R_0}, \quad R_0 = \sum_{j=1}^{K} \frac{F^j}{R_0^j} \tag{1}$$

$$R(\vec{r}) = \frac{1}{\alpha_{out}} \frac{T_{in}^{air} - T_{out}^{air}}{T(\vec{r}) - T_{out}^{air}} \tag{2}$$

After the local heat engineering parameters of the filler structure are defined through the first part of the measurement the found values can be used to calculate the average heat transfer resistance. The equation 1 shows the typical way to calculation this resistance. In the equation F is the surface of the envelope, F_j is the surface of a fragment of the envelope and R_j is the corresponding resistance value, K is the number of the surfaces. A special model is used to distribute these values to the whole envelope of the building. The model compares the temperature of the each point of the image with the corresponding heat transfers resistance value (figure 2, right). The comparison rule is presented by formulae 2 where T_{in}^{air} is the temperature of the inner building air, T_{out}^{air} is thee environment temperature and $T(\vec{r})$ is the temperature of the current point $\vec{r}$ of the surface of the envelope. a_{out} is the external thermal emmisivity of the envelope surface. The calculation procedure requires the infrared image of all of the parts of the envelope (figure 2, left). The estimations show that the error of the averaged heat transfer resistance calculation does not exceed 15 %. After the resistance value is calculated the researcher also can use the infrared images to find structural defects.

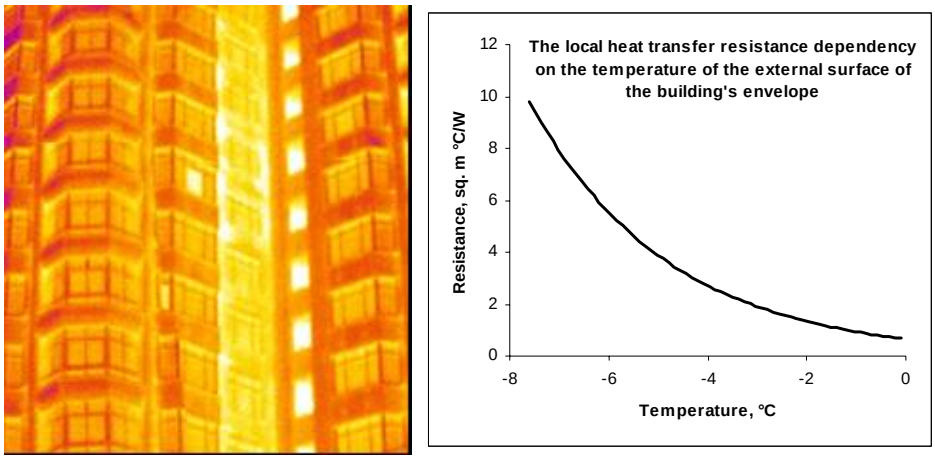

Figure 2. Calculating the averaged heat transfer resistance using special model.

This technology was used to estimate the quality of buildings by request of Moscow Government. More than 500 buildings including civil structures, many-storied buildings, palaces, industrial buildings were surveyed. Some of the corresponding methods have been certified by “State Standard” and agreed with Federal Agency of science and education of Russian Federation and “State City Technical Supervision”.

Submitted for oral presentation at QIRT 2006

DETERMINATION OF CRITICAL MOISTURE CONTENT IN POROUS MATERIALS BY IR THERMOGRAPHY

A. Tavukcuoglu[1], E. Grinzato[2],

[1] Middle East Technical University, Department of Architecture, Ankara - Turkey
[2]Consiglio Nazionale delle Ricerche, CNR-ITC Padova – Italy

Abstract

It is well-known that weathering conditions are more damaging for the porous materials in the presence of water above the critical moisture content (Θ_{cr}). IR thermography is one of the non-invasive techniques and the most practical one used in-situ for the detection of moisture in historical buildings. This study is a step towards monitoring damp zones non-invasively whether the moisture content is above or below the Θ_{cr} and to achieve a quantitative information by infrared imaging applied in-situ.

The Θ_{cr} level for some tuffs and repair bricks, especially manufactured for the restoration of historical buildings, were examined in laboratory. Two methods, IR thermography and standard weighing method by RILEM (1980) were used together for this laboratory analysis. Several saturated samples were prepared in varying thicknesses with the same top surface area allowing evaporation, while the other surfaces being vapour tight. Drying phase was examined for constant boundary conditions of 20°C and 40%RH under the effect of steady and low air velocity. They were monitored during the moisture desorption in terms of evaporation rate (*ER*) and a new informative parameter called Evaporative Thermal Index (*ETI*). *ETI* is related to the surface temperature and defined as the normalized temperature difference between actual and dry surface, multiplied by a suitable constant. The standard evaporation rate test is based on the sample weight loss change in time, during the drying process, knowing the evaporating area. Then, the evaporation rate is computed as a function of the moisture content. The moisture content was calculated by the weight loss, normalized by the sample volume. The surface temperatures were assessed as a function of time by means of a infrared sequence taken through an infrared window, during the evaporation rate test. Tests have been run inside a chamber, with controlled temperature and humidity, allowing steady boundary condition. Then, *ETI* is expressed in terms of the moisture content.

The emphasis was given to the transition stage between the saturated and dry phases of the samples which has been defined in literature as the critical moisture content (Θ_{cr}) level. Above Θ_{cr} it happens that liquid transfer in capillaries, with the highest evaporation rate; while below it moisture transfer occurs only by vapour transfer, with a sharp decrease in evaporation rate.

A good correlation was achieved between the *ER* and *ETI* both for the saturated and almost dry phases. Some differences appear close to the Θ_{cr} values, due to the uneven concentration of water inside the sample. In fact, while *ER* gave data in relation to the total moisture content of the whole sample, *ETI* reflected purely the water content of a shallow layer close to the evaporating surface. Furthermore, it was seen that *ETI* can be used to determine the Θ_{cr} and is very sensitive compared with the weighing method about the range of Θ_{cr}. It is interesting to note that thicker samples were found to have higher critical moisture content. This may initiate a discussion on the standard dimensions of samples to be examined for their Θ_{cr} characterization.

Further studies by means of IR thermography started to determine the relationship between the capillary suction coefficient (*A*), the range of Θ_{cr} and the moisture diffusion of particular materials. The results obtained in the laboratory were promising to give the hints of methods for quantitative moisture content measurements and in-situ IR investigation.

Keywords: critical moisture content; porous materials; IR thermography; evaporation rate

Submitted for Poster presentation at QIRT 2006

title

Thermal NdE of FRP applied to civil structures

Authors

E.Grinzato[(1)]; V.A.M. Luprano[(2)]; S. Marinetti[(1)]; P.G. Bison[(1)]; A.Tundo[(2)]; A. Tatì [(3)]

[1] Consiglio Nazionale delle Ricerche, CNR Padova - Italy
[2] ENEA S.S. 7 Appia km 714 -72100 Brindisi– Italy
[3] ENEA Casaccia - S.Maria di Galeria - Roma– Italy

Abstract

The use of advanced composite materials for the reinforcement of civil structures as Fibre-Reinforced Polymers (FRP) is becoming more and more common. The strengthening and restoring of buildings is achieved applying composites made of fibres as glass, carbon or aramid within a polymeric matrix, such as epoxy resin. The FRP reinforcement techniques found its success on the perfect adhesion between the FRP and the underlying material. For this reason, it is essential to use Non-Destructive Testing (NDT) to assess the bond quality. In particular, the interface between FRP and different kind of materials as concrete, bricks and wood is examined in order to characterize the perfect matching with FRP.

In the recent literature, IR thermography appears as one of the most advantageous methods. By means of thermography, it is possible to find out defects that cause alterations of the normal distribution of the surface temperatures, when a suitable heat flux is imposed on the surface. Different techniques have demonstrated identifying artificial defects inserted at the interface to simulate a lack of adhesion. The fibres orientation, fabric and number of layers have been considered according to the most frequent practice.

The main aim of this work is to develop a reliable and confident non destructive testing procedure to characterize the extension of the delamination and its location. In facts, the more advanced standards set the limit for acceptable defects, both in terms of number and size.

An experimental study on samples bonded with FRP and containing defects appropriately applied at the interface, will be presented. The influence of the FRP material, the kind of fabric and of the finishing layer of the reinforcement, on the evaluation of defects will be analysed.

Different algorithms have been applied at the evaluation stage in order to estimate the defect size and location.

Finally, a comparison between thermography and ultrasonic wave measurements will be carried out. The cross evaluation is essential to analyse not only artificial defects but natural ones.

Restoration mortars at IRT: optical and hygroscopic properties of surfaces

N.Ludwig (1), E. Rosina (2)

(1) IFGA, University of study of Milan, V. Celoria 16, 20133 Milano, Italy, ludwig@mailserver.unimi.it, +39 02 50317423
(2) BEST Dept., Polythecnic of Milan, V. Ponzio 31, 20133 Milano, Italy, elisabetta.rosina@polimi.it, +39 02 23994150

IRThermography usefully integrates the visual inspection and the videomicroscopy in the field. Microscopy allows to recognize the texture of the surfaces and the state of conservation. Texture of the material affects the distribution of surface temperature [1], especially in transient condition. Moreover, the roughness of surface has some influence on the absorbance of the surface.
The research starts from the observation in the field of the hygroscopic behaviour of different texture of mortars [2] with high RH rate and low ambient temperature: textures obtained with hard tools (e.g. spatula, wooden float, trowel) have harder surfaces, more compacted, which facilitate the condensation of water vapour; soft tools finishing (sponge, sponge float) have a rough surface, which facilitate the absorption and evaporation of moisture. In case of contiguity between two different finishing, the edges of rougher surface (around more compact texture) show major damage.
In restoration of plasters and mortars, the operators use both kinds of instruments, only dependently on the extension of the "patch" and the final aesthetic effect.
Early detection of these risk areas, by use of IRT, is a great deal for preservation of historical buildings without a controlled HACV system, and an advancement for the restoration techniques of precious surfaces.
For that, authors studied the surfaces properties of responding to thermal stimulation and humidity exchange between surfaces and ambient, by means of NDT as IRT.

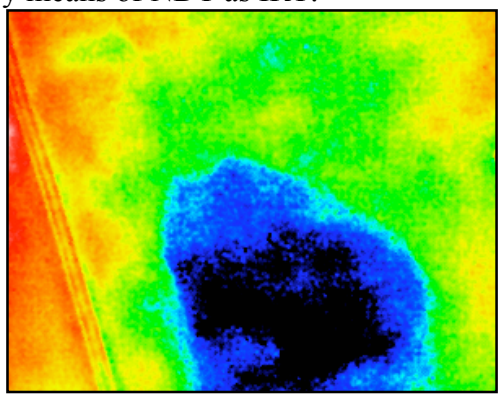

Fig. 1, S.ta Maria in Strada, sec XVII, visual image of the ceiling
Fig. 2, IRThermography of the same zone at transient condition

In several study cases use IRT showed different plasters up (in fig. 2, IRT reveals a large patch of plaster, which was accurately covered by decoration). In some of them [3], physical-chemical analysis of samples allowed to exclude that the composition and density of mortars could be differentiated between the mortars. Further assessment, at a very close distance form the surface, allows authors and restorers to hypothize that the roughness (and therefore the kind of finishing) could be responsible for the different heating distribution on the surface.
The identification of the key factors which determines the observed different absorption curves of heating required to reproduce the test in the laboratory. 24 bricks supported 12 different plasters, which were spread using four different tools (spatula, trowel, wooden float, sponge; about 3 mm thickness). Among the samples, a mortar ($CaCO_3$, rich lime and sand) resulted differently responding to thermal stimulation, according to the different finishing. In a further step of the research, the researchers produced 72 new samples, with controlled ingredients and the same proportions (including the water) and geometry, the mortar at whole thickness (6 mm), using the almost the same tools for finishing (a sponge float substituted the wooden one).
Several thermographic sequences, recaptured at a rate of 10 and 60 seconds, served to obtain the heating curve of the surfaces. The final thermal gradient is some degrees, depending on the time of heating. Authors evaluated the affection of surface roughness on the heat absorption by irradiation and also by convection, using a climatic room (T_{air}=35°C, RH= 50%). The thermographic sequences of the heating allowed to obtain the heating curve of small areas for each sample (fig. 3).
The trend is similar in each area, and it is possible to group together sponge/trowel and spatula/float. The first group' trend shows a higher heating from the beginning (360 seconds), probably due to a higher

absorption of infrared irradiation. Particularly, the higher increase of temperature is measured on the sponge finishing (1°C higher than the trowel finishing). The videomicroscopy (magnifying 100 x) confirmed the hypothesis: operators shot four images for each samples, choosing zone with similar texture and avoiding any defect of the surface. Moreover, a further image processing of these images allowed to calculate the area of the projection of the exposed sand grains over the plan which intersect the microscope focus, and which is parallel to the analysed surface. Because of the plan is kept equal for each image, the average area calculated for each image can be comparable. In this way, authors connected the roughness of the surface to a quantitative parameter, EGAA (Exposed Grains Average Area). The highest values of EGAA correspond to the roughest surface. The prominent presence of sand grains, determines the optical properties of the surface, and consequently the properties of irradiation balance of the surface, which directly affects the thermal behaviour of the sample surface.

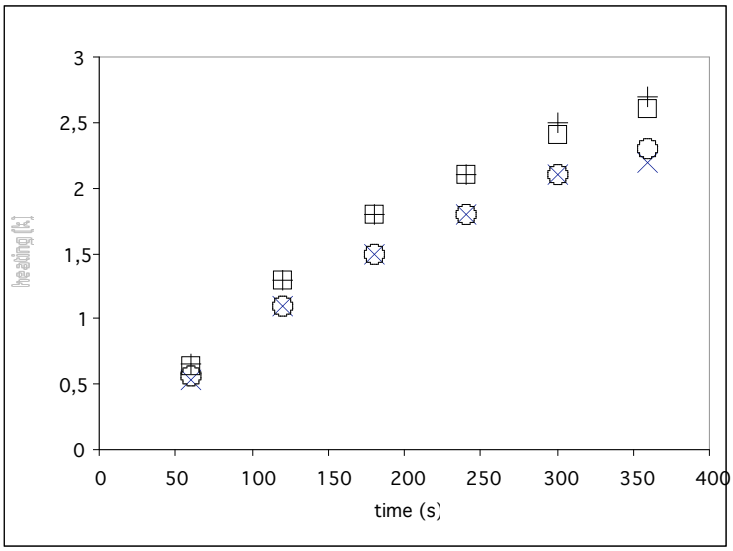

Fig. 3, graph of the increase of temperature vs. time on brick and mortar samples (heating by radiation)
○ spatula, + sponge, X wooden float, □ trowel finishing

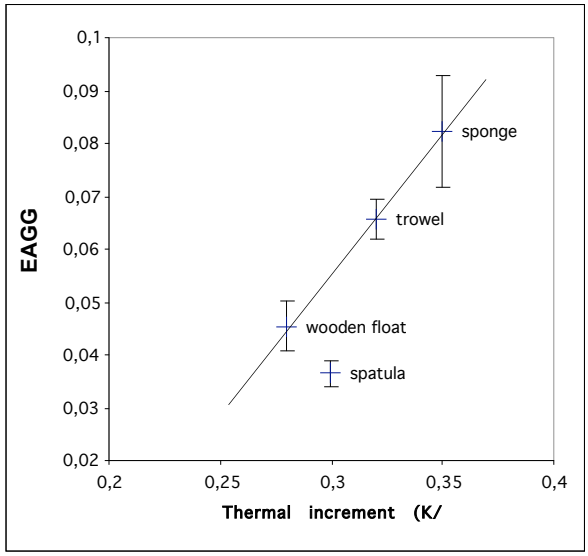

Fig. 4, graph of the EGAA factor vs. the increment of temperature during the heating: it shows a direct correlation between the kind of finishing and the temperature, but only the spatula

Verification of the absorbance properties in the visible-NIR spectral band (400-1100 nm) and emissivity at thermal IR (8-14 micron) confirmed the presented hypothesis. As a conclusion, the comparison between thermal behaviour and localization of mortar grains allows to evaluate how much the finishing techniques affect the thermal characteristics.

Bibliography

[1] S. Della Torre, E. Rosina, S. D'Ascola, S. Caglio, *Restauri a rischio, microclima e differenze superficiali dei materiali in opera*, 11 Conferenza Nazionale PND, Milano 2005

[2] S. Della Torre, E. Rosina, M. Catalano, C. Faliva, G. Suardi, A Sansonetti, L. Toniolo, *Early Detection and Monitoring Procedures by Means of Multispectral Image Analysis*, Art 2005, Lecce 2005

[3] S. Della Torre, E. Rosina, V. Pracchi, G. Suardi, N. Ludwig, V. Redaelli, A. Sansonetti, R. Negrotti, *Le indagini multispettrali per il riconoscimento telemetrico degli interventi di restauro nelle pitture murali*, in atti del XXI Convegno Internazionale, Bressanone 2005

Feasibility of different thermal analysis of FRP – reinforced concrete

U. Galietti[(1)]; P. Corvaglia[(2)]; A. Largo[(2)]; S. Nenna[(2)]; L. Spagnolo[(1)]

[1] Dipartimento Ingegneria Meccanica e Gestionale – Politecnico di Bari;
viale Japigia 182; 70126 Bari – Italy; E. mail: galietti@poliba.it; spagnolo@poliba.it
[2] Department of Materials and Structures Engineering – CETMA Consortium;
s.s. Appia km 706+030, 72100 Brindisi – Italy; e-mail: paolo.corvaglia@cetma.it; alessandro.largo@cetma.it

There are a number of situations where it may become necessary to increase the load – carrying capacity of a structure in service. These include change of loading or use, and the cases of structures that have been damaged as a result of impact or material deterioration. In the past, the increase in strength has been usually provided by casting additional reinforced concrete, while more recently, by attaching steel plates to the tension zone surface by use of adhesive and bolts. These conventional rehabilitating techniques provide promising strengthening solutions in civil concrete applications; unfortunately, the weight penalty and the corrosion of the steel material may eventually increase the overall maintenance cost.
Thereby, this requires the development and application of new materials and technologies, which can extend the service life of the structures, reducing the time and cost maintenance and improving durability.
Thus, the use of FRP (Fiber Reinforced Plastic) materials such as glass or carbon fibers in polymer matrices is becoming increasingly important to extend the service life of civil structures in the last few years.
However, in order to assure an effective FRP reinforcement, perfect adhesion between FRP and concrete must be obtained; for this reason, it is essential to use Non-Destructive Testing (NDT) to assess the quality of the bonding. In the "ICC Evaluation Service" standards, bonding defects are allowed if less than 13 [cm^2] for a maximum of 10 delaminations per about 1 [m^2].
Among the NDT, InfraRed Thermography (IRT) is becoming increasingly attractive, allowing the analysis of the effects induced by defects on the thermal behaviour of the material. It is then possible to spot defects that cause alterations of the temperature distribution of the surface stimulated by a heat source.
The aim of this work is to develop a reliable and precise non destructive testing technique based on infrared thermography and on post processing of the thermograms by means of Neural Networks. In particular, two experimental procedures were implemented: the first consists mainly in the "impulsive" heating of the structure and in the analysis of the superficial thermal response by means of a thermocamera during the cooling phase; the second is based on the use of the "Lock – in" method . The procedures require a detailed set-up, in order to assess their feasibility. In this work the study case of a concrete structure strengthened by bonded FRP, with imposed well-known defects is presented.
The results obtained by means of infrared thermography, with the two described procedures, were compared in order to make a comparative analysis between them. Moreover, the thermographic results were also compared with results obtained by ultrasonic testing.

Key words: Thermography, FRP, Concrete, Neural networks, Bonding

EXPERIMENTAL SET UP

The reinforcement of a concrete structure, by means of FRP (Carbon and Glass), was investigated. Some samples were accurately prepared, imposing bonding defects of well-known dimensions

between different layers of composite or between composite and concrete. In particular 16 defects were inserted between the underlying concrete structure and the CFRP in a single sample. Two types of defects with different dimensions were imposed:

- delamination, by means of the interposition of two bonded Teflon foils ;
- lack of bonding of the FRP, by means of a simple Teflon foil.

The surface of the sample was analysed by thermocamera after an "impulsive heating" and with the "Lock – in" method.
The same sample was analysed by means of ultrasonic C-Scan inspection in pulse echo mode with a water-jet as coupling fluid.

ANALYTICAL RESULTS

Thermographic data were processed with Almond's half maximum contrast method. Almond's method is based on the evaluation of the thermal contrast of the thermogram, defined as the difference between the temperature in the pixels under investigation and the temperature of a sound region, in which there are no defects. A generic pixel is then considered part of the damaged zone if it is characterised by a contrast equal or greater than the half of the maximum contrast relative to the damaged zone.
A particular matlab routine was implemented in order to apply Almond's procedure to the whole thermogram. In Fig.1 an example of a thermogram of the reinforced sample is presented.

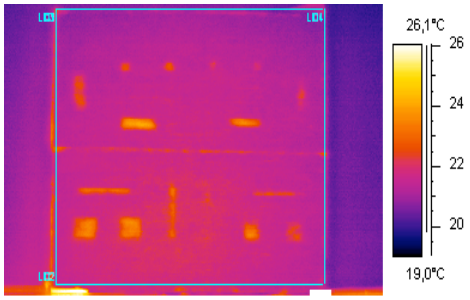

Fig.1. Thermogram of the CFRP sample with imposed defects

References

ICBO; "Acceptance criteria for inspection and verification of concrete and reinforced and unreinforced mansory strengthening using fiber-reinforced polymer (FRP) composite systems"; ICBO Evaluation Service, INC, 05/2001.
Peters S.T., Handbook of Composites, Chapman & Hall, London (UK), 1998.
X.P.V. Maldague; "Theory and Practice of Infrared Technology for Nondestructive Testing"; A Wiley-Interscience Publication, John Wiley & Sons Inc.; N.Y. 2001.
D.P. Almond, R. Hamzah, P. Delpech, Peng Wen, M.H. Beheshty, M. B. Saintey; "Experimental investigations of defect sizing by transient thermography"; QIRT 96-Eurotherm Series 50 ETS ed., Pisa 1997, pp.233-238.
Muscio, S. Marinetti, P. G. Bison, A. Ciliberto, G. Cavacini, E. Grinzato; "Modelling of Thermal Non-Destructive Evaluation Techniques for Composite Materials and the European Aerospace Industry"; AITA-Advanced Infrared Technology and Applications, Venezia, 1999, pp.143-153.
J.G. Sun; "Analysis of quantitative measurement of defects by pulsed thermal imaging"; Review of QNDE, D.O. Thompson and D.E. Chimenti Eds., vol. 21, 2002, pp. 572-576.
M. B. Saintey, D. P. Almond, "An artificial neural network interpreter for transient thermography image data"; NDT&E International, vol. 30, N° 5, 1997, pp. 291-295.

Advances of Quantitative IR-Thermal Imaging in Medical Diagnostics

A. Z. Nowakowski
Department of Biomedical Engineering, Gdansk University of Technology, Gdansk, Poland

Abstract—**This review will show the state of the art in thermal IR-imaging from the point of view of medical diagnostics. Advantages and limitations of IR thermal imaging, including tomography procedures, based on thermal properties of living tissues, will be presented. Properties of this modality will be discussed mainly from the point of view of skin burn evaluation.**

Keywords— **thermal tissue properties, thermal tomography, medical diagnostics**

I. Introduction

Living organism may be regarded as a source of different signals, which are interpreted from the point of view of medical diagnostics. IR thermal imaging is known as a very important modality in determination of local sources of hot or cold spots (increased or decreased metabolism), e.g. showing places of cancer development or deficit of blood flow.

The goal of this presentation is to discuss the diagnostic role of thermal tissue properties. The main questions concern such problems as limitations in investigation of living organs, diagnostic meaning of measurements, etc. Advances in construction of measurement systems will be shortly presented.

The discussion is illustrated by solutions and measurements performed at the Department of Biomedical Engineering Gdansk University of Technology (TUG) in cooperation with several clinics of Medical University of Gdansk (MUG) and the Department of Animal Physiology of Gdansk University (UG).

II. Infrared thermal imaging

Infrared thermal imaging is present in medical diagnostics for almost 50 years [1,2,3,4,5]. Unfortunately lack in preserving standard "golden rules" in diagnostic procedures evoked a great critical dispute of the value of thermography in medical diagnostics [6] and as a result, this modality was almost forgotten. This was a mistake as IR thermal imaging has a lot of advantages. It is non-contact, therefore aseptic and safe, gives no interaction with tissues, it is fast and easy to use; storage of data is simple as well as presentation of surface temperature is very attractive. Recently one may observe a great progress of this technology, what makes it extremely attractive again. Advances of thermography in medicine are presented in several books, as e.g. [7]. Broad bibliography of classical thermography in medicine is available in Glamorgan University [8]. At present in USA several institutions are strongly involved in promotion of new ideas in IR thermal imaging, e.g. [9,10,11]. In Europe very active is the group of institutions acting in the field of non-destructive testing - Quantitative Infrared Thermography QIRT [12,13]; in medicine new projects concern standardization of procedures [14,15,16]. Also in Poland some publications are dealing with IR imaging in medicine [17,18,19].

In most of those publications classical IR thermal imaging methods are described. Distribution of the body surface temperature, usually as a steady state, frequently based on observation of symmetries, is holding diagnostic information. Living organism itself is generating heat; therefore distribution of surface temperature may be giving a lot of information, which has important diagnostic value. Advances in IR instrumentation, especially increased thermal resolution and implementation of digital signal processing, also introduction of new matrices of FPA detectors (*Focal Plane Array*) are pushing this technology and made it is easy accessible. In medical applications cameras of the speed of 30 frames/second, thermal resolution at the level of 0.1^{o}C and pixel resolution 240x320, with handy room temperature operation, are fully acceptable in practice. Also prices of such cameras are falling down, what makes this equipment to be accessible even in private practice. In research much better cameras of thermal resolution even at the level of 0.01 ^{o}C and with high time & spatial resolution (respectively more than 1000 frames/second and 1 million pixels) are already available. Adding advances in computer technology, data processing and visualization one may claim this is a real technological revolution in IR thermal imaging.

Such trends as use of digital analysis of enhanced resolution thermal images [20], advanced model based analysis of thermal objects [21] or of characteristic thermal signatures [9,22] are representing the modern approaches. Important are projects concerning accessible from the global net databases containing reference data for normal, healthy and diagnosed cases [15,23]. Important are methods using advanced quantitative statistic analysis of images [24,25], or some other advanced mathematic tools, as e.g. neural networks [26], thermal texture maps [27] or extraction of functional features of thermal images [28]. Another interesting proposal concerns very fast registration of thermal images and Fourier analysis, allowing presentation of very subtle temperature changes [29]. Unfortunately, here a high performance camera is necessary.

Probably first active dynamic thermography experiments for medical diagnostics have been proposed in VUB [30]. The microwave energy was applied to enhance

thermal effects of breast cancer. At this time Vavilov [31] introduced for the first time the term *Thermal Tomography*.

Thermal Tomography allows identification of geometry of a tested object based on thermal properties of tissues. Generally, thermal excitation applied to a tested object is responsible for temperature transients on its surface. Results of measurements of surface transient processes are compared with results of simulations of an equivalent model of the object. Solving the inverse problem the internal structure of the object of known thermal properties or thermal properties for defined object geometry may be calculated. We are intensively involved in development of active dynamic thermography **(ADT)** as well as thermal tomography **(TT)** in such medical applications as: classification of skin burns, inspection of cardiosurgical interventions, detection of the breast cancer and some other.

The main difference comparing ADT and TT to classical thermal imaging is in investigation of thermal properties of tissues, not just simple distribution of temperature. In both techniques external excitation is applied and thermal transients are registered. Usually, based on an equivalent thermal model, a tested structure is determined or some synthetic parameters, strongly correlated to this structure are visualized. We proved the value of such measurements in *in vivo* animal experiments and in clinics [32 – 45], where basic limitations of both methods have been analyzed and defined. The conclusions show different meaning of both modalities and their special role as monitoring techniques.

We asked the following questions:

- What is the practical value of ADT and TT?
- Could ADT and TT be used for reliable intra-operation monitoring in cardiosurgery interventions, in skin burn evaluation, in mammography, etc.?

Concluding, even thermal properties of different tissues may be not strong the heat transfer by blood is responsible for getting strong contrast in thermal images. ADT and TT are limited to rather thin layers, as the skin is, where evaluation of burns was proved to be efficient. Both modalities may be used for evaluation of tissues of affected vascularisation. Method's surface resolution depends on optical system and may be very high. ADT and TT are non-contact, assuring aseptic applications. Still, limited knowledge of emissivity is influencing accuracy of data acquisition.

Depending on time I may also compare TT and EIT (electrical impedance tomography) - Is there any correlation between thermal and electrical properties of biological tissues?

The main element of comparison is the relation of thermal and electrical parameters, which are shown in Tab.1. The values are of approximate character, as a big diversity of different parameter values for a living tissue exists. It is clearly seen that thermal properties do not differ importantly; therefore it would be difficult to use TT for discrimination of deep internal body structure. Much better situation is in electrical domain, where properties of different tissues are better differentiated. Additional factor limiting TT is slow speed of thermal transients, what always should be taken into account.

Table 1. *Thermal and electrical parameters of different tissues (approximate values taken from measurements and literature)*

Parameter / Tissue	Density Δ [kg/m^3]	Thermal conductivity k [W/{(m)(K)}]	Thermal effusivity β [J/(m^{2}Ks$^{1/2}$)]	Electrical conductivity σ [S/cm]
Heart muscle	1060	0.53	1440	$2.5\ 10^{-3}$
Skeletal muscle transverse	1044	0.49	1370	$0{,}62\ 10^{-3}$
Skeletal muscle longitudinal	1045	0.49	1370	$(3.35 - 7.4)\ 10^{-3}$
Brain	1034	0.54	1440	$1.7\ 10^{-3}$
Kidney	1050	0.51	1404	$2.7\ 10^{-3}$
Liver	1060	0.53	1280	$(1.2 - 2.7)\ 10^{-3}$
Lungs	1050	0.39	1100	$(0.4 - 0.94)\ 10^{-3}$
Fat	850	0.22	725	$0.335\ 10^{-3}$
Blood	1060	0.49	1370	$6.7\ 10^{-3}$

Tomography is giving in each case data of great importance in terms of the evaluation of surgical procedures as well as visualization of actual state of the tested heart. Electroimpedance measurements allow direct inspection of the state of the heart. The main disadvantage is that only contact measurements are possible, limiting the spatial resolution of the method to dimensions dependent on the electrode size and position. Only surfaces accessible for measurements may be inspected. Electroimpedance measurements are giving local information of the state of inspected tissue while IR imaging shows full structure. Both modalities allow easy discrimination of necrosis as well as of increased vascularisation. In both cases quantitative data describe objective state of the tissue under investigation, allowing application of advanced digital data processing important for proper diagnosis. Electrical measurements are cheaper although direct contact, e.g. to the heart tissue, is necessary causing a lot of aseptic problems.

ACKNOWLEDGMENT

The author thanks the co-workers and Ph.D. students from TUG, MUG and UG, who participated in the presented research. Most of the names are listed in the attached bibliography as co-authors of common publications.

REFERENCES

[1] Williams K. L., Williams F. L., Handlay R. S., Infrared radiation thermometry in clinical practice, *Lancet*, 1960, 958.

[2] Williams K. L., Williams F. L., Handlay R. S., Infrared thermometry in the diagnosis of breast disease, *Lancet*, 1961, 1378 - 1381.

[3] Lawson R. N., Chughtai M. S., Breast cancer and body temperature, *Can. Med. Ass. J.*, v. 82, no 2, 1963, 68.

[4] Barnes R. B., Gerson-Cohen J., Thermography of the human body, *Science*, v. 140, 1963, 870-877.

[5] Gershen-Cohen J., Haberman J. Brueschke E. E., Medical thermography: A summary of current status, *Radiol. Clin. North Am.*, 1965, 3, 403-431.

[6] Report of the Working Group to Review the National Cancer Institute Breast Cancer Detection Demonstration Projects, *Journal of National Cancer Institute*, v. 62, 1979, 641-709.

[7] Nowakowski A., Kaczmarek M., Hryciuk M., Ruminski J., *Advances in thermography – medical applications (in Polish),* Wyd. Gdanskie, Gdansk, 2001.

[8] Jones B. Ed. CD – Acta Thermogrphica & Thermology Archive of Papers, University of Glamorgan, 2000;

[9] Paul J.L., Lupo J.C., Application of infrared imaging and automatic target recognition image processing for early detection of breast cancer, *IEEE Eng. in Medicine and Biology*, v. 21, 6, 2002, 34 – 35.

[10] Qi H., Diakides N., Thermal infrared imaging in early breast cancer detection – a survey of recent research, *Proc. IEEE EMBC*, Cancun, 2003, 1109 – 1112.

[11] Kayserlink J., Ahlgren P., Yassa M., Belliveau N., Overview of functional infrared imaging as part of a multi-imaging strategy for breast cancer detection and therapeutic monitoring, *Proc. EMBS-BMES Conf*., Houston, 2002, 231.

[12] *Proc. QIRT*, Chatenay-Malabary-1992, Naples-94, Stuttgart-1996, Lodz-1998, Venice-2000, Reims-2002, Brussels-2004.

[13] *QIRT Journal*, published since April 2004.

[14] Ring E.F.J., Standardisation of Thermal Imaging Technique, *Thermology Oesterrich*, 3, 1993, 11 – 13.

[15] http://www.comp.glam.ac.uk/pages/staff/pplassma/MedImaging/Projects/IR/Atlas/index.html

[16] Ammer K., Ring E.F.J., Plassmann P., Jones B.F., Rationale for standard capture and analysis of infrared images, *IFMBE Proc. 2-nd European Medical and Biological Engineering Conf.*, Vienna, 2002, 1608 – 1609.

[17] Jung A., _uber J., Ring F., *A casebook of infrared imaging in clinical medicine*, Medpress, Warsaw, 2003.

[18] Nowakowski A., Wrobel Z., IR thermography in medical diagnostics, *in Polish*, 475 – 614; Nowakowski A., Kaczmarek M., Hryciuk M., Thermal Tomography, 615 – 696, in Chmielewski L., Kulikowski J.L., Nowakowski A., *Obrazowanie Biomedyczne*, *Biocybernetyka i In_ynieria Biomedyczna 2000*, v. 8, EXIT, Warszawa, 2003.

[19] *Thermovision Measurements in Practice* (in Polish - *Pomiary Termowizyjne w Praktyce*, Praca zbiorowa), Agenda Wydawnicza PAKu, Warszawa, 2004.

[20] Arena F., Barone C., DiCicco T., Use of digital infrared imaging in enhanced breast cancer detection and monitoring of the clinical response to treatment, *Proc. IEEE EMBEC Conf*., Cancun, 2003, 1129 – 1132.

[21] Nowakowski A., Kaczmarek M., Ruminski J., Hryciuk M., Renkielska A., Grudzinski J., Siebert J., Jagielak D., Rogowski J., Roszak K., Stojek W., Medical applications of model based dynamic thermography, *Proc. SPIE*, v. 4360, 2001, 492 – 503.

[22] Irvine J.M., Applicability of automated target recognition technique to early screening for breast cancer, *IEEE Eng. in Medicine and Biology*, v. 21, 6, 36 – 40, 2002.

[23] Murawski P., Jung A., _uber J., Kalicki B., The project of an open and extendable database for thermal images archiving, *IFMBE Proc. 2-nd European Medical and Biological Engineering Conf*., Vienna, 2002, 1618 – 1619.

[24] Jones B., Plassman P., Computational approaches to image processing for improved interpretation and analysis, *IEEE Eng. in Medicine and Biology*, v. 21, 6, 2002, 41 - 48.

[25] Jakubowska T., Wiecek B., Wysocki M., Drews-Peszynski C., Thermal signatures for breast cancer screening comparative study, *Proc. IEEE EMBEC*, Cancun, 2003, 1117–20.

[26] Szu H., Kopriva I., Hoekstra P., Diakides N., Diakides M., Buss J., Lupo J., Early Tumor Detection by Multiple Infrared Unsupervised Neural Nets fusion, *Proc. IEEE EMBC*, Cancun, 2003, 1133 – 1136.

[27] Qi H., Kuruganti P.T., Liu Z., Early detection of breast cancer using thermal texture maps, *IEEE Int. Symp. On Biomedical Imaging*, Washington DC, 2002, 309 – 312.

[28] Keyserlingk J. R., Ahlgren P. D., Yu E., Belliveau N., Yassa M., Functional Infrared Imaging of the Breast, *IEEE Engineering in Medicine and Biology Magazine*, vol. 19, No 3, 2000, 30-42.

[29] Anbar M., Physiological, clinical and psychological applications of dynamic infrared imaging, *Proc. IEEE EMBC*, Cancun, 2003, 1121 – 1123.

[30] Steenhaut O., Van Denhaute E., Cornelis J., Contrast enhancement in infrared thermography by the application of microwave irradiation applied to tumour detection, *Proc. MECOMBE'86*, 1986, 485-488.

[31] Vavilov V., Shirayev V., Thermal Tomograph – *USSR Patent* no. 1.266.308, 1985.

[32] Nowakowski A, Kaczmarek M., Dynamic thermography as a quantitative medical diagnostic tool, *Medical and Biological Eng. and Computing incorp. Cellular Eng.*, 37, suppl.1, p.1, 1999, 244 – 245.

[33] Kaczmarek M., Ruminski J., Nowakowski A., Measurement of thermal properties of biological tissues – Comparision of Different Thermal NDT Techniques, *Proc. Advanced Infrared Technology and Application*, Venice 1999, 2001, 322-329.

[34] Kaczmarek M., Nowakowski A., Renkielska A., Rating Burn Wounds by Dynamic Thermography, *Quantitative InfraRed Thermography 5*, 2000, 376 – 381.

[35] Nowakowski A., Kaczmarek M., Debicki P., Active thermography with Microwave Excitation, *Quantitative InfraRed Thermography 5*, 2000, 387 – 392.

[36] Ruminski J., Nowakowski A., Kaczmarek M., Hryciuk M., Model-based parametric images in dynamic thermography, *Polish Journal of Medical Physics and Eng*., 6(3), 2000, 159-164.

[37] Ruminski J., Kaczmarek M., Nowakowski A., Medical Active Thermography – A New Image Reconstruction Method, *Lecture Notes in Computer Science*, LNCS 2124, Springer, Berlin-Heidelberg, 2001, 274-181.

[38] Hryciuk M., Nowakowski A., Renkielska A., Multilayer thermal model of healty and burned skin, *Proc. 2nd European Medical and Biological Engineering Conference*, EMBEC´02, v. 3, Pt. 2., Vienna, 2002, 1614-1617.

[39] Nowakowski A., Kaczmarek M., Siebert J., Rogowski J., Jagielak D., Roszak K., Stojek W.,Topolewicz J., Role of Thermographic Inspection in Cardiosurgery, *ibid.,* 1626-1627.

[40] Hryciuk M., Nowakowski A., Evaluation of thermal diffusivity variations in multi-layered structures, *Proc. 6 QIRT*, Zagreb, 2003, 267-274.

[41] Kaczmarek M., Rumunski J., Nowakowski A., Renkielska A., Grudzinski J., Stojek W., In-vivo experiments for evaluation of new diagnostic procedures in medical thermography, *ibid*., 260-266.

[42] Kaczmarek M., Nowakowski A., Analysis of Transient Thermal Processes for Improved Visualization of Breast Cancer Using IR Imaging, *Proc. IEEE EMBC*, Cancun, 2003, 1113-1116.

[43] Nowakowski A, Kaczmarek M., Wtorek J., Siebert J., Jagielak D., Roszak K., Topolewicz J., Thermographic and electrical measurements for cardiac surgery inspection, Proc. of 23rd Annual International Conference IEEE EMBS, CD-ROM, Istanbul, 2001.

[44] Renkielska A., Nowakowski A., Kaczmarek M., Dobke M.K., Grudzinski J., Karmolinski A., Stojek W.. Static thermography revisited – an adjunct method for determining the depth of the burn injury. *Burns* 2005, **31**: 768-775.

[45] Renkielska A., Nowakowski A., Kaczmarek M., Ruminski J., Burn depth evaluation based on IR thermal imaging – a preliminary study", Burns 2006, accepted for publication.

THERMOGRAPHIC ANALYSIS OF PHACOEMULSIFICATION BASED CATARACT SURGERY PROCEDURES (ORAL PRESENTATION)

Andrea Corvi[1], Bernardo Innocenti[1], Rita Mencucci[2]

[1]Dipartimento di Meccanica e Tecnologie Industriali – Università degli Studi di Firenze, via di S. Marta 3, 50139, Firenze, Italy
[2]Dipartimento di Scienze Chirurgiche Oto-Neuro-Oftalmologiche - II Clinica di Oftalmologia – Università degli Studi di Firenze, viale Morgagni 85, 50134, Firenze, Italy

Reprint requests to:
Bernardo Innocenti, Mech. Eng.
Dipartimento di Meccanica e Tecnologie Industriali
Università degli Studi di Firenze
via di Santa Marta 3, 50139 Firenze, ITALY.
Tel: (+39) 348 8605172
Fax: (+39) 055 4796400
e-mail: bernardo.innocenti@unifi.it

In this study a thermographic system has been used with the task of in vivo monitoring the temperature values of the eye during surgical cataract operations based on phacoemulsification technique (fig. 1). This analysis method, as compared to ones used by other researcher based on thermocouple measurements, has the advantage of being totally non-invasive both for the surgeon and the patient. The temperature values are in fact measured by an infrared camera placed at due distance from both patient and surgeon, so that it neither hinders nor limits the surgeon's movements. Thermographic measurement has the further advantage of assessing the temperature of all points in the measurement zone, rather than one point only; nor does it alter the temperature of the eye during measurement, not being in contact with it [1-5].
Thermography has been employed to analyze and compare three phacoemulsification based cataract surgery procedures performed in vivo: the Sovereign phacoemulsification system with traditional technique (called group A, applied to 20 patients), the Sovereign WhiteStar phacoemulsification system with traditional technique (called group B, applied to 15 patients) and the Sovereign WhiteStar phacoemulsification system with bimanual technique (called group C, applied to 15 patients).
In this experimental study the patients (average age 72 years, 32 females, 18 males) presented cataracts of similar hardness (nuclear sclerotic grade 2 or 3) and were free from systemic or ophthalmologic pathologies. Furthermore, they presented no alterations in the lachrymal film nor refraction defects greater than 3 D (sphere) and 1.5 D (cylinder). All of the phacoemulsification procedures were conducted utilizing a clear cornea incision and the 'stop & chop' technique. The procedures were carried out by the same surgeon, in the same operating room, with the same ambient conditions (T=25°C, Humidity=55%). The operating room parameters, for each of the 50 operations analyzed, were within clinical standards.
The thermocamera was set taking account of the temperature and humidity conditions of the operating room and the emissivity parameters of the ocular tissue ($\varepsilon = 0.975$). The results of all of the procedures were successful and no post-operative complications occurred.
The instrumentation utilized in the tests consists of an Agema THW® 880 thermocamera interfaced with a Thermovision® 800 BRUT (Burst Recording Unit) system consisting of a dedicated control computer with hard disk. The 880 LWB thermocamera can measure temperatures ranging from -20 to 1500°C with a sensitivity, expressed in terms of noise equivalent temperature difference, of 0.07 °C at 30°C.
Thermographic analysis has been used to monitor the temperature values of the ocular surface throughout the entire procedure (fig. 2). In particular, temperature values were monitored in the area in which the phaco probe was inserted into the eye. Since the aim of this study is that of evaluated the highest temperature reached during a surgical procedure, the maximum temperature values in an area of interest were monitored. The size of this area was identified through a square made up of sixteen pixels (about 3 mm per side), positioned in the thermographic image, centered on the phaco tip and integral with it throughout the procedure. The decision to utilize a square of these dimensions was made in the pre-test stage, in which it was observed that such a square is always able to contain and follow the phaco tip during the surgical procedure. In this way the measured values correspond to the temperature of the phaco probe in contact with the eye, and thus also to the temperature of the portion of the eye in contact with the phaco probe.
During the course of the operation the temperature values were monitored only in the stages in which ultrasonic emissions were used, without taking into consideration the stage of filling the anterior chamber with the viscoelastic gel, the stage of removing the anterior capsule of the crystalline lens or that of inserting the intraocular lens.
The temperature values in the area where the phaco probe was inserted in the eye were measured, and the quantities of heat transmitted to the eye in the different procedures were assessed through suitable indices. In this study the highest temperature measured for each procedure during the surgical operation was: 44.9°C for the Sovereign

phacoemulsification system with traditional technique, 41°C for the Sovereign WhiteStar phacoemulsification system with traditional technique and 39.3°C for the Sovereign WhiteStar phacoemulsification system with bimanual technique, which is also the surgical procedure having the lowest thermal impact on the eye, i.e., the one in which the temperature peaks are lowest in intensity and the least amount of heat is transmitted to the eye. Thermography, used in this study as a temperature monitoring instrument, has allowed analysis to be effected through a useful and advantageous methodology, totally non-invasive as regards both surgeon and patient, and has been applied in vivo without requiring any change in the surgical procedure.

All of the analyzed procedures have had positive results on the patients and no corneal burns have occurred. This is justifiable because in the literature studies have been reported which show how burns in the ocular tissue have occurred at the ocular surface temperature of 51.5°C while in this study the highest temperature reached was 44.9°C [6].

Thermography has thus shown itself to be an effective tool that can be routinely applied in the operating room as a monitoring instrument. Moreover, it has the further advantage of being a totally non-invasive methodology for both patient and surgeon. In future it can thus be a useful means of documenting, during surgical procedures, the temperature and the heat for each operation, as is already routinely done with the optic telecamera.

In this study thermography has been employed to compare three types of procedure utilizing the same surgical technique. In future it would be interesting to use thermography for comparing different surgical techniques in order to determine which of them has the least thermal impact on the eye, so as to reduce any possible surgical complications (e.g., corneal burns) caused by the excessive release of heat which phacoemulsification can at times produce in eyes, provoking damage that is in most cases irreparable.

Keywords: biomedical application, in vivo measurement, cataract surgery.

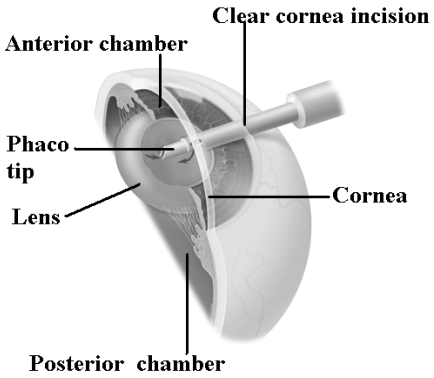

Fig. 1: Position of the phaco tip during a phacoemulsification cataract surgery

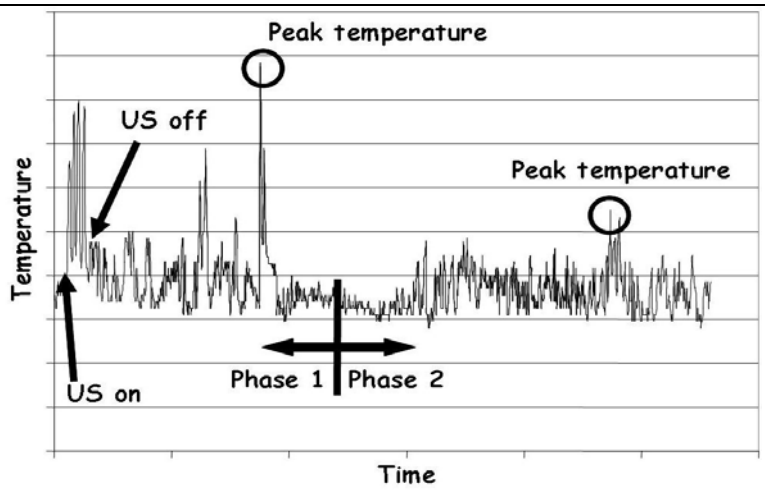

Fig.2: Generic behavior of the temperature values monitored during a cataract operation. The most significant points are localized on the graph. Phase 1 and Phase 2 represents the principal phases of the procedures i.e. the lens fracture (Phase 1) and the debris aspiration (Phase 2)

References

1. Soscia, W., Howard, J.G., Olson, R.J., 2002. Bimanual phacoemulsification through 2 stab incisions, a wound temperature study. J. Cataract Refract Surg 28, 1039-1043.
2. Donnenfeld, E.D., Olson, R.J., Solomon, R., Finger, P.T., Biser, S.A., Perry, H.D., Doshi, S., 2003. Efficacy and wound temperature gradient of WhiteStar phacoemulsification through a 1.2 mm incision. J Cataract Refract Surg 29, 1097-1100.
3. Bissen-Miyajima, H., Shimmura, S., Tsubota, K., 1999. Thermal effect on corneal incisions with different phacoemulsification ultrasonic tips. J Cataract Refract Surg 25, 60-64.
4. Ernest, P., Rhem, M., McDermott, M., Lavery, K., Sensoli, A., 2001. Phacoemulsification conditions resulting in thermal injury. J Cataract Refract Surg 27, 1829-1839.
5. Tsuneoka, H., Shiba, T., Takahashi, Y., 2001. Feasibility of ultrasound cataract surgery with a 1.4 mm incision. J Cataract Refract Surg 27, 934-940.
6. Mackool, R.J., 2003. Incision Burns. J Cataract Refract Surg 29, 233-236.

Advancements in biomedical applications of infrared imaging

Introduction

Infrared imaging permits to map the surface thermal distribution of the human body. A large number of studies has been so far established to assess the contribution that such information may provide to the clinicians. Cutaneous temperature distribution depends on complex relationships defining the heat exchange processes between cutaneous tissue, inner tissue, local vasculature, and metabolic activity. All of these processes are mediated and regulated by the sympathetic and parasympathetic activity to keep the thermal homeostasis. At a local level, diseases and disorders can affect the heat balance or exchange processes resulting in modification of the cutaneous temperature and of its functional with respect to healthy conditions. Therefore, the characteristic parameters modeling the spontaneous activity of the cutaneous thermoregulatory system can be used as quantitative diagnostic parameters. The functional Infrared Imaging (fIRI)– also named Infrared Functional Imaging (IRFI) – is the study for diagnostic purposes, based on the modeling of the bio-heat exchange processes, of the functional properties and alterations of the human thermoregulatory system. In this paper, we will review some of the most important recent clinical applications of the functional infrared imaging.

Quantifying the Relevance and Stage of Disease with the τ Image Technique.

Infrared imaging can provide diagnostic information according different possible approaches. The approach generally followed consists of the detection of significant differences between the cutaneous thermal distributions of the two hemisoma or in the pattern recognition of specific features with respect to average healthy population [1]. More valuable and quantitative information can be obtained from the study of the cutaneous temperature dynamics in the unsteady state, where the processes involved and controlled by the thermoregulatory system can be modeled and described through their characteristic parameters [2-7]. The presence of diseases interfering with the cutaneous thermoregulatory system can be then inferred by the analysis of its functional alterations [8-18]. Merla et al. [7, 17, 20, and 21] proposed a new imaging technique, based on this approach, for the clinical study of a variety of diseases. Starting from a general energy balance equation, they have demonstrated that the recovery time from any kind of thermal stress for a given region of interest depends from the region thermal parameters.

The proposed model accept an exponential solution and suggests to use the time constant τ as a characterizing parameter for the description of the recovery process after any kind of controlled thermal stress, with τ mainly determined by the local blood flow and thermal capacity of the tissue.To pictorially describe the effect of the given disease, an image reporting pixel to pixel the τ recovery time can be used to characterize that disease [7, 17, 20, and 21].

The τ image technique has been first proposed as complementary diagnostic tool for the diagnosis of muscular lesions, Raynaud's phenomenon and Deep Vein Thrombosis [7, 17 20, 21].

Raynaud's Phenomenon and Scleroderma

Raynaud's phenomenon (RP) is defined as a painful vasoconstriction - that may follow cold or emotional stress - of small arteries and arterioles of extremities, like fingers and toes. RP can be primary (PRP) or secondary (SSc) to scleroderma. None of the physiological measurement techniques currently in use, but infrared imaging, are completely satisfactory in focusing primary or secondary RP [3]. Thermography protocols [3-5, 24-28] usually include cold patch testing to evaluate the capability of the patient hands to re-warm. The pattern of the re-warming curves is usually used to depict the underlying structural diseases. Merla et al. [14, 16] proposed study the natural response of the fingertips to exposure to a cold environment through a simple bioheat model to compute the amount of heat produced by the local thermoregulatory system and stored in the fingertip as a possible diagnostic parameter. Such a parameter has been used in [14, 16] to discriminate and classify PRP, SSc and healthy subjects on a set of 40 (20 PRP, 20 SSc) and 18 healthy volunteers.

The sensitivity of the method in order to distinguish patients from normal is 100%. The specificity in distinguishing SSc from PRP is 95%.

Diagnosis of Varicocele and Follow Up of the Treatment

Varicocele is a widely spread male disease consisting into a dilatation of the pampiniform venous plexus and of the internal spermatic vein. Consequences of such a dilatation are an increase of the scrotal temperature and a possible impairment of the potential fertility [36, 37]. fIRI has been used to determine whether altered scrotal thermoregulation is related to subclinical varicocele [15]. In a study conducted in 2001, Merla and Romani enrolled 60 asymptomatic volunteers that underwent to clinical examination, echo color Doppler imaging (the gold standard) and fIRI. The latter technique accurately detected 22 no symptomatic varicocele. The control of the scrotum temperature should improve after varicocelectomy as a complementary effect of the reduction of the blood reflux. Moreover, follow-up of the changes in scrotum thermoregulation after varicocelectomy may provide early indications on possible relapses of the disease. To answer the above questions, Merla et al. [9] used fIRI to study changes in the scrotum thermoregulation of 20 patients that were judged eligible for varicocelectomy on the basis of the combined results of the clinical examination, Echo color Doppler imaging, and spermiogram. fIRI documented the changes in the thermoregulatory control of the scrotum after the treatment and proved that the surgical treatment of the varicocele induces modification in the thermoregulatory properties of the scrotum, reducing the basal temperature of the affected testicle and pampiniform plexus, and slowing down its recovery time after thermal stress.

Conclusions

fIRI is a biomedical imaging technique that relies on high resolution infrared imaging and on the modeling of the heat exchange and control processes at the cutaneous layer. fIRI is aimed to provide further information about the studied disease to the physicians, like explanation of the possible physics reasons of some thermal behaviors and their relationships with the physiology of the involved processes. One of the great advantages of fIR imaging is the fact that is not invasive and it is a touchless imaging technique. fIR is not a static imaging investigation technique. Therefore, data for fIR imaging need to be processed adequately for movement. Adequate bio heat modeling is also required. The medical fields for possible applications of fIR imaging are numerous, ranging from those described into this chapter, to psychometrics, cutaneous blood flow modeling, peripheral nervous system activity, and some angiopathies. The applications described in this paper show that fIR imaging provides highly effective diagnostic parameters. The method is highly sensitive, but also highly specific into discriminating different conditions of the same disease.

References

Aweruch, M.S., Thermography: its current diagnostic status in muscular-skeletal medicine, Med. J. Aust, 154, 441, 1991.

Prescott, et at., Sequential dermal microvascular and perivascualr changes in the development of scleroderma, *J. Pathol.*, 166, 255, 1992.

Herrick, A.L. and Clark, S., Quantifying digital vascular disease in patients with primary Raynaud's phenomenon and systemic sclerosis, *Ann. Rheum. Dis.*, 57,70, 1998.

Darton, K. and Black, C.M., Pyroelectric vidicon thermography and cold challenge quantify the severity of Raynaud's phenomenon, *Br. J. Rheumatol.*, 30,190,1991.

Javanetti, S., et al., Thermography and nailfold capillaroscopy as noninvasive measures of circulation in children with Raynaud's phenomenon, *J. Rheumatol.*, 25, 997,1998.

Merla, A., et al., Dynamic digital telethermography: A novel approach to the diagnosis of varicocele, *Med. Biolog. Eng. Comp.*, 37,1080, 1999.

Merla, A., et al., Correlation of telethermographic and ultrasonographic reports in the therapeutic monitoring of second-class muscular lesions treated by hyperthermia, *Med. Biolog. Eng. Comp.*, 37, 942, 1999.

Merla, A, Biomedical applications of functional infrared imaging, presented at the 21st Annual Meeting of Houston Society of Engineering in Medicine and Biology, Houston, TX, Feb 12-13, 2004.Merla, A., et al., Assessment of the effects of the varicocelectomy on the thermoregulatory control of the scrotum, Fertility and Sterility, 81,471, 2004.Merla, A., et al., Recording of the Sympathetic Thermal Response by means of Infrared Functional Imaging, *in Proc. of the 25th Annual International Conference of the IEEE Engineering in Medicine and Biology Society*, Cancun, Mexico, Sept 17-21, 2003.

Merla, A., et al., Infrared Functional Imaging applied to the study of emotional reactions: preliminary results, *in Proc. of the 4th International Non Invasive Functional Source Imaging*, Chieti, Italy, Sept, 9-13, 2003.

Merla, A. and Romani, G.L., Cutaneous blood flow rate mapping through functional infrared imaging, *in Proc. of the World Congress of Medical Physics WC2003*, Sidney, Aug, 24-29, 2003.

Merla, A., Cianflone, F., and Romani, G.L., Cutaneous blood flow rate estimation through functional infrared imaging analysis, *in Proc. of the 5th International Federation of Automatic Control Symposium on Modelling and Control in Biomedical Systems*, Melbourne, Aug, 19-23, 2003.

Merla, A., et al., Raynaud's Phenomenon: infrared functional imaging applied to diagnosis and drugs effects, *Int. J. Immun. Pharm.*, 15, 41, 2002.

Merla, A., et al., Use of Infrared Functional Imaging to detect impaired thermoregulatory control in men with asymptomatic varicocele, *Fertility and Sterility*, 78, 199, 2002.

Merla, A., et al., Infrared Functional Imaging Applied to Raynaud's Phenomenon, *IEEE Eng. Med. Biol. Mag.*, 21, 73, 2002.

Merla, A., et al., Quantifying the Relevance and Stage of Disease with the Tau image Technique. *IEEE Eng. Med. Biol. Mag.*, 21, 86, 2002

Merla, A., et al., Infrared Functional Imaging: Analysis of cutaneous temperature during exercise, *in Proc.of the 24th IEEE Engineering in Medicine and Biology Society Conference*, Houston, Oct 23-25, 2002.

ASHRAE: Handbook Fundamentals SI Edition, ASHRAE, Atlanta, GA, 1985

Merla, A., et al., Time Recovery Image: a diagnostic image technique based on the Dynamic Digital Telethermography, *Thermol. Intern.*, 10, 142, 2000.

Merla, A., et al.,. Tau image: a diagnostic imaging techinque based on the dynamic digital telethermography, *in Proc. of the WC2000 Chicago World Congress on Medical Physics and Biomedical Engineering and 22th International Conference of IEEE Engineering in Medicine and Biology Society*, Digest of Papers CD, track 1,TU-FXH, Jul 2000, Chicago.

Allen, E.V. and Brown, G.E., Raynaud's disease: a critical review of minimal requisites for diagnosis, *Am. J. Med. Sci.*, 183,187, 1932.

Subcommittee for Scleroderma Criteria of the American Rheumatism Association Diagnostic and Therapeutic Criteria Committee, Preliminary criteria for the classification of systemic sclerosis (scleroderma), *Arthritis Rheum*., 23,581,1980.

O'Reilly, D., et al., Measurement of cold challenge response in primary Raynaud's phenomenon and Raynaud's phenomenon associated with systemic sclerosis, *Ann. Rheum. Dis.*, 51,1193, 1992.

Clarks, S., et al., The distal-dorsal difference as a possible predictor of secondary Raynaud's phenomenon, *J. Rheumatol.*, 26,1125, 1999.

Schuhfried, O., et al., Thermographic parameters in the diagnosis of Secondary Raynaud's Phenomenon, *Arch. Phys. Med. Rehabil.,* 81,495, 2000.

Ring, E.F.J., Cold Stress test for the hands, in *The thermal image in Medicine and Biology*, Uhlen Verlag, Ed., Wien, 1995.

Merla, A., et al., Combined approach to the initial stage Raynaud's phenomenon diagnosis by means of dynamic digital telethermography, capilloroscopy and pletismography: preliminary findings, *Med. Biol. Eng. Comp.*, 37, 992, 1999.

Shitzer, A., et al., Lumped parameter tissue temperature-blood perfusion model of a cold stressed finger, *J. Appl. Physiol*., 80,1829, 1996.

Cooke, E.D., et al., Reflex sympathetic dystrophy and repetitive strain injury: temperature and microcirculatory changes following mild cold stress, *J. Royal. Soc. Med.,* 86,690, 1993.

Di Benedetto, M., Regional hypothermia in response to minor injure, *Am. J. Phys. Med. Rehabil.,* 75,270, 1996.

Garagiola, U., Use of telethermography in the management of sports injuries, Sports Med., 10, 267, 1990.

Maricq, H.R., et al., Diagnostic potential of in vivo capillary microscopy in scleroderma and related disorders, Arthr. Rheum., 23,183,1980.

Rodnan, G.P., Myerowitz, R.I., and Justh, G.O., Morphological changes in the digital arteries of patients with progressive systemic sclerosis and Raynaud Phenomenon, *Medicine*, 59,393,1980.

Tucker, A., Infrared thermographic assessment of the human scrotum, *Fertil. Steril.,*74,802, 2000.

Mieusset, R. and Bujan, L., Testicular heating and its possible contributions to male infertility: a review, *Int. J. Andr.,*18,169, 1995.

Trum, J. W., The value of palpation, varicoscreen contact thermography and colour Doppler ultrasound in the diagnosis of varicocele, *Hum. Reprod.,*11,1232, 1996.

ACTIVE DYNAMIC THERMOGRAPHY IN CARDIOSURGERY

Mariusz Kaczmarek, Antoni Nowakowski

Gdansk University of Technology/Department of Biomedical Engineering, Gdansk, Poland
tel. +48 58 347 26 78; fax. +48 58 347 17 57; mariusz.kaczmarek@biomed.eti.pg.gda.pl

Key words : cardiosurgery, dynamic thermography, parametric imaging

The goal of the presented research was to apply dedicated data processing and external thermal excitations to get objective, quantitative thermal data of tested tissues [1]. It allows validation of active dynamic thermography (ADT) in medical diagnostics and development of new diagnostic procedure. Our studies in that field are concentrated on applications to diagnostics of burns, skin transplants and open heart surgery evaluation [2]. The aim of this study is preparation of tools applicable in real clinical environment for continuous inspection of interventions in open-heart surgical procedures. Our notice is concentrated on heart ischaemia and methods which allows to prevent risk of such failure.

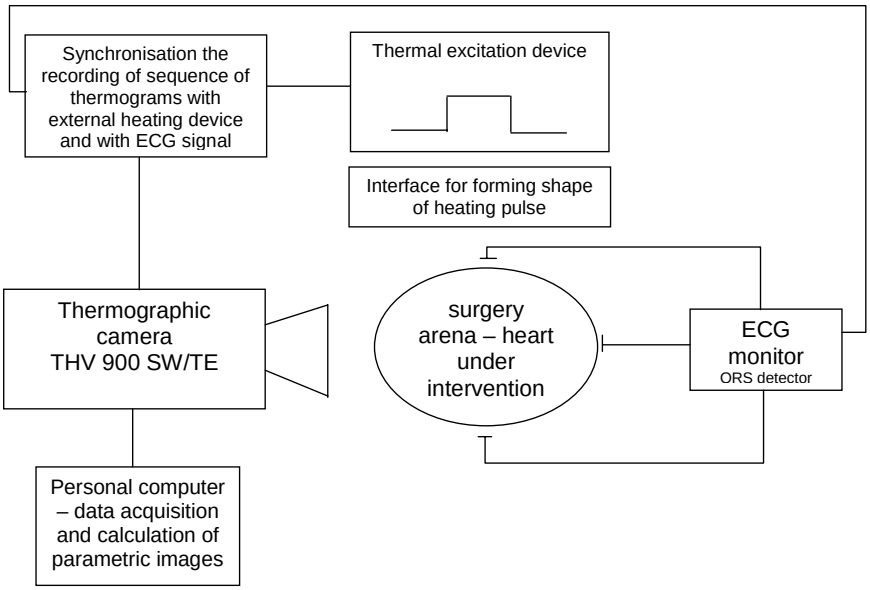

Fig. 1. Measurements set-up for active dynamic thermography in cardiosurgery applications

For i*n vivo* experiments on animals (performed according to all legal regulations and permission of the Local Ethics Commission for Experimentation on Animals at the Medical University of Gdansk, Poland) the pigs have been studied due to the closest to human physiological and anatomical structure of the heart muscle and the circulatory system. . The chest was open to have full access to the heart muscle. Intubation was applied during all experiment time. To evoke the heart muscle ischaemia the left descending artery was clamped totally blocking delivery of the blood.

Thermal state of the heart is monitored by simple registration of IR radiation emitted by the observed surface of the heart while thermal properties of the heart muscle are calculated from active dynamic thermography (ADT) experiments based on external thermal excitation.

The general concept of measurements performed in *ADT* is shown in Fig. 1. First, the steady state temperature distribution on the tested surface is recorded using an IR camera. Next, external thermal excitation (heating or cooling) is applied, followed by measurements of temperature transients on the tested surface. Typically, a set of halogen lamps may be applied as the thermal excitation source but we have tested cooling using cold air forced flow, too. Finally, tested tissue can be quantitatively assessed by means of the thermal time constant ***(τ)*** – one of the exponential equation parameter: $T(t)=T_s+\sum_{j=1}^{m}\Delta T_j\cdot e^{-\frac{t}{\tau_j}}$, where t – time, T_s – temperature in steady state.

As an example of measurements performed using the acquisition system shown in Fig.1 typical measurement results are presented in Fig. 2. Thermal properties of the heart muscle are affected by ischemia. This is not only due to limited vascularisation but also by visible changes in cell structures in the affected regions.

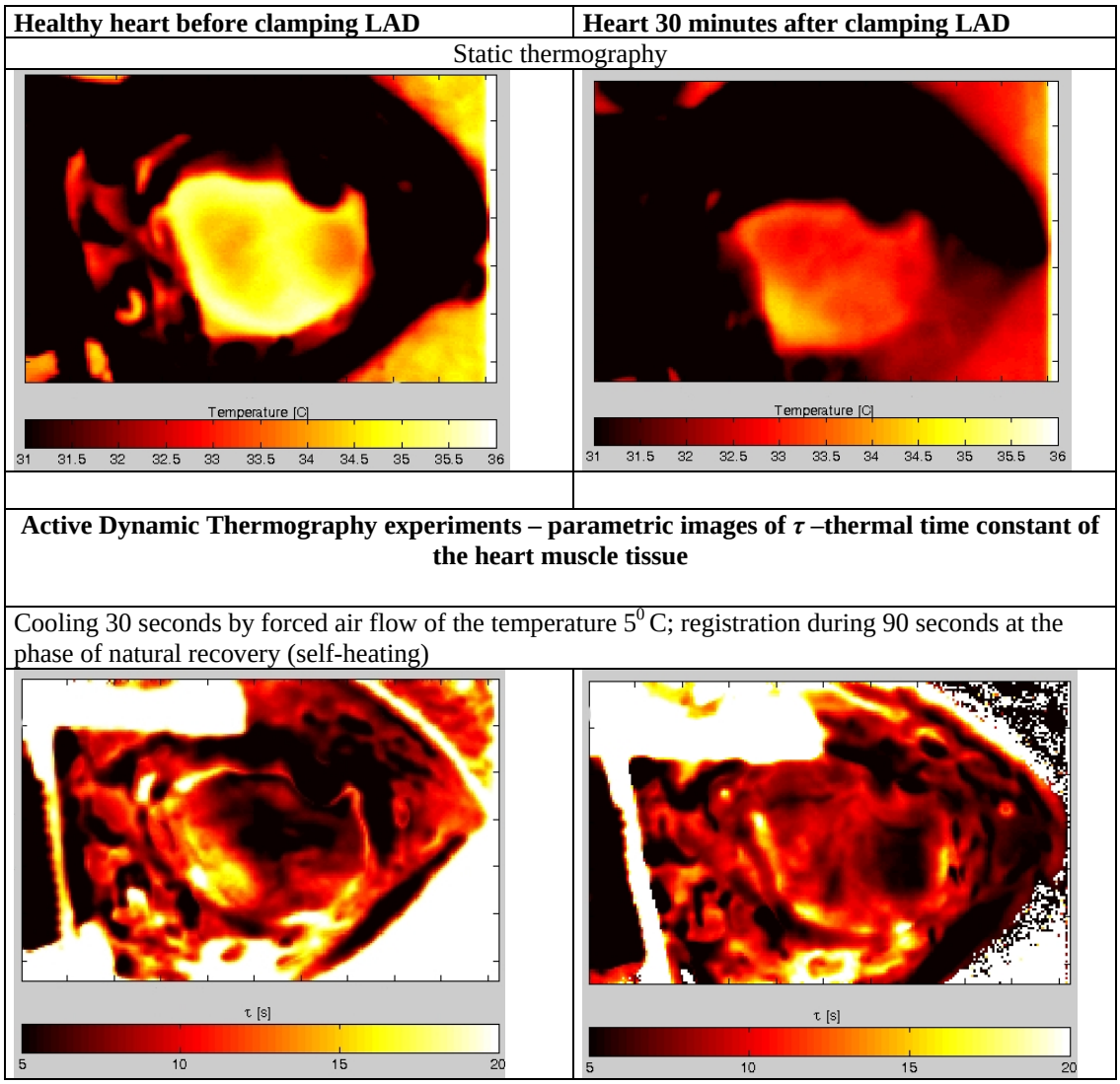

Fig. 2. Static IR-images and ADT parametric images for air cooling taken respectively before and after 30 min of clamping LAD.

The set of ADT parametric images gives rather structural information of the tested tissue. Properties of tissue are dependent on blood flow and physical structure which is devastated after long lasting processes of ischemia. Blood arrest has damaging influence on the structure of cells what may be easy evidenced by histopathology. Therefore the ADT images are differentiating tissues already affected but are not sensitive to short deficits in blood flow.

References

1. Maldague XPV. Theory and practice of infrared technology for non-destructive testing, J. Wiley & Sons, Inc., New York, 2001.
2. Nowakowski A., Kaczmarek M., Ruminski J., Hryciuk M., Renkielska A., Grudzinski J., Siebert J., Jagielak D., Rogowski J., Roszak K., Stojek W., Medical applications of model based dynamic thermography, Proc. SPIE, v. 4360, 2001, 492 – 503.

APPLICABILITY OF I.R. THERMOGRAPHY TO THE MEASUREMENT OF STRESS IN RABBIT

Nicola Ludwig[1], Marco Gargano[1], Fabio Luzi[2], Corrado Carenzi[2], Marina Verga[2]
[1]Istituto di Fis. Gen. Applicata, Facoltà di SFMN via G. Celoria, 16, 20133 Milano
[2]Istituto di Zootecnica, Facoltà di Med. Vet., via G. Celoria, 10, 20133 Milano

Corresponding Author: Dr. Nicola Ludwig - Università di Milano. Italy
Tel. +39 02 50317473 - Fax: +39 02 50317422 - Email: nicola.ludwig@unimi.it

Keywords: ***Rabbit , Stress, IR-thermography***

ABSTRACT: The problem in evaluating stress in animals is related to the need to avoid as much as possible to induce other stress reactions due to handling. Among the physiological stress indicators, the body temperature evaluation is very important and innovative because it may be monitored without interacting with the animal. Thermographic technique has been successfully applied in order to evaluate the stress response in some research on domestic animals, although it has not yet been used in rabbits. In the preliminary step this research activity has been addressed to define methods for measuring rabbit temperature by using an infrared camera. Main problems occurring in rabbit temperature measuring by infrared thermography are skin/fur emissivity determination as well the definition of a stress factor. In our study, the rabbit species was chosen due to its physiological and behavioral characteristics and the high reproductive rhythm, which allow analyzing a high number of animals with homogeneous morphological traits. The use of a thermographic system (Avio TVS 700 microbolometric uncooled LW) has proved to be a very suitable method in order to measure rabbit temperature by means of a complete non-invasive way. Zones of the rabbit skin most suitable for the temperature monitoring during stress reactions was singled out during the first testes. Variations of the observed temperature are in fact limited in a range of few degrees, so emissivity coefficient can be considered constant. Furthermore we were interested in detecting temperature differences related to different stress response of the same subject and variation due to individual metabolism was not taken into account. Ten hybrid rabbits (8 fatteners and 2 does) were observed during different phases of stress reaction. The areas selected (see fig 1) as reference for the detection of the temperature changes were: internal auricle pavilion and the ocular area. The last one showed to be the most uniform inside the same subject and between different subjects. The mean of the temperature variation of the analyzed subjects were σ_{ey} = 0.2°C and σ_{ear} = 0.5°C respectively for the eye zone and for the auricular zone.

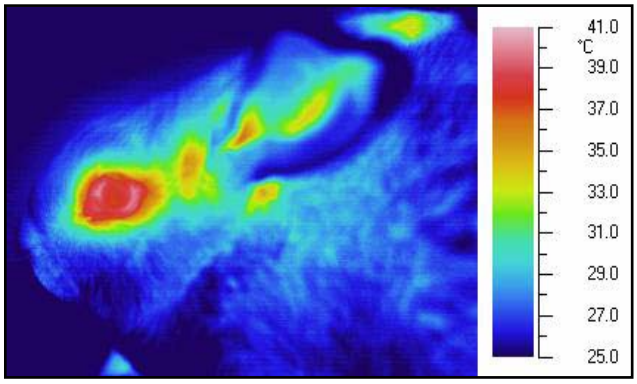

Fig. 1.Temperature distribution of a rabbit under laboratory condition.

The first results concerning the effect of stress on body temperature showed an increasing of 0.8°C and of 1.3°C in the first two sequence trial (ocular area), going by basal conditions to acute stress.
Preliminary results of this research show that the thermographic technique is a suitable method for the evaluation of temperature variation on the rabbit's skin. In fig 2 are showed two sequence of measurement (blue and red) that correlate the increasing of ocular temperature to the increasing of the stressor (arbitrarily defined in a scale ranging from 0 to 5).

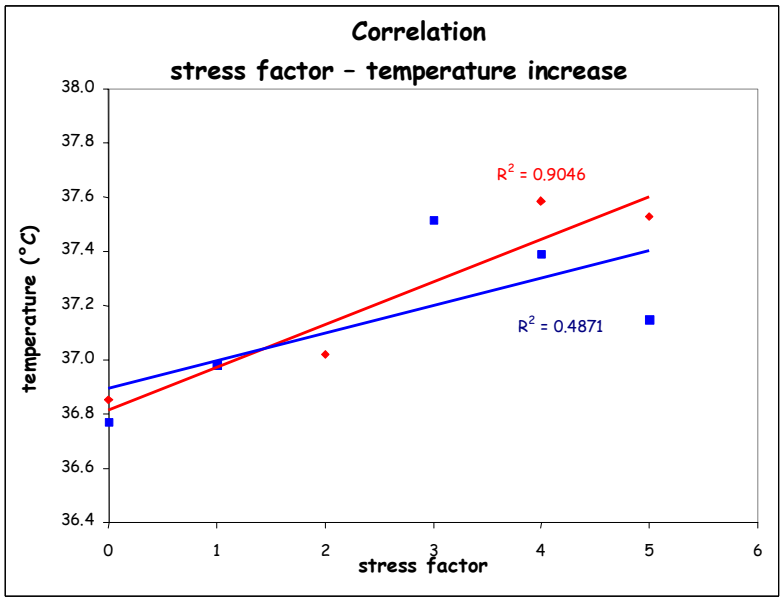

Fig. 2. Sequence of measurement showing the increasing of rabbit ocular temperature with the stress factor.

(0=basal conditions in group housing; 1=stressors in group housing; 2=tonic immobility; 3=basal conditions in individual housing; 4=individual housing; 5=stressors in individual housing.

The high correlation obtained in the second sequence (red line) seems to be correlated to the *better* repeatable experimental condition in which the state of tonic immobility has been introduced (stress factor=2).
In a second phase of research, temperature measurements in the two aforesaid reference areas were also compared to the ones obtained from a shaved area and from internal body temperature. Furthermore, a correlation was studied among cutaneous temperature and corticosterone levels. The latter represents a stress indicator related to the activation of the HPA (hypothalamus-pituitary-adrenal) axis.
The results of this first preliminary research in rabbits are very promising. In fact, thermography allows evaluating a physiological indicator of stress with a not invasive method. In the next future the correlation among body temperature and other stress indicators, such as behaviour and physiology (corticosterone levels) needs further and deeply investigations.

A theoretical study of medical imaging by optical tomography using a radiative transfer model

H. Trabelsi and R. Ben Salah

Institut Supérieur des Technologies médicales de Tunis. 9 Rue Z. Essafi 1006 Tunis. Tunisia.

Abstract

A new method for image reconstruction from optical tomography is developed.The radiative transfer equation is used to describe the photon propagation in participating media. The reconstruction method consists on two steps : - Development of a forward model based on the discrete ordinates method associated with a finite volume scheme. - The use of a downhill Simplex algorithm to perform a minimization of the objective function that provides values of the differences between the detected and the predicted data. The studied medium is a tissue-like medium. The scattering is modeled making use of the Henyey- Greenstein function. The accuracy of the proposed method is tested in a rectangular geometry. Some results are given using simulated data. In recent years there has been attempts to develop a diagnostic imaging modality based on near-infrared radiation . This new imaging modality is commonly known as optical tomography (OT). Changes in the optical properties are closely related to physiological and pathological changes of different tissues.The OT imaging process is based on the reconstruction of the distribution of optical properties inside a medium by using results of light-transmission measurements obtained on the surface. This provides information of human organs without having to draw upon surgery ; so this technique could be a good candidate to fulfilling conditions of a low cost, non-ionizing tomography method easily movable and even capable of on-line monitoring. Light-transmission measuring technology on human subjects is nowadays available. Then a crucial research task is to perform adapted algorithms that transform these measurements into medical images. It is established that the quality of reconstructed image depends on the accuracy of the model of photon transmission in human tissue-like media. One way to model propagation of near-infrared light is diffusion equation. It is an approximation of the photon transport equation in very high scattering biologocal tissue. Many of commonly known reconstruction algorithms are based on this approach. However low scattering regions in human body such as the cerebrospinal fluid of the brain, the synovial fluid of human finger joints and the amniotic fluid in the female uterus could be not accurately represented by this model. Also highly absorbing regions such as hematoma and liver tissue risk to be out of media concerned by diffusion

approximation model.Therefore, for a general biological tissue-like medium, it is desirable to have a reconstruction method based on radiative transfer equation itself. Some works have been already developed concerning radiation inverse problem. A majority of these attempts has dealt with one dimensional geometry configuration. Other works have used very complicated algorithms such as GIIR methods that overcome some limitations but they demand a lot of derivative calculus.Monte Carlo methods have been also used in reconstruction problems based on radiative transfer theory but they risk to have high time-price. In this work we present a finite volume discrete ordinates method for the solution of the radiative transfer equation as a forward model. The reconstruction method is based on minimizing an objective function using a downhill simplex algorithm. This method requires only functions evaluation , not derivatives. Some results are given from simulated data for media with varying scattering coefficients.

Key words: Optical tomography - Radiative Transfer Equation - Discrete Ordinates Method - Simplex Algorithm - Medical Imaging.

Mathematical relation between Thermal skin surface data and its electrical counterpart.

(M. Piquemal:MD,EE; B.Baran:PhD computer sciences; A.Lheureux: Eng. Computer sciences; A.Hermosilla:Eng.Industrial)

1. Introduction.

Human skin is not just only considered by Medical investigations field as a barrier to protect body from injure (physical, chemical, bacterial..). In our computed and interconnected world we tend to think that skin should be also considered as an communication interface between two different but interrelated spaces: the little organic inner space (body) and its surroundings (Nature). As one of predictive Nature' laws is to function with lower energetic level, to reduce any unnecessary energetic waste in the body, permanent physiological adaptation has to occur, at any time. In this way of thinking, skin interface should be worked too as a determinant system to inform body of any outer change. Due to embryological development, back skin surface, for keeping track of dermatoma, is selected. Dermatoma is a physiological unit, easy to identify in the back region that associates in a delimited cutaneous territory, nerves, muscles, blood vessels and special organ functions that are projected on this vertical slice of skin.

Two Passive ways of investigation on skin surface are chosen to be linked: Infra red blood flow measurement and Bio difference of electrical potential (Bio-DDP).

Understanding, in a quick reliable passive mode of data capture, any change in skin pattern information of these dermatoma, should be lead us to catch functional disturbance to prevent any higher organic disorder in the future.

In previous works[1,2], statistical correlation between thermal and electrical matrices, allow us to foresee high possibility to be linearly correlated. Present mathematical investigation attempts to determine linear equation relating thermal to electrical data taken from particular points belonging to acupuncture (*Bei shu* points), as historically, the electrical field of these points are clinically known to reflect shifts in functioning of specific organs.

2 Material and method

- Data process

To get the two basic matrixes (thermal one and electrical one) to be interrelated, a couple of methods will be used: I.R. Thermography and electrical measurement. These will be made in the skin of the back of 8 patients, from the third dorsal to the fifth lumbar vertebras.

-Thermography is accomplished using an InfraMetrics Model 520 cooled Imaging radiometer.

-Bio DDP is based on a differential measurement of electric potential. A digital high input impedance electro voltmeter is chosen. Electrical reference point is situated on the front, to be known as one of the most electropositive point of the body. Interface skin- electrodes will be solved using electrochemical electrodes in order not to generate secondary electrode potential [3,4]. Capture of signal is done in an electromagnetic free environment. Filters are used too to guaranty a quite noiseless signal from patient.

At the end of the process two thermal and electrical matrices are built. First one comes from IR imaging, that is being analyzed after a standardized digitalized process involving only the double set of 10 *Bei shu* points, been previously localized on the global matrix picture. Electrical matrix is directly built in real time, picking up signals from the 10 symmetric *Bei shu* point localized with respect to the spinal bones. So both matrices to be correlated are ten rows and two, columns after these reducing data process from back skin dermatoma.

- Statistical process .

Regressive statistical analysis of this bio metrics data is done. Linear relationship is attempted to be determined between thermal and electrical matrix. Is it possible to stand a mathematical linear equation where Y stands for electrical matrix and variable is the thermal matrix?

To solve this equation, a set of variable is proposed. Definitive equation looks like:

$$Y=m1X1+m2X2\ldots..+m6X6+b$$

Where X1 stands for the thermal matrix.; X2 .Sex of patient is taken into account (1=Female;-1=Male) ; -X3. Maxima Arterial blood pressure from left side ;-X4.Minima Arterial blood pressure from left side.

3. Results

Regression Variable Results

Parameter	Value	Standard Error	t-ratio	Prob(t)
m1	-0,557338	0,020277	-27,485692	0
m2	-0,252448	0,002438	-103,561285	0
m3	3,822182	0,088361	43,256413	0
m4	-5,104005	0,077576	-65,793385	0
b	1,477514	0,019812	74,577062	0

4. Interpretation, conclusion

Only it was possible to write electrical matrix as a linear combination of thermal data and other variables like arterial pressure. To better understand the reason why only one way of mathematical linear expression is possible, it is important to know about how Bio-DDP arise from skin (J.Pontigny engineer's hypothesis). Bio-DDP is the sum of three quantifiable biological sources of electrical potential. Primary bioelectrical difference of potential takes form from epidermis. It is a stable dc -40 mV voltage. Secondary and tertiary Bio-DDP are variables. Both of them arise from dermis histological structure. Secondary bio-difference in electrical potential, originate itself from rich blood vessels. 95% of blood vessels in the dermis serve autonomic nervous system function purposes. Blood should be understood as an electric charge carrier and of course as a thermal fluid. Tertiary Bio-difference in electrical potential takes form from the interplay between skin and autonomic nervous system regulating tonal fluctuation of the blood vessel according to local possible feed back control loop between environment and inner organ functions.

To establish only one way linear relationship between theses two different matrix origins, shows that Bio_DDP is not only an exclusive function of thermal data but too of nervous trains of impulse.

To relate thermal to electrical data on a linear mode with a set of easy personal data to get, allows indistinctly in the future, the use of thermal as electrical data. Thanks to linear conversion, versatility in the data capture methods will increase biometrics information database.

Linear equation linking thermal data to electrical ones should be part of higher project allowing skin information capture to foresee functional disturbances, to prevent organic failure, in the body.

6. Bibliography

1.Piquemal M. Clinical correlation between cutaneous bioelectric potential and thermographic imaging of blood flow. Coherence 2000;2:8-11.

2. L'Heureux A., Piquemal M. Sistema innovador de captura de datos para la electrorraquigrafía en la fase de captura y análisis [Tesis]. Asunción:Universidad Columbia del Paraguay; 2002.

3. Pontigny A, Pontigny J. Instrumentation et acupuncture. Sainte Ruffine: Maisonneuve; 1989.

4. Becker RO. The bioelectric Field Pattern in the salamander and Its Stimulation by an Electronic Analog. IRE Transacions on Medical Electronics.February 1960:202-5.

5. Pontigny A, Pontigny J. Les biodifferences de potentiel de surface. Meridiens 1992; 97:73-84.

6. Cantoni G, Pontigny J. Recherche Scientifique française et acupuncture. Sainte Ruffine: Maisonneuve; 1989.

Emissivity of the popular dental materials

M. Dabrowski[1], R. Dulski[1], P. Zaborowski[2], St. Zmuda[3]

[1] Institute of Optoelectronics, Military University of Technology, ul. Kaliskiego 2, 00-908 Warsaw, Poland, rdulski@wat.edu.pl
[2] Military Institute of the Health Services, ul. Szaserów 128, 00-909 Warsaw, Poland
[3] Central Military Surgery, ul. Koszykowa 78, 00-911 Warsaw, Poland

ABSTRACT

Knowledge of emissivity is essential to ensure high accuracy of temperature measurements when using non-contact methods. Emissivity coefficients were calculated using the reflective method. The authors introduce and compare average and spectral directional emissivity of the most popular dental materials in spectral bands commonly used in modern IR cameras.

The measurements of temperature in dentistry are important because of the fact that dental procedures can bring on uncontrolled increasing in temperature inside the oral cavity. It is known [1-3] that temperature increase inside the pulp of about 5°C can lead to irreversible changes in the pulp itself and thus can be very danger to patient's health. During examination of thermal injury of dental equipment in clinical circumstances we are interested in real temperature values rather than apparent ones [4, 5], which cannot be measured using IR cameras without knowledge of emissivity of observed objects.

This fact appears well in Fig. 1 where the apparent temperature distribution of four different dental materials placed on the homogeneous background is shown.

Unfortunately, most real materials including dental ones are selective. In such a case its emissivity depends on wavelength. Many people who use IR cameras are not familiar enough with IR technique and what's more, data about value of object's emissivity in real measurement conditions are often difficult to find in literature.

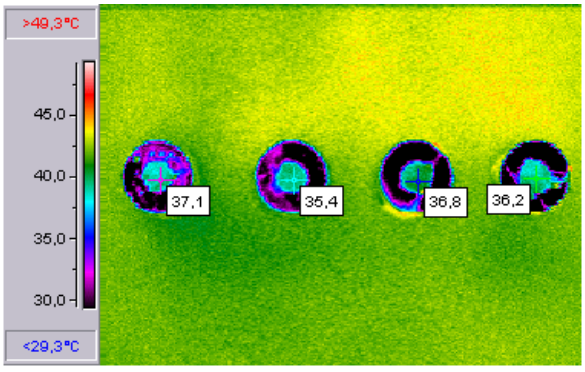

Fig. 1. Apparent temperature distribution of dental materials

Another problem is that the operating spectral band of IR camera depends on its design, especially on the detector's type (i.e., microbolometric FPA works in different spectral band than QWIP or PtSi ones) and the value of emissivity used for correction should be calculated in the same spectral band as operating spectral band of the IR camera used.

Spectral directional emissivity for each material was determined using the reflective method [7], i.e. indirectly by processing measured values of reflectance.

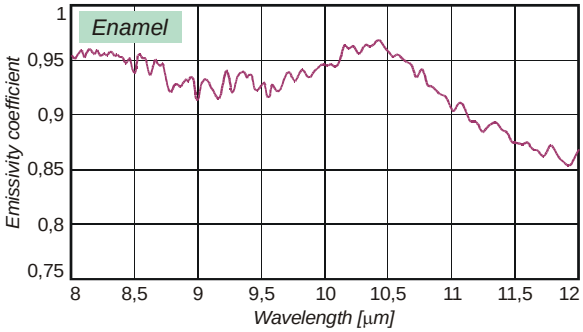

Fig. 2. Emissivity coefficient of the enamel

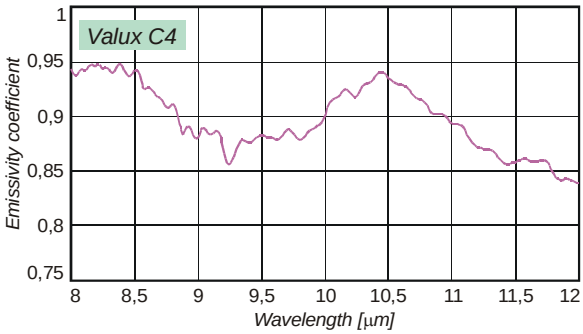

Fig. 3. Emissivity coefficient of an example dental material

Example results of the spectral directional emissivity calculations for the enamel and a dental material are shown in Fig. 2 and Fig. 3, respectively.

References

1. Zach L, Cohen G., Thermogenesis in operative techniques, comparisons of four methods, J Prosthet Dent 1962; 12:977-84.
2. Noyborg H, Brannstrom J., Pulp reaction to heat, J Prosthet Dent 1968; 19:605-12.
3. Carson J, Rider T, Nash D., A thermographic study of heat distribution during ultra-speed cavity preparation, J Dent Res 1979; 48:1681-4.
4. M. Dąbrowski, R. Dulski, S. Żmuda, P. Zaborowski, C. Pogorzelski, The use of thermovision camera to represent physiological and pathological conditions of oral cavity mucous membrane, Infrared Physics & Technology, 43 (2002) p. 265-269.
5. H. Madura, M. Dąbrowski, R. Dulski, S. Żmuda, P. Zaborowski, Thermographic method for evaluation of thermal influence of Nd:YAG laser on a tooth root during sterilization process, Infrared Physics & Technology, 46 (2004) p. 167-171.
6. S. Żmuda, P. Zaborowski, P. Trykowski, M. Dąbrowski, R. Dulski, Effect of hte emission properites of detal materiale and hard detal tissues of the teeht on indirect temperature measurement of the teeth., *Stomatologia Współczesna*, Suplement nr 1/2000, p. 8-12 (in Polish).
7. Ascetta J.S., Shumaker D.L., eds, The Infrared and Electro-Optical Systems Handbook, SPIE Optical Engineering Press, Bellingham (1993).

ON THE USE OF AN INFRA-RED CAMERA FOR THE MEASUREMENT OF TEMPERATURE IN FIRES OF VEGETATIVE FUELS

Frédéric RINIERI*, Jacques Henri BALBI, Paul Antoine SANTONI
Université de CORSE UMR 6134 Quartier Grossetti, BP 52, 20250 CORTE, France
*phone : (33) 4 95 45 01 11, fax : (33) 4 95 45 01 62
Email: {rinieri, balbi, santoni}@univ-corse.fr

KEYWORDS: temperature measurement, application to flame

PREFERENCE: Oral Presentation

ABSTRACT

We have recently proposed a semi-physical model of forest fire [1], validated at the laboratory scale for fires across litters of pine needles, under both wind and slope condition. This model must now be tested at the field scale. It is based on a reaction-diffusion formulation representing in overall way the exchanges between the combustion area and its immediate surrounding. It is called semi-physical because it has a physical core and contains a share of empiricism for the identification of the model's parameters. These parameters are identified thanks to the temperature recorded in experimental fire fronts. Up to now, the temperature was measured by using thermocouples at the laboratory scale. However, these measurements are tricky to carry out at the field scale.

In this work, we propose an original methodology based on infra-red thermography to measure the temperature in the flames and embers of a fire of vegetation. An infra-red camera provides digital levels in output that can be used to retrieve the temperature of the target. The method usually used to obtain this temperature follows a formalism resulting from the law of Planck [3], [4]. By taking into account the recommendations given in [5], we have developed a new approach based on the assumption that the flame can be view as a grey surface [6], of emissivity ε, and of average temperature *T*. The answer of the apparatus is modelled by the following relationship $N - N_0 = aT^4$, where *T* is the temperature of the target, *N* is the digital level of the camera, *a* and N_0 are parameters. Both relationships were compared for static and spreading fires. The proposed approach provides better agreement with experiments than the classical method. To illustrate, the effectiveness of this method, measurements by infra-red camera are presented in figure 1. Its main advantages are the following: it requires the calibration of two parameters instead of three for the existing method and the identification of these parameters is simple. The variation of the parameters *a* and N_0, in function of the distance and in function of the vegetative fuel was also studied. *a* and N_0 remain unchanged for different species and do not depend on the point of measurement in the flames. The main reason is that the digital levels are quasi-constant in the continues zones of the flames. By way of example, infra-red images of flames of needles *Pinus pinaster* and *Helichrysum italicum* are presented in figure 2. The measurement was then used to identify the parameters of the model of fire spread. These results are also discussed and concluded in the full paper.

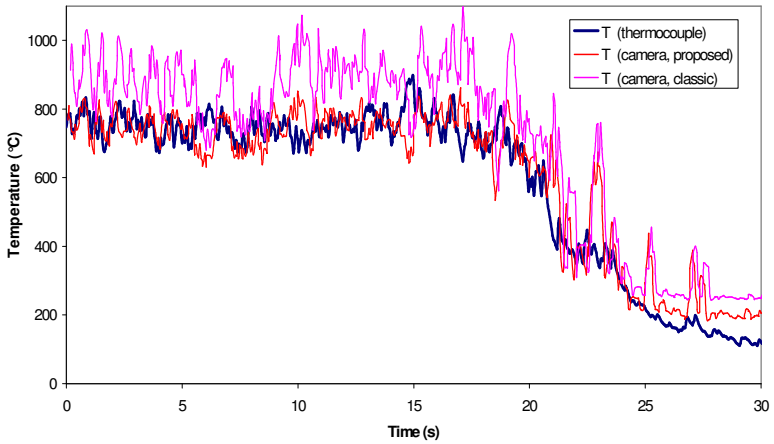

Fig. 1. Temperature measured by thermocouple and by infra-red camera in a flame of *Pinus Pinaster*

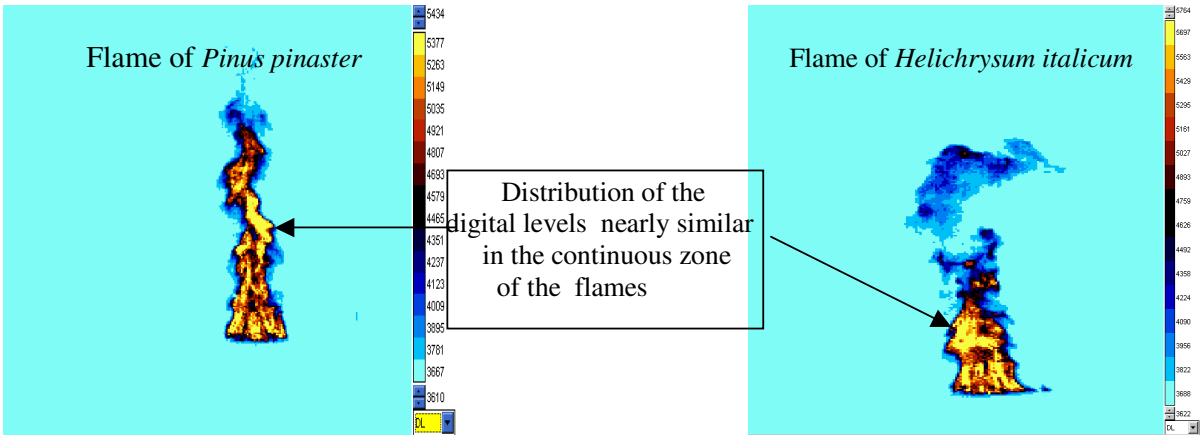

Fig.2. Infra-red images of a flame of *Pinus pinaster* and *Helichrysum italicum*

REFERENCE

[1] F. MORANDINI - A. SIMEONI - P.A. SANTONI - J.H. BALBI, A model for the spread of fire across a fuel-bed incorporating the effects of wind and slope, Combustion science and technology, 177(7):1381-1418 (2005)

[2] J.L. DUPUY, Mieux comprendre et prédire la propagation des feux de forêt: expérimentation, test et proposition de modèle Thèse de doctorat de l'Université de Lyon (1997).

[3] D. PAJANI, Thermographie infrarouge. Quelle longueur d'onde choisir ? Techniques d'applications MESURES, 52(8):71-76, (mai 1987).

[4] A. ARCONADA - A. ARGIRIOU - F. PAPINI – R. PASQUETTI, la mesure en thermographie infrarouge : calibration et traitement du signal, journal of modern optics, 34(10):1327-1335, (1987).

[5] D. BALAGEAS – A. DEOM – D. BOSCHER, La mesure de température par camera infrarouge, journée d'étude: mesure des températures, Revue Pratique de Contrôle Industriel, 164:61-74, Paris, (19-20 juin 1990).

[6] F. MORANDINI - P.A. SANTONI - J.H. BALBI, « The contribution of radiant heat transfer to laboratory-scale fire spread under the influences of wind and slope ». Fire Safety J., 36: 519-543 (2001).

EXPERIMENTS ON SCALE REDUCTION IN INFRARED LAND-MINE DETECTION

Alberto Muscio°, Luca Tarozzi, Mauro A. Corticelli

DIMeC – Dipartimento di Ingegneria Meccanica e Civile, Università di Modena e Reggio Emilia
Via Vignolese 905/B, 41100 Modena, Italia
°Phone +39-059-2056194, Fax +39-059-2056126, E-mail: alberto.muscio@unimore.it

Keywords: Buried object detection, Infrared measurements, Non-destructive testing, Rapid prototyping, Solar radiation

Presentation preference: oral presentation

1. INTRODUCTION

A method has been proposed to reproduce in the laboratory the heating and cooling cycles of a soil with a buried land-mine. The method allows the length-scale and time-scale of the experiments to be drastically decreased. This is achieved by dimensional analysis of the thermal problem. A preliminary confirmation of the used approach was obtained with simplified tests [1-3].

In the present work, the method is verified experimentally. Models of different types of land-mine are produced for this purpose. Full-scale and scaled-down models are built by a rapid prototyping technique, using materials with thermal properties similar to those of the actual land-mines.

The response of the soil surface is monitored during the thermal cycles by an infrared camera. Preliminarily, the surface response measured above full-scale models is cross-checked against that measured above actual land-mines. Full-scale and scaled-down models are then tested outdoors and in the laboratory, respectively. The measured distribution and time-evolution patterns of surface temperature are eventually compared, in order to assess the reliability of the scale reduction method.

2. MATHEMATICAL FORMULATION

Along a day cycle, heat transfer in a soil with a buried landmine depends on a large number of parameters, regarding system geometry, material properties, and heat exchange at the soil surface. However, dimensional analysis of the thermal problem shows that this actually depends on a relatively small number of dimensionless parameters:

$$Fo = \frac{\alpha_{soil} t_0}{L^2}, \alpha^* = \frac{\alpha_{mine}}{\alpha_{soil}}, \kappa^* = \frac{\kappa_{mine}}{\kappa_{soil}}, Bi = \frac{h_{atm} L}{\kappa_{soil}}, \Delta T_{atm}^* = \frac{\Delta T_{atm}}{q_0 L / \kappa_{soil}}$$

where the most significant terms are the thermal diffusivities α_{mine} and α_{soil} [m^2/s], the thermal conductivities κ_{mine} and κ_{soil} [W/(m·K)] of soil and landmine, the time-cycle t_0 [24 h], the solar constant q_0 [1367 W/m^2], the heat transfer coefficient at the soil surface h_{atm} [$W/(m^2K)$], the amplitude of daily

oscillation of the air temperature ΔT_{atm} [K], and an additional term L [m]. The latter is a reference length of the thermal system, in our case the radius of the landmine.

Dimensional analysis shows that in outdoor and indoor experiments of infrared landmine detection, the same distribution and time-evolution patterns of the dimensionless temperature $T^*=(T-T_{atm,ave})/(q_0 L/\kappa_{soil})$ is produced in terms of the dimensionless coordinate system (x^*=x/L,y^*=y/L,z^*=z/L) and of the dimensionless time $t^*=t/t_0$, when the geometrical similitude and the values of all the above mentioned dimensionless groups are conserved.

The geometrical similitude is relatively easy to achieve. Besides, there is little difficulty in using the same materials as in on-field experiments, thus keeping unmodified the diffusivity and conductivity values. This allows devising a procedure for reduction of both the time-scale and the length-scale of experiments. The procedure is described into details in previous work [1-3]. It was theoretically tested by numerical modeling, with excellent outcomes [1-2]. Positive results were also given by a few preliminary experiments with reduced scale, carried out in the laboratory. [2-3]. In those experiments, the land-mines were represented by plastic cylindrical disks, totally or partially filled with a wax having thermal properties similar to those of the TNT explosive.

3. EXPERIMENTS WITH SIMULACRA OF REAL LANDMINES

In this work, a more complete verification of the scale-reduction method was carried out by experimental means. Accurate models of real land-mines were built, either in full-scale or scaled-down, by a rapid prototyping technique (figs. 1-2).

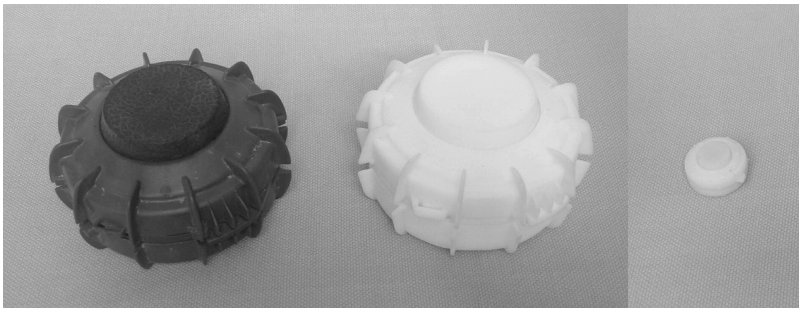

Figure 1. Landmine type VS50: actual landmine (dark color), full scale and reduced-scale simulacra (white).

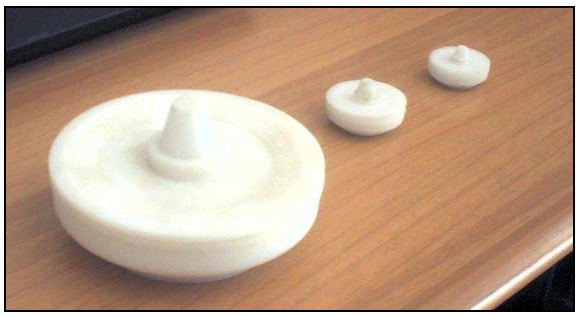

Figure 2. Landmine type AUPS: full scale and reduced-scale simulacra (white).

The surface response measured above full-scale simulacra was cross-checked against that measured above actual land-mines, with positive outcomes. The soil surface was monitored along the whole day cycle by an infrared camera. Comparable surface and time-evolution patterns of temperature were obtained in outdoor experiments (see fig. 3 for representative results).

Full-scale and scaled-down simulacra were then tested outdoors and in the laboratory, respectively. The measured distribution and time-evolution patterns of surface temperature were eventually compared, (see fig. 4 for representative results). Further experiments are in progress.

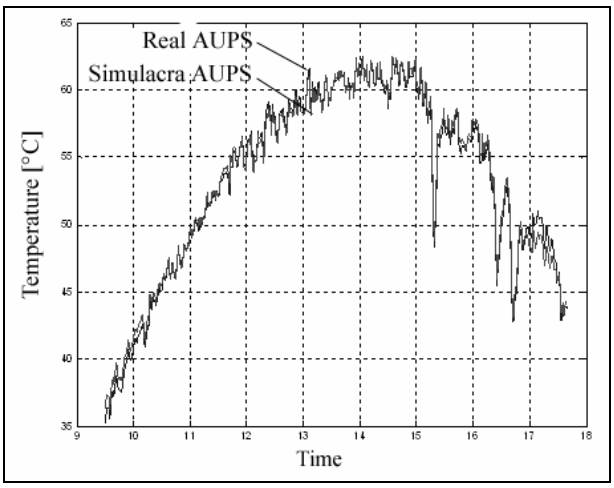

Figure 3. Landmine type AUPS: patterns of surface temperature above actual landmine and full scale simulacrum.

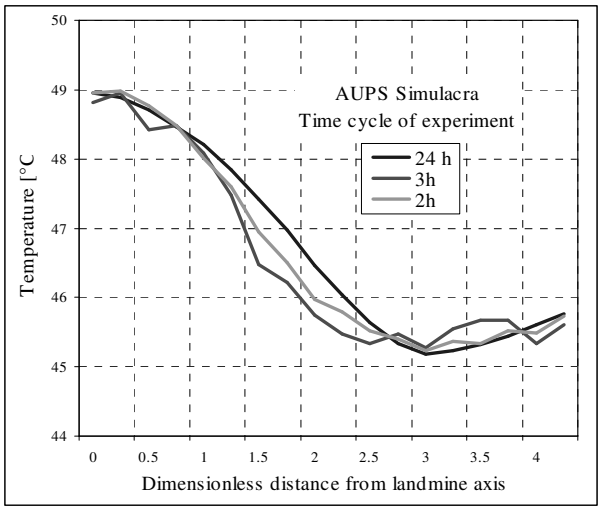

Figure 4. Landmine type AUPS: patterns of surface temperature above full scale and reduced-scale simulacra (diameter lines).

Overall, a verification of the scale-reduction method was again obtained. Moreover, an approach was developed to produce quickly and easily landmine simulacra, in full-scale or with reduced-scale. All that is expected to pave the way to extensive experimentation, dealing with different climates and different types of landmine, but working in the laboratory with accelerated operations.

REFERENCES

[1] L. Tarozzi, A. Muscio, M.A. Corticelli, "Ricerca di mine mediante termografia infrarossa: riduzione della scala degli esperimenti", *Proc. 21st UIT National Heat Transfer Conference*, Udine (Italia), 23-25 June 2003, ISBN 88-86281-79-X, pp. 51-58 (2003).

[2] A. Muscio, M.A. Corticelli, "Land-mine detection by infrared thermography: reduction of the size and duration of the experiments", *IEEE Transaction on Geoscience and Remote Sensing*, vol. 42, n. 9, September 2004, pp. 1955-1964 (2004).

[3] A. Muscio, M.A. Corticelli, "Experiments of thermographic landmine detection with reduced size and compressed time", *7th A.I.T.A.*, Pisa (Italia), 9-11 September 2003, published on *Infrared Physics and Technology*, vol. 46, n. 1-2, December 2004, pp. 101-107 (2004).

Air borne laser IR thermographic system for detecting gas leaks

V. Vavilov[1], O. Ershov[2], A. Klimov[2]

[1]Tomsk Polytechnic University, Russia 634028, Tomsk, 28 Savinykh St., 7
E-mail: vavilov@introscopy.tpu.ru
[2]Pergam Engineering, Russia 129164, Moscow, Olminsky St., 3A
E-mail: info@pergam.ru

There is a growing demand for remote and fast gas detection systems in Russia with its enormous network of buried and ground-based pipelines. The principle of IR thermographic monitoring can be used in two types of gas detectors: 1) backscatter/absorption gas IR imaging systems, and 2) trivial thermal imaging systems which detect leaks by purely thermal phenomena.

The first type systems implement irradiating a scene with a laser operating on a wavelength which is well absorbed by gases containing CH radicals, such as methane. The work distance of such systems is limited with some tens meters, thus being used mainly in workshop conditions. The second type systems utilize the phenomenon of gas expansion through small-size holes accompanied by local cooling. The reputation of such technique is controversial because of the necessity of advanced data treatment of IR thermographic indications on the background of noise which is of a multiple nature.

In this paper, a three-channel air borne IR system intended for remote gas detection is described. A 15 mW laser unit operating at 1.65 μm is a core of the system. This unit allows detecting leaks of methane at 20-150 m from a pipeline by the back-scattered laser radiation, i.e. without using any additional reflector. On-line inspection results are presented as sets of gas content profiles of whose true coordinates are provided by a built-in GPS system. Gas leaks are seen in these profile as distinct signal spikes. The second system channel is IR thermographic and its primary purpose, according to our present experience, is in evaluating changing depth of piping rather than detecting gas leaks. In parallel, the route details are recorded on a standard video-system which is the third system channel. The specialized software enables matching the data obtained by each of three channels to true ground position coordinates and comparing images captured in visual and IR wavelength bands. The sensitivity of the system by the laser channel is estimated to be about 100 ppm*m at 100 m (by methane).

The system implies the module principle that allows its easy installation on a helicopter (a Russia-made Kamov-26 helicopter has been used in on-flight monitoring). It is supposed to use it in the inspection of high voltage transmission lines where the IR thermographic channel is supposed to be crucial.

Monitoring of the Degradation Dynamics of agricultural films by IR Thermography

P. Mormile [a], L. Petti [a], M. Rippa [a], B. Immirzi [b], M. Malinconico[b]

[a] *Istituto di Cibernetica-CNR, via Campi Flegrei 34, 80078 Pozzuoli*
[b] *Istituto di Chimica e Tecnologia dei polimeri-CNR, via Campi Flegrei 34, 80078 Pozzuoli*

In the last decade biodegradable films for agriculture are attracting a great deal of attention because of the well known problems concerning the environmental impact produced by the traditional films after their use. The landfill of million and million tons of plastic films represents a serious problem for the environment also because, while consumption continuously increases, the recycling system in any country doesn't work as it should. Biodegradable materials are the ideal solution to this kind of problems which are involving the whole channel food year by year.
The research activity is focusing the efforts on new materials. The BIO.CO.AGRI Project, one of the LIFE Project funded by EC, recently aimed to the realization and characterization of new biodegradable films to be employed in agriculture.
One of the activities planned for the project was the acquisition of information about the degradation process of the films. Normally in order to study this process several pictures are taken at different times and then analysed. The comparison between the photos of the first week, of the second one and so on, indicate that the film is modifying itself. The novelty that we introduced is the use of thermography to monitor the dynamic of the degradation process. This approach allows to evaluate the local modifications of the material investigated as a function of time and according to the changing of the thermal properties induced by the degradation dynamics.
In our experiment we put on soil in open fields all the materials of interest in our project. The main characteristic of these materials is that they are originally liquid and they are sprayed on soil and immediately after they cross-link in a film state. This is the first time that sprayable films are proposed in agriculture for mulching soil instead of the traditional plastic ones. Due to their nature, their belonging to alginate and polysaccharides families, they are biodegradable.
Through an IR thermal camera we monitored the state of the films day by day and we analysed the thermal images to detect the continuous changing of them. Thanks to the dedicated software we studied also the temperature profiles in a selected target area of each material.
In figure 1 we report the images after an elaboration describing the dynamic process of its degradation.

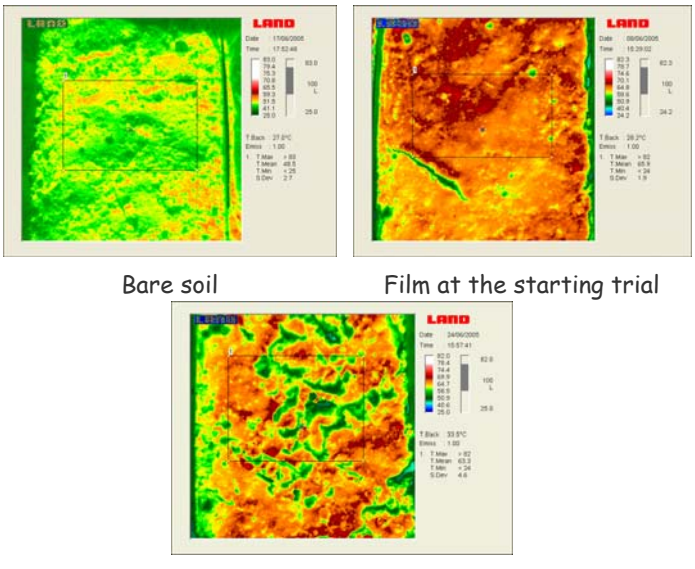

Figure 1: Thermal images of a film analysed vs time

In figure 2, it is reported the ratio of the average temperature per unit area of the films on the soil temperature as a function of time. This ratio as shown in figure decreases according to the degradation dynamic. It is worthwhile to notice that the values of two different biodegradable materials (c-d) after three weeks come to converge with the value of bare soil (b) and of a traditional plastic film (a).

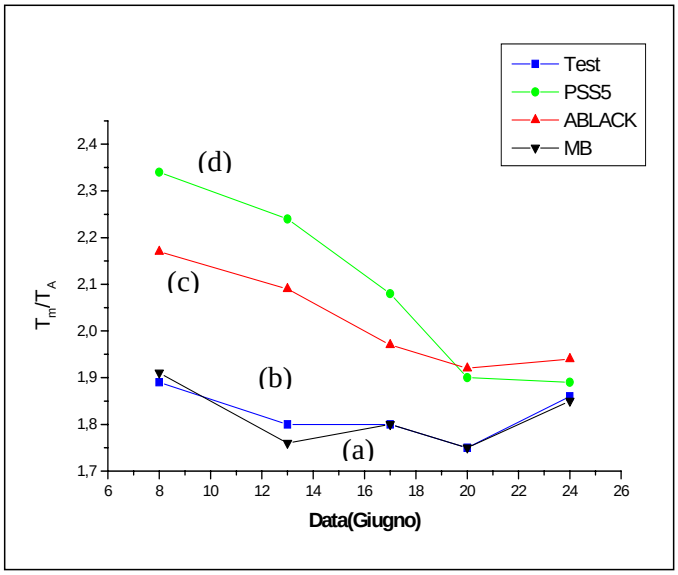

Figure 2: Experimental data reporting the normalised average temperatures per unit area of each material vs time; (a): traditional plastic film; (b): bare soil; (c), (d) biodegradable sprayed films.

Our experimental results show that thermography technique can be a very good tool in order to monitor the degradation process of a film in the agriculture field but also to give information on the degradation mechanism related to the soil state. Furthermore we believe that the ratio values of temperatures reported in figure 2 could be considered as a reference parameter in order to indicate the degradation state of a material employed in agriculture.

Non-destructive analyses of defects and effects of airborne pollutants in historical buildings

C. Bonifazzi[a,e,] , G. Maino[b], S. Massari[b] , L. Roversi[b] , C. Selvatici[c] and A.Tartari[d,e]

[a]*Department of Biomedical Science, University of Ferrara – Italy*
[b]*ENEA, Applied Physics Division, Bologna – Italy*
[c]*DAPT, Alma Mater Studiorum, University of Bologna – Italy*
[d]*Department of Physics, University of Ferrara – Italy*
[e]*INFM, National Institute of Matter, Genova – Italy*

Keywords. Material testing, Termography, ECoSp, PCA, Cultural Heritage Conservation.

Different imaging techniques are presented and applied to the study of historical buildings, mainly belonging to Renaissance time, in the city of Bologna, where the arenaria (sandstone) of which they are constituted is largely degradated in the surfaces due to the effects of pollutants present in the atmosphere. In the following figures, present status and a map od degradation effects is shown for two well-known palaces once belonging to honorable families, Bevilacqua and Fantuzzi (upper and lower figures).

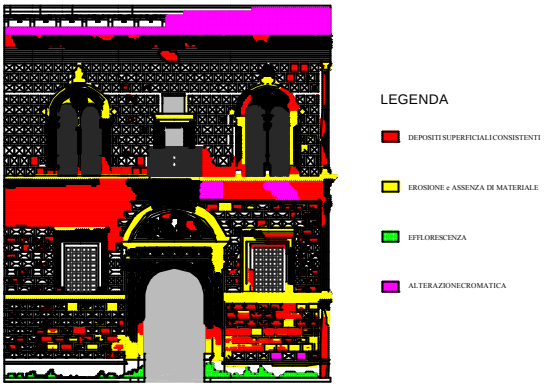

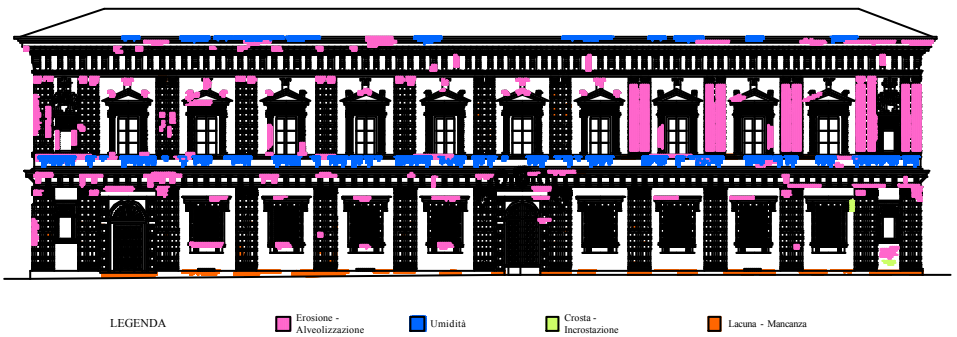

We based our investigation on multispectral techniques ranging from infrared reflectography, digitag termography and ultraviolet fluorescence. In addition, an original portable equipment based on the detection of Compton scattering photons and a further statistical analysis of the collected data has been utilized. The photon detection has been performed by the Enhanced Compton Spectrometer (ECoSp), a recently devised instrument that allows to collect the backscattered photons by investigating the tested sample from one side only. Photons collected during the planar scanning of a given area are used to describe the electronic density of the sample as a density image; afterwards, the Principal Component Analysis (PCA) was applied to the multispectral image processing, resulting from the mathematical combination of all the adopted imaging techniques. As a case study, a non-destructive testing of plaster substrates supporting mural paintings has been performed using this technique, searching for flaws, defects, fractures, and so on. Results are shown in the following figures in comparison with usual termographic analyses.

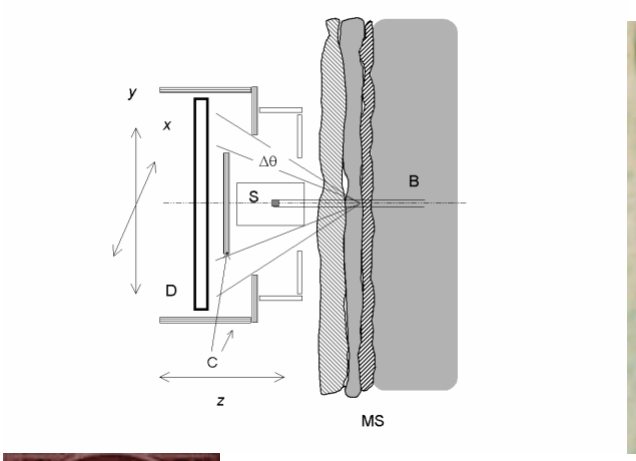

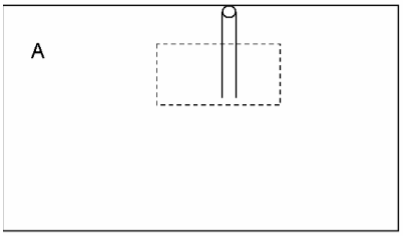

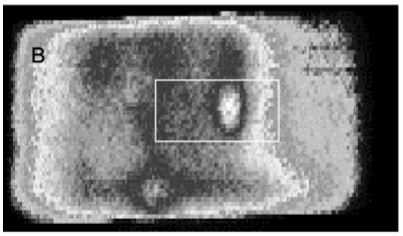

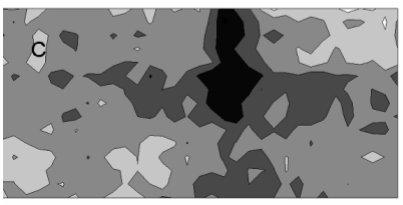

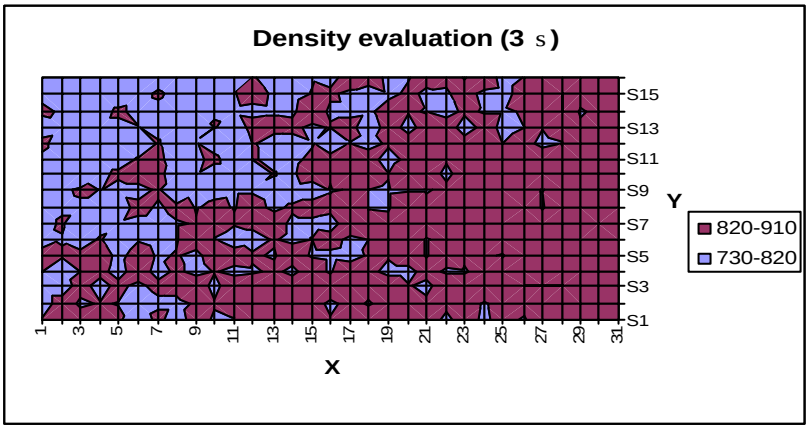

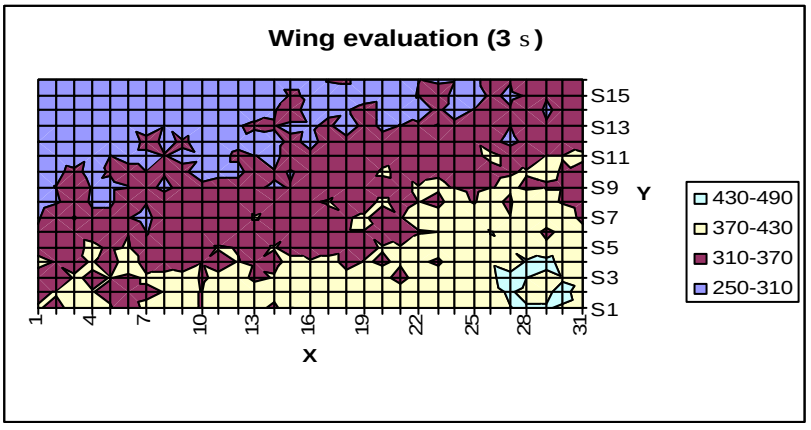

Measurement of forest fire parameters with multi-spectral imaging in the medium infrared

Juan Meléndez, José Manuel Aranda, Antonio J. de Castro, Fernando López.
Laboratorio de Sensores Teledetección e Imagen Infrarroja (LIR). Dept. Física.
Universidad Carlos III, Avda. Universidad, 30, 28911-Leganés. Madrid

phone: +34 91 624 94 12
fax: +34 91 624 87 49
e-mail: juan.melendez@uc3m.es

In the last years, infrared (IR) cameras have been used increasingly in forest fire related applications, like ground-based detection and monitoring. IR cameras are valuable in early detection of fires, due to their high sensitivity, and in fire monitoring because of their ability to see the fire front through smoke.

IR imaging is also a very attractive technology for fire studies, because it can provide, in principle, remote measurements of the main fire parameters (rate of spread, temperature, fire intensity, etc). These parameters are essential for forest fire propagation models, but their measurement with standard techniques is inaccurate, time consuming, and often impossible in field conditions. For instance, standard temperature measurements in a forest fire require the previous deployment of a grid of thermocouples over the whole area to be burned. As another example, smoke obscuration can make impossible rate of spread measurements by visual inspection. In both cases, IR imaging is an appealing alternative. However, its use for quantitative measurements faces difficulties, due to the complex spatial and spectral structure of fires.

A forest fire is a complex target, in which several different regions (flames, fire front, embers, ashes…) may be distinguished. The spatial distribution of each region changes with time, and their spectral profiles of emission may be very different from that of a blackbody. This means that each region is affected by atmospheric absorption in a different way, and that brightness temperatures may be very different from real temperatures. Thus, radiometric calibration is not enough to provide quantitative measurements of fire parameters: a previous scene analysis is mandatory.

Figure 1.: *(Left) Visible aspect of the 180 burn. (Right) The same scene in the 3,6 mm band. The fire front, propagating upward, is clearly seen.*

In this work it is shown that some of these difficulties can be overcome by using multi-spectral images of fires. Images were acquired with a radiometrically calibrated camera that operates in the medium infrared (MIR) band, and is provided with a rotating four filter wheel. One of the filters (F1) corresponds to the full band, and the others are centred, respectively, at: F2 = 4,8 μm, F3 = 4,2 μm, and F4 = 3,6 μm, all of them with a full width at half maximum of 0,4 μm. Sensitivity was adjusted to obtain a good signal to noise ratio at the F2, F3 and F4 bands, being band F1 consequently saturated. Measurements of forest fires at short (7 m), medium (180 m) and large (650 m) distances have been performed. Figure 1 shows a snapshot of the 180 burn in the visible band and in the 3.6 μm band.

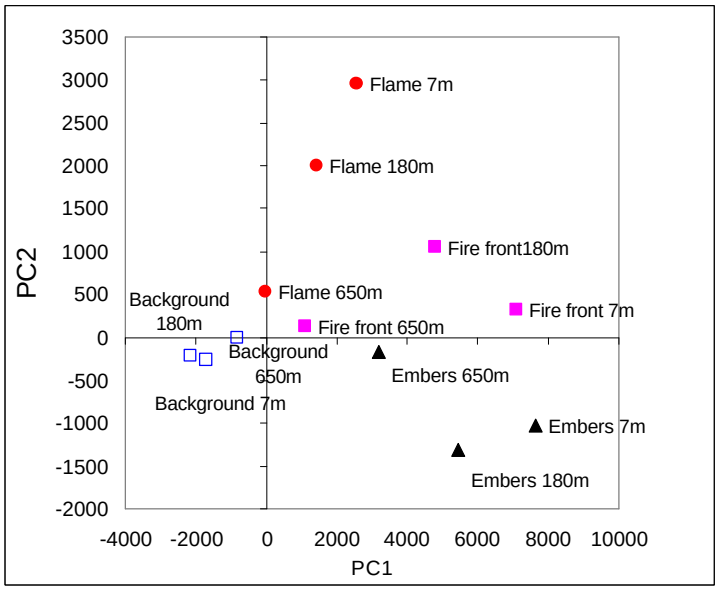

Figure 2.: *Values of the first two principal components for typical fire regions at the three distances studied. As distance increases, representative points tend to the origin, but discrimination between regions is still possible at 650 m.*

By applying classification techniques, a standard tool for the analysis of satellite multi-spectral images, the scene can be classified into different fire regions. Classification makes possible also an accurate definition of the fire front position, thus improving the measurement of the fire rate of spread.

As expected, classification gets worse with increasing distance. However, principal component analysis (PCA) of the F2, F3 and F4 bands has shown that region discrimination is possible even in the long distance measurements (see Figure 2).

The spectral behaviour of each fire region has been studied with spectral measurements obtained with a Fourier-Transform (FTIR) spectro-radiometer in laboratory experiments. This makes possible to take into account properly atmospheric absorption and to estimate the total radiated power for each fire region, thereby providing a figure for the “radiated fire intensity”. Heat radiated per unit area is estimated also by integration over time of radiated power.

In order to be able to estimate the total released power, a series of laboratory experiments has been conducted to compare radiated power and heat values (obtained from IR measurements) with total power and heat values (derived from heat of combustion and fuel consumption). The relationship obtained makes possible to estimate forest fire intensity from IR measurements alone.

Two-dimensional thermal analysis of organic materials by IR thermography

Junko Morikawa, Toshimasa Hashimoto,
Tokyo Institute of Technology,
2-12-1, O-okayama, Meguro-ku, Tokyo 152-8552, Japan
tel&fax: 81-3-5734-2435, e-mail : jmorikaw@o.cc.titech.ac.jp. toshimas@o.cc.titech.ac.jp

Keywords: two-dimensional thermal analysis, latent heat, differential image, thermal diffusion

1. Introduction

Two-dimensional micro scale thermal analysis for the measurement of latent heat released from the organic materials and cells during phase transition is proposed by use of high-speed infrared focal plane arrays. The thermo graphically observed latent heat spreading over the homogeneous / inhomogeneous structures of the materials allow estimating the two-dimensional distribution of the thermal properties. The influence of the inter-cellular and intra-cellular thermal diffusion of the released latent heat in the freezing of biological tissues is presented.

2. EXPERIMENTAL

2.1 Instruments

2.1.1 IR (Infra red) FPA (Focal plane arrays) system

The schematic diagram of apparatus is shown in Fig. 1. When temperature wave (TWA)[1)] is inputted, function generator and lock-in amplifier are also settled in the system. The specimen is directly put on the thin gold plate (with thickness 100 μm) fixed on a Peltier chip with a heat sink in a vessel. The specimen holder was controlled at a constant temperature scan rate of 1~80°C/min in the temperature range of –20°C~150 °C. To avoid condensation of water on a specimen surface the atmosphere in the vessel is filled with dried nitrogen gas. The observation of temperature was carried out through a sapphire glass window.

High-speed IR FPA system, Phoenix (Indigo) and Radiance HS

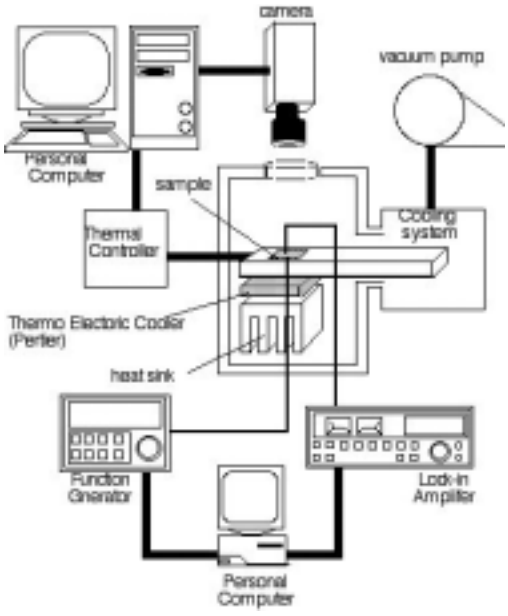

Fig.1 Schematic diagram of high-speed IR measuring system with TWA technique.

(Raytheon), having an indium-antimony (InSb) sensor array of 320x256, or 256x256 pixels with the optimum wavelength 3μm~5μm was used for the measurement. The frame rate for taking image was selected 250 ~1000 frames/s (4msec~1msec per one picture) in this study. By silicon germanium made microscopic lens, it can visualize the area size of 1.9mmx 1.9mm corresponding to the spatial resolution of 3.0μm~ 7.5μm. The length and distortion are calibrated by using a standard micro-scale (Nikon).

3. Results and Discussion

3.1 Freezing of tissues of plant cells:

Fig. 2 shows IR image photographs of onionskin cell at a moment of freezing. The brighter parts indicate high temperature while dark parts relatively low temperature. The release of latent heat proceeds, which is observed as a proceeding of a temperature rise in each single cell. It is observed randomly in the unit cell scale, cell by cell, but the freezing of adjacent cells were rarely observed at the same time. A temperature rise starts at a point on the cell wall at an inter-cellular interface and propagates to the whole part of the cell. It suggests that the cell wall has some important roles from the viewpoint of thermal behavior such as controlling thermal diffusion.

The inter-cellular thermal analysis is shown in Fig.3 for alphabetically numbered pixels A~E in the five different adjacent cells. At a moment of freezing after being super cooled to –8.5°C, an obvious temperature rise generated by the release of latent heat from each cell is observed in the complicated way.

In each pixel, characteristic profile is obviously observed as a superposition of several peaks, that is, one main peak and several smaller side peaks. The highest peak in each pixel results from the latent heat on the freezing of the cell itself and the temperature rise is almost constant at 5°C. On the other hand, the smaller peaks are induced by the heat conduction from the adjacent cells, in which a latent heat is generated at a different time. The peak height of smaller side peak corresponds to the distance from the influential cell. The summation of temperature rise of all pixels corresponds to the thermo grams of the conventional thermal analysis.

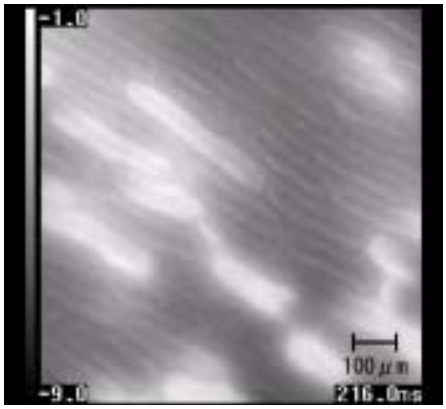

Fig.2. Two-dimensional IR images of onion skincells just at a moment of freezing in the cooling

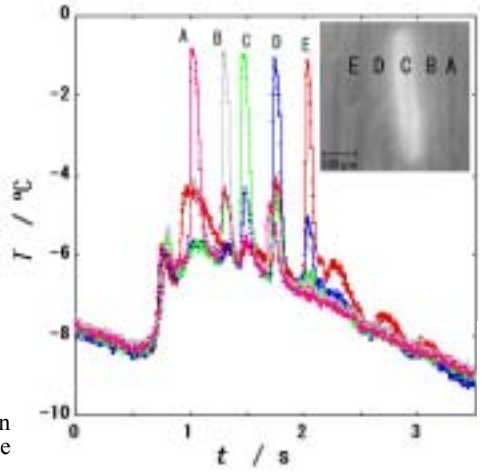

Fig. 3 Temperature profiles at pixels A, B, C, D, and E in neighbouring cells in a cooling scan.

Reference

1) J. Morikawa, T. Hashimoto Jpn. J. Apply. Phys., 37, (1998) L1484

Thermal characterization of multi-layer polymer films by IR thermography

Junko Morikawa, Toshimasa Hashimoto,
Tokyo Institute of Technology,
2-12-1, O-okayama, Meguro-ku, Tokyo 152-8552, Japan
tel&fax 81-3-5734-2435 e-mail jmorikaw@o.cc.titech.ac.jp, toshimas@o.cc.titech.ac.jp
Roberto Li Voti, Universita di Roma "La Sapienza",
Via Scarpa, 14-00161 Roma Italy
tel 06-49916540, fax 06-44240183 e-mail Roberto.Livoti@uniroma1.it

Keywords: temperature wave, thermal interface, thermal diffusivity, thermal effusivity, thermal impedance

1. INTRODUCTION

To design and control the thermal interface is one of the important challenge especially in industry in view of the efficient power control. The methodology and experimental technique to quantify and determine the thermal characterization of the interface is still under discussion. In this study the thermal characterization of the cross section of polymer film layers including the interface was performed by an edge view observation of IR thermography and the Fourier- transformed phase shift image. An analytical simulation of thermal wave in multi layers assuming the thermal impedance on the interface was applied to analyse the thermal characterizatin of the interface.

2. EXPERIMENTAL

2.1 Instruments

2.1.1 IR (Infra red) FPA (Focal plane arrays) system

InSb FPA (Phoenix, Indigo Systems, and Radiance HS, Raytheon) was used which is sensitive in 3~5μm spectral band. The array of 256x256 pixels and IR optics allowed 1.9x1.9mm^2 specimen area giving a spatial resolution of 7.5μm~3μm/pixel with SiGe micro lens (ai-phase Co., Ltd.). The frame rate varied from 60Hz to 5000Hz, corresponding to the pixel size 256x256~64x64. The time resolved IR photograph of the temperature wave on the specimen was obtained in the above conditions, and

simultaneously the time profiles of temperature at all pixels were obtained. The measurement was performed both in the atmospheric and the reduced pressure.

3. Results and Discussion

3.1 Phase image of temperature wave

The cross section of the three layered polyimide films with and without heat conductive grease compounds at the interface were observed by IR thermography with different frequency of temperature wave generated by a.c. Joule heating on the outside surface. The time resolved IR thermograph (Fig.1) was analyzed at each pixel as phase and amplitude image by Fourier transform. Fig. 2 shows the Fourier transformed phase image at 1Hz temperature wave.

3.2 Numerical simulation of the thermal boundary resistance

The experimental data of phase shift have been compared and fitted by appropriate numerical simulations of the thermal field in the multilayered polymeric samples. Since the geometry of the interfaces and the heater have both a plane symmetry (1D geometry) the theoretical approach analyses the thermal field in each layer as a superposition of forward and backward plane thermal waves in the out of plane direction. [1]. The phase and amplitude jumps observed experimentally, indicates the presence of a thermal boundary resistance between each layer. This effect has been modelled by introducing thin surface skins of poor conductors (air, grease) among polymeric layers. The numerical analysis allows estimating the thickness of these skin layers of less than3 μm.

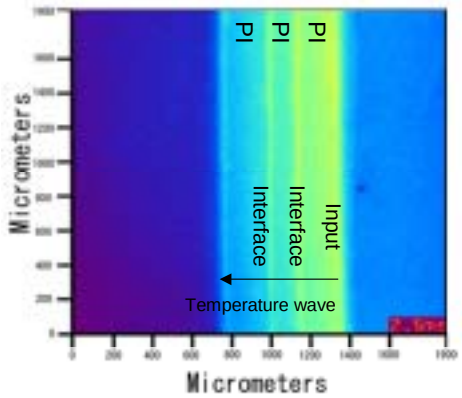

Fig.1 Thermal image of Interface of a cross section of three layered polyimide (125μm-75μm-125μm) films with the impression of temperature wave by IR-FPA in 1.9mmx1.9mm area size with 7.5μmx7.5μm pixel size.

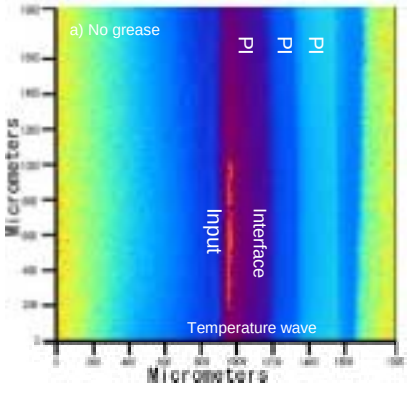

Fig.2 Fourier transformed phase image of three layered polyimide film with an applied temperature wave (frequency:1Hz) captured by IR-FPA with 7.5μmx7.5μm pixel size.

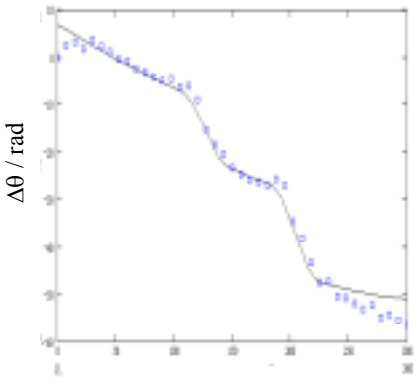

Fig.3 Numerical simulation (line;—) and the experimental results (circles; ○) of phase shifts Δθ of temperature wave (1Hz) in the three layered polyimide films.

Reference [1] M.Bertolotti, M.Firpo, **R.Li Voti,** S.Paoloni, C.Sibilia, F.Tani and G.L.Liakhou - *Thermal characterization of multilayer material*, Progress in Natural Science Suppl. Vol.6 p.219 (1996).

IR thermographic evaluation of thermal diffusivity anisotropy: comparative analysis of some algorithms

V. Vavilov*, D.D. Burleigh**, V. Shiryaev*

*Tomsk Polytechnic University, Russia 634028, Tomsk, 28 Savinykh St., 7
E-mail: vavilov@introscopy.tpu.ru
**Surfside Consulting, Box 178232, San Diego, CA, U.S.A.
E-mail: ddburleigh@aol.com

Anisotropic thermal diffusivity of orthotropic materials can be characterized in Cartesian coordinates by two lateral (α_x, α_y) and one transverse (α_z) components. The transverse component can be routinely determined by using some classical techniques of which the Parker's method is probably the most popular. Evaluating lateral components of thermal diffusivity by using classical methods represents a more difficult task which requires either preparing material samples cut in particular directions or solving 3D heat conduction problems. In the latter case, the measurement of lateral, 'in plane' diffusivity requires the injection of a heat pulse into the material while monitoring the propagation of the heat in lateral directions. The heat pulse spatial distribution may be a Gaussian spot, square area, line heating, etc. To interpret temperature information that is contained in an image sequence, a *spatial Fourier transformation* technique is typically used.

In this study, we have used three approaches conventionally named by I.Filippi et al. [1], J.-C.Krapez et al. [2] and P.Bison et al. [3]. The procedure of determining anisotropic components of CFRP thermal diffusivity is illustrated with Fig. 1. A slit-mask "footprint" (Fig.1a) is converted into a Fourier spectrum where a basic frequency can be well detected as a specific spike (Fig. 1b). The Fourier temperature logarithmic ratio curve shown in Fig. 1c allows reliable determining the α_x component by the curve slope. The same curves for the α_y component shown in Fig. 1d, e are more noisy but still significant while applying a data fitting procedure.

The corresponding CFRP diffusivity values have been found as follows: $\alpha_x = 4.6 \cdot 10^{-7}$ m^2/s, $\alpha_y = 19.1 \cdot 10^{-7}$ m^2/s and $\alpha_z = 4.6 \cdot 10^{-7}$ m^2/s.

By producing artificial image sequences, we have analyzed the following parameters which affect accuracy of determining lateral diffusivity: 1) finite heat pulse duration, 2) acquisition interval, 3) time period chosen for fitting logarithmic curves, 4) ratio between sample surface and heated area, and 5) noise.

The images were calculated numerically using the ThermoCalc-6L program (Innovation, Ltd., Russia). Forty three data sequences of up to 250 images in a 200x200 format were analyzed to determine α_x, α_y of Carbon Fiber Reinforced Plastic (CFRP) composite.

The conclusions have been as follows.

- It has been shown that providing the Dirac-pulse behavior of a heat pulse in time is more important than shaping a heat pulse in space. However, in case of slit-mask heating, some results appeared better when longer heat pulses were applied.
- With noise-free data, accurate results appear at many Fourier frequencies except those where the heat pulse spectrum energy drops to zero.
- In case of slit-mask heating, choosing a spatial area on sample surface has proved to be an important factor. Another crucial factor influencing identification accuracy has been the time period where the temperature data is to be processed that is particularly true on sample rear surface
- Noise might seriously corrupt calculated diffusivity values if the noise amplitude is comparable to the amplitude of sample excess temperatures. From this point of view, the

slit-mask approach seems to be more noise-resistant due to the presence of a carrier frequency.

- Experimentally, the lateral diffusivity components were found to be α_x =(4.5-6.5)·10^{-7} m^2/s and α_y =(17.9-20.6)·10^{-7} m^2/s in case of unidirectional CFRP composites. The value of α_z was found to be 4.6·10^{-7} m^2/s.

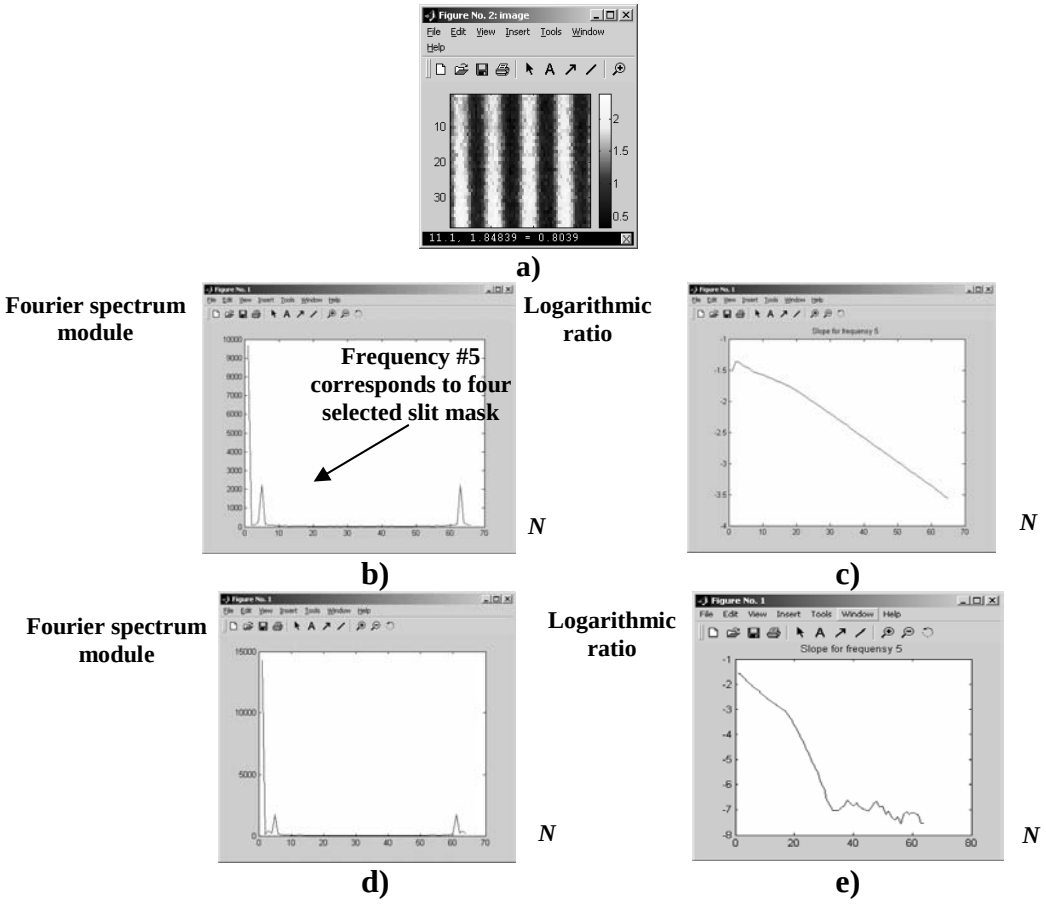

Fig. 1. Evaluating thermal diffusivity by using a slit-mask method (CFRP sample, slit mask period 10 mm, heating time 3 s):

a – area of interest, *R*-surface,

b - α_x component, Fourier spectrum,

c - $Ln[\tilde{\tilde{T}}(\omega_x,0,z,\tau)/\tilde{\tilde{T}}(0,0,z,\tau)] = Ln[\Phi(\omega_x,0)/\Phi(0,0)] - \alpha_x\omega_x^2\tau$ as a function of time,

d - α_y component, Fourier spectrum,

e - $Ln[\tilde{\tilde{T}}(\omega_y,0,z,\tau)/\tilde{\tilde{T}}(0,0,z,\tau)] = Ln[\Phi(\omega_y,0)/\Phi(0,0)] - \alpha_y\omega_y^2\tau$ as a function of time

References

1. I. Philippi, J.-C. Batsale, D. Maillet, A. Degiovanni. Measurements of thermal diffusivities through processing of infrared images. // Rev. Sci. Instrum., Jan. 1995. V. 66(1). P. 132-138.

2. J.-C. Krapez, L. Spagnolo, M. Frieß. Measurement of in-plane diffusivity in non-homogeneous slabs by applying flash thermography. // Intern. J. of Thermal Sciences, 2004. V. 43. P. 967-977.

3. P.G. Bison, E. Grinzato, S. Marinetti. Local thermal diffusivity measurement. // J. Quant. Infr. Thermogr., 2004. Vol. 1. No. 2. P. 241-250.

Ageing evaluation of Thermal Barrier Coating: comparison between Pulsed Thermography and Thermal Wave Interferomety.

P.G. Bison[1], F. Cernuschi[2], E. Grinzato[1], S. Marinetti[1], D. Robba[2]

[1] CNR-ITC, C.so Stati Uniti 4, 35127 Padova, Italy - paolo.bison@itc.cnr.it
[2] CESI, via Rubattino 54, 20134 Milano, Italy - cernuschi@cesi.it

Ceramic thermal barrier coatings (TBC) are widely applied for protecting from combustion gases hot path components of gas turbines for both aero- and land- based applications. In order to prevent the detachment of TBC, it would be essential to monitor their degradation in terms of sintering kinetic. As sintering strongly affects also the thermal diffusivity of TBC, the idea is to measure the latter parameter to account for the former.
The technique to measure thermal diffusivity variation with ageing was recently presented [1]. Tests and results concerning the in-depth thermal diffusivity on TBC specimens artificially aged were reported. Pulsed Thermography together with the model that leads to the identification of diffusivity for both in-depth and lateral diffusion were used for that purpose.
Thermal Wave Interferometry (TWI) is a photothermal technique used to evaluate thermal parameters when steady periodic conditions are applied to the material [2]. Developed in the eighties of the last century, it was recently considered as a tool for the evaluation of the coatings thermal properties, being them either isotropic and anisotropic [3].
In the present work a recall of the main results obtained with the Pulsed Thermography for this application is given. After that the TWI technique is used to measure again the in-depth thermal diffusivity of the same samples artificially aged and yet tested with Pulsed Thermography. With this completely alternative and non invasive technique we want to validate what was obtained in the previous work.
The work is complemented with an analysis of the conductivity behaviour of porous material, such as the TBCs, when pores are evacuated (e.g. when measured with a laser flash technique in vacuum chamber), filled with air at atmospheric pressure (as in Pulsed Thermography test at ambient conditions), or filled with high pressure gases (as during working conditions inside the combustion chamber of a turbine).

Bibliography

[1] P.G. Bison, F. Cernuschi, E. Grinzato, S. Marinetti, D. Robba. AGEING EVALUATION OF THERMAL BARRIER COATINGS BY THERMAL DIFFUSIVITY. Presented to the 8th AITA. Submitted to *Infrared Physics and Technology*.
[2] D.P. Almond, P.M. Patel. Photothermal Science and Techniques. Chapman & Hall, 1996.
[3] T.D. Bennet. Determining Anisotropic Film Thermal Properties Through Harmonic Surface Heating With a Gaussian Laser Beam: A Theoretical Consideration. Journal of Heat Transfer, June 2004, Vol. 126, pp. 305-311.

Two dimensional velocity mapping in the case of three dimensional transient diffusion: "Flash" method and infrared image sequence analysis

M. Bamford*, J.C. Batsale*, O. Fudym**, D. Reungoat*
* *TREFLE-ENSAM, UMR 8508 CNRS, 33405 Talence* Cedex – FRANCE –
Phone : (33) 5 56 84 54 25 -Fax : (33) 5 56 84 54 36
Jean-christophe.batsale@bordeaux.ensam.fr, matthieu.bamford@bordeaux.ensam.fr, reungoat@enscpb.fr
** *Ecole des Mines d'Albi Carmaux, Laboratoire de Génie des Procédés des Solides Divisés, Campus Jarlard, UMR 2392 CNRS-EMAC,* 81013 *Albi* Cedex 09, – FRANCE –
Phone : (33) 5 63 49 30 24 -Fax : (33) 5 63 49 32 43
olivier.fudym@enstimac.fr

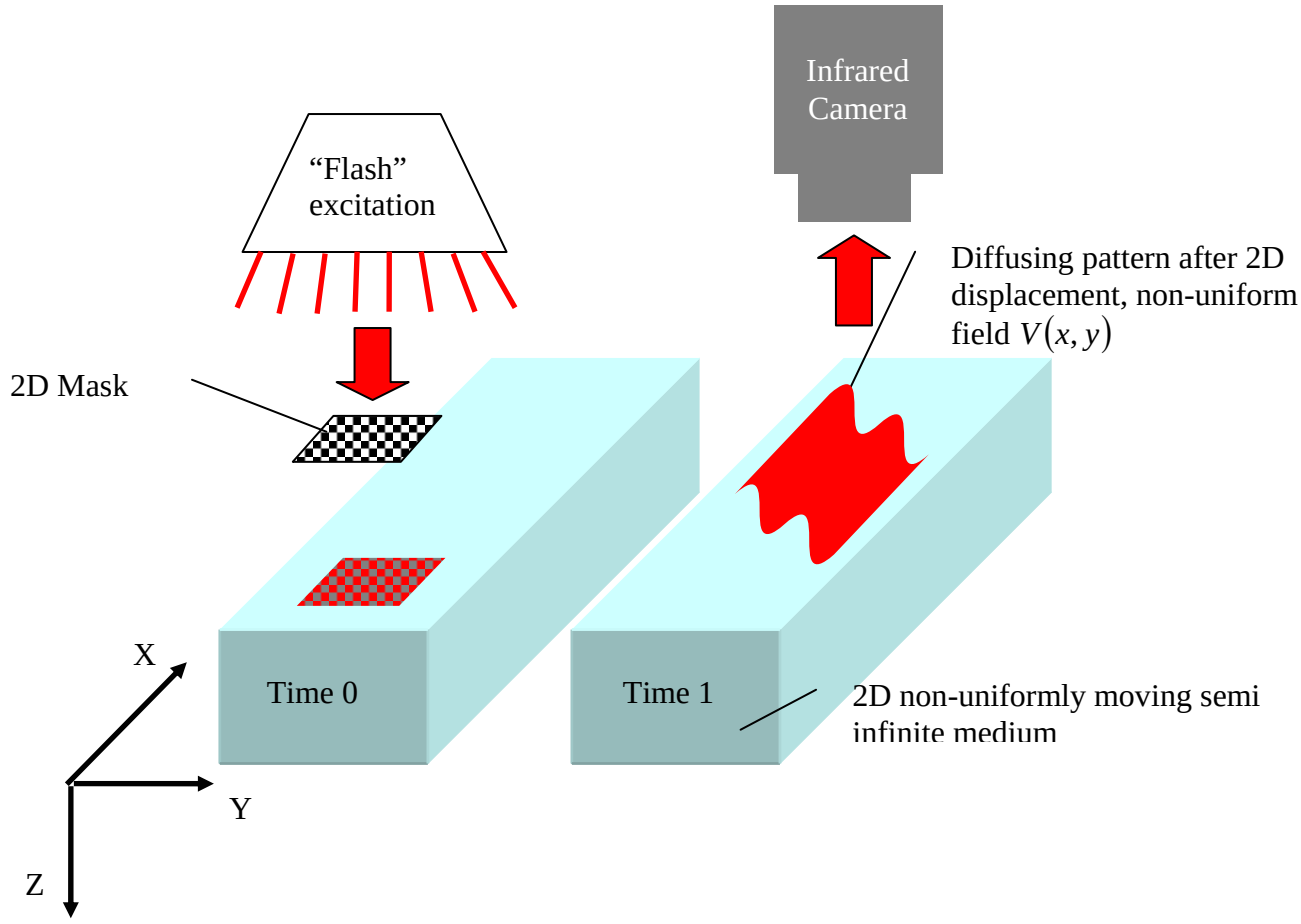

Keywords:
Velocity field estimation, Infrared thermography, Flash method

Abstract:

The aim of this work is to study the two dimensional velocity mapping from the processing of infrared image sequences after a flash experiment. This work takes place in a scientific context where a lot of papers related to the "optical flow estimation" from the processing of visible image sequences exist (see Jähne et al. 1998). These recent methods consist in solving the local "violated" conservation equations such as:

$$\frac{\partial I(x,y,t)}{\partial t}+V_x(x,y)\frac{\partial I(x,y,t)}{\partial x}+V_y(x,y)\frac{\partial I(x,y,t)}{\partial y}=a\cdot\left(\frac{\partial^2 I(x,y,t)}{\partial x^2}+\frac{\partial^2 I(x,y,t)}{\partial y^2}\right)+g(x,y,t)$$

Where $V_y(x,y)$ (respectively $V_x(x,y)$) is the velocity component versus y (respectively x) at location (x,y), $I(x,y,t)$ is the image brightness at location (x,y), $g(x,y,t)$ stands for a local source term, and a is the diffusivity.

When replacing $I(x,y,t)$ with a signal proportional to temperature $T(x,y,t)$ in the case of infrared images, it should be noticed that the previous equation is close to the heat diffusion equation within two dimensional thin plates. Therefore it seems to make sense to transpose the methodology developed in the visible spectrum to infrared images.

Unfortunately, excepted in the case of adiabatic thin layers, heat transfer is often three-dimensional, transient, and the diffusion versus the thickness of the medium is an important component that can not be neglected in a simplified model.

Such phenomena can be dealt with when considering some separability properties in the case of the "Flash" excitation.

Let $T(x,y,z=0,t)$ be the infrared image intensity at location $(x,y,z=0)$ and time t, and then consider that it is proportional to the surface temperature. The governing heat equation in the semi-infinite medium is:

$$\frac{\partial T(x,y,z,t)}{\partial t}+V_x(x,y)\frac{\partial T(x,y,z,t)}{\partial x}+V_y(x,y)\frac{\partial T(x,y,z,t)}{\partial y}=a\cdot\left(\frac{\partial^2 T(x,y,z,t)}{\partial x^2}+\frac{\partial^2 T(x,y,z,t)}{\partial y^2}+\frac{\partial^2 T(x,y,z,t)}{\partial z^2}\right)+\Phi(x,y,z,t)$$

We know (see [1], chap. 5) that for semi-infinite media with constant properties in the z direction $T(x,y,z,t)=T_{x,y}(x,y,t)\cdot T_z(z,t)$ where $T_z(0,t)$ is known analytically. Therefore if we note $T_{x,y}(x,y,t)=\dfrac{T(x,y,z=0,t)}{T_z(0,t)}$, this new pseudotemperature distribution verifies a 2D general conservation equation such as:

$$\frac{\partial T_{x,y}(x,y,t)}{\partial t}+V_x\frac{\partial T_{x,y}(x,y,t)}{\partial x}+V_y\frac{\partial T_{x,y}(x,y,t)}{\partial y}=a\cdot\left(\frac{\partial^2 T_{x,y}(x,y,t)}{\partial x^2}+\frac{\partial^2 T_{x,y}(x,y,t)}{\partial y^2}\right)+\phi(x,y,t)$$

We may thus implement the techniques mentioned in [2] to study the optical flow variations and deduce both the medium thermal diffusivity and a 2D velocity mapping from brightness variations study in IR images sequences. Nevertheless precautions must be taken to avoid noise amplification due to the division of $T(x,y,z=0,t)$ by $T_z(0,t)$. We will also compare the efficiency of various estimators and numerical schemes used for this purpose with respect to accuracy, robustness, and computation time.

References:

[1] Maillet D., Batsale J.C, Degiovanni A., André S., Moyne C., Thermal Quadrupoles, solving the heat equation through integral transforms (J. Wiley and sons 2000)

[2] Bernd Jähne, Horst W. Haussecker, Hanno Scharr, Hagen Spies, D. Schmundt, Uli Schurr: Study of Dynamical Processes with Tensor-Based Spatiotemporal Image Processing Techniques. ECCV (2) 1998: 322-336

Application of the flash method to rods and tubes

Agustín Salazar[1], Alberto Oleaga[1], Fernando Alonso[2] and Idurre Sáez-Ocáriz[2]

[1]*Departamento de Física Aplicada I, Escuela Técnica Superior de Ingeniería, Universidad del País Vasco, Alameda Urquijo s/n, 48013 Bilbao, Spain. E-Mail: agustin.salazar@ehu.es*
[2]*Centro de Tecnologías Aeronáuticas (CTA), Parque Tecnológico de Álava, Juan de la Cierva 1, 01510 Miñano, Spain.*

The flash method is the most acknowledge technique to measure the thermal diffusivity at high temperatures. It consists of heating the front surface of an opaque slab by a short laser pulse and detecting the temperature evolution at its rear surface. The thermal diffusivity is obtained by measuring the time corresponding to the half maximum of the temperature rise ($t_{1/2}$), that is related to the thermal diffusivity through the expression: $t_{1/2} = 0.1388L^2/D$, where L is the sample thickness and D is the thermal diffusivity. This procedure works under ideal conditions: negligible laser pulse duration and heat losses.

We have extended the classical flash method to be used with rods and tubes. We proceed as follows. First, the temperature distribution when these samples are illuminated by a modulated light beam is calculated. Then, using the inverse Laplace transform, the temperature evolution of the sample after being heated by a short light pulse is obtained.

Let us consider an infinite and opaque hollow cylinder with an outer radius a and an inner radius b, that is illuminated uniformly by a modulated light beam of intensity I_o and frequency f ($\omega = 2\pi f$). Its cross-section is shown in Fig. 1. The temperature oscillation at any point of the cylinder can be written as[1,2]

$$T(r,\phi,\omega) = \sum_{m=-\infty}^{\infty} A_m J_m(qr) e^{im\phi} + \sum_{m=-\infty}^{\infty} B_m H_m(qr) e^{im\phi} \qquad (1)$$

where $q = \sqrt{i\omega/D}$ is the thermal wave vector, and J_m and H_m are the mth order of the Bessel and Hankel functions of the first kind respectively. The first term in Eq. (1) represents the ingoing cylindrical thermal wave starting at the sample surface, while the second one is the corresponding reflected wave at the inner surface. A_m and B_m are obtained from the heat flux continuity at the cylinder surfaces. In this way an analytical solution is obtained

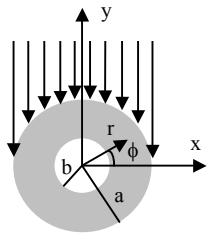

Fig.1.- Geometry

$$T(r,\phi,\omega) = \frac{I_o}{2Kq} \sum_{m=-\infty}^{\infty} \frac{(-i)^m}{\pi(1-m^2)} \cos\left(m\frac{\pi}{2}\right) e^{im\phi} \times \frac{H'_m(qb)J_m(qr) - J'_m(qb)H_m(qr)}{J'_m(qa)H'_m(qb) - J'_m(qb)H'_m(qa)} \qquad (2)$$

where J'_m and H'_m are the derivatives of the Bessel and Hankel functions respectively. A simplified expression can be found for a solid cylinder by making $b = 0$.

Now, using the inverse Laplace transform, the temperature evolution after the absorption of a light pulse can be calculated. Following this procedure the temperature rise of the rear surface of three stainless steel samples (K = 14.5 $Wm^{-1}K^{-1}$, D = 3.8 mm^2s^{-1}) after the absorption of a Dirac pulse has been simulated: (a) a 3 mm-thick-slab, (b) a solid cylinder of 3 mm in diameter whose temperature is measured at the bottom pole, $\phi = -\pi/2$, and (c) a hollow cylinder with an outer diameter of 3 mm and an inner diameter of 2 mm, whose temperature is measured at $\phi = -\pi/2$. Their normalized temperature histories are shown in Fig. 2. Calculations performed for a wide variety of materials indicate that the time required by the back surface to reach the half of the maximum

temperature rise ($t_{1/2}$) only depends on the thermal diffusivity and on the sample size, through the equation:

$$t_{1/2} = A\frac{d^2}{D}, \qquad (3)$$

where d is the thickness in the case of a slab or the diameter ($2a$) in the case of a cylinder. For slabs A is the well-known 0.1388, while for solid cylinders we found $A = 0.1068$. A simple formula has not been encountered for hollow cylinders.

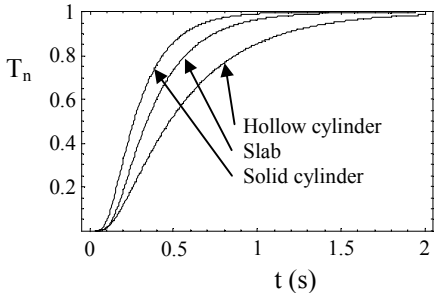

Fig.2.- Calculation of normalized temperature

The validity of the theory has been tested experimentally by measuring the following AISI-304 stainless steel samples: A rod whose diameter is 4 mm, a hollow cylinder with an outer diameter of 2.05 mm and an inner diameter of 1.55 mm, and a 2 mm-thick-plate that has been used as a reference. The samples have been illuminated by a 6 kJ flash lamp and their rear surface temperature has been measured by an infrared camera (Thermacam SC 2000 from FLIR Systems) at a frequency rate of 50 frames per second.

In Fig. 3 the temperature rise after the flash light for the three samples under study is shown by dots. In the case of the two cylindrical samples the temperature is the average of 100 pixel placed along the cylinder axis. In the three cases the temperature reaches a constant value at long times after the flash light, indicating that the influence of heat losses is negligible. Using Eq. (3), D = 3.76±0.10 mm^2/s and D = 3.70±0.14 mm^2/s are obtained for the slab and the rod respectively. The continuous lines in Fig. 3 are the fit to the theoretical model. The fitted thermal diffusivity of the tube is 3.84±0.16 mm^2/s, while for the slab and for the rod the same thermal diffusivity values as those found using Eq. (3) are obtained. All values are consistent and fall inside the typical thermal diffusivity values of AISI-304 that can be found in the literature (3.7-4.0 mm^2/s).

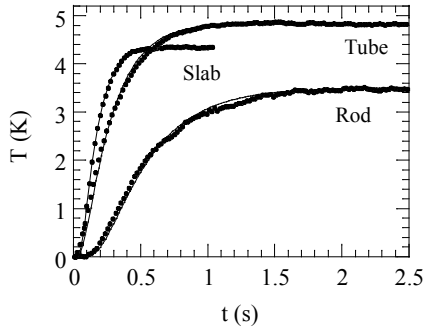

Fig. 3.- Experimental results

Finally, let us compare the flash method as applied to a slab and to the inner side of a tube (i.e., the temperature is measured at $r = b$ and $\phi = +\pi/2$) with the same thickness as that of the slab. It is surprising that the corresponding temperature rise curves are almost indistinguishable even for tubes of small radii. Figure 4 shows the error in the calculated thermal diffusivity of an AISI-304 tube 2 mm thick as a function of the outer diameter, a, when Eq. (3) with A = 0.1388 is applied. This result suggests the possibility of applying the classical flash method to a wide variety of curved plates.

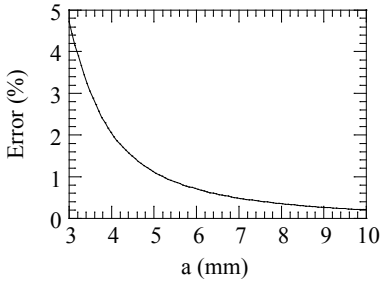

Fig. 4.- Thermal diffusivity error

This work has been supported by the Ministerio de Educación y Ciencia (MAT2005-02999).

[1]J. Sinai and R.C. Waag, *J. Acous. Soc. Am.* **83**, 1729 (1988).
[2]Y.S. Joo, J.G. Ih, and M.S. Choi, *J. Acous. Soc. Am.* **103**, 900 (1998).

Thickness measurement system of multilayer films

With radiation measurement techniques every material can be analysed in such a way, that even the smallest differences in radiation density can be registered by the arsenco sensor and processed by any computer.

The measurement of heat conductivity, capacity, or specific mass in thin layers requires a precise, very accurate synchronisation between a pulse source, the IR sensor, and the electronic. In conjunction with different energy pulse technologies, the high-speed arsenco sensor delivers information about layer thickness, adhesion, layer quality and other factors of interest for industrial production. The measured results can indicate porosity, formation of cracks or faults within a layer, chemical variations or residual voltage. The measurement is done without contact and causes no damage.

The measuring system allows the fast and ongoing monitoring of running production processes, the evaluation of product quality during production, the measuring of heat conductivity in very thin layers, or the selective measuring of a layer thickness to the micrometer - even in multiple superimposed layers.

The new sensor is suitable for the measurement of extremely fast events in a wide spectrum. Its advantages compared to conventional sensors are its high spectral flexibility, exact synchronisation via external pulse sources, software-supported access to the integration and readout time of the individual sensor elements, and the high readout dynamic.

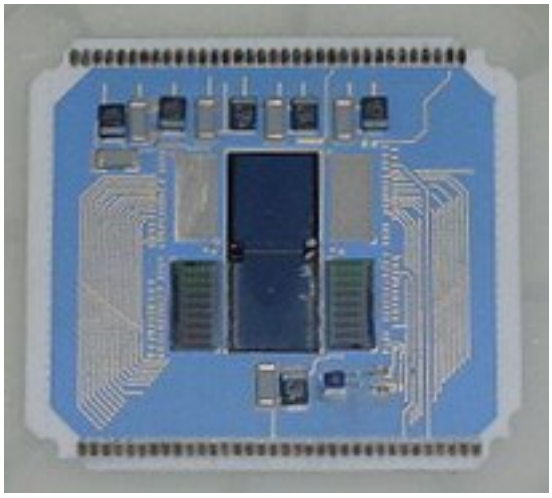

arsenco ag Industriezone Schächenwald Tel: +41 (0)41 875 75 00 info@arsenco.com
CH – 6460 Altdorf, Switzerland Fax: +41 (0)41 875 75 20 www.arsenco.com

A semi-analytical model for the temperature distribution of thermo-inductive heating

B. Oswald-Tranta, G. Wally*, J. Oswald*[+]
** Institute for Automation, University of Leoben, Austria*
[+] *Institute for Physics, University of Leoben, Austria*
beate.oswald@unileoben.ac.at

PREFERENCE: oral presentation

In the case of thermo-inductive heating the workpiece is heated by induced eddy currents, while an infrared camera is recording the temperature distribution of the surface. Irregularities and failures in the surface or closely below the surface cause anomalies in the temperature distribution. Therefore, the thermo-inductive method can be used to detect failures or cracks in electric conductive materials, as e.g. in metals.

Mid- and high frequency (20-300kHz) is used to induce the eddy current. Because of the well-known skin effect the eddy current decays exponentionally below the surface. The value of the penetration depth depends on the frequency and on the material properties as e.g. the magnetic permeability value. Magnetic steel with high relative permeability has a very small penetration depth of the eddy current (0.03mm at 200kHz) and non-magnetic steel has a much higher penetration depth (about 0.8mm) at the same frequency. Experiments show that in non-magnetic steel the corners of a workpiece are not warmed-up (see Figure 1). In contrast, the tip of a crack becomes warmer than other parts.

A semi-analytical model has been developed to calculate this phenomenon. In a first step the distribution of the electrical current streamlines around the crack is determined (see Figure 2). This is done with the aid of an appropriate conform transformation, which is transforming a Cartesian grid line system to the geometry of the surface crack, while keeping the angle of 90° between the grid lines. In Figure 2 one can see, that the current streamlines don't penetrate into the corners, but densify around the tip of the crack. In a second step the generated heat along the streamlines is determined. In the last step the propagation of the heat is calculated according to the heat conductivity. In such way the temperature distribution can be calculated (see Figure 3). The comparison of the calculated and measured results show very good agreement.

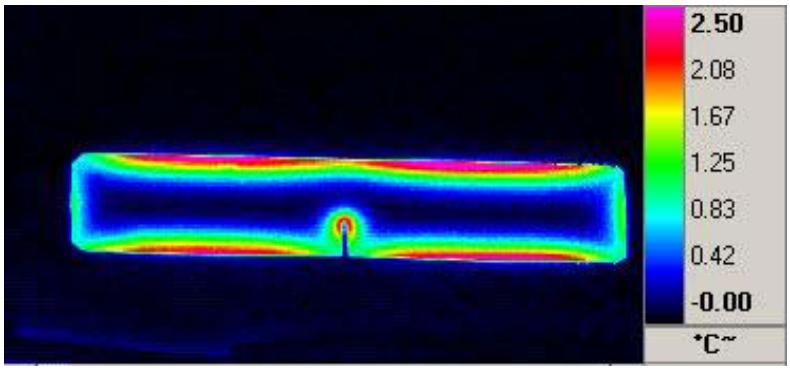

***Figure 1**: Infrared image of an inductive heated workpiece after 0.2 sec.*

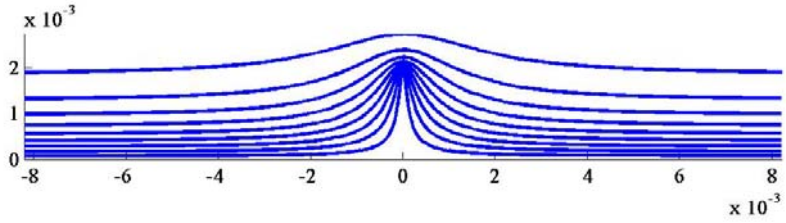

***Figure 2**: Calculated electrical current strealines around a surface crack with a depth of 2 mm at position of (0,0).*

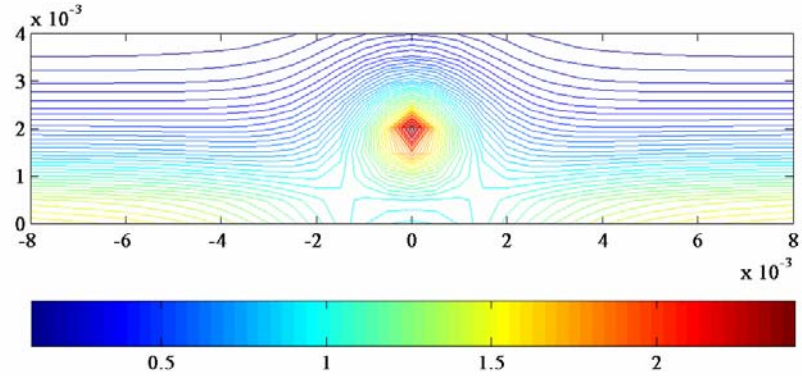

***Figure 3**: Calculated temperature around a surface crack with a depth of 2 mm at position of (0,0).*

Some peculiarities of modeling defects in polyaramide composite materials

W. Świderski*, V. Vavilov**

*Military Institute of Armament Technology, Zielonka, Poland
E-mail: waldemar.swiderski@wp.pl
**Tomsk Polytechnic University, Tomsk, Russia
E-mail: vavilov@introscopy.tpu.ru

In military, composites are increasingly used in manufacturing light ballistic protections which withstand well bullets and small arm fragments. Such composites are typically made on the basis of very resistant aramide and polyethane fibers joined with phenolic and polyurethane resins and other elastic mixtures. They are light-weight, non-corrosive and flexible to fit well surface to be protected. Composites can be also applied in conjunction with steel sheets and ceramics, thus increasing their protecting efficiency.

The defects which can appear in the above-mentioned composites are typically deficiencies in glue layers, as well as stratifications and delaminations occurring if a composite is impacted by 'hard objects'.

Thermal nondestructive testing (NDT) is regarded as a fairly relevant technique for detecting defects in composite materials. In this paper, the accent is made on some inspection and modeling peculiarities which require further improvement of defect models to simulate possible modifications of sample geometrical and thermal properties in defect sites.

Five samples made of polyaramide layers (0.6 mm-thick) joined with formaldehyde resin glue (0.04 mm-thick) were inspected (see Fig. 1). Defects were simulated by Teflon inserts and air gaps. All samples were subjected to both front- (F) and rear (R)-surface tests (τ_h-heat pulse duration; Q-heat power density).

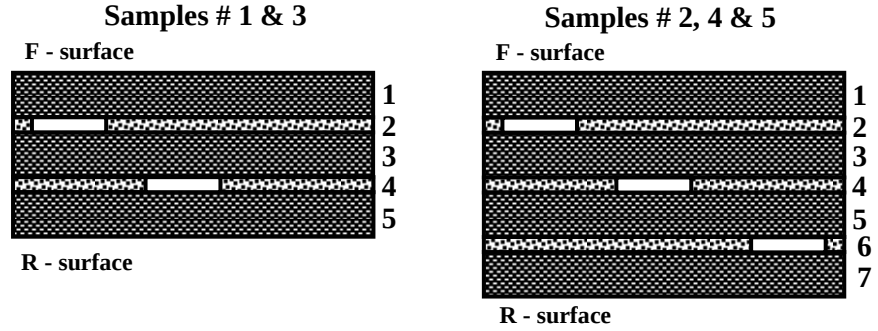

Fig. 1. Sample schemes

The thermal properties of the materials are assumed as follows: aramide – conductivity perpendicular to fibers $\lambda_{\perp} = 0.142 W/(m \cdot K)$; conductivity parallel to fibers $\lambda_{\parallel} = 1.69\ W/(m \cdot K)$; density $\rho = 1330\ kg/m^3$; heat capacity $C = 1047\ J/(kg \cdot K)$; diffusivity perpendicular to fibers $\alpha_{\perp} = 0.1 \cdot 10^{-6}\ m^2/s$; diffusivity parallel to fibers $\lambda_{\parallel} = 1.19 \cdot 10^{-6}\ m^2/s$; formaldehyde resin - $\lambda = 0.2\ W/(m \cdot K)$; $\rho = 1200\ kg/m^3$; $C = 1850\ J/(kg \cdot K)$; $\alpha = 2.22 \cdot 10^{-6}\ m^2/s$; air (in thin gaps) - $\lambda = 0.07\ W/(m \cdot K)$; $\rho = 1.2\ kg/m^3$; $C = 1005\ J/(kg \cdot K)$; $\alpha = 5.8 \cdot 10^{-5}\ m^2/s$; Teflon - $\lambda = 0.23\ W/(m \cdot K)$; $\rho = 2210\ kg/m^3$; $C = 1050\ J/(kg \cdot K)$; $\alpha = 0.99 \cdot 10^{-7}\ m^2/s$.

In experiments, samples were optically heated with a set of lamps that allowed sample F-surface excess temperature to reach 65°C for τ_h=3 s; thus absorbed energy density was estimated to be Q=3.2 kW/m^2. Temperature was monitored with a Thermovision 900 IR thermographic system. The example of experimental results is shown in Fig. 3 where the left column represents the 'optimal' raw image and the right column contains the phasegram.

The theoretical analysis has been done on two defect models shown in Fig. 4. It has been demonstrated that the main difference between these models takes place in a two-sided (R-surface) test. In case of thin composites of which thermal properties are close to air and Teflon, *Defect model #1* might produce higher R-surface temperature under air-filled defects. Introducing *Defect model #2* where the total sample thickness is increased by the thickness of a defect, allows overcoming this difficulty.

Fig. 3. Experimental results in the inspection of Sample #3 (F-surface): optimal source image (left) and phasegram (right)

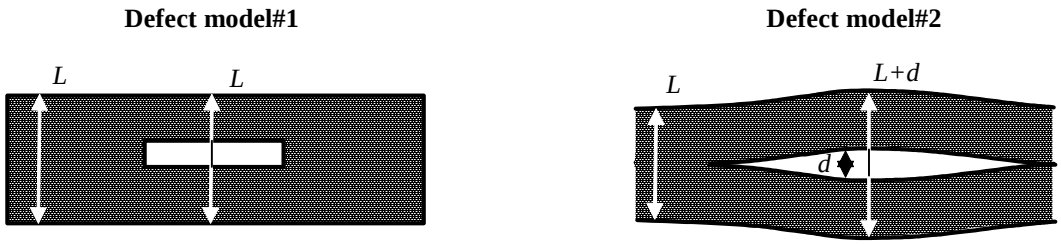

Fig. 4. Modeling defects in composites:

a – Defect model #1 (a defect substitutes a host material, sample thickness remains the same)
b – Defect model #2 (a defect increases a sample thickness)

The following conclusions have been made by comparing theoretical and experimental data:

- Thermal NDT can be applied for evaluating thin polyaramide composites but appearing temperature signals might be low that requires using advanced data processing techniques, such as Pulse Phase Thermography.
- In a one-sided test, defect detectability appeared to be better than in a two-sided test, probably, due to close thermal properties of materials involved and higher temperature signals on F-surface.
- In layered polyaramide structures, simulating defects in formaldehyde resin layers with Teflon or air gaps might lead to inconsistent results because of combination of some factors, such as sample compression or enlargement, modification of sample material thermal properties, etc. Modeling thermal NDT in this case requires further improvement of existing numerical and analytical models.

Detection of thermal bridges in insulating stratified media with thermography- A 3D transient direct model suitable to implement a Total least square estimation method.

Matthieu BAMFORD*, Jean-Christophe BATSALE*, David MOURAND***, Abdelhakim BENDADA**
*TREFLE-ENSAM, UMR 8508 CNRS, 33405 Talence Cedex – FRANCE –
Phone : (33) 5 56 84 54 25 -Fax : (33) 5 56 84 54 36
Jean-christophe.batsale@bordeaux.ensam.fr, matthieu.bamford@bordeaux.ensam.fr,
**LVSN, Université de Laval, Pavillon Adrien-Pouliot, G1K-7P4 – QUEBEC –
Phone : (1) 418 656 2131, ext. 3552 -Fax : (1) 418 656 3159
bendada@gel.ulaval.ca
***THERMICAR, esplanade des arts et métiers, 33405 Talence Cedex – FRANCE –
Phone : (33) 5 56 84 44 70-Fax : (33) 5 56 84 44 79
thermicar@bordeaux.ensam.fr

Keywords:.
Infrared Thermography- Thermal Insulating Systems-Thermal Quadrupoles-Total Least Squares estimation

ABSTRACT:
The aim of this work is to conceive a thermal NDE method in order to detect thermal bridges in insulating stratified media (see figure 1 and see Mourand et al., 1997).

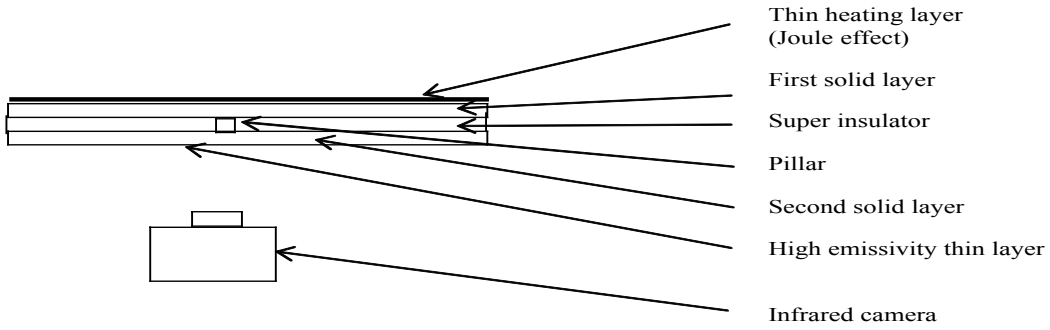

Fig. 1: Scheme of the superinsulating system.

At the opposite to the detection of delamination in composite samples (see for example Balageas et al, 1991), such situation induces strong 3D transient effects which force us to consider the spatial correlation between the pixels (see one simulation example of the temperature field on figure 2)

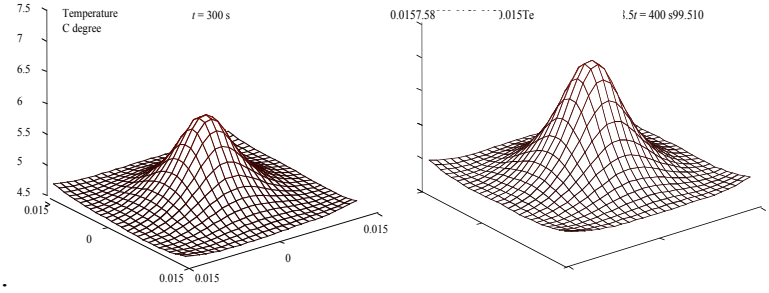

Fig. 2: Examples of evolution of calculated temperature field

In order to avoid a heavy direct model, we develop a suitable approximation of the exact analytical model of heat diffusion:

$$R(x,y)\cdot\left[\frac{\partial T(x,y,z=2e,t)}{\partial t}-a\cdot\left(\frac{\partial^2 T}{\partial x^2}+\frac{\partial^2 T}{\partial y^2}\right)(x,y,z=2e,t)\right]=\frac{Q}{(\rho c\cdot e)^2}\cdot t$$

Such approximation can be implemented with numerical methods by considering only the instantaneous time and space derivatives at each pixel. An estimation of the 2D field of thermal bridges is then available (in fact, such field is represented as a thermal contact resistance field inside the heat transfer model).

The Total Least Squares (TLS) method (see Jähne et al. 1998) is then very suitable because it estimates a thermal resistance $R(x,y)$ at each pixel thanks to an eigenvalue analysis of the following ▮ matrix, which is implemented in an autoregressive fashion:

$$\blacksquare=\begin{bmatrix}\sum_t\left(\frac{\partial^2 T}{\partial x^2}+\frac{\partial^2 T}{\partial y^2}\right)^2 & -\sum_t\left(\frac{\partial^2 T}{\partial x^2}+\frac{\partial^2 T}{\partial y^2}\right)\times t & -\sum_t\left(\frac{\partial^2 T}{\partial x^2}+\frac{\partial^2 T}{\partial y^2}\right)\times\left(\frac{\partial T}{\partial t}\right)\\ sym & \sum_t t^2 & \sum_t\left(\frac{\partial T}{\partial t}\right)\times t\\ sym & sym & \sum_t\left(\frac{\partial T}{\partial t}\right)^2\end{bmatrix}$$

Such situation allows studying the heat losses caused by pillars of very small diameter which are the only thermal bridges between the front and the rear plate. In such cases, the spatial camera resolution or the considered layer thickness are limiting the estimation of the contact real size. Nevertheless, a local thermal resistance can be estimated and constitutes a first approach in order to study very small contacts.

References:

[1] Balageas D., Delpech P., Boscher D., Deom A., "New developments in stimulated infrared thermography applied to non destructive evaluation of laminates", *Review on Progress in Quantitative Non-Destructive Testing*, ED Thompson and Chimienti (Plenum Press, New York, 1991, Vol 10 A, pp 1073-1081

[2] Batsale J.C., Maillet D., Degiovanni A., " Extension de la méthode des quadripoles thermiques à l'aide de transformations intégrales-Application au défaut plan bidimensionnel ", *Int J. Heat Mass Transfer,* 1994, Vol 37, n1, pp111-127.

[3] Bendada A., Maillet D., Batsale J.C. et Degiovanni A. - "Reconstruction of a non-uniform interface thermal resistance by inverse conduction". *Inverse Problems in Engineering* - Vol 6, 1998, p. 79-123.

[4] Bernd Jähne, Horst W. Haussecker, Hanno Scharr, Hagen Spies, D. Schmundt, Uli Schurr: Study of Dynamical Processes with Tensor-Based Spatiotemporal Image Processing Techniques. ECCV (2) 1998: 322-336

[5] Mourand D., Batsale J.C., Battaglia J.L., (2001) Infrared image processing for the evaluation of thermal bridges in high performance insulating systems. Image Analysis & Stereology, N° 20 (2) supl. 1, 498-503.

APPLICATION OF CONTROL VOLUME NUMERICAL METHOD IN THERMOGRAPHIC ANALYSIS OF RELATIVE MATERIAL LOSS

S. ŠVAIĆ, I. BORAS
University of Zagreb, Faculty of Mechanical Engineering and Naval Architecture, 10000 Zagreb, Croatia; e-mails: srecko.svaic@fsb.hr, ivanka.boras@fsb.hr

Application of IR thermography for revealing and estimation of corrosion intensity seems to have a good perspective as a non destructive method. Beside the limitations which are the results of IR camera itself and thermal properties of the material detected, when combined with adequate numerical method the acceptable results can be obtained.
The paper presents the comparison of the results obtained by simulation by means of software developed by authors and the results obtained by thermographic measurement presented by Marinetti, Bison and Grinzato in reference [1].
The subject of the research was the sample shown on figure 1. The sample was made from steel having known properties. The intensity of corrosion was simulated by means of six cylindrical cavities which represents the material loss of: 50%, 30%, 20%, 10%, 5% and 2%. In the numerical simulation it is assumed that there are no alternations in material properties caused by corrosion, but only material loss.

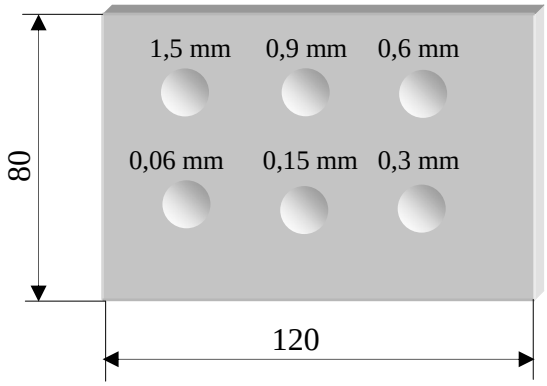

Figure 1. Geometry of the observed model

Numerical simulation of heat transport enables a separate analysis of relevant parameters which characterize heat dissipation in material, like: intensity and duration of heat stimulation, properties of material and start conditions, as well as the time distribution of certain parameters.
The comparison of numerical simulation and thermographic measurements presented in reference [1] shows a very good corresponding in results. The importance to determine the moment when the contrast reached its maximum can be clearly seen from numerical analysis. The analysis also shows that a relative material loss and the diameter of defect can be estimated with best accuracy in the moment when current contrast reaches the maximum.

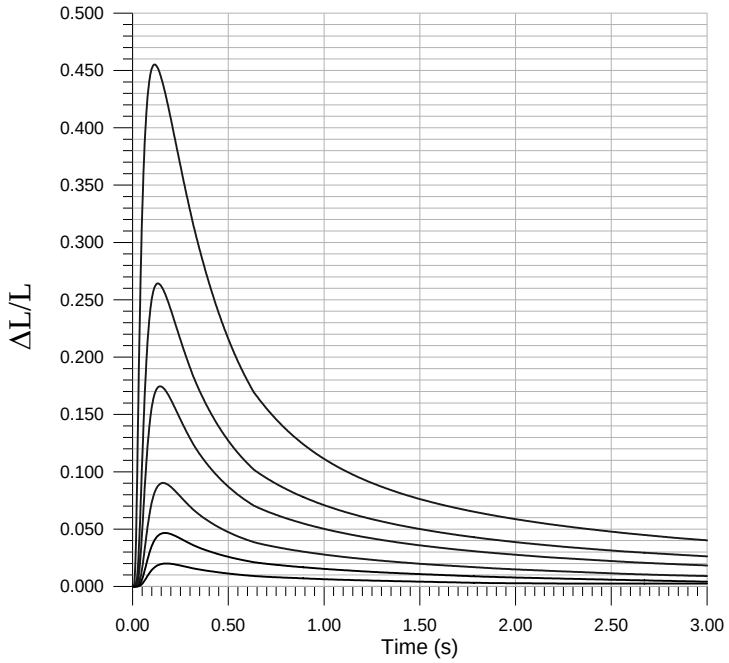

Figure 2. Time development of function for determination of relative material loss

The particular attention in the analysis was given to investigate the influence of heat stimulation parameters and the type of the material on optimal time for corrosion detection. On figure 3 the numerically obtained surface temperature distribution is shown for the optimal time.

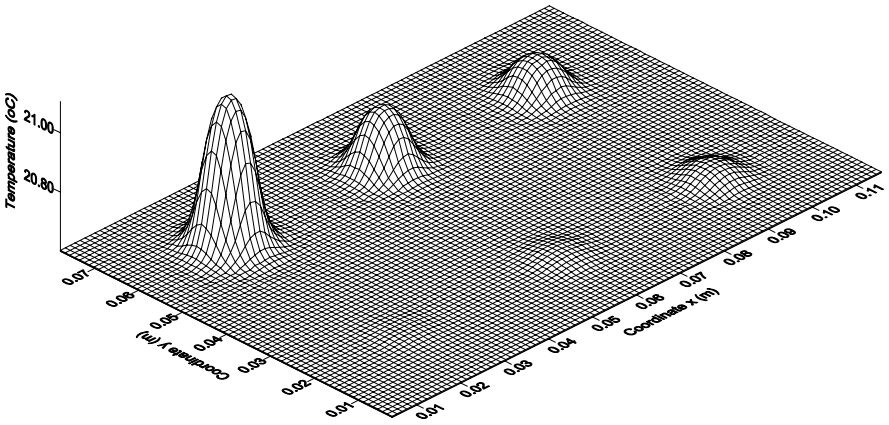

Figure 3. Temperature distribution after 0,1 s

Grzegorz Gralewicz[1], Grzegorz Owczarek[1], Bogusław Więcek[2]
1-Central Institute for Labour Protection - PIB, Warsaw
2-Institute of Electronic, Technical University of Łódź, Łódź

THERMAL MODEL OF MULTILAYER STRUCTURE TO INCLUDE THERMAL RESISTANCE AND THERMAL CAPACITY

Abstract

This paper presents the study on the mechanism of heat transport in multilayer solid body with the assumption that the heat transfer proceeds with the aid of thermal conductivity. It presents a test conducted with lock-in thermography on four-layer structure with implanted defect. The structure is made from materials of different thermal conductivity k (fig. 1.)

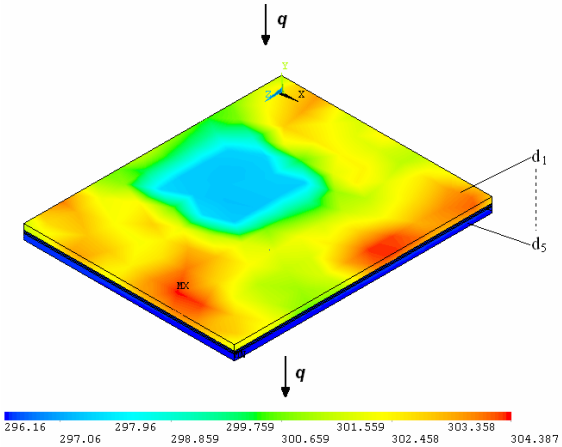

Fig. 1. four multilayer structure with implanted defect

The boundary conditions for a 1-D model are, as follows: $T = T_1$ for $x = 0$, $T = T_2$ for $x = d_1$, $T = T_3$ for $x = d_2$, $T = T_4$ for $x = d_3$, $T = T_5$ for $x = d_4$, $T = T_6$ for $x = d_5$. The equation of temperature distribution for each layer was received as: $q = -k\frac{dT}{dx}$. The stream of warmth out steady state of heat conductivity for every layer is the same and equal to: $q = \frac{T_1 - T_2}{R_{th1}} \dots q = \frac{T_5 - T_6}{R_{th5}}$ where: $R_{th1} = \frac{d_1}{k_1 A} \dots R_{th5} = \frac{d_5}{k_5 A}$. The thermal resistance of multilayer structure is a sum of thermal resistance of each layer: $R_{th} = \sum_i R_{thi}$.

The heat transfer is the same for all layers. In the time Δt the heat transfer equals: $q = C_{th}\frac{dT}{dt}$, so the amount of heat accumulated in the object the heat transfer it equals: $Q = \int_{T_1}^{T_2} C_{th} dT$. The total capacity of multilayer structure complies with the parallel connection of capacity of all layers: $C_{th} = \sum_i C_{thi}$. In such a case different layers of tested object described by thermal resistance and thermal capacity create supplementary circuit, as shown in fig. 2. The model contains the elements of the reactance character and can be used not only in qualification of static schedule of temperature, but also in investigation of transient processes.

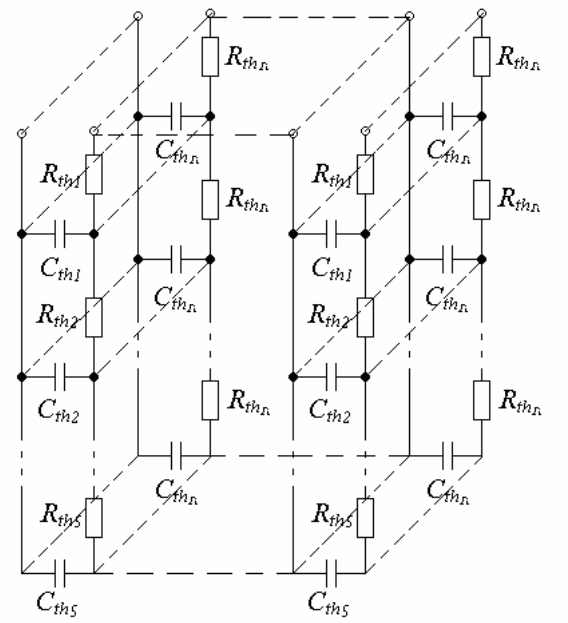

Fig. 2. Thermal model

MODELISATION OF THE COAL PULVERISE COMBUSTION

SAADAOUI M.*, MAHJOUB SAID N.*, MHIRI H.*, LE PALEC G.**, BOURNOT Ph.**
* Unité de thermique et environnement, Ecole Nationale d'Ingénieurs de Monastir, route de Ouardanine 5020 MONASTIR, Tunisie
** Equipe IMFT, Institut de Mécanique de Marseille, UNIMECA, 60 rue Juliot - Curie, Technopôle de Château- Gombert, 13453 MARSEILLE Cedex 13, France,

The development of the clean coal techniques passes initially by the setting in conformity of the power stations with pulverized coal, where the fuel is pulverized in very fine dust in the crushers to facilitate combustion, is mixed with heated air and finally injected into the combustion chamber of the vapor generator. To decrease the emission in the atmosphere of polluting gases, one can add installations of denitrification and/or desulphurization. These processes act either on the level of combustion, or by a treatment of the fume.

The objective of this work is to lead and control combustion with the coal pulverized while knowing to observe the parameters of combustion, to establish a diagnosis, to bring the corrective actions with the permanent concern to optimize the output of combustion and to reduce the emissions of gaseous pollutants.

This work treats the numerical modeling of the combustion of a pulverized jet of solid combustion [1]. Our simulation is based on the resolution of the average equations of Navier-stokes coupled with the conservation equation of the enthalpy and the conservation of the species. For the closing of the equations of turbulence we chose the model k-ε Standard [2]. The modelling of the reactions of devolatilisation and combustion is made according to the model of assessment of density of probability (PDF) [3]. We used the method of the volumes finished for the numerical resolution of the partial derivative equations.

Bibliography

[1] F. C. Lockwood et A. P. Salooja (1983), The prediction of some pulverized bituminous coal in a furnace, Combustion and flame, vol. 56, pp 23-32.

[2]B. E. Launder and D. B. Spalding, *Lecture sin Mathematical Models of Turbulence*, Academic Press, London, England, 1972.

[3] Borghi R. Destriau M., La combustion et les flammes; *technip 1995, pp 37.3.*

Transient Thermal Radiation Analysis of a polymer Fiber

Parham. Sadooghi

K.N.T University of Technology, Tehran – Iran

Email: parhampari2002@yahoo.com

Abstract:

When a solid or stationary fluid is translucent, energy can be transferred internally by radiation in addition to heat conduction. Since radiant propagation is very rapid, it can provide energy within the material more quickly than diffusion by heat conduction. This is important for evaluating the thermal performance of translucent materials that are at high elevated temperatures, are in high temperature surroundings, or are subjected to large incident radiation. Convective heating or cooling can also be applied at the boundaries. Radiant effects are accentuated as temperatures rise; it can be the temperature of material, the temperature of the surroundings, or both. Examples are heating a window by radiation emitted at high temperature from the sun, cooling a white hot ceramic by radiation loss to lower temperature surroundings, heating an insulating shield during atmospheric reentry, and heating translucent plastic with infrared lamps to soften it for manufacturing processes.

Interests in polymer fibers derived from synthetic organic polymers, has grown substantially over the past 25 years. Underlying this growth is the remarkable range of mechanical properties exhibited by polymer fibers. They are widely used in the chemical, metallurgical and food and construction material industries as well as in the other branches of industry for the filtration of gaseous, aggressive liquid and high –temperature substances. Their application in the electrical and electronic industries is especially important, because it has enabled a real increase in the reliability of electrical machines and the development of materials for IC’s and microelectronics.

In this paper, transient radiative and conductive heat transfer in a translucent medium (polymer) with isotropic optical properties is investigated. The radiative two-flux equation is coupled with the transient energy equation and both equations are solved simultaneously. Transient solutions are obtained for a plane layer with refractive index

equal or larger than one, and with external convection and radiation at each boundary. First, it is placed in a hot radiative environment while being cooled by convection at both boundaries. The transient temperature distributions can have rapidly varying shapes when the optical thickness is large, so the absorption of incident energy is concentrated near the boundaries. An important effect of refractive index is that internal reflections promote the distribution of radiative energy within the layer; this makes the transient temperature distribution more uniform. When the boundary conditions are changed and the layer is heated by radiation on one side and is cooled by convection and radiation on the other, the result shows that, if the optical thickness is less than about 10, internal reflections provided by refractive index of two have a substantial effect in equalizing the temperature distributions.

Illustrative results obtained with the two –flux method show the effects of changing parameters such as optical thicknesses, refractive index, conduction-radiation parameter and scattering on the transient temperature distribution within the layer. Results are given at different instances during the transient and the distribution for the largest time is at or very close to steady state.